CHEMICAL REVIEWS

Review

pubs.acs.org/CR

Next Generation of Fluorine-Containing Pharmaceuticals, Compounds Currently in Phase II–III Clinical Trials of Major Pharmaceutical Companies: New Structural Trends and Therapeutic Areas

Yu Zhou,[†] Jiang Wang,[†] Zhanni Gu,[†] Shuni Wang,[†] Wei Zhu,[†] José Luis Aceña,[*,‡,§] Vadim A. Soloshonok,[*,‡,∥] Kunisuke Izawa,[*,⊥] and Hong Liu[*,†]

[†]Key Laboratory of Receptor Research, Shanghai Institute of Materia Medica, Chinese Academy of Sciences, 555 Zu Chong Zhi Road, Shanghai 201203, China

[‡]Department of Organic Chemistry I, Faculty of Chemistry, University of the Basque Country UPV/EHU, Paseo Manuel Lardizábal 3, 20018 San Sebastián, Spain

[§]Department of Organic Chemistry, Autónoma University of Madrid, Cantoblanco, 28049 Madrid, Spain

[∥]IKERBASQUE, Basque Foundation for Science, María Díaz de Haro 3, 48013 Bilbao, Spain

[⊥]Hamari Chemicals Ltd., 1-4-29 Kunijima, Higashi-Yodogawa-ku, Osaka, Japan 533-0024

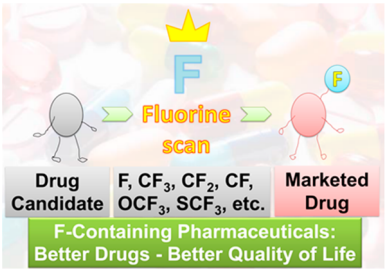

CONTENTS

1. Introduction 423
1.1. Multidisciplinary Impact of Fluorine on Chemical Industry 423
1.2. Fluorine in Pharmaceuticals 423
1.3. Synergy between Fluorine Bioscience and Methodology Development 424
2. Compounds Containing One Fluorine Atom 427
2.1. Afatinib and Dacomitinib 427
2.2. Trametinib 429
2.3. Olaparib 429
2.4. Cabozantinib 430
2.5. Cediranib and Brivanib Alaninate 431
2.6. Idelalisib 433
2.7. Edivoxetine 434
2.8. Blonanserin 435
2.9. Vorapaxar 435
2.10. Tedizolid Phosphate 436
2.11. Zabofloxacin 439
2.12. Solithromycin 439
2.13. Sofosbuvir 440
2.14. Clevudine 443
2.15. Elvitegravir 447
2.16. Riociguat 448
2.17. Setipiprant 450
2.18. Vonoprazan 451
2.19. Ulimorelin 452
2.20. Ripasudil 454
2.21. Canagliflozin and Ipragliflozin 456
2.22. Trelagliptin 458
3. Compounds Containing Two Fluorine Atoms 459
3.1. Omarigliptin 459
3.2. Isavuconazole 459
3.3. Dolutegravir 461
3.4. Ledipasvir 464
4. Compounds Containing Three Fluorine Atoms 468
4.1. Dabrafenib 468
4.2. Cobimetinib 469
5. Compounds Containing One Trifluoromethyl Group 470
5.1. Radotinib and Ponatinib 470
5.2. Tasquinimod 472
5.3. Telotristat Ethyl 474
5.4. Buparlisib 475
5.5. Enobosarm 475
5.6. Siponimod 477
5.7. Teriflunomide 479
5.8. Pradigastat 480
5.9. Delamanid 481
6. Compounds Containing Two Trifluoromethyl Groups 483
6.1. Netupitant and Rolapitant 483
6.2. Evacetrapib 485
7. Compounds Containing Both Trifluoromethyl Groups and Fluorine Atoms 487
7.1. Enzalutamide 487
7.2. Regorafenib 488
7.3. Bitopertin 489
7.4. Elagolix 490
7.5. Odanacatib 491
7.6. Anacetrapib 493
7.7. Darapladib 495
8. Summary of Therapeutic Areas and Drug Indications 496

Received: July 6, 2015
Published: January 12, 2016

DOI: 10.1021/acs.chemrev.5b00392
Chem. Rev. 2016, 116, 422–518

9. Conclusions 498
Author Information 499
Corresponding Authors 499
Notes 499
Biographies 499
Acknowledgments 500
References 500

1. INTRODUCTION

1.1. Multidisciplinary Impact of Fluorine on Chemical Industry

Fluoroorganic chemistry has become essential in the evolution of many different but interconnected research fields. These include the development of new materials with a broad range of applications as represented by photovoltaic solar cells,[1−3] or diagnostic tools such as positron emission tomography (PET) that employs radiotracers labeled with ^{18}F nuclei.[4,5] In addition, the high sensitivity of ^{19}F in nuclear magnetic resonance (NMR) experiments makes this nucleus ideal for biological studies,[6,7] requiring the previous preparation of fluorine-containing amino acids[8−11] and their further incorporation into proteins.[12−15] A closely related diagnostic technique is ^{19}F magnetic resonance imaging (MRI),[16] usually relying on the design and synthesis of polyfluorinated (fluorous) molecules.[17] Furthermore, fluorous reagents, catalysts, and supports also enable the application of synthetic methodologies in a more efficient manner that allows recovering and recycling of valuable materials.[18−20]

Nevertheless, the highest impact of fluorine in the biochemical sciences is undoubtedly associated with the development of agrochemicals[21,22] and, most importantly, in medicinal chemistry.[23−26] Thus, selective fluorination of bioactive molecules is a well-established strategy in the design of new drugs to increase pharmaceutical effectiveness, biological half-life, and bioabsorption.[27−30] This becomes noticeable in the continuous increase of the number of fluorinated drugs already approved or drug candidates entering clinical trials. As a result, some of the best performing, top-selling drugs on the current pharmaceutical market contain fluorine atoms in their structures (see section 1.2).

The benefit of introducing fluorine atoms or fluoroalkyl groups into organic compounds is a consequence of the alteration of their physicochemical characteristics, which in some cases are substantially modified in comparison to their nonfluorinated counterparts. For instance, the modulation of the acidity and lipophilicity, as well as the control of conformational bias, can be achieved by rational substitution of hydrogen atoms or functional groups by fluorine, and ultimately this may result in an improvement of the biological and/or pharmacological properties. Another useful approach is the blocking of potential oxidation sites in order to prevent undesired metabolic pathways, exemplified in the replacement of methyl-arene substituents by trifluoromethyl. Even if there is a certain degree of predictability when designing bioactive fluoroorganic compounds, medicinal chemists still need to synthesize a large number of derivatives through a trial and error process until the desired molecule is finally reached. In addition, the access to a desired fluorine-containing molecule might not be straightforward because of synthetic reasons, as we briefly discuss in section 1.3, and sometimes the choice of a given drug candidate results from a delicate balance between optimal bioactivity and synthetic availability. A more extended discussion on these issues would overlap with already published monographs,[27−30] and readers are also referred to two very recent review articles that try to bring light into these questions.[31,32]

As a continuation of our previous projects in this field,[33−35] we focus herein on a new collection of 51 fluorine-containing molecules that either were approved after 2011 by the corresponding agencies or still are in clinical development. These compounds cover a large number of therapeutic areas, and on this occasion, we decided to classify them according to the number of fluorine atoms or fluorinated moieties. In each case, the structures and modes of action of these new drugs are revised, with a particular focus on the role of fluorine in the biological and pharmaceutical properties, when appropriate. Finally, representative synthetic routes are highlighted.

1.2. Fluorine in Pharmaceuticals

Since the first approval in 1955 by the U.S. Food and Drug Administration (FDA) of a fluorine-containing drug, the steroid fludrocortisone (**1**),[36] nearly 150 fluorinated molecules have succeeded in reaching the market (Figure 1). In 2010 it was

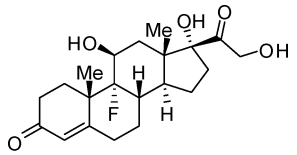

1

Figure 1. Structure of fludrocortisone (**1**).

calculated that about 20% of administered drugs contained fluorine atoms or fluoroalkyl groups.[26] However, the current trend is increasing from 20% to about 30% for all new approved drugs (excluding biopharmaceutical products), in the most recent years. These fluorinated drugs cover all possible therapeutic areas, possess a broad structural diversity, and, despite the limited connectivity of fluorine atoms compared to other heteroatoms, the variety of fluorinated moieties is noteworthy.[37] According to a recent survey, several fluorine-containing drugs are among the most-prescribed and/or profitable in the U.S. pharmaceutical market.[38,39] Some of them are featured in this section.

Statins are a group of 3-hydroxy-3-methylglutaryl CoA (HMG-CoA) reductase inhibitors for the treatment of hypercholesterolemia. A member of this family, rosuvastatin (trade name: Crestor, **2**), became the fourth best-selling ($5.2 billion) and the 13th most prescribed drug in 2013 (Figure 2).[40] In fact, rosuvastatin surpassed another prominent member of the statins, atorvastatin (trade name: Lipitor, **3**), which was the most profitable drug ever until its patent expiration in 2011. However, atorvastatin is still the 16th most prescribed drug in several generic forms.[41]

Another successful fluorine-containing drug is fluticasone propionate (**4**), which in combination with salmeterol (trade name: Advair Diskus) is an oral inhaler for the treatment of asthma, being in sixth place in both prescription and sales rate ($5.0 billion) (Figure 3). Fluticasone propionate is a trifluorinated derivative of fludrocortisone (**1**) acting as a selective agonist of the glucocorticoid receptor, also administered for treating several other inflammatory disorders.[42]

DOI: 10.1021/acs.chemrev.5b00392
Chem. Rev. 2016, 116, 422−518

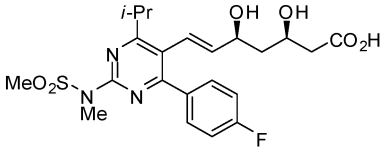

2

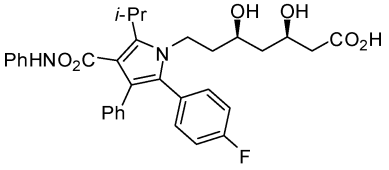

3

Figure 2. Structures of rosuvastatin (**2**) and atorvastatin (**3**).

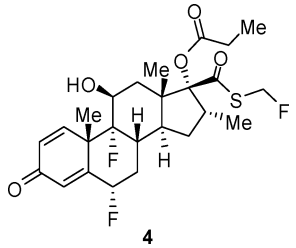

4

Figure 3. Structure of fluticasone propionate (**4**).

Nowadays, triple combination therapy has become the standard treatment for human immunodeficiency virus (HIV) infection. The most successful of these combinations contains two fluorinated drugs, emtricitabine (**5**) and efavirenz (**6**), along with tenofovir under the trade name Atripla ($2.8 billion in sales, 14th place of all pharmaceuticals) (Figure 4). Emtricitabine and efavirenz are nucleoside and non-nucleoside inhibitors of HIV type 1 reverse transcriptase, the enzyme responsible for the virus replication.[43]

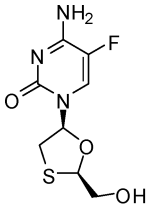

5

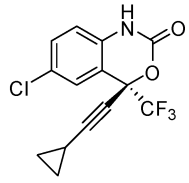

6

Figure 4. Structures of emtricitabine (**5**) and efavirenz (**6**).

Sitagliptin (**7**) is an antidiabetic drug belonging to the group of gliptins or inhibitors of dipeptidyl peptidase 4 (DPP-4) (see sections 2.22 and 3.1) (Figure 5). Sitagliptin phosphate (trade name: Januvia) was the first of this class of compounds

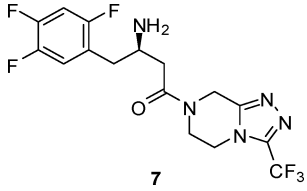

7

Figure 5. Structure of sitagliptin (**7**).

approved for the treatment of diabetes mellitus type 2, making it the 15th most sold drug ($2.8 billion).[44]

Finally, the 21st fluorine-containing drug in sales ($2.2 billion) is celecoxib (trade name: Celebrex, **8**), a nonsteroidal anti-inflammatory drug that is used to reduce pain in several indications, including arthritis and related disorders (Figure 6). The mechanism of action of celecoxib is the blocking of prostaglandin synthesis by selective inhibition of cyclo-oxygenase-2 (COX-2).[45]

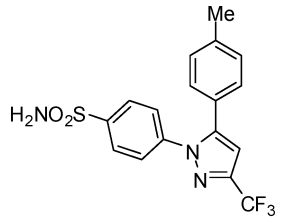

8

Figure 6. Structure of celecoxib (**8**).

1.3. Synergy between Fluorine Bioscience and Methodology Development

The remarkable success of the fluorine-containing drugs discussed above provides an enormous motivation for chemists to discover new methods for preparation of organofluorine compounds. This interest in synthetic methods incorporating fluorine into organic molecules is at an all-time high, ever, showing tremendous ingenuity and breaking all records in number of publications and citations.[46−51] In this chapter, we highlight several most recent breakthroughs in the methodology development for preparation of selectively fluorinated organic compounds.

Retrospectively, the access to simple fluorinated building blocks was far from straightforward and usually required tedious multistep processes. However, medicinal chemists now have a much wider arsenal of available synthetic protocols, with the benefit of being employed in late stages of a synthetic route without affecting already existing functional groups.[52] Furthermore, recently developed fluorination and trifluoromethylation methods are designed with the ultimate goal of being further implemented in industrial processes.[53]

A vast majority of the molecules highlighted in this review contain aromatic rings substituted with one or more fluorine atoms and/or trifluoromethyl groups. In contrast, pharmaceuticals possessing fluorine in aliphatic chains are represented only by solithromycin (section 2.12), sofosbubir (section 2.13), clevudine (section 2.14), ledipasvir (section 3.4), telotristat ethyl (section 5.3), bitopertin (section 7.3), and odanacatib (section 7.5). Although all drugs selected herein were developed in the last years, this statistical conclusion can be extrapolated to the overall number of fluorinated drugs previously in development.

Early examples of direct monofluorination of aromatic rings include the Balz−Schiemann reaction for converting anilines into fluoroarenes (see sections 2.10, 2.15, and 2.18).[54] On the other hand, the nucleophilic displacement of aryl halides can take place with several fluoride sources, although for best results it necessitates the use of anhydrous fluoride anion.[55] Nevertheless, a number of metal-catalyzed methods are now available, usually operating under milder reaction conditions and compatible with a range of functional groups.[56−58] An

DOI: 10.1021/acs.chemrev.5b00392
Chem. Rev. 2016, 116, 422−518

illustrative example is the pioneering work on *ortho*-directing electrophilic fluorination of pyridylarenes **9** under Pd(II) catalysis (Scheme 1).[59] Alternatively, aryl triflates **11** have been converted into aryl fluorides **12** by nucleophilic fluorination with CsF in the presence of catalytic Pd(II) complexes.[60]

Scheme 1. Monofluorination of Aromatic Rings

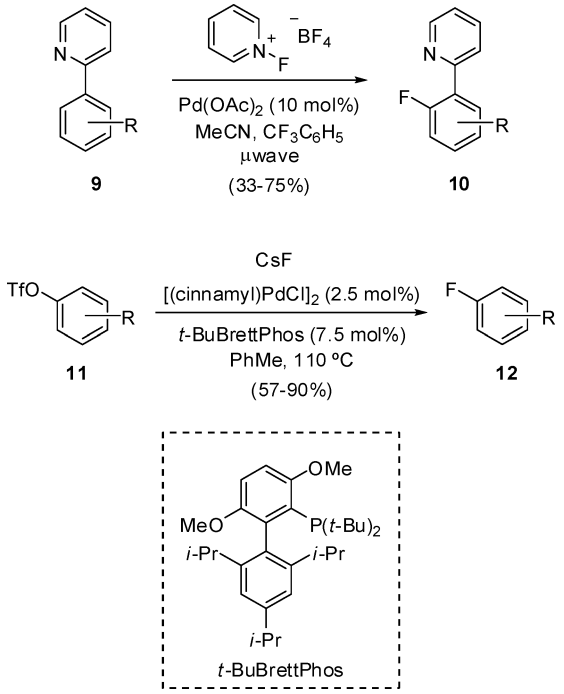

Regarding trifluoromethylations at sp^2 carbons, the use of the Ruppert–Prakash reagent (Me_3SiCF_3) for nucleophilic substitution of aryl halides is a classic protocol (see sections 5.6 and 7.6),[61,62] usually in the presence of stoichiometric amounts of metal salts although catalytic methods have been recently reported.[63] Otherwise, electrophilic trifluoromethylations are possible under a variety of conditions, in the presence of Umemoto's[64] or Togni's family of reagents[65,66] among others (Figure 7). However, these methods suffer from the use of

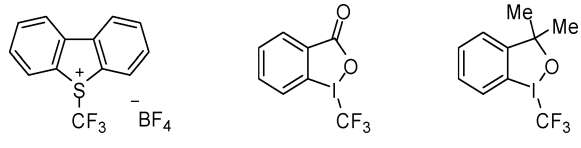

Figure 7. Structures of Umemoto's (**13**) and Togni's (**14** and **15**) reagents.

relatively high cost reagents and somewhat harsh reaction conditions, and therefore a number of alternative synthetic protocols have appeared in recent years. Among them, C–H activation of arenes **16** by reaction with CF_3SO_2Cl under photoredox catalysis is an efficient way of accessing trifluoromethylbenzenes **12**, although mixtures of regioisomeric products are unavoidably obtained (Scheme 2).[67] Another source of CF_3 radical is the Langlois reagent (CF_3SO_2Na) that was used to prepare a number of trifluoromethyl heterocyclic systems such as pyridines **18**.[68]

Scheme 2. Radical Trifluoromethylations of Aromatic and Heteroaromatic Rings

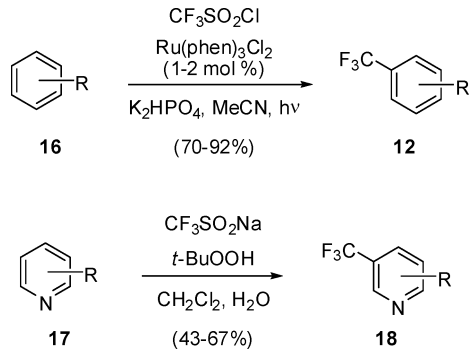

Quite a hectic activity in this field of trifluoromethylation has already exhausted all available sources of trifluoromethyl radical focusing the current research on refining reaction conditions and improving chemo/regioselectivity. Therefore, it is very important to mention the most recent discovery of a new reagent capable of generating a trifluoromethyl radical. Perfluoro-3-ethyl-2,4-dimethyl-3-pentyl radical **19**[69] is a rather unconventional source of the CF_3 radical and initiated various radical polymerization processes.[70−72] Most importantly, for the subject of this review, it worked quite well for radical trifluoromethylation of various simple aromatic compounds showing generally better chemical yields and regioselectivity as compared with the conventional reagents (Scheme 3).[73]

Scheme 3. Structure and Reactivity of Perfluoroalkyl Radical Reagent 19

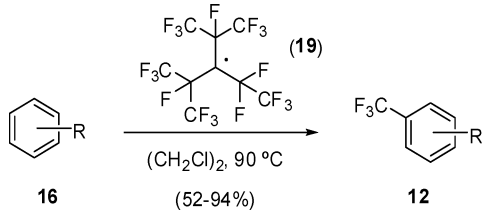

Meanwhile, important examples of fluorination at sp^3 carbons are deoxofluorination reactions that convert alcohols into alkyl fluorides, mostly using R_2N-SF_3 reagents such as (diethylamino)sulfur trifluoride (DAST, **20**) (see sections 2.13 and 7.5) or bis(2-methoxyethyl)aminosulfur trifluoride (Deoxo-Fluor, **21**) (see section 3.4) (Figure 8).[74] Deoxofluorinations also serve to prepare difluoroalkanes from the corresponding carbonyl derivatives. Alternatively, electrophilic fluorinations have been carried out with reagents such as *N*-

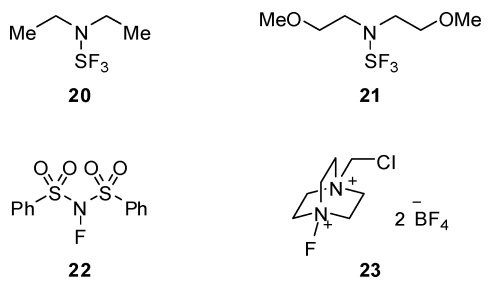

Figure 8. Structures of DAST (**20**), Deoxo-Fluor (**21**), NFSI (**22**), and Selectfluor (**23**).

DOI: 10.1021/acs.chemrev.5b00392
Chem. Rev. 2016, 116, 422–518

fluorobenzenesulfonamide (NFSI, **22**) (see sections 2.12 and 3.4) or 1-chloromethyl-4-fluoro-1,4-diazoniabicyclo[2.2.2]-octane bis(tetrafluoroborate) (Selectfluor, **23**) (see sections 2.12 and 2.14).[75]

The above reactions usually entail the achievement of full stereocontrol as an additional challenge.[76] While most of those examples usually work well in a diastereoselective manner when starting from chiral substrates, a number of enantioselective protocols have been reported in recent years. For instance, organocatalytic methods provide access to α-fluorocarbonyl derivatives **25** by electrophilic fluorination of aldehydes **24** with NFSI (**22**) in the presence of chiral catalysts in good to excellent enantiomeric excesses (ee's) (Scheme 4).[77−79]

Scheme 4. Enantioselective α-Fluorination of Aldehydes

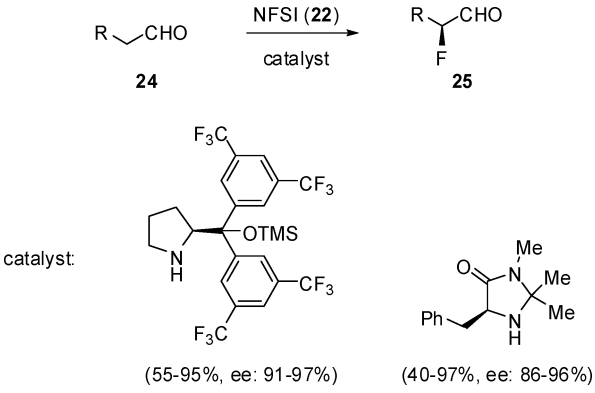

Conversely, an important example of enantioselective catalytic α-trifluoromethylation of aldehydes employed CF_3I as a source of trifluoromethyl radical, in the presence of a metallic photocatalyst, a chiral organocatalyst, and visible light using a regular household bulb, to afford α-CF_3-substituted aldehydes **26** in very good ee's (Scheme 5).[80]

Scheme 5. Enantioselective α-Trifluoromethylation of Aldehydes

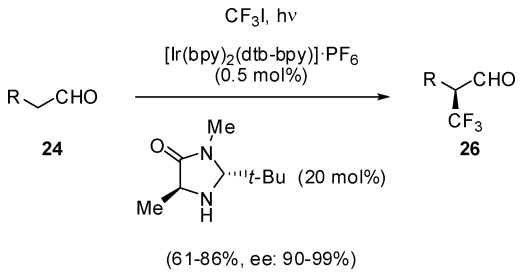

The synthesis of α-(trifluoromethyl)amines is routinely performed by means of nucleophilic additions to chiral CF_3-imines (see section 7.5).[81] In this context, one of quite successful findings is (*S*)- or (*R*)-*N*-*tert*-butylsulfinyl-3,3,3-trifluoroacetaldimine **27** (Scheme 6).[82−84] In molecule **27** the trifluoromethyl[85−87] and *tert*-butylsulfinyl[88−90] groups are two strongly stereocontrolling substituents usually providing excellent stereochemical outcome of nucleophilic additions across the C=N double bond. Compound **27** is readily available in both (*S*) and (*R*) enantiomeric forms, and can be prepared on a large scale.[91] The research reported so far on the chemistry of imine **27** quite convincingly demonstrates that it can be used as an extraordinary general reagent for installation

Scheme 6. Synthetic Applications of Reagent 27

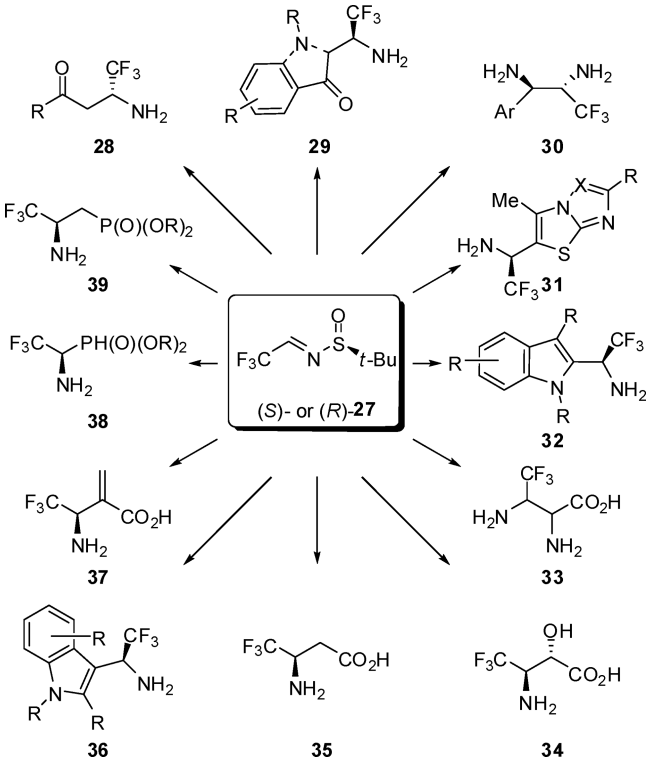

of the β,β,β-trifluoro-α-(amino)ethyl pharmacophoric [CF_3−$CH(NH_2)$−] group into biologically relevant organic compounds. Among the successful applications of chiral imine **27** are the following nucleophilic additions: in situ decarboxylatively generated enolates (compounds **28**),[92] ketone-derived Li enolates (**29**),[93−96] decarboxylatively generated Schiff base C-nucleophiles (**30**),[97] Li nucleophiles derived from various heterocyclic compounds (**31**),[98−101] including indoles (**32**),[102] glycine Schiff bases (**33**),[103,104] α-hydroxy ester derived nucleophile (**34**),[105] malonic acid derivatives (**35**),[106,107] Friedel−Crafts reactions (**36**),[108] aza-Baylis−Hillman reactions (**37**),[109] dialkyl phosphites (**38**),[110] dialkyl methylphosphonates (**39**),[111,112] and other.[113−116] As pointed out above, all these reactions occur with synthetically useful stereochemical outcome and can be readily scaled up.[117]

Reactions of fluoro-enolates with electrophilic species, such as imines or carbonyl compounds, is one of the most valuable and generalized approaches for preparation of a variety of polyfunctional fluorine-containing derivatives of high pharmaceutical potential. Most of the research in this area is based on the application of difluoroenoxysilanes **40** (Scheme 7).[118−120] However, compounds **40** are quite expensive and difficult to make on a large scale. Thus, the practical potential of greatly biologically valuable derivatives of type **41**−**44** and related compounds was rather unavailable for drug development. Therefore, the discovery of the detrifluoroacetylative in situ generation of fluoro-enolates **47** can be regarded as a truly methodological breakthrough in recent years.[121] Mechanistically, it is based on haloform-type reaction[122−126] of perfluorocarbonyl compounds **45**[127−130] and can be conducted under very mild conditions. The reaction types reported so far are Mannich,[131−134] aldol,[135−138] and halogenation[139] reactions. The Mannich and aldol additions can be quite successfully performed in an asymmetric sense using stoichiometric or

DOI: 10.1021/acs.chemrev.5b00392
Chem. Rev. 2016, 116, 422−518

Scheme 7. Detrifluoroacetylative in Situ Generation of Fluoro-Enolates 47

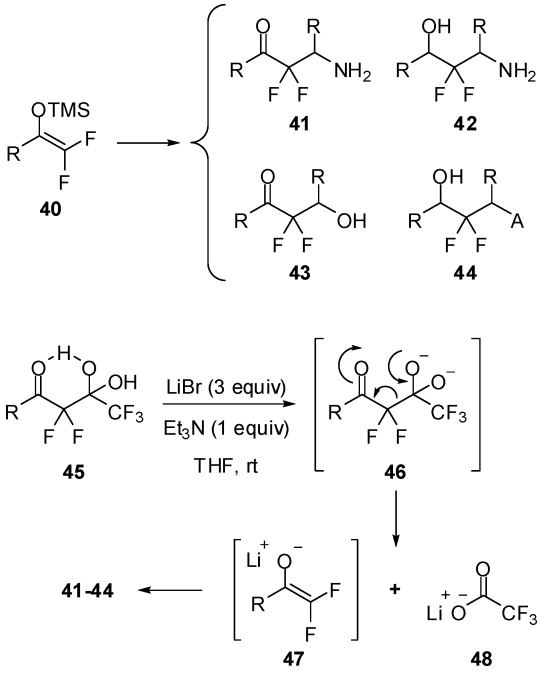

catalytic mode. Furthermore, the detrifluoroacetylative generation of fluoro-enolates **47** features remarkable substrate generality, yields, and stereochemical outcome, the characteristics that bode well with widespread applications of this approach.

The methodological achievements highlighted herein are rather arbitrary, but they provide a realistic snapshot of incredible scope and extraordinary quality of the research activity in the field of organofluorine chemistry. All these new methods will soon be subjected to the ultimate test of practical application for preparation of fluorine-containing pharmaceuticals. In the following sections, we profile 51 compounds, critically highlighting, where it is possible, the source of fluorine and the methodological choices in light of the past and current developments.

2. COMPOUNDS CONTAINING ONE FLUORINE ATOM

2.1. Afatinib and Dacomitinib

Afatinib (BIBW2992, **49**) was developed by Boehringer Ingelheim for the potential treatment of non-small-cell lung cancer (NSCLC) and other solid tumors,[140,141] while a closely related molecule, dacomitinib (PF-299804, **50**), was selected by Pfizer for the same indication (Figure 9).[142] In July 2013, afatinib was approved by the FDA for NSCLC treatment, and was then launched in the United States in October 2013 with the trade name Gilotrif. Eventually, the European Commission, Health Canada, Mexico, Japan, and Taiwan have also approved afatinib. In contrast, dacomitinib is still progressing through phase III clinical trials.

Both afatinib and dacomitinib are oral irreversible inhibitors of the ErbB family or receptor tyrosine kinases, including the epidermal growth factor receptor (EGFR) and the human epidermal growth factor receptor (HER2). They derived from the previously launched EGFR inhibitor gefitinib (**51**), with which they share the 6,7-disubstituted quinazoline core as well as the fluorinated aniline fragment. In fact, previous work

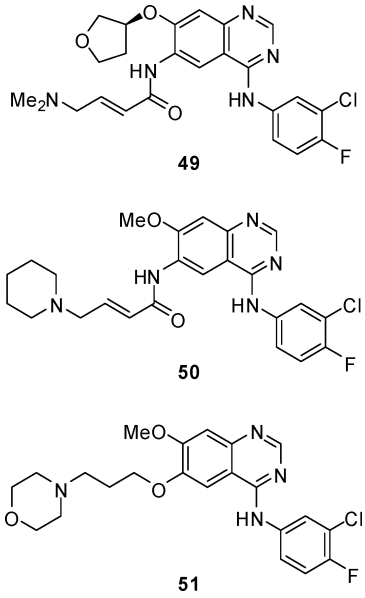

Figure 9. Structures of afatinib (**49**), dacomitinib (**50**), and gefitinib (**51**).

showed that the 3′-Cl substituent would bind to a lipophilic pocket in the ATP binding domain and notably the 4′-F substituent would afford longer in vivo half-lives by slowing down the rate of metabolism.[143,144]

The development of afatinib started from the hit compounds **52** and **53**, which were designed to form covalent bonds through their Michael acceptor moiety with the sulfhydryl group of Cys-773 in EGFR for irreversibly blocking EGFR autophosphorylation (Scheme 8).[145] Modeling analyses of

Scheme 8. Discovery of Afatinib (49)

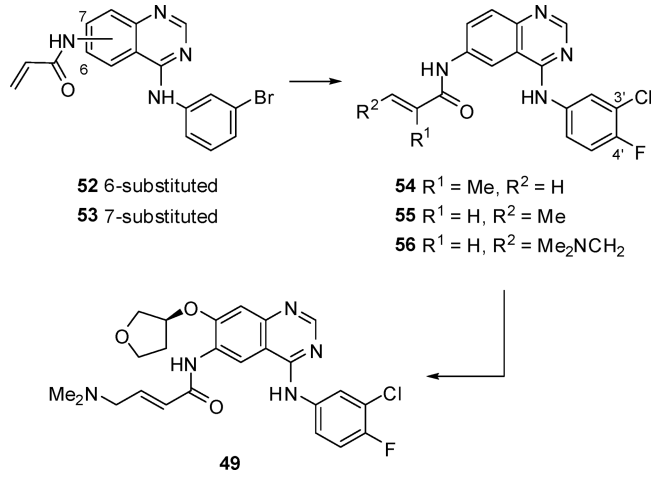

former reversible inhibitors demonstrated that both the 6- and 7-positions of the quinazoline ring emerged out of the ATP binding pocket toward the solvent,[146] while the 6-substituted side chain was 2-fold closer to Cys-773 than the 7-substituted side chain, showing a much faster alkylation rate.[144] The aniline ring was modified as in gefitinib, and further alterations of the Michael acceptor fragment resulted in 1-methylacrylamide **54**, but this compound exhibited a complete loss of irreversible inhibition of EGFR, whereas the 2-methylacrylamide **55** reduced the enzyme alkylation rate with only partial

DOI: 10.1021/acs.chemrev.5b00392
Chem. Rev. 2016, 116, 422−518

Scheme 9. Synthetic Route to Afatinib (49)

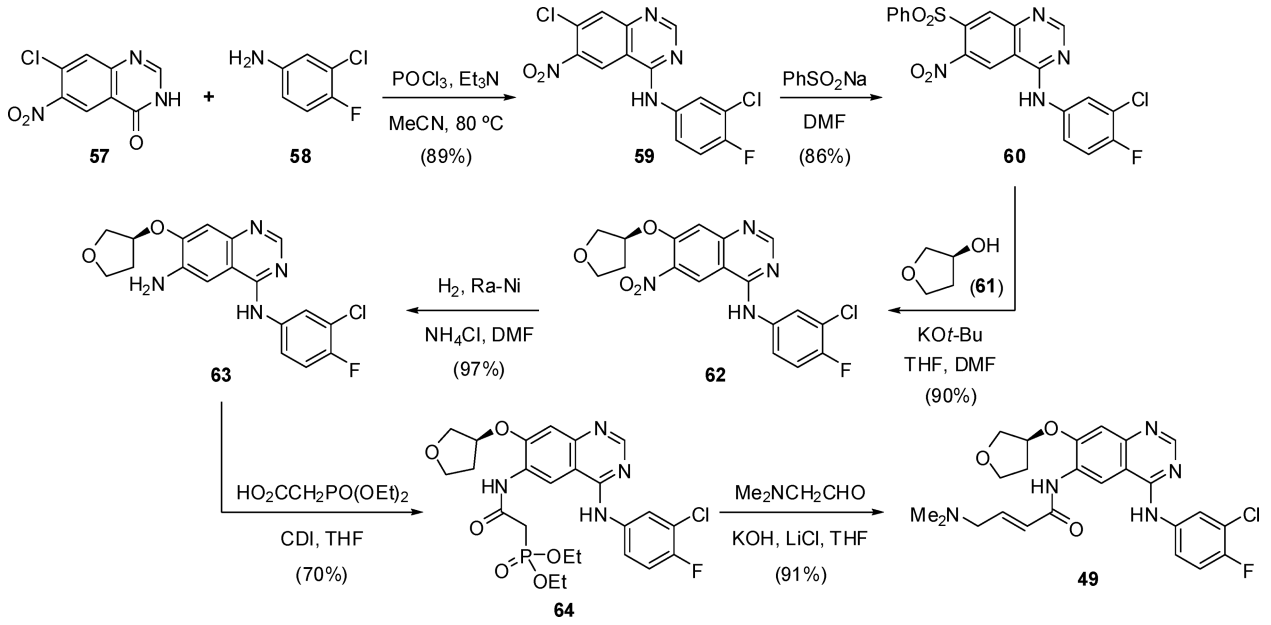

Scheme 10. Synthetic Route to Dacomitinib (50)

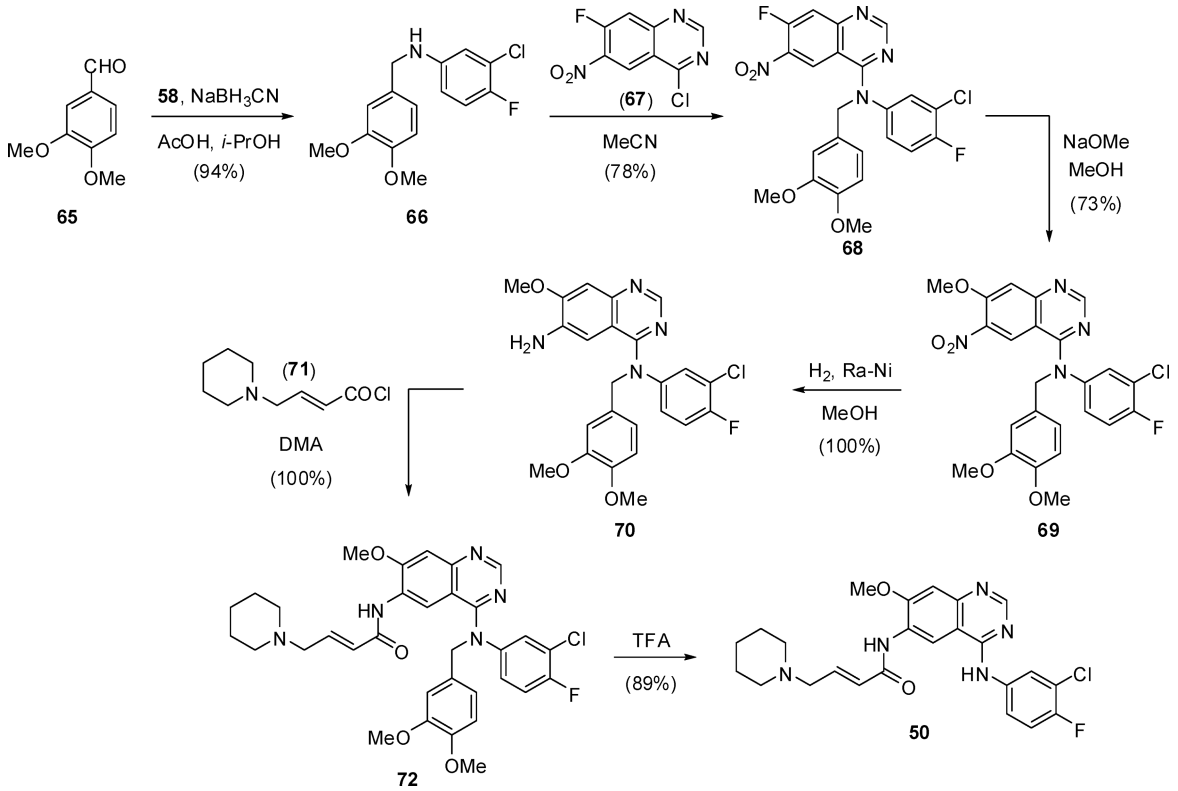

irreversibility.[147] Meanwhile, incorporation of a dimethylamino group at the amide chain as in **56** not only accelerated the alkylation of the sulfhydryl group with the Michael acceptor through a cyclic catalytic mechanism, but also improved the oral bioavailability by enhancing the solubility under physiological conditions.[148,149] Finally, structure optimization by introduction of soluble groups at the 7-position of the quinazoline led to the discovery of afatinib (**49**). The existence of a covalent bond between afatinib and EGFR has been demonstrated by several techniques including X-ray analysis and mass spectrometry.[150]

Afatinib was synthesized as shown in Scheme 9. The source of fluorine was 3-chloro-4-fluoroaniline (**58**), which is commercially available in multikilogram amounts and also accessible by nitration and fluorination of 1,2-dichlorobenzene.[151] Quinazolinone **57** was heated in the presence of $POCl_3$, followed by addition of aniline **58** to afford amine **59**. Nucleophilic substitution of **59** with benzenesulfinic acid sodium salt gave sulfone **60**, which was treated with (*S*)-3-

DOI: 10.1021/acs.chemrev.5b00392
Chem. Rev. 2016, 116, 422−518

hydroxytetrahydrofuran (**61**) and KO*t*-Bu to provide aryl ether **62**. After hydrogenation of the nitro group, condensation of aniline **63** with diethylphosphonoacetic acid yielded amide **64**, and final Horner−Wadsworth−Emmons olefination with dimethylaminoacetaldehyde (prepared from the corresponding diethyl acetal) produced afatinib (**49**).[152]

Conversely, dacomitinib was prepared as depicted in Scheme 10. Reductive amination of substituted benzaldehyde **65** with aniline **58** afforded secondary amine **66**, which was treated with quinazoline **67** to yield tertiary amine **68**. Substitution of a fluorine atom in **68** by a methoxy group with NaOMe provided **69**, which was hydrogenated with Raney nickel as catalyst to give intermediate **70**. Next, unsaturated amide **72** was prepared by coupling of **70** with acid chloride **71**, and finally the target molecule dacomitinib (**50**) was obtained by debenzylation of amide **72** in TFA.[153]

2.2. Trametinib

The RAS/RAF/MEK/ERK mitogen-activated protein kinase (MAPK) pathway is a complex signaling network involving a family of protein kinases that regulates many essential cellular processes, including cell proliferation, survival, differentiation, motility, apoptosis, and angiogenesis. However, abnormalities in some of its components may lead to the development of many human malignancies.[154] It was demonstrated that BRAF may be the most important activator associated with melanoma, and BRAF-mutated cell lines are extremely sensitive to MEK inhibition. Therefore, the inhibition of MEK is a promising therapeutic strategy for melanoma patients with activating mutations involving the MAPK pathway.[155]

The first MEK inhibitor, trametinib (GSK1120212, **73**), was approved by the FDA in May 2013 for the treatment of patients with unresectable or metastatic melanoma with $BRAF^{V600E/K}$ mutations (Figure 10). In January 2014, the combination of

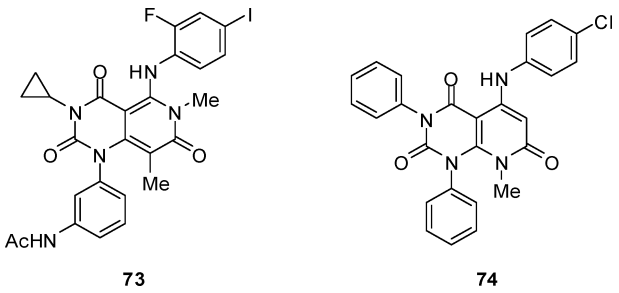

Figure 10. Structures of trametinib (**73**) and lead compound **74**.

trametinib and dabrafenib (see section 4.1) was granted accelerated approval in the United States for the same indications. Marketed as the DMSO-solvate form (trade name: Mekinist), trametinib was originally discovered by Japan Tobacco and then developed and launched by GlaxoSmithKline. It is a potent orally bioavailable allosteric ATP noncompetitive inhibitor of both MEK 1 and MEK 2 protein kinases.[156] In addition, trametinib may also inhibit the activation of MEK by preferentially inhibiting phosphorylation at Ser-217 to impact normal dual phosphorylation of MEK, leading to a mainly monophosphorylated protein at Ser-221.[157]

The lead compound (**74**) of trametinib was originally discovered from a high-throughput screening as a $p15^{INK4b}$ inducer for inhibiting the cyclin-dependent kinase (CDK) 4/6.[158] SAR studies demonstrated that the introduction of one fluorine atom at the 2-position of the aniline moiety improved the antitumor potency by 4-fold and led to a small increase in hydrophobicity. Besides, the presence of sterically demanding substituents such as iodine in the 4-position increased the potency by nearly 500-fold, compared with the compounds without *para*-substituents. The introduction of the 3′-acetamido group contributed to the better bioavailability and potency. Moreover, the liposolubility was greatly reduced by replacement of the phenyl group by a cyclopropyl ring on the pyrimidinedione.[159]

The synthesis of trametinib started from 2-fluoro-4-iodo-1-isocyanatobenzene (**75**), which was combined with cyclopropylamine and then reacted with malonic acid to give the cyclization product **77** (Scheme 11). Compound **77** was chlorinated by treatment with $POCl_3$ to give intermediate **78**, although the regioselectivity was not reported. Replacement of the chlorine with methylamine afforded compound **79**. Reaction of **79** with diethyl methylmalonate led to cyclization product **80**, which underwent a substitution reaction through the corresponding triflate **81** to furnish nitrobenzene **82**. Under weakly basic conditions, the isomeric nitrobenzene **83** was formed via an intramolecular rearrangement. Finally, the nitro group was converted to amine **84** that was acetylated to yield trametinib (**73**).[159]

2.3. Olaparib

Olaparib (AZD-2281, KU-59436, **85**) was discovered by KuDOS Pharmaceuticals and later developed by AstraZeneca for the potential treatment of BRCA-mutated ovarian and breast cancer as a monotherapy, as well as other tumors such as gastric, prostate, and non-small-cell lung cancer (NSCLC) when combined with DNA-damaging agents (Figure 11). As one of the leads of numerous poly(ADP-ribose) polymerase (PARP) inhibitors, olaparib exhibited potent activity in a cell-based assay (potentiation factor at 50% growth inhibition, PF_{50} = 25.8) with good pharmacokinetic and physicochemical properties for oral administration.[160,161] Regulatory filing submission for gBRCAm platinum-sensitive recurrent (PSR) ovarian cancer in the United States was successful, and FDA approval for olaparib (trade name: Lynparza) was granted in December 2014.[162]

The discovery process of olaparib was envisaged from the hit compound **86**, obtained from high-throughput screening of the Maybridge collection, showing low-micromolar inhibitory potency against human PARP-1 (IC_{50} = 0.77l μM) (Scheme 12). Preliminary structure-guided modifications around the *meta*-substituents of the benzyl moiety, supported by the homology model of chicken PARP-1, resulted in a diverse library of anilides as PARP-1 inhibitors with enhanced potency, among which propionanilide derivative **87** exhibited the most potent PARP-1 inhibition (IC_{50} = 10 nM). However, it displayed poor pharmacokinetic properties with high clearance rate in vitro in mouse hepatic microsomes (CL = 12 mL/min/g), which might be caused by the metabolic instability of the pendant anilide moiety.[163] Interestingly, reversal of this possible metabolic point to give the corresponding amide **88** exhibited a significantly improved metabolic stability in vitro with retained inhibitory potency (CL < 1 mL/min/g, IC_{50} = 50 nM). Further structural elaborations of the amide moiety, based on the above observation, led to the disclosure of compound **89**, which exhibited good inhibitory potency at both the enzyme level and the cellular level (PARP-1: IC_{50} = 9 nM, PF_{50} = 2.4). Notably, introduction of fluorine at the *para*-position of the benzyl group significantly enhanced cellular activity, while maintaining

DOI: 10.1021/acs.chemrev.5b00392
Chem. Rev. 2016, 116, 422−518

Scheme 11. Synthetic Route to Trametinib (73)

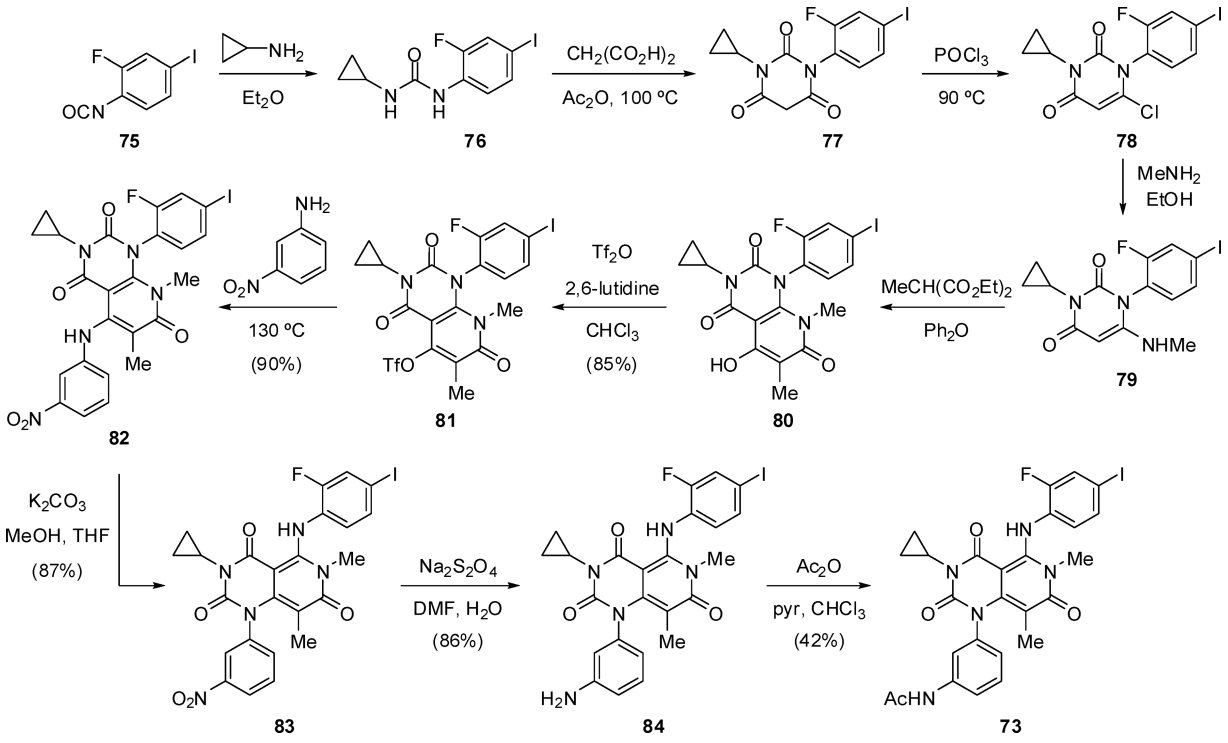

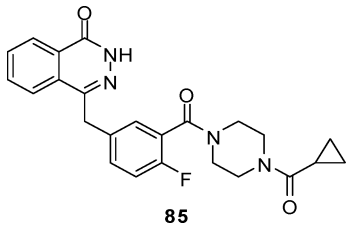

Figure 11. Structure of olaparib (**85**).

Scheme 12. Discovery of Olaparib (85)

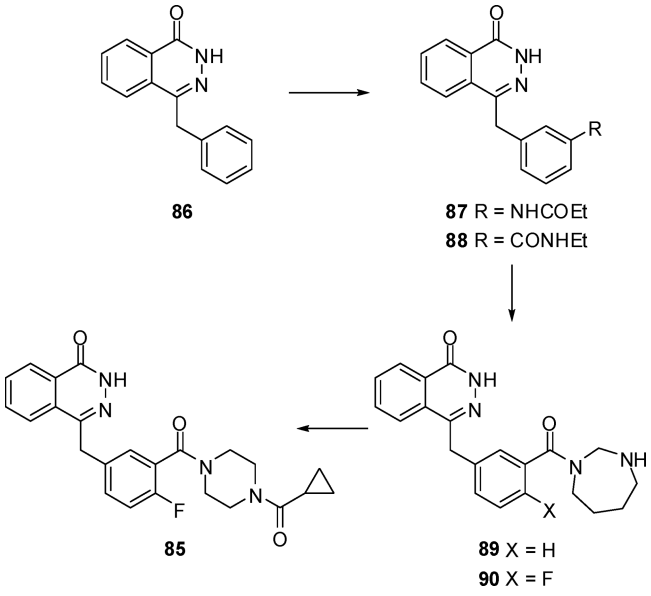

potency at the enzyme (**90**, PARP-1: IC_{50} = 7 nM, PF_{50} = 12.6).[164] Researchers postulated that the repulsive electrostatic interactions between fluorine and the C-3 carbonyl could possibly confine the conformational rotation and lower the molecular entropy, which consequently enhanced the permeability of the fluorine-substituted derivative. Finally, the pharmacokinetic screen of distal nitrogen substituted derivatives led to the discovery of olaparib (**85**) with excellent potency and improved oral availability (PARP-1: IC_{50} = 5 nM, PF_{50} = 25.8).[165]

The synthetic route to olaparib is illustrated in Scheme 13. Treatment of 2-formylbenzoic acid (**91**) with dimethyl phosphite and NaOMe afforded phosphonate **92**, which underwent Horner−Wadsworth−Emmons olefination with fluoro-substituted benzaldehyde **93**[166] to give **94** as a mixture of geometrical isomers. Hydrolysis of the nitrile group in **94** under basic conditions, followed by ring rearrangement with hydrazine hydrate, yielded benzoic acid **95**, which was condensed with cyclopropyl(piperazin-1-yl)methanone (**96**) in the presence of HBTU and *i*-Pr_2NEt (Hünig's base)[167] to afford the targeted product olaparib (**85**).[165]

A metal-free protocol for the production of carbon monoxide from carbon dioxide has been successfully applied to the carbonylative coupling of late-stage intermediate **97** with piperazine **96** to afford olaparib (**85**) in excellent yield (Scheme 14). The process occurred in a two-chamber vessel connected with a glass tube to allow gas transfer and is amenable for preparing ^{13}C-labeled olaparib using readily available $^{13}CO_2$ as starting material.[168]

2.4. Cabozantinib

Cabozantinib (XL-104, **98**) was developed by Exelisis as a multitargeted tyrosine kinase (such as MET, VEGFR2, RET, Kit, and Flt3) inhibitor, for the oral treatment of metastatic medullary thyroid cancer (MTC) (Figure 12).[169−172] Although prescribing information on cabozantinib carried a boxed warning highlighting the risks of perforations and fistulas and severe, sometimes fatal hemorrhage, it was finally approved in

DOI: 10.1021/acs.chemrev.5b00392
Chem. Rev. 2016, 116, 422−518

Scheme 13. Synthetic Route to Olaparib (85)

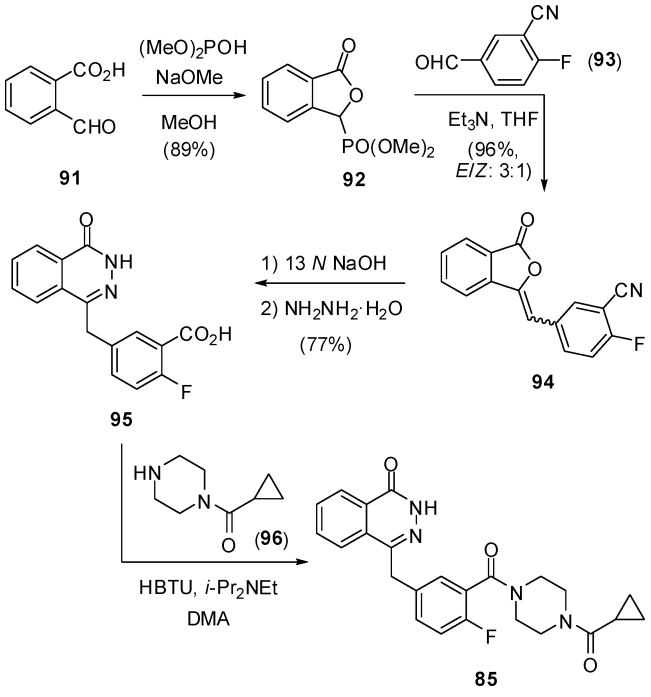

Scheme 14. Preparation of Olaparib (85) via Aminocarbonylation Reaction

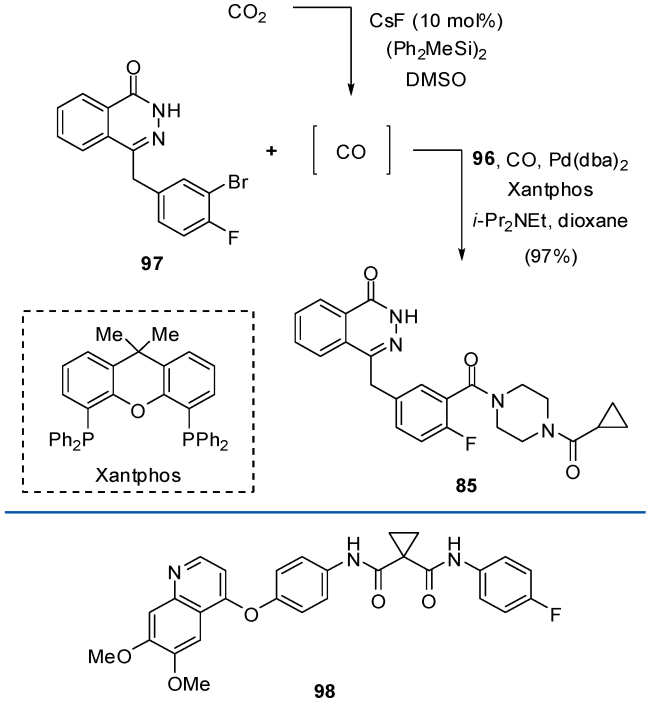

Figure 12. Structure of cabozantinib (**98**).

the United States in November 2012 and in the EU in March 2014 (trade name: Cometriq). A number of clinical trials for several types of cancer are also in process.

Cabozantinib was synthesized as shown in Scheme 15. Quinolinol **99** was heated with $POCl_3$ to give chloroquinoline **100**, which was substituted with 4-aminophenol to afford aniline **101**. Conversely, cyclopropane-1,1-dicarboxylic acid (**102**) was stirred with $SOCl_2$ and Et_3N, followed by treatment

Scheme 15. Synthetic Route to Cabozantinib (98)

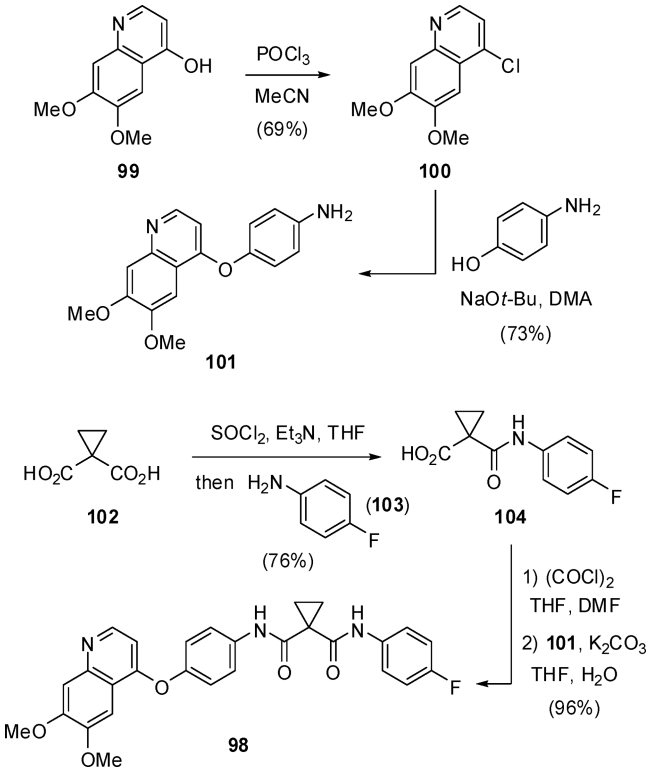

with 4-fluoroaniline (**103**) to yield amide **104**. Activation of **104** as its corresponding acid chloride with $(COCl)_2$ and subsequent condensation with aniline **101** provided the target molecule cabozantinib (**98**).[172,173]

2.5. Cediranib and Brivanib Alaninate

Cediranib (AZD2171, **105**) was developed by AstraZeneca as an orally bioavailable inhibitor of pan-vascular endothelial growth factor (pan-VEGF) receptor tyrosine kinase for the potential treatment of cancer (Figure 13).[174−176] A phase II/III study for non-small-cell lung cancer (NSCLC) commenced in November 2005 although it was discontinued for toxicity imbalances in February 2008, and a phase II trial for gastric cancer was initiated in January 2012 in Japan. In December 2010, the FDA awarded orphan drug status to cediranib for glioblastoma treatment.

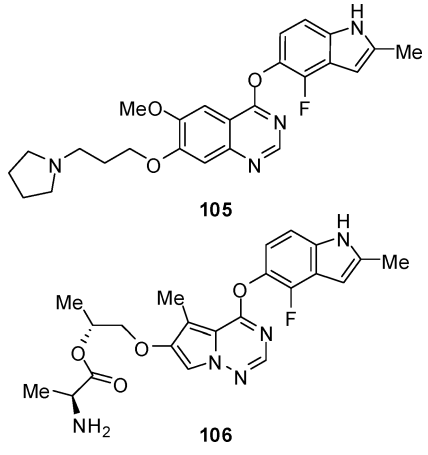

Figure 13. Structures of cediranib (**105**) and brivanib alaninate (**106**).

DOI: 10.1021/acs.chemrev.5b00392
Chem. Rev. 2016, 116, 422−518

The fluorinated indole ring of cediranib is also found in another anticancer drug, brivanib alaninate (BMS-582664, **106**), which was reported by Bristol-Myers Squibb as an orally active dual inhibitor of the VEGFR-2 (KDR) and FGF receptor tyrosine kinases.[177] Currently, phase III trials for hepatocellular carcinoma (HCC) are ongoing.

The scaffold of cediranib derived from a series of quinazoline-based inhibitors of receptor tyrosine kinases with potent inhibitory activities against EGFR, as in gefitinib discussed earlier (see section 2.1). After replacing the aniline moiety found in gefitinib by a substituted indolol fragment, the corresponding compound exhibited good inhibitory potency against VEGFR. Incorporation of fluorine at the 4′-position of the indole ring would further improve the in vitro inhibition of VEGFR.[178,179]

In the case of brivanib alaninate, the hit compound **107**, which also derived from gefitinib, demonstrated relatively good potency against EGFR (IC_{50} = 100 nM) (Scheme 16). After

Scheme 16. Discovery of Brivanib Alaninate (106)

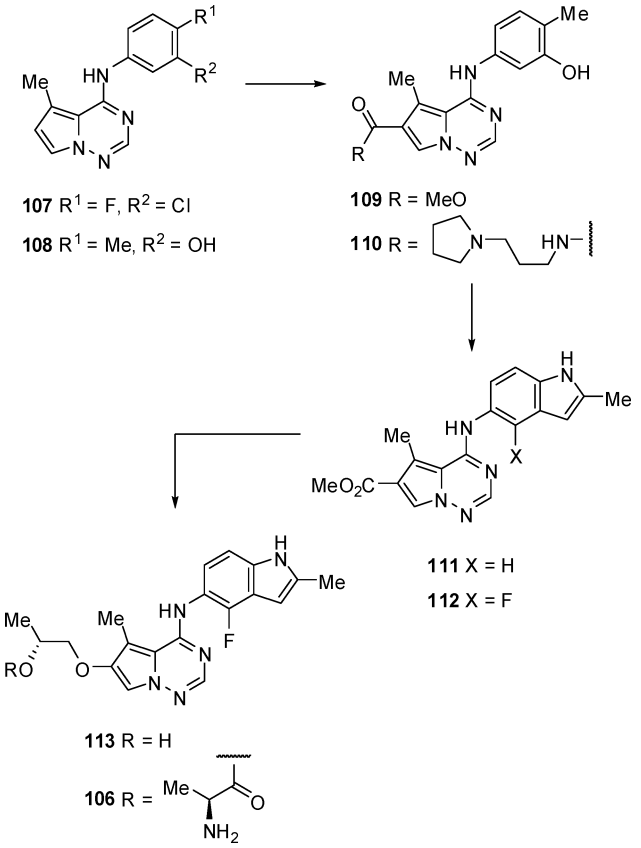

replacing the substituents of the aniline ring, the inhibition of EGFR in the corresponding compound **108** was reduced to some extent, but in contrast the inhibition of VEGFR-2 was considerably improved (EGFR: IC_{50} = 346 nM, VEGFR-2: IC_{50} = 66 nM).[180] This inhibitory activity was preserved, when an ester moiety was incorporated at the C-6 position, but the resulting derivative **109** showed facile glucuronidation at the phenolic oxygen. Introduction of a basic amino group on the C-6 substituent decreased the rate of glucuronidation, but compound **110** failed to provide the desired in vivo pharmacokinetic properties.[181] To overcome the metabolic instability, the phenol fragment was replaced by an indole to give compound **111** (VEGFR-2: IC_{50} = 78 nM). Notably, the fluorine-substituted indole moiety in **112** achieved a 4-fold increase in potency against VEGFR-2 (IC_{50} = 17 nM). Further SAR studies at the C-6 position led to the discovery of brivanib (BMS-540215, **113**) in the consideration of its relatively low inhibition activity of hERG and cytochrome P450 (CYP) enzyme CYP3A4 (VEGFR-2: IC_{50} = 25 nM, hGER: IC_{50} = 18 μM, CYP3A4: IC_{50} = 18 μM).[182] Finally, the (*S*)-Ala-substituted prodrug brivanib alaninate (**106**) was designed to improve the aqueous solubility, exhibiting favorable CYP profile and excellent pharmaceutical properties.[177]

The synthesis of the fluoroindole moiety common in both cediranib and brivanib alaninate was performed from 1,2,3-trifluoro-4-nitrobenzene (**114**)[183] by nucleophilic substitution with ethyl 3-oxobutanoate followed by decarboxylation reaction under acidic conditions (Scheme 17). The resulting arylpropa-

Scheme 17. Synthesis of Fluorinated Indole 117

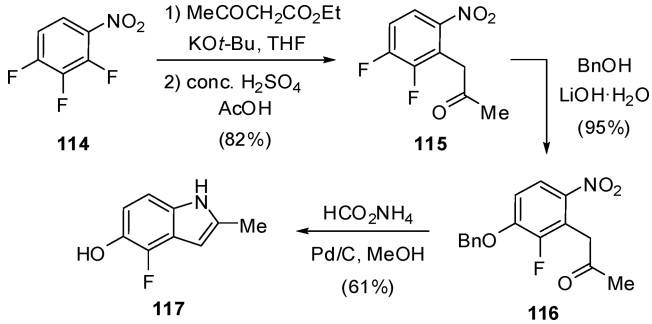

none **115** further underwent another S_NAr reaction by heating with LiOH and benzyl alcohol to yield benzyl ether **116**. The intermediate indole **117** was next prepared by hydrogenation and sequential annulation using ammonium formate and Pd/C.[178]

The quinazoline core of cediranib was constructed from phenol **118** that was first protected as its benzyl ether **119**, followed by nitration to give nitrobenzene **120** (Scheme 18). Hydrogenation of **120** using Pt/C provided aniline **121**, which was heated with ammonium formate in DMF to yield quinazolinone **122**. Chlorination of **122** with $POCl_3$ furnished quinazoline **123**, and subsequent nucleophilic substitution with indole intermediate **117** gave indole ether **124**. Deprotection of intermediate **124** provided phenol **125**, which was heated with ammonium salt **126** to afford the target product cediranib (**105**).[179]

Brivanib alaninate was synthesized as shown in Scheme 19. The pericyclic reaction between methyl but-2-enoate (**127**) and toluenesulfonylmethyl isocyanide (TosMIC) under basic conditions and subsequent acylation by treatment with $AlCl_3$ and CCl_3COCl afforded pyrrole **128**. The pyrrolotriazine nucleus was constructed by N-amination of pyrrole **128** with diphenyl phosphoryl hydroxylamine and subsequent annulation reaction by heating with formamide to render **129**. Treatment of **129** with $POCl_3$ afforded chloroimidate **130** that was transformed into aromatic ether **131** by nucleophilic substitution with indole **117**. Addition of MeMgBr to **131** yielded tertiary alcohol **132**, which was oxidized by treatment with H_2O_2 to afford pyrrolotriazinol **133**. Base-catalyzed epoxide opening of (*R*)-(+)-propylene oxide by reaction with **133** gave brivanib (**113**), which underwent condensation reaction with

DOI: 10.1021/acs.chemrev.5b00392
Chem. Rev. 2016, 116, 422−518

Scheme 18. Synthetic Route to Cediranib (105)

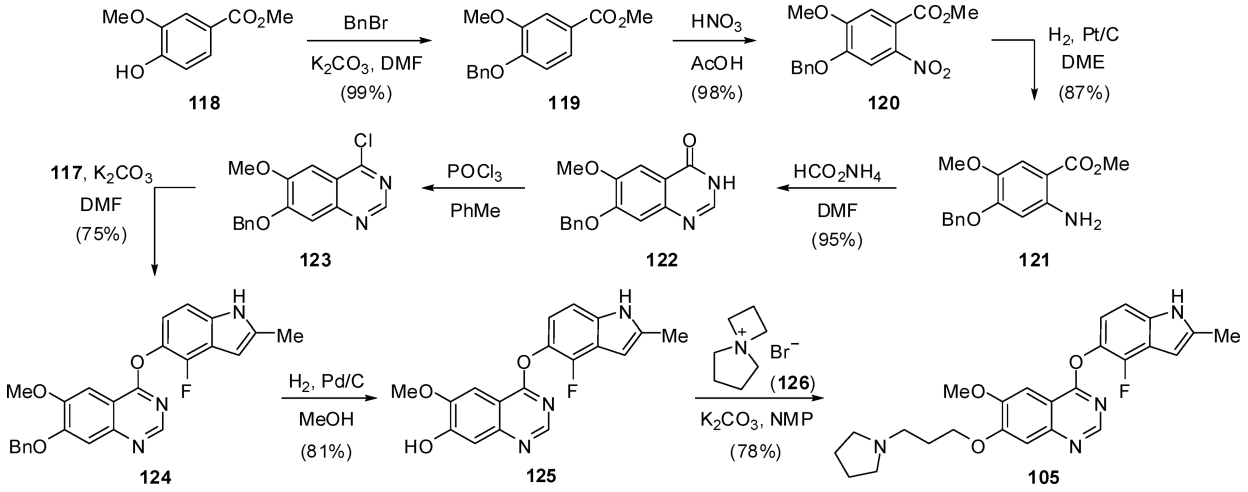

Scheme 19. Synthetic Route to Brivanib Alaninate (106)

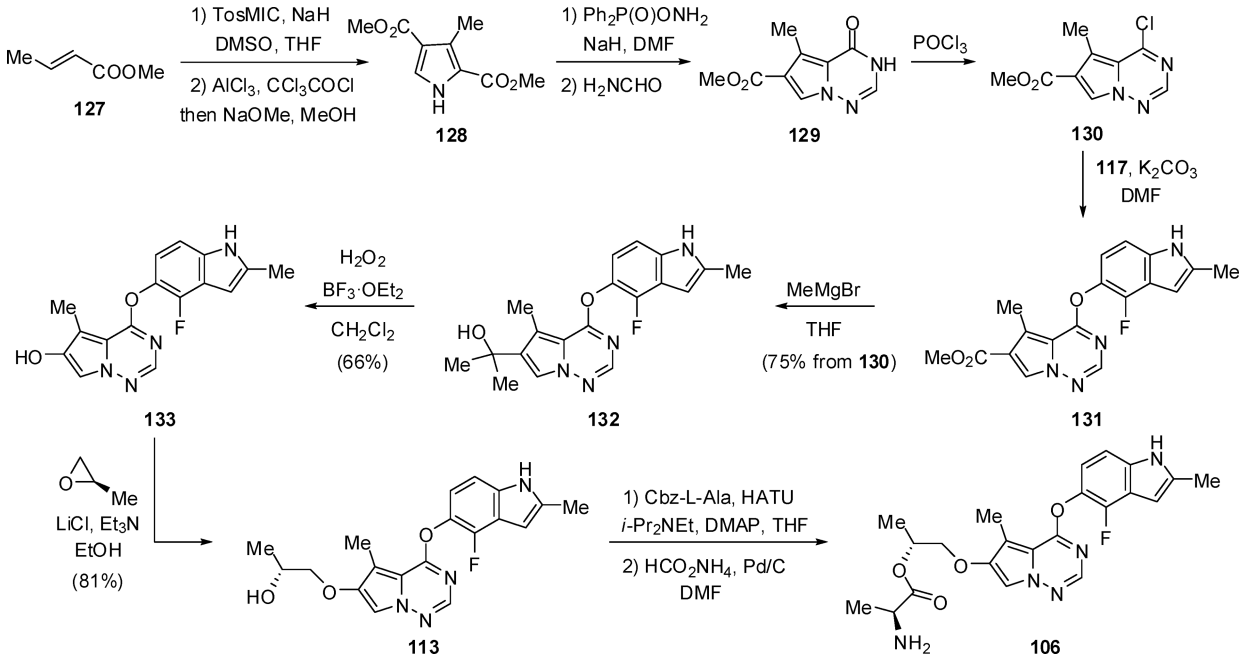

suitably protected alanine to yield the prodrug brivanib alaninate (**106**) after removal of the Cbz group.[177,181]

2.6. Idelalisib

Idelalisib (GS-1101, CAL-101, **134**), the first oral selective inhibitor of phosphatidylinositol 3-kinase p110δ (PI3Kδ) (IC_{50} = 2.5 nM), was approved by the FDA on July 23, 2014, for the treatment of three types of relapsed blood cancer: chronic lymphocytic leukemia (CLL), follicular B-cell lymphoma (FL), and small lymphocytic lymphoma (SLL) (Figure 14).[184] The combination of idelalisib and rituximab, an anti-CD20 antibody, was approved for the treatment of patients with relapsed CLL, which apparently increased progression free survival time, compared with treatment with rituximab monotherapy and a placebo. For patients with FL or SLL, idelalisib is used for those who have already received two or more systemic therapies.[185] Moreover, it has also been given accelerated approval to the treatment of patients with relapsed follicular B-cell non-Hodgkin lymphoma (NHL) and relapsed SLL who have received at least two preferential therapies.[186] Idelalisib was discovered by Calistoga Pharmaceuticals, and later developed and marketed by Gilead Sciences (trade name: Zydelig).

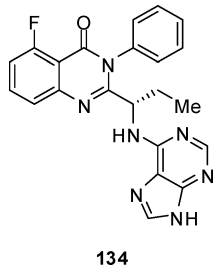

Figure 14. Structure of idelalisib (**134**).

Idelalisib plays a highly selective role in inhibiting the δ isoform of class I phosphatidylinositol 3-kinase, and hence it can effectively block the PI3Kδ/Akt/mTOR signaling pathway and promote cell death.[187] This inhibition takes place by

DOI: 10.1021/acs.chemrev.5b00392
Chem. Rev. 2016, 116, 422−518

reversible and noncovalent binding to PI3Kδ, by opening a hydrophobic pocket at the ATP-binding site in which the fluoroquinazolinone moiety accommodates as demonstrated by X-ray analysis of an idelalisib−PI3Kδ complex.[188] Also, idelalisib can interfere with BCR signal pathway (including MEK and ERK phosphorylation) and reduction of chemokine secretion (CCL2, CCL3, CCL4, and CCL22) by malignant B cells, which in turn attracts accessory cells, such as T cells, to the effect tissue immune microenvironment.[189] Compared with compounds where fluorine is on the 4-position or fluorine is replaced by chlorine, idelalisib exhibits a better selectivity toward PI3Kδ.[190]

The synthesis of idelalisib was initiated from commercially available 2-fluoro-6-nitrobenzoic acid (**135**) (Scheme 20).[191]

Scheme 20. Synthetic Route to Idelalisib (134)

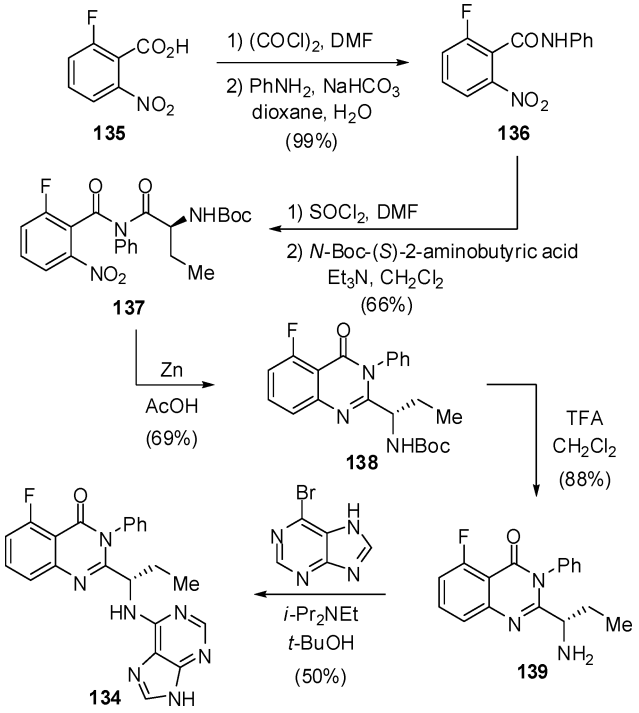

First, reaction of the acid chloride derived from **135** with aniline afforded amide **136**, which was next coupled with *N*-Boc-(*S*)-2-aminobutyric acid to obtain chiral imide **137**. The Zn/AcOH catalytic system promoted the reduction of the nitro group and a subsequent cyclization reaction leading to intermediate **138**. Finally, after removal of the *N*-Boc protecting group, idelalisib (**134**) was successfully prepared by substitution with 6-bromopurine.[192]

2.7. Edivoxetine

Edivoxetine (LY-2216684, **140**) is an oral second-generation, highly selective, and potent norepinephrine reuptake inhibitor (NERI) for the potential treatment of psychiatric indications, including attention deficit hyperactivity disorder (ADHD)[193] and adjunctive therapy of major depressive disorder (MDD) (Figure 15).[194] Edivoxetine was developed by Eli Lilly and Co. and advanced to phase III clinical trials in the above indications.[195] However, in December 2013 edivoxetine failed to meet its primary end point in phase III MDD trials and its development was discontinued, although an ongoing trial assessing the long-term maintenance effect of the drug would continue to completion.

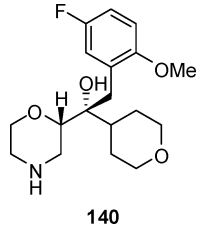

140

Figure 15. Structure of edivoxetine (**140**).

Early compounds in the development of edivoxetine were potent inhibitors of α-methyl-*m*-tyrosine (α-MMT)-induced norepinephrine depletion in vivo, but significant toxicity issues were revealed during a 3-month dog toxicology study. Further optimization around the phenyl group led to edivoxetine with K_i values of 15.6 and 5050 nM against norepinephrine and 5-HT uptake, respectively. In the dog, the oral bioavailability of edivoxetine is 88%, the half-life is 4 h with a good exposure in vivo (AUC = 793 ng·h/mL).[196] In addition, edivoxetine dose-dependently displaced the NET-specific PET ligand in rhesus monkeys. Phase I studies indicate that edivoxetine is safe and well tolerated in healthy volunteers.[197] The absorption of edivoxetine was rapid with an average time to reach maximum plasma concentration (C_{max}) of 2 h. Edivoxetine is extensively metabolized, predominantly via the cytochrome P450 (CYP) enzyme CYP2D6 and CYP3A4. Following a single dose oral administration of edivoxetine, renal or hepatic impairment patients did not appear to influence overall subject tolerability.[198]

Preparation of edivoxetine started from the cyclocondensation between 2-(benzylamino)ethanol (**141**) and 2-chloroacrylonitrile (**142**) in the presence of KO*t*-Bu (Scheme 21). The resulting morpholinocarbonitrile **143** was then converted to

Scheme 21. Synthetic Route to Edivoxetine (140)

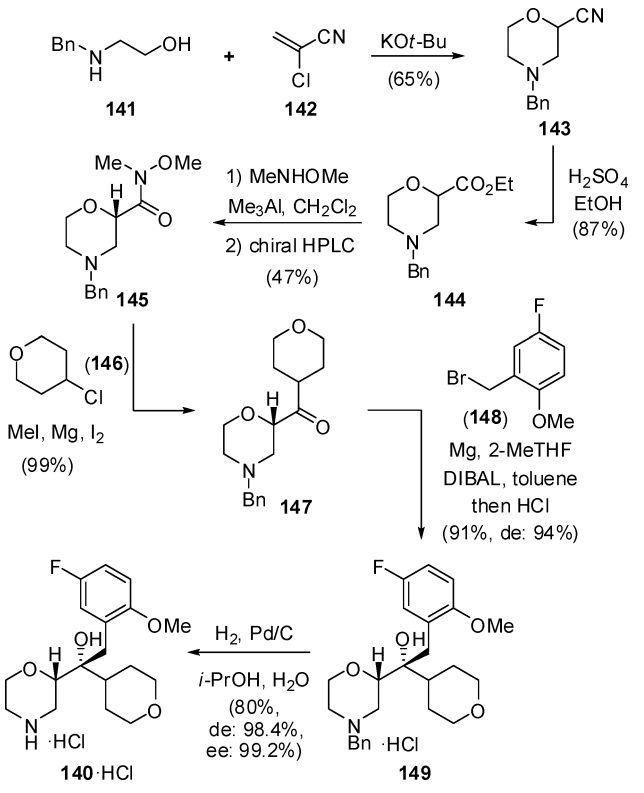

DOI: 10.1021/acs.chemrev.5b00392
Chem. Rev. 2016, 116, 422−518

ester **144** by acidic treatment. Condensation of **144** and *N,O*-dimethylhydroxylamine in the presence of trimethylaluminum led to racemic Weinreb amide *rac*-**145**. This compound was resolved by chiral HPLC to give the desired (*S*)-enantiomer. Reaction of **145** with the Grignard reagent derived from 1-chlorotetrahydropyran (**146**) gave intermediate **147** in good yield. The next reaction with another Grignard reagent, prepared from 2-(bromomethyl)-4-fluoro-1-methoxybenzene (**148**), afforded tertiary alcohol **149**. Finally, N-debenzylation with H_2 over Pd/C gave edivoxetine hydrochloride (**140**·HCl).[199]

2.8. Blonanserin

Blonanserin (AD-5423, **150**) is a relatively selective antagonist of serotonin 5-HT_{2A} and dopamine D_2 receptors, resulting in a novel oral atypical antipsychotic drug (APD) indicated for the treatment of schizophrenia in adults (Figure 16).[200] Blonanserin was developed and launched by Dainippon Sumitomo Pharma and approved in Japan (2008) and Korea (2009).[201] Because of its reasonably selective pharmacological properties, blonanserin displayed the advantages of low risk of excessive sedation, few adverse side effects, and a lower possibility of prompting orthostatic hypotension compared to other atypical APDs.[202] Clinical trials conducted in Japan have indicated that blonanserin is well tolerated and effective in the treatment of both positive and negative symptoms of schizophrenia.[203] Blonanserin can also treat delirium in the intensive care unit.[204] Sales for blonanserin (trade name: Lonasen) stated by Dainippon Sumitomo Pharma for 2012 were $133.8 million, indicating a year to year increase of 9.2% in 2011.

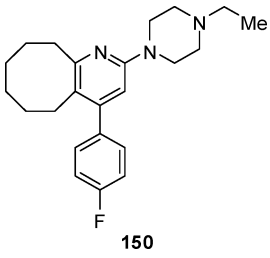

150

Figure 16. Structure of blonanserin (**150**).

Blonanserin is derived from an earlier series of 4-phenyl-2-(1-piperazinyl)pyridines, being selected as the most promising candidate because of its in vitro binding affinity to a variety of potentially important receptors. Relatively high binding affinity for serotonin 5HT_{2A} and dopamine D_2 receptors in rat has been shown, with K_i values of 3.98 and 14.8 nM, respectively.[205] Thus, blonanserin has a binding affinity for the dopamine D_2 receptor that is similar to that of haloperidol (K_i = 8.79 nM), but superior to that of clozapine (K_i = 149 nM), whereas the binding affinity for 5HT_2 receptor is better than that of clozapine (K_i = 8.66 nM) and much greater than that of haloperidol (K_i = 26.8 nM). Blonanserin exhibits a low binding affinity for the adrenergic α_1 receptor and virtually none for the D_1 receptor. Furthermore, the binding affinity for 5-HT_1, 5-HT_3, adrenergic α_2, adrenergic β, histamine H_1, muscarinic, and GABA receptors is low.[206]

The absorption of blonanserin is rapid after oral administration in healthy volunteers, with a time to reach peak plasma concentration of around 1.5 h. It is readily absorbed and its metabolism proceeds through the cytochrome P450 enzyme CYP3A4, being further eliminated mainly by the urine (59%) and feces (30%) as metabolites.[200] Many metabolites of blonanserin were detected and identified in animal pharmacokinetic studies. For instance, all stereoisomers of the two major hydroxyl metabolites of blonanserin in humans, 7-hydroxylated blonanserin (**151**) and 8-hydroxylated blonanserin (**152**), displayed a lower binding affinity to the D_2 and 5HT_{2A} receptors than that of blonanserin itself (Figure 17).[207]

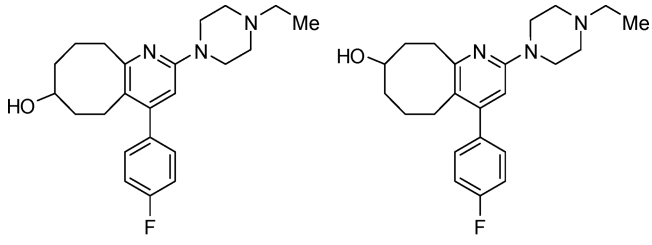

151 152

Figure 17. Structures of the major metabolites of blonanserin, compounds **151** and **152**.

Blonanserin was synthesized in a simple three-step process as shown in Scheme 22. First, 4-fluorobenzoylacetonitrile (**153**) was condensed with cyclooctanone (**154**) by heating in polyphosphoric acid (PPA) to afford compound **155**, which was converted into the corresponding 2-chloro derivative **156** by treatment with phenylphosphonic dichloride. Finally, substitution of **156** with *N*-ethylpiperazine (**157**) afforded the target compound blonanserin (**150**).[207,208]

Scheme 22. Synthetic Route to Blonanserin (150)

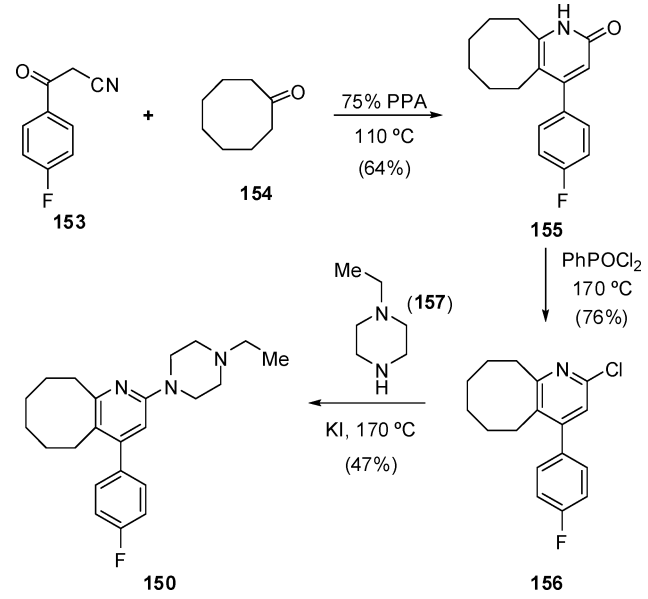

2.9. Vorapaxar

Vorapaxar (SCH 530348, **158**) is an oral platelet thrombin receptor antagonist developed by Schering-Plough (now Merck & Co.) for the treatment of thrombosis (Figure 18).[209,210] After completion of phase III clinical trials for acute coronary syndrome (ACS) and secondary prevention of cardiovascular events, vorapaxar (trade name: Zontivity) received approval by the FDA in May 2014. Generally, oral administration of vorapaxar was well tolerated in clinical trials and did not cause

DOI: 10.1021/acs.chemrev.5b00392
Chem. Rev. 2016, 116, 422−518

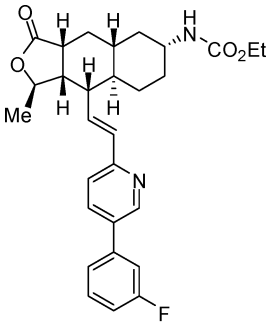

158

Figure 18. Structure of vorapaxar (**158**).

thrombolysis in myocardial infarction (TIMI) bleeding, when combined with aspirin or clopidogrel.[211]

The thrombin receptor, also known as protease-activated receptor-1 (PAR-1), is the most potent cell surface inducer of platelet activation.[212] Vorapaxar is a synthetic tricyclic 3-phenylpyridine analogue of natural product himbacine (**159**) (Scheme 23).[213] SCH 205831 (**160**) and compound **161** were also based on the structure of *ent*-himbacine, being high-affinity, orally active, low-molecular-weight non-peptide competitive PAR-1 antagonists, with excellent oral efficacy in an ex vivo platelet aggregation model in cynomolgus monkeys.[214,215] However, compound **161** generated a metabolite **162**, which is a 7,8-dihydroxy derivative. A series of novel himbacine derivatives **163** was next developed in order to change the metabolic pathway of compound **161**, by incorporating heteroatoms into the C-ring of the tricyclic motif.[216] Finally, the introduction of a fluorine atom in the phenyl ring increased the potency leading to the discovery of vorapaxar (**158**).[217]

Vorapaxar is a highly selective, virtually irreversible PAR-1 antagonist, displaying an oral antiplatelet effect in a cynomolgus monkey model of agonist-induced ex vivo platelet aggregation, after oral administration at 0.1 mg/kg, and complete inhibition (100%) of platelet aggregation for 24 h. Vorapaxar was selective against PAR-2 and PAR-4 showing an excellent pharmacokinetic profile, with a half-life of 6.2 h, and an oral bioavailability of 62% in the cynomolgus monkey model. The crystal structure of human PAR-1 in complex with vorapaxar has been reported. Vorapaxar binds to the extracellular surface of PAR-1 through the fluorophenyl ring that $\pi-\pi$ stacks with the side chain of Phe-271, and the pyridine also makes a hydrogen bond with the side chain of Tyr-337.[218]

The synthetic route to vorapaxar is illustrated in Scheme 24. Bromoalkene **164** was subjected to a Heck reaction with methyl acrylate to give the corresponding acid **165** after ethyl ester hydrolysis. Condensation of dienoic acid **165** and chiral allylic alcohol **166** in the presence of *N*,*N*′-dicyclohexylcarbodiimide (DCC) and 4-pyrrolidinopyridine (PPY) afforded triene **167**, which underwent a fully diastereoselective intramolecular Diels–Alder cycloaddition followed by base-mediated epimerization of the α-carbonyl proton to afford tricyclic lactone **168** containing four newly created stereogenic centers. Two consecutive hydrogenations in compound **168** reduced the double bond and removed the benzyl ester moiety, and the resulting acid **169** was transformed into aldehyde **170** by reduction of the corresponding acid chloride with *n*-Bu_3SnH under palladium catalysis. Next, Horner–Wadsworth–Emmons olefination with pyridyl phosphonate **171** produced (*E*)-alkene **172**. Triflate **173** was easily accessed from **172** and was used in

Scheme 23. Discovery of Vorapaxar (158)

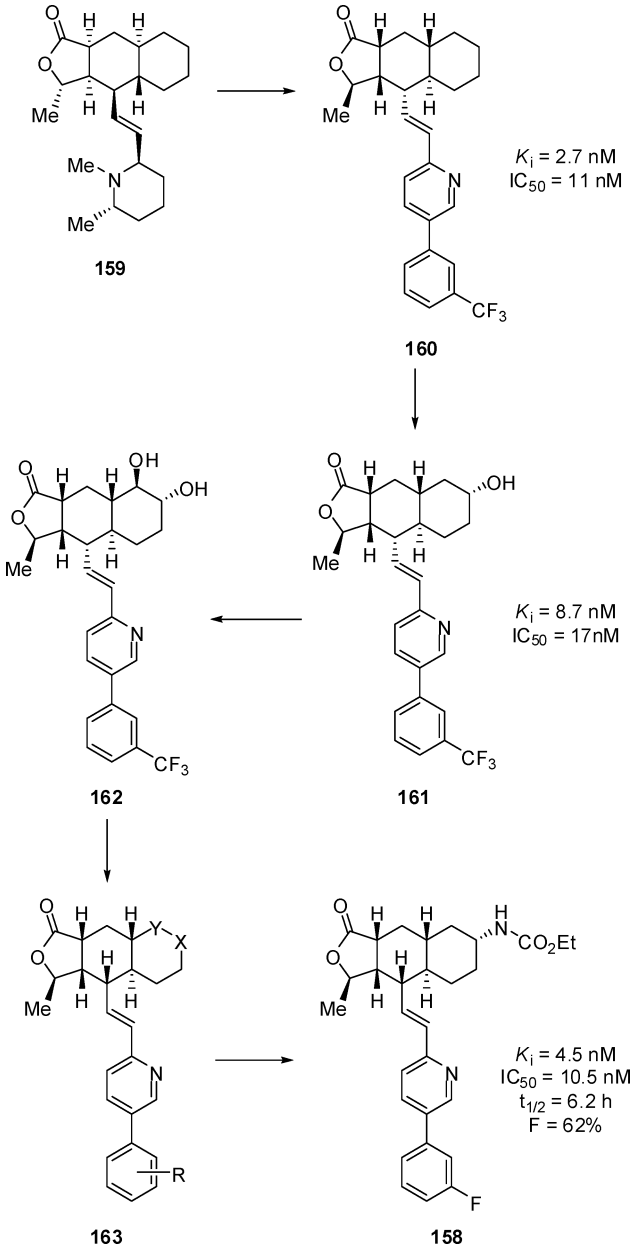

the subsequent Suzuki cross-coupling with 3-fluorophenylboronic acid (**174**) to furnish intermediate **175**. Removal of the cyclic acetal in **175** led to ketone **176**, and its further reaction with ammonia followed by reduction with $NaBH_3CN$ produced a mixture of diastereomeric primary amines albeit in low yield. After chromatographic separation, the major amine **177** was finally transformed into vorapaxar (**158**) by reaction with ethyl chloroformate.[215,217]

2.10. Tedizolid Phosphate

In June 2014, the FDA approved tedizolid phosphate (trade name: Sivextro, **178**), the prodrug of tedizolid, for both intravenous and oral treatment of acute bacterial skin and skin structure infections (ABSSSI) caused by certain susceptible bacteria, such as *Staphylococcus aureus* (including methicillin-resistant strains (MRSA) and methicillin-susceptible strains), various *Streptococcus* species, and *Enterococcus faecalis* (Figure 19). Tedizolid (also known as torezolid) is a second-generation

DOI: 10.1021/acs.chemrev.5b00392
Chem. Rev. 2016, 116, 422–518

Scheme 24. Synthetic Route to Vorapaxar (158)

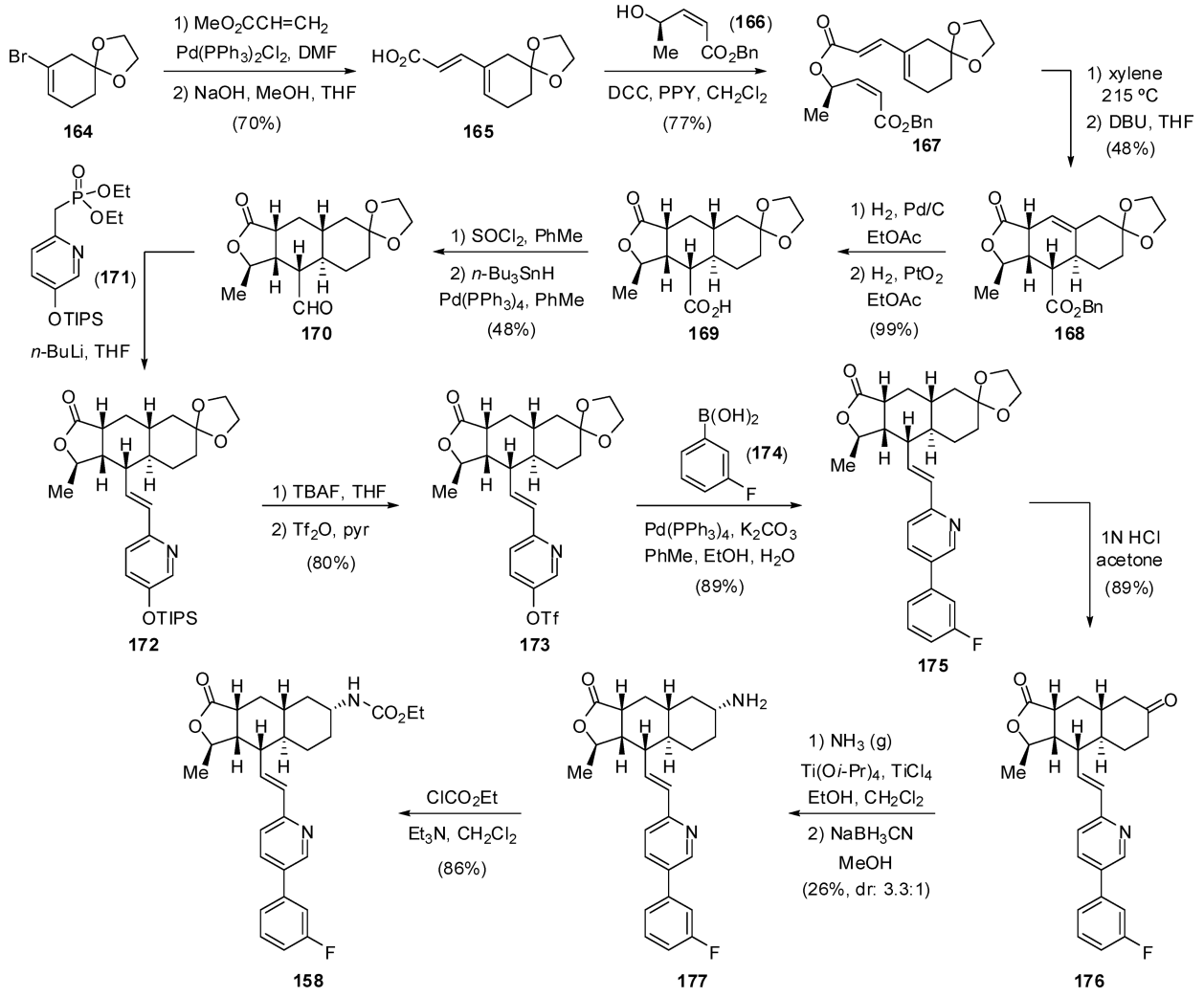

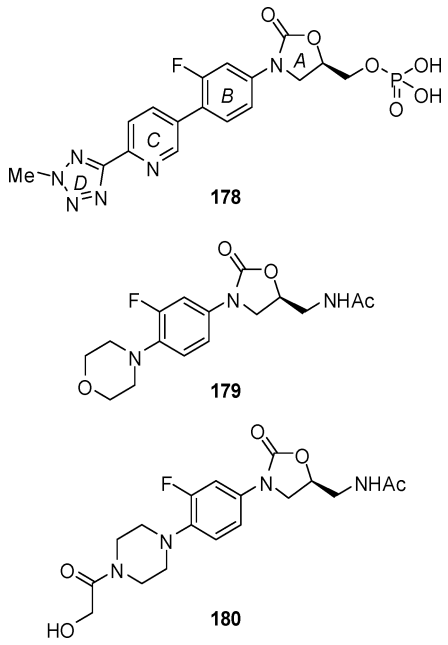

Figure 19. Structures of tedizolid phosphate (**178**), linezolid (**179**), and eperezolid (**180**).

oxazolidinone antibiotic developed by Cubist Pharmaceuticals (following acquisition of Trius Therapeutics) and Dong-A Pharmaceutical, in partnertship with Bayer. Similar to linezolid (**179**), the first oxazolidinone launched in 2000, tedizolid inhibits the formation of the 70S initiation complex by binding the 50S subunit of ribosome at a site close to the 30S subunit, therefore blocking the early step of protein synthesis. This unique mechanism makes it difficult to develop cross-resistance with other classes of antibiotics.[219]

Structurally, the drug follows the typical A−B ring system of previous oxazolidinone derivatives like linezolid (**179**) and eperezolid (**180**). This 3-fluorophenyloxazolidinone backbone was initially identified by Upjohn Co. since eperezolid was found as the best lead compound to balance the antibacterial activity, pharmacokinetics, aqueous solubility, and synthetic convenience compared to its nonfluorinated and 3,5-difluorophenyl congeners.[220,221] Replacement of the morpholino group of linezolid by a methyl tetrazole substituted pyridine conferred superior activities against several antibiotic resistant strains, which may be attributed to the additional interactions of the tetrazole and the pyridine with the binding pocket. Besides, the activity varied with the substituted forms of the tetrazole and the position of the methyl group.[222] According to SAR studies on the 5-position of the oxazolidinone, the 5-hydroxymethyl derivative (tedizolid) was chosen as a candidate

DOI: 10.1021/acs.chemrev.5b00392
Chem. Rev. 2016, 116, 422−518

Scheme 25. Synthetic Route to Tedizolid Phosphate (178)

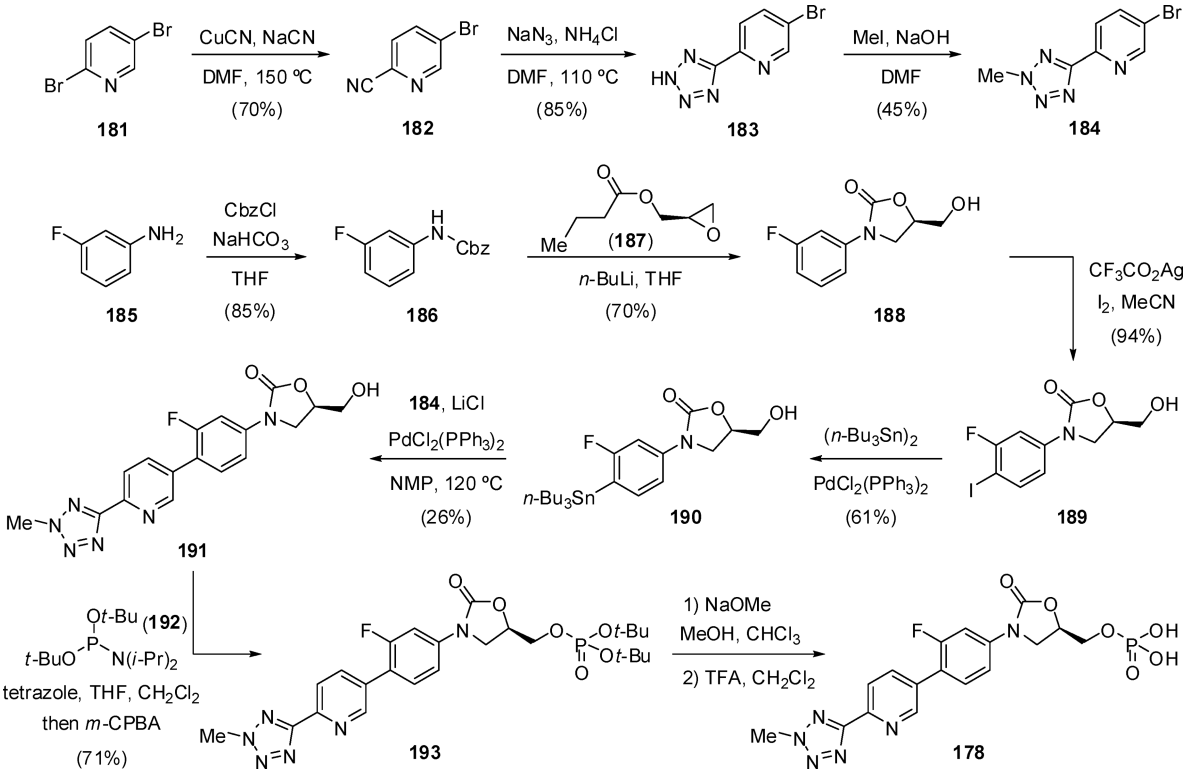

for its higher potency, longer half-life, activity against linezolid-resistant strains, and low risk of causing new resistance. A prodrug strategy was also utilized and led to tedizolid phosphate (**178**) with promising aqueous solubility (>50 mg/mL in deionized H_2O), pharmacokinetic properties (oral bioavailability: F > 90%), and improved in vivo efficacy compared to linezolid.[223]

The first convergent route to tedizolid phosphate used 2,5-dibromopyridine (**181**) and 3-fluoroaniline (**185**) as starting materials (Scheme 25). Pyridine **181** reacted with CuCN and NaCN in refluxing DMF to afford **182**, which upon cycloaddition with sodium azide under high temperature provided tetrazole **183**. Methylation of **183** with iodomethane following isolation with silica-gel column chromatography gave the desired 2-methyltetrazolylpyridine **184**, as well as its 1-methyl regioisomer in almost equimolecular amount. Conversely, Cbz-protected fluoroaniline **186** was directly converted into 5-hydroxymethyl oxazolidinone **188** by reacting with (*R*)-glycidyl butyrate (**187**) and *n*-BuLi. Iodination of **188** followed by palladium-catalyzed reaction with hexabutylditin afforded the tributylstannyl derivative **190**. Then, the two intermediates, **184** and **190**, were cross-coupled via a Stille reaction that gave tedizolid (**191**). Reaction of alcohol **191** with phosphamidite **192** in the presence of tetrazole followed by oxidation with *m*-CPBA furnished phosphoric acid di-*tert*-butyl ester derivative **193**, and final treatment with NaOMe generated the desired compound tedizolid phosphate (**178**).[223,224]

To avoid the toxicity of residues from tin-based couplings, Trius Therapeutics disclosed another process in which the pyridinyl phenyl moiety was synthesized through a Suzuki coupling. Starting from 4-bromo-3-fluoroaniline (**194**), Cbz-protected aniline **195** was thus prepared (Scheme 26). Reaction of **195** with triisopropyl borate and *n*-BuLi and subsequent hydrolysis with 20% aqueous NH_4Cl gave boronic acid **196**.

Scheme 26. Process Preparation of Tedizolid Phosphate (178)

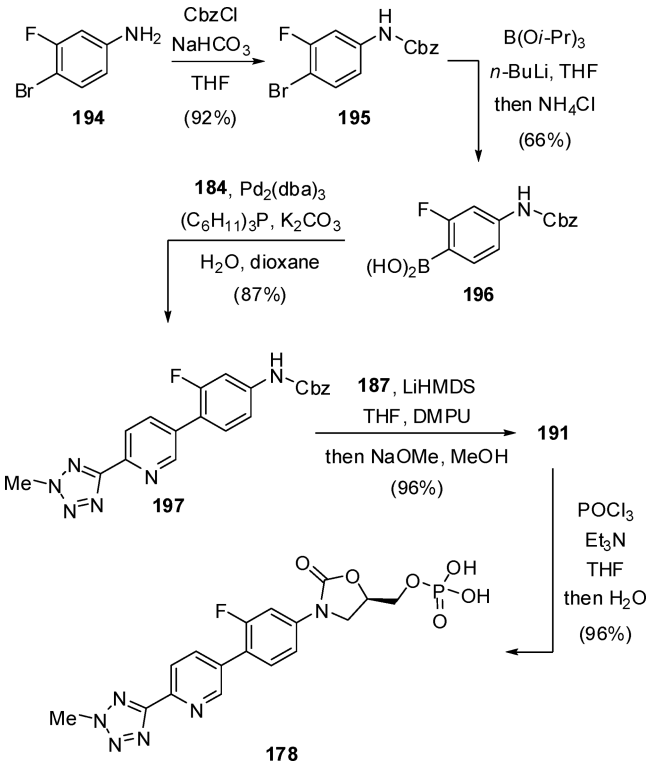

Accordingly, Suzuki coupling between **196** and **184** provided intermediate **197**. The oxazolidinone ring was then constructed by using LHMDS and DMPU in the reaction of **197** with chiral glycidyl ester **187** to give tedizolid (**191**) in good yield. Finally,

DOI: 10.1021/acs.chemrev.5b00392
Chem. Rev. 2016, 116, 422−518

treatment of **191** with Et_3N and $POCl_3$ in THF and quenching with water furnished phosphate **178**.[225]

A cheap and convenient route to prepare fluorine-containing aniline **185** from *m*-aminoacetanilide hydrochloride (**198**) was described through diazotization followed by fluorination and hydrolysis (Scheme 27).[226] In addition, substrate **194** can be obtained in over 95% yield by bromination of **185** with NBS in DMF.[227]

Scheme 27. Preparation of Fluorine-Containing Anilines 185 and 194

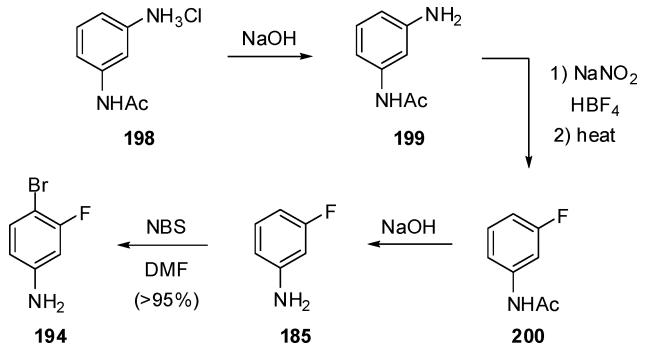

2.11. Zabofloxacin

Dong Wha Pharmaceuticals, together with IASO Pharma (formerly Pacific Beach BioSciences), developed zabofloxacin (DW-224a, **201**), an oral antibacterial fluoronaphthyridone DNA gyrase and topoisomerase IV inhibitor, for the potential treatment of bacterial respiratory tract infections (Figure 20).[228] The drug has entered a phase III trial for the treatment

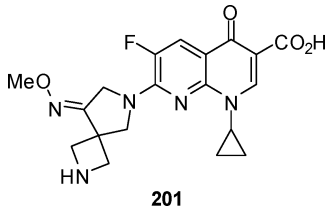

201

Figure 20. Structure of zabofloxacin (**201**).

of acute bacterial exacerbation of chronic obstructive pulmonary disease (COPD) in South Korea and a phase II trial for pneumonia in the United States.

As a new member of fluoroquinolone antibiotics, zabofloxacin is also a typical fluorine-containing drug. Since the C-6 fluorine is quite crucial for both high DNA gyrase complex binding activity and great bacterial cell penetration of this class of antibiotics, nearly all of the newly invented quinolones keep this C-6 fluorine substituent in place.[229,230] To meet the needs for compounds with enhanced activities against Gram-positive bacteria and quinolone-resistant strains, researchers introduced a novel 2,6-diazaspiro[3.4]octane (with an alkoxyimino group on it) to the 7-position of a traditional naphthyridine scaffold and discovered the unique structure of zabofloxacin (**201**),[231] which displays a higher antibiotic potency, wider spectrum, better safety, and limited adverse events than the marketed drugs of the same class.[232,233]

Scheme 28 shows an available synthetic route to zabofloxacin. Pyrrolidinone **202** was hydroxymethylated with formaldehyde to afford alcohol **203**, which reacted with *O*-methylhydroxylamine to give the corresponding oxime **204**. Then, alcohol protection and ester reduction yielded the hydroxymethyl derivative **206**, which was treated with NaN_3 to afford azide **207**. The reaction of **207** with MsCl provided mesylate **208**, which upon reduction with hydrogen and Raney nickel gave amine **209**. The subsequent annulation occurred in the presence of DBU and gave the 2,6-diazaspiro[3.4]octane derivative **210**. Protection with Boc_2O and selective hydrogenolysis over Pd/C furnished the monoprotected diamine **212**, which condensed with naphthyridinone **213** to give **214** in good yield. Finally, the target molecule zabofloxazin (**201**) was obtained by deprotection of **214** with TFA.[231]

A four-step, one-pot reaction using a single solvent was disclosed for preparation of the fluorine-containing intermediate **213** (Scheme 29). Starting from ethyl 3-(2,6-dichloro-5-fluoropyridin-3-yl)-3-oxo-propanoate (**215**),[234] reaction with triethyl orthoformate and acetic acid in toluene afforded derivative **216**, which was then condensed with cyclopropylamine. The resulting enamine **217** was cyclized using 40% aqueous tetrabutylammonium hydroxide and 10 N NaOH to give **218**, followed by hydrolysis with concentrated HCl to afford intermediate **213** in high purity and excellent overall yield after simple washings of the collected solid compound.[235]

2.12. Solithromycin

Solithromycin (CEM-101, OP-1068, **219**) developed by Cempra Pharmaceuticals (under license from Optimer Pharmaceuticals) is the first fluoroketolide antibiotic that has progressed to phase III clinical trials as oral and intravenous formulation for the treatment of moderate to moderately severe community-acquired bacterial pneumonia (CABP) (Figure 21).[236] The drug blocks protein synthesis and thus prevents bacterial growth and reproduction by reversibly binding to the 50S subunit of the bacterial ribosome. Solithromycin has proven activity against macrolide-resistant strains, because it binds to three regions on the bacterial ribosome, unlike one or two sites for current macrolides.[237]

Traditional macrolides, such as erythromycin (**220**), are characterized by a 14-atom macrolactone ring containing two sugar moieties, namely cladinose and desosamine at the C-3 and C-5 positions, respectively. Efforts to overcome macrolide resistances led to the discovery of ketolides, which have a C-3 keto group and a C-11,12 alkyl-aryl side chain, being the marketed drug telithromycin (**221**) a representative example.[238] To optimize domain II binding and antibacterial activity, a series of ketolides possessing a 1,2,3-triazole were designed, and solithromycin (**219**), also featuring a C-2 fluorine substituent and an aminophenyl-1,2,3-triazolylbutyl-11,12-carbamate side chain, entered further development.[239] The structure of solithromycin complexed to the *E. coli* ribosome revealed the proximity (2.7 Å) of the C-2 fluorine to the N-1 of C2611, which may lead to a tighter binding of the compound to ribosome in which A2058 has been dimethylated by Erm methyltransferase. Compared with its nonfluorinated analogue, solithromycin exerts superior inhibition against growth of streptococci carrying the Erm methyltransferase gene, which is thought to be the main cause of macrolide resistance.[237]

The initial route to solithromycin adopted the antibiotic clarithromycin (**222**) as starting material (Scheme 30). Reaction of **222** with Ac_2O provided the corresponding diacetyl derivative which was treated with 1,1-carbonyldiimidazole (CDI) and NaH to give intermediate **223**. Cyclization of **223** with 4-aminobutanol produced alcohol **224**, which

DOI: 10.1021/acs.chemrev.5b00392
Chem. Rev. 2016, 116, 422−518

Scheme 28. Synthetic Route to Zabofloxacin (201)

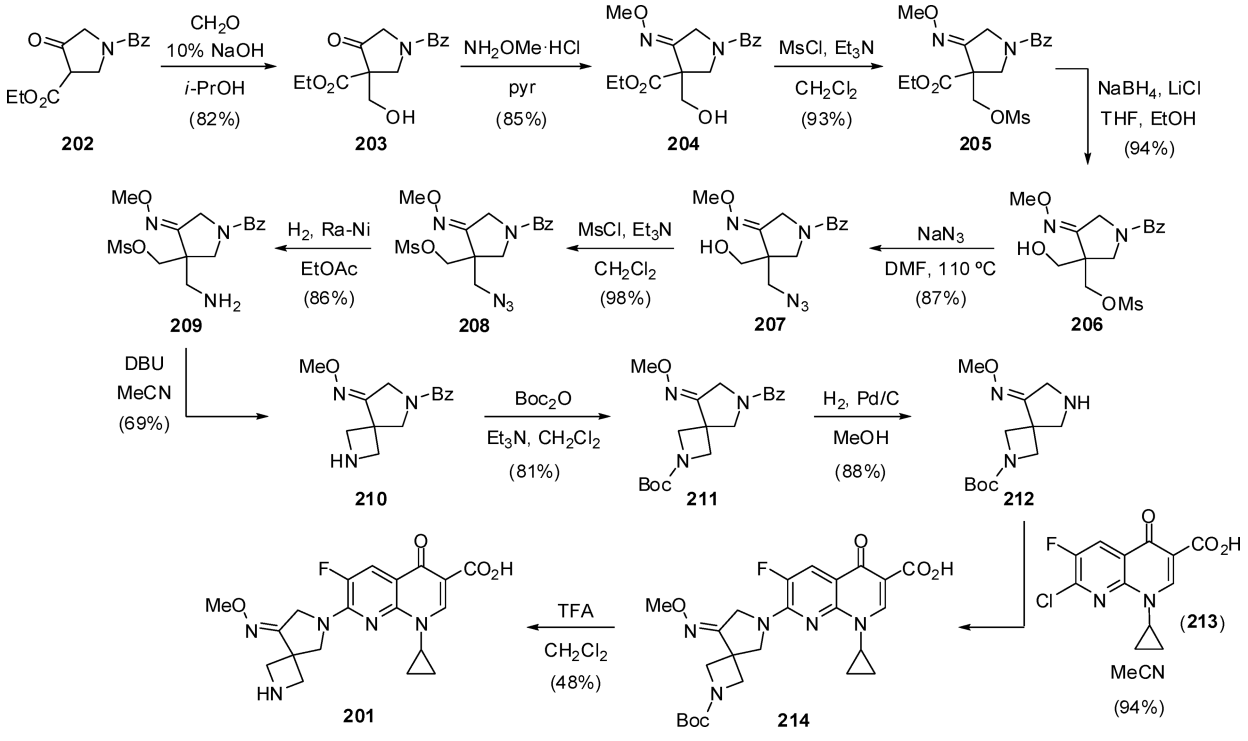

Scheme 29. Synthesis of Naphthyridinone 213

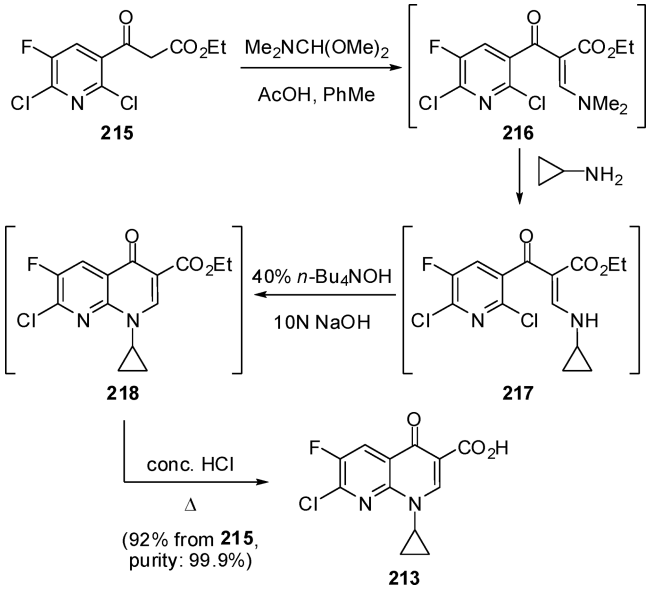

underwent tosylation with TsCl and further substitution with NaN_3 to produce azide **225**. After hydrolysis of the cladinose fragment, the resulting alcohol was converted into ketone **226** by Swern oxidation. Then, regioselective electrophilic fluorination was performed with Selectfluor (**23**) in the presence of KO*t*-Bu. After deacetylation to fluoro-azide derivative **227**, the target compound solithromycin (**219**) was finally accessed via a copper-catalyzed azide−alkyne cycloaddition with 3-ethynylaniline (**228**).[239,240]

An improved synthetic process involved the protection of **222** with benzoic anhydride, and the subsequent reaction with CDI and DBU to afford **229** (Scheme 31). Cyclization with 4-azidobutylamine (**230**) [obtained in turn from 1,4-dibromobutane (**234**) by substitution with NaN_3 and Staudinger reduction[128,241,242] with PPh_3] gave 11,12-cyclic carbamate **231**. Acidic hydrolysis of **231** was followed by oxidation of the C-3 hydroxyl group with Dess−Martin periodinane (DMP) to yield ketone **232**. Fluorination at the C-2 position was accomplished using NFSI (**22**) and KO*t*-Bu to afford fluoro-azide **233**. Cycloaddition between **228** and **233** in the presence of CuI followed by deprotection in refluxing MeOH provided solithromycin (**219**).[243,244]

2.13. Sofosbuvir

Hepatitis C is an infectious disease of the liver which is estimated to affect 130−150 million people worldwide.[245] Infection by hepatitis C virus (HCV) is the most common chronic blood-borne infection in the United States, where approximately 2.7 million persons are chronically infected and 8000−10000 annual deaths are attributed to HCV infection.[246] Furthermore, chronic infection by HCV greatly increases the risk of hepatic carcinoma. The current standard treatment for hepatitis C is pegylated interferon combined with ribavirin.[247] However, the viral response rate of this treatment is assessed in only less than 50% of the patients infected with the genotype 1 virus.[248] Over the past decade, ribonucleoside analogues containing a 2′-*C*-methyl substituent were identified as potent and selective inhibitors of NS5B polymerase of the HCV replication complex.[249] For instance, 2′-deoxy-2′-fluoro-2′-*C*-methylcytidine (PSI-6130, **236**) was initially selected for clinical development based on its superior profile,[250] and currently its diisobutyroyl prodrug mericitabine (RG7128, **237**) is in phase IIb clinical trials for hepatitis C in Hoffmann La Roche (Figure 22).[251] A similar investigational, nonfluorinated molecule is valopicitabine (NM283, **238**).[252]

Scientists at Pharmasset were further interested in developing a second generation of agents with improved potency and pharmacokinetic properties. Metabolism studies showed that PSI-6130 (**236**), as well as its monophosphate **240**, could be

DOI: 10.1021/acs.chemrev.5b00392
Chem. Rev. 2016, 116, 422−518

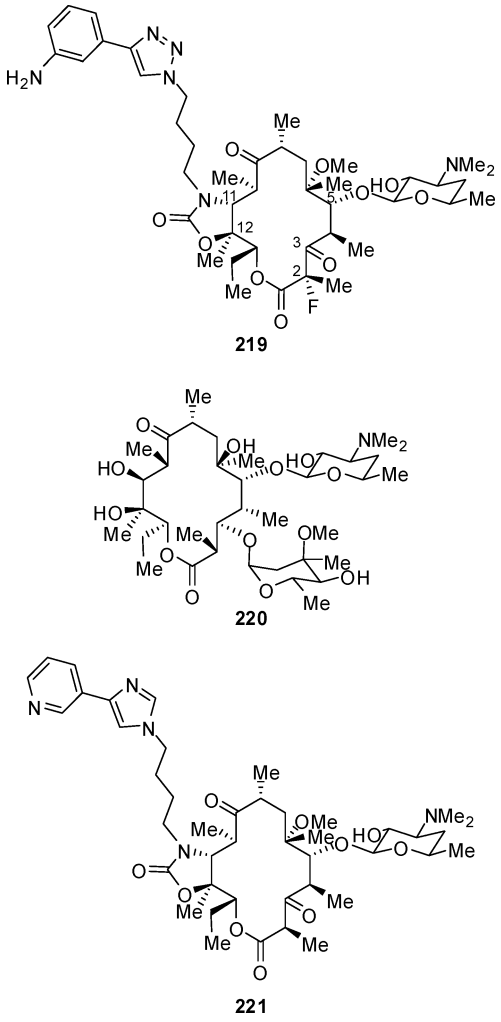

Figure 21. Structures of solithromycin (**219**), erythromycin (**220**), and telithromycin (**221**).

deaminated to the uridine derivatives **241** and **242**, respectively, and the latter subsequently anabolized to the triphosphate **243** by uridine−cytidine monophosphate kinase (YMPK) and nucleoside diphosphate kinase (NDPK) (Scheme 32).[253] This uridine triphosphate **243** displayed a long intracellular half-life. However, earlier studies had shown that compound **241** was inactive in the HCV replicon assay indicating the lack of deoxyuridine kinase activity.[254] Therefore, in order to accomplish the delivery of high liver concentrations of the desired triphosphate **243**, many prodrugs of the monophosphate **242** were examined.

In this context, the phosphoramidate prodrugs enhanced the potency of the nucleoside in vivo, because of an increase of the intracellular concentration of the active compound.[255] This type of prodrug provided suitable pharmacokinetic properties for in vivo absorption and liver targeting characteristics. Once in the liver, the phosphoramidate was metabolized to the monophosphate nucleotide through a cascade of steps starting with the cleavage of the amino acid ester by esterases. After a screening of suitable phosphoramidate derivatives, sofosbuvir (PSI-7977, **239**) was selected as a second generation nucleoside inhibitor of HCV NS5B RNA-dependent RNA polymerase.[253] Sofosbuvir (trade name: Sovaldi) was discovered by Pharmasset and developed by Gilead Sciences in the United States, being approved by the FDA on December 2013 and by the European Commission on January 2014.[256] Sofosbuvir is also used as a combination therapy with ledipasvir, an NS5A inhibitor, which also has potency against HCV genotypes 1a and 1b (see section 3.4).

Synthetic approaches to sofosbuvir were based on the prior preparation of PSI-6130 (**236**). One of the key issues for its synthesis was the stereoselective functionalization of the C-2′ position in order to generate a tetrasubstituted center having 2′-*C*-methyl and 2′-fluoro substituents. The discovery synthesis of **236** was rather straightforward using cytidine (**244**) as starting material (Scheme 33). Cytidine was first transformed into its 2′-*C*-methyl arabinoside analogue **248** in six conventional steps. Then, fluorination of the C-2′ tertiary alcohol in **248** with DAST (**20**) gave the desired product **249** with inversion of the configuration. However, the yield of **249** was very low due to the accompanying formation of byproducts (**250** and **251**) by elimination and hydrolysis, and the need of chromatographic separation of this mixture represented an additional problem for the scale-up of this protocol. PSI-6130 (**236**) was finally accessed by removal of the benzoyl protecting groups in **249**.[250]

Thus, an alternative synthesis of the benzoylated cytidine precursor **249** from inexpensive D-xylose was developed. The intermediate methyl furanoside **252**, obtained from D-xylose according to literature methods,[257] was oxidized with NaOCl/TEMPO to the ketone **253** followed by stereoselective methylation to give the desired 3,5-di-*O*-benzyl-2-*C*-methyl-β-D-arabinofuranoside (**254**) (Scheme 34). Fluorination was again carried out using DAST (**20**) to give the desired fluorinated product **255** albeit in only 19% yield after purification by silica gel chromatography. The benzyl groups were replaced with benzoyl groups by transfer hydrogenolysis followed by treatment with benzoyl chloride to afford **257** in good yield. Furanoside **257** was then converted into the key intermediate **259** via cleavage of the methyl furanoside moiety and subsequent benzoylation. Vorbrüggen condensation with silylated N^4-benzoylcytosine **260** in the presence of $SnCl_4$ afforded the desired product **249** along with its α-anomer 2-*epi*-**249**. The pure β-anomer **249** was obtained by silica gel chromatography in 37% yield from the crude mixture.[258]

Another synthesis of the sugar moiety of sofosbuvir was disclosed starting from the protected derivative of D-erythronolactone **261** (Scheme 35). Compound **261** was converted into 3,4-*O*-isopropylidene-2-*C*-methyl-D-arabino-1,5-lactone (**262**) by successive addition of MeMgBr and NaCN, followed by hydrolysis and in situ lactonization. Next, the corresponding triflate **263** was reacted with tris(dimethylamino)sulfur trimethylsilyl difluoride (TASF) to carry out fluoride displacement, and further, acetonide deprotection, and in situ lactone rearrangement led to 2-deoxy-2-fluoro-2-*C*-methyl-D-1,4-ribonolactone (**265**) as the major product. Treatment of **265** with benzoyl chloride afforded the key intermediate **267**.[259]

More recently, a more practical synthesis of PSI-6130 (**236**) was reported using commercially available isopropylidene-D-glyceraldehyde (**268**) as starting material (Scheme 36). Wittig reaction of **268** with commercially available (carbethoxyethylidene)triphenylmethylphosphorane proceeded with high *E*/*Z* selectivity (97:3 ratio). The intermediate pentenoate ester was used for the next dihydroxylation step without purification to afford diol **269** as a pure D-isomer after aqueous workup and recrystallization, thus avoiding chromatographic techniques. Sharpless AD-mix-β efficiently catalyzed

DOI: 10.1021/acs.chemrev.5b00392
Chem. Rev. 2016, 116, 422−518

Scheme 30. Synthetic Route to Solithromycin (219)

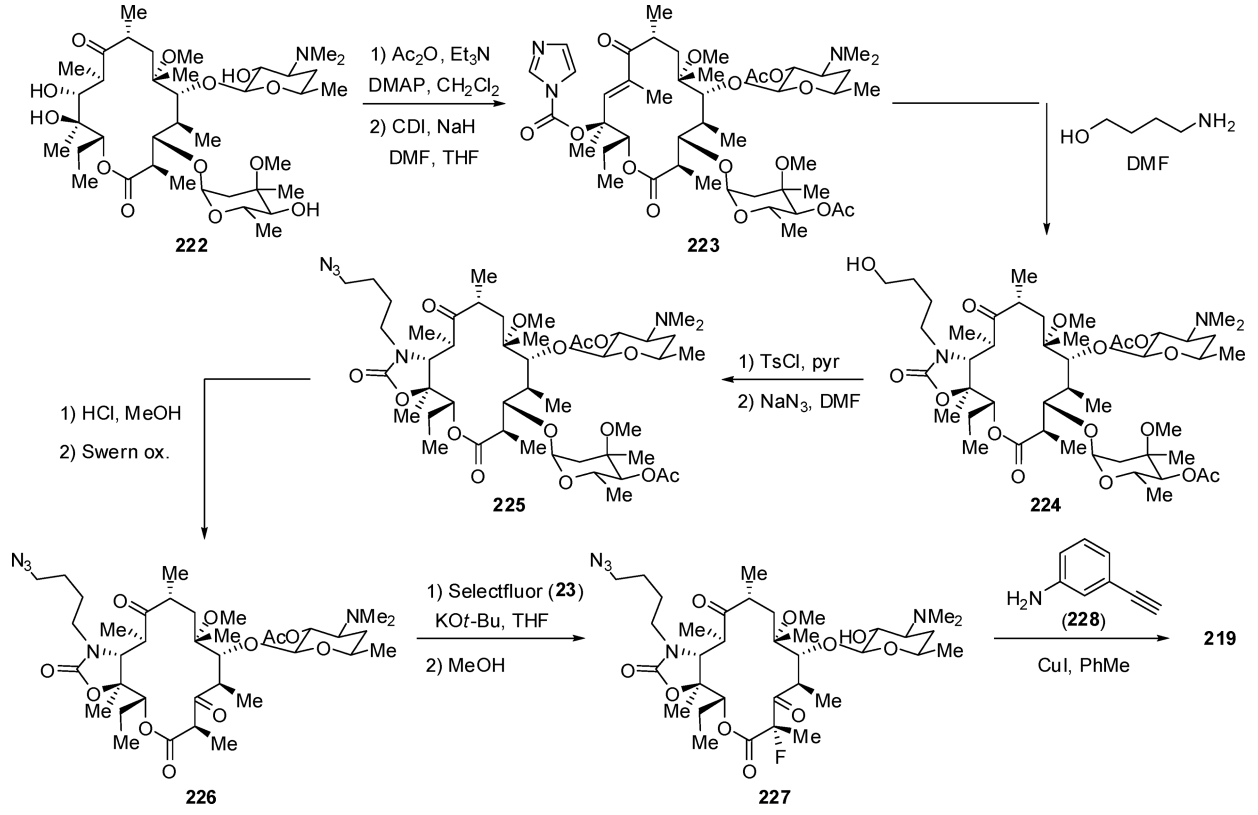

Scheme 31. Improved Process for the Synthesis of Solithromycin (219)

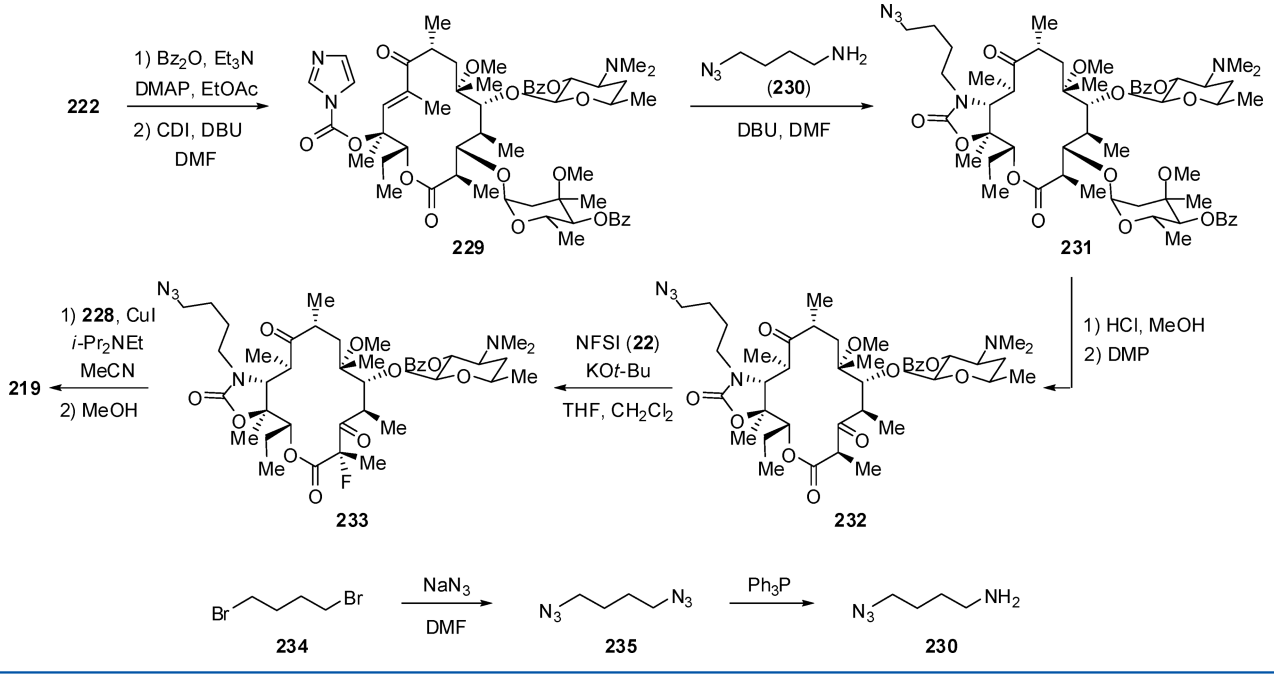

this dihydroxylation in good yield and stereoselectivity, but the most practical conditions, found after extensive studies, involved the much cheaper $KMnO_4$ reagent. The secondary C-3 hydroxyl group of diol **269** could be selectively benzoylated, thus allowing for a selective fluorination of the C-2 tertiary alcohol with DAST (**20**); however, the yield of the fluorination step dropped dramatically when the process was scaled up, and concurrently this approach required multiple chromatographic separations. Cyclic sulfates derived from 2,3-dihydroxyesters experienced the ring opening by substitution at the C-2 position with high selectivity.[260] As a result, an alternative approach involved cyclic sulfate **270**, which was prepared from **269** using a two-step process, namely cyclic sulfite formation with $SOCl_2$ and then oxidization to the cyclic sulfate with catalytic TEMPO and NaOCl. Although **270** could be directly prepared from diol **269** with SO_2Cl_2, the former

DOI: 10.1021/acs.chemrev.5b00392
Chem. Rev. 2016, 116, 422−518

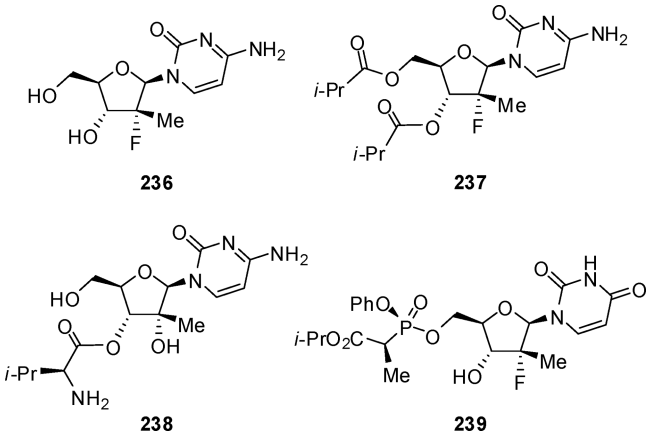

Figure 22. Structures of 2′-*C*-methyl nucleoside analogues **236**–**238** and sofosbuvir (**239**).

Scheme 32. Metabolism of 236 to Both the Active Triphosphate 243 and the Inactive Nucleoside 241

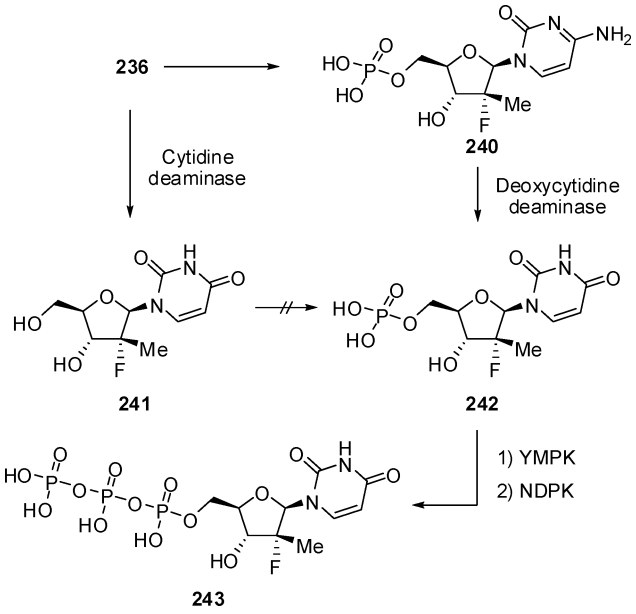

method gave higher and more reproducible yields. After an aqueous workup, **270** could be used without further purification. Then, a number of nucleophilic fluorinating reagents and conditions were examined, and tetraethylammonium fluoride hydrate was selected as the reagent of choice, since no regioisomer resulting from fluorination at the C-3 position could be observed. The reaction mixture was used directly in the next step, and hence hydrolysis of the sulfate followed by lactonization afforded compound **271**, which was next benzoylated to give the key intermediate **267**. Reduction of the lactone ring in **267** with lithium aluminum tri-*tert*-butoxy hydride gave a mixture of anomeric lactols (2:1 ratio), and for the subsequent coupling with cytosine reagent **260**, the derived acetate **272** was best employed leading to intermediate **249** as a 4:1 ratio of β/α anomers. After workup, the pure β-anomer crystallized from a methanol solution. As mentioned before, the final deprotection of **249** to PSI-6130 (**236**) was carried out by treatment with methanolic ammonia.[261]

The initial synthesis of sofosbuvir was accomplished from **249** (the precursor of **236**) by preparing first the uridine derivative **273** followed by removal of the benzoyl protecting groups using an ammonolysis reaction (Scheme 37). The resulting compound **274** was next reacted with the chlorophosphoramidate **275** (prepared from alanine isopropyl ester and phosphorodichloridate) to afford a 1:1 mixture of the diastereomers of sofosbuvir at the phosphorus atom. The active isomer of sofosbuvir has (S_P) configuration, and was isolated by sequential crystallization (CH_2Cl_2/*i*-Pr_2O, CH_2Cl_2) from the diastereomeric mixture.[253]

However, the above crystallization approach was not efficient for the industrial production of sofosbuvir, because half of the advanced intermediate **274** was consumed in the last step of the synthesis, when preparing a diastereomeric mixture. Therefore, an effort to develop a more convergent diastereoselective synthesis of sofosbuvir was undertaken through the intermediacy of a diastereomerically pure phosphoramidate reagent. Thus, a stable phosphoramidate sufficiently reactive to allow ester bond formation with a nucleophilic 5′-OH group was required, while maintaining intact the desired phenolic phosphate ester. Eventually, pentafluorophenyl phosphoramidating reagent **277** was found to be suitable for the synthesis of sofosbuvir (Scheme 38). The optically pure reagent **277** was readily prepared by reacting phenyl dichlorophosphate and (*S*)-alanine isopropyl ester (**276**) in the presence of triethylamine, followed by addition of pentafluorophenol to give a mixture of diastereomers. Crystallization of the mixture from EtOAc/hexane led to the isolation of the (S_P) isomer with a diastereomeric excess greater than 98.0%. A multigram synthesis of sofosbuvir was then carried out by addition of *t*-BuMgCl to uridine **274** followed by reagent **277**. Aqueous workup followed by two crystallizations afforded sofosbuvir (**239**) as a 99.8% pure crystalline material with a diastereomeric excess of 99.7%.[262]

2.14. Clevudine

Clevudine or 2′-fluoro-5-methyl-β-L-arabinofuranosyluracil (L-FMAU, **278**) is an antiviral drug with an inhibitory effect on DNA polymerase for the treatment of chronic hepatitis B (Figure 23).[263] It was approved in South Korea and Philippines, and marketed by Bukwang Pharmaceuticals in South Korea and by HI-Eisai in Philippines under the trade names Levovir and Revovir, respectively. The approval in South Korea was revoked due to considerable resistance and some myopathy cases in patients.[264,265] However, the Korean FDA scrutinized all of the safety data including muscle-related symptoms and then decided that clevudine could be marketed, because its associated myopathy is not life-threatening and is reversible, when the patient is taken off the drug.[266]

As with other nucleoside reverse transcriptase inhibitors (NRTIs), clevudine, as a triphosphate, directly inhibits DNA synthesis of hepatitis B virus (HBV).[267] It is noteworthy that, in contrast to many other known nucleoside analogues, clevudine is not considered a chain terminator due to the presence of the 3′-OH group, and the inhibition of viral polymerase activity is likely attained without being incorporated into viral DNA.[268] Furthermore, clevudine is not incorporated into DNA by the Epstein–Barr virus or cellular DNA polymerases, indicating it does not serve as a substrate for DNA synthesis by the polymerases.[269,270] Since clevudine inhibits HBV replication through a fundamentally different mechanism from that of other nucleoside analogues, a synergistic inhibitory effect was observed when combined with other NRTIs.[271] Recently, the

DOI: 10.1021/acs.chemrev.5b00392
Chem. Rev. 2016, 116, 422–518

Scheme 33. Initial Synthesis of PSI-6130 (236)

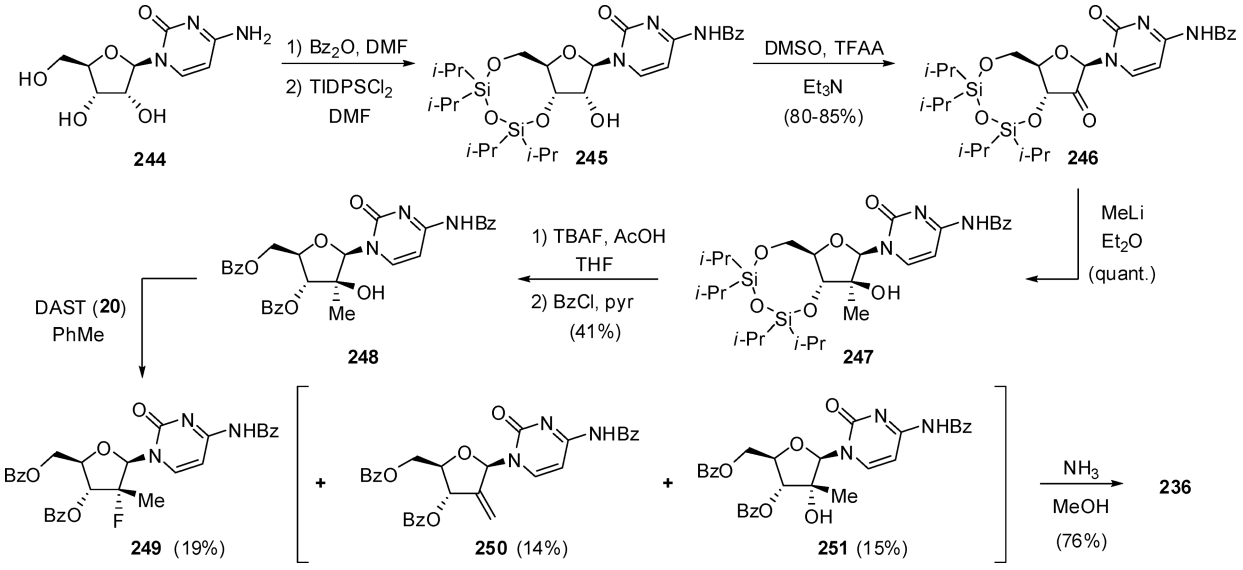

Scheme 34. Alternative Synthesis of Intermediate 249

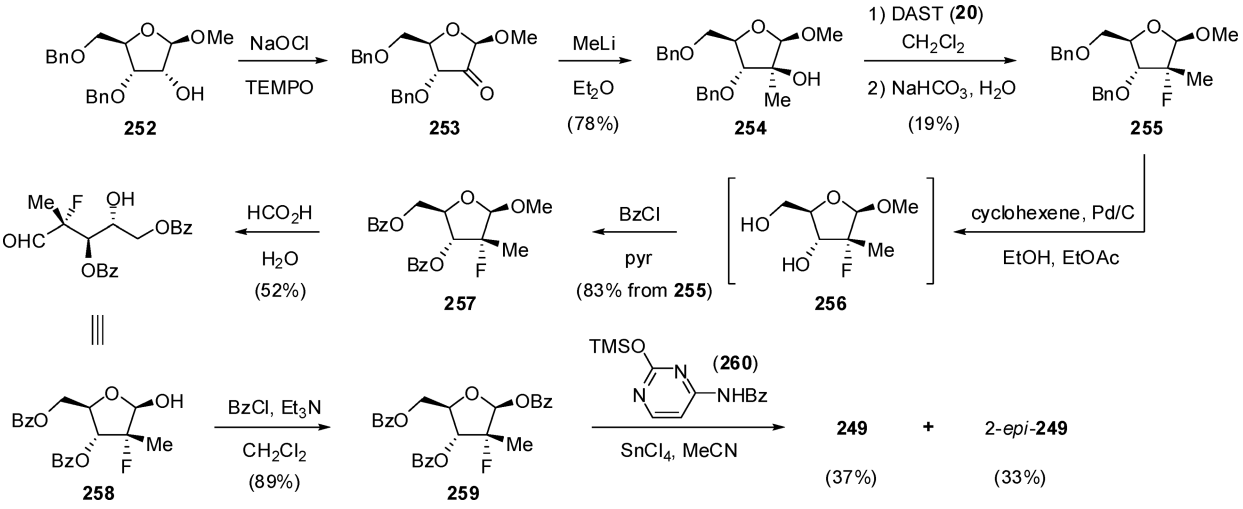

combination therapy of low-dose clevudine and adefovir is under evaluation.[266]

HBV is known to be a major cause of chronic liver disease leading to cirrhosis and hepatocellular carcinoma. Although safe and effective vaccines are available for prevention of HBV infection, hundreds of millions of people worldwide are still chronically infected with HBV. Current treatments for chronic HBV infection include pegylated α-interferon and NRTIs. However, interferon therapy is effective only in a limited number of patients and it is associated with side effects. On the other hand, five NRTIs have been approved by the FDA for HBV treatment, including lamivudine (**279**), telbivudine (**280**), entecavir (**281**), adefovir dipivoxil (**282**), and tenofovir disoproxil fumarate (**283**) (Figure 24).[272,273] NRTIs suppress HBV replication in most patients, but are not curative, requiring potentially lifelong treatment that may be associated with drug resistance and toxicity. Interestingly, clevudine (**278**) as well as compounds **279** and **280** are L-nucleosides,[274] and therefore, they do not interfere with the mitochondrial functions and showed no bone marrow toxicity up to 100 μM in vitro.[275] In addition, it has been reported that clevudine did not show significant virus rebound after cessation of the drug treatment.[276,277]

Originally, clevudine was prepared from L-ribose adapting a synthetic method previously developed for D-FMAU.[278] Since L-ribose was not easily obtained in large amounts, its preparation from readily available L-xylose was also described. Thus, 1,2-*O*-isopropylidene-α-L-xylofuranose (**285**) was synthesized from L-xylose (**284**), and selectively protected at the 5-OH with BzCl to give compound **286** (Scheme 39). Among various oxidation reagents, pyridinium dichromate (PDC) gave the best yield of ketone **287**. This ketone was stereoselectively reduced with $NaBH_4$ to the desired ribose derivative **288**, apparently due to the stereoelectronic effects of the 1,2-*O*-isopropylidene group. Compound **288** was then benzoylated to give the dibenzoyl ribose derivative **289**, which was successively treated with HCl, BzCl, and then Ac_2O in acidic media without isolation of intermediates to render the protected ribose **290** as a crystalline product. Treatment of **290** with saturated hydrogen chloride in CH_2Cl_2 followed by hydrolysis and accompanying benzoyl group transfer gave **291**, which was treated with SO_2Cl_2 and imidazole to afford the imidazolyl

DOI: 10.1021/acs.chemrev.5b00392
Chem. Rev. 2016, 116, 422−518

Scheme 35. Synthesis of Fluorine-Containing Sugar Moiety 267

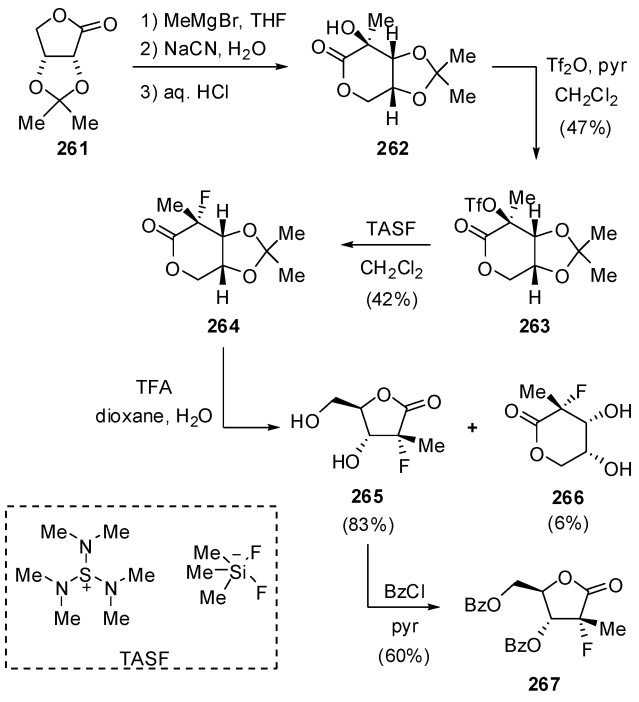

Scheme 36. Practical Synthesis of PSI-6130 (236)

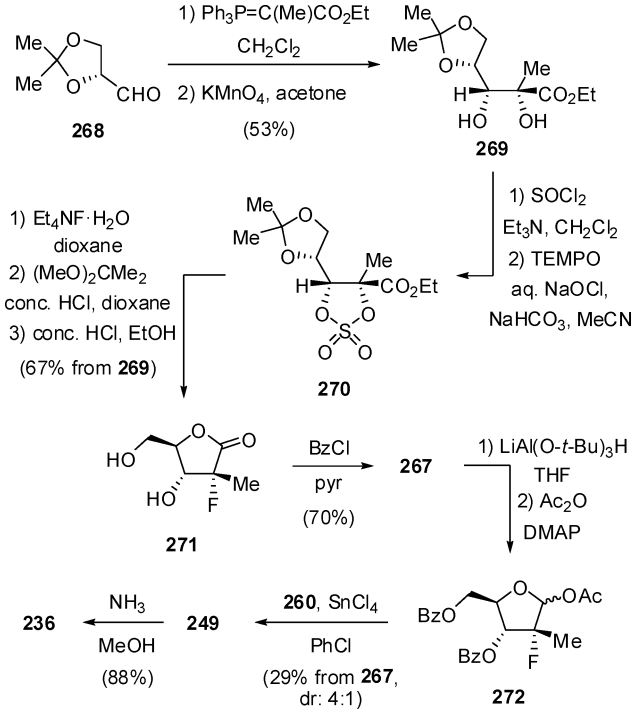

Scheme 37. Initial Synthetic Route to Sofosbuvir (239)

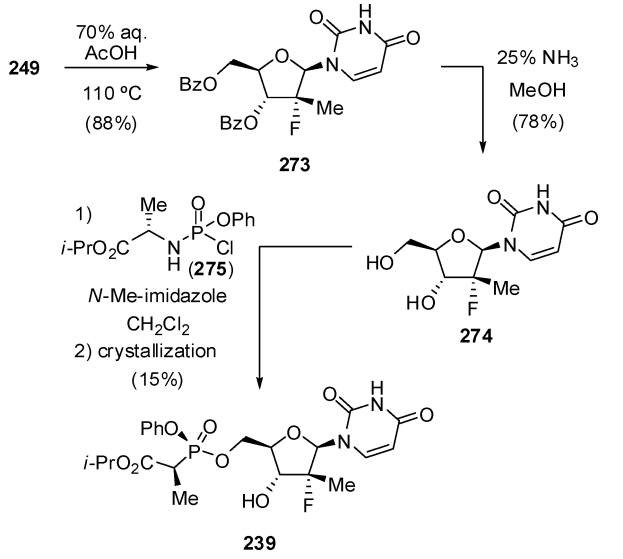

Scheme 38. Improved Process for the Synthesis of Sofosbuvir (239)

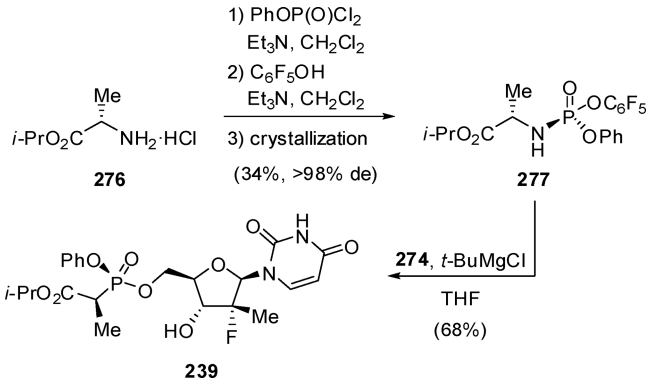

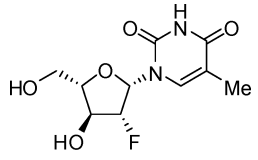

Figure 23. Structure of clevudine (**278**).

sulfonate **292**. Fluorination of the sulfonate derivative **292** was achieved with KHF_2 and 48% HF/H_2O to give the key intermediate, 1,3,5-tri-*O*-benzoyl-2-fluoro-α-L-arabinofuranose (**293**). Bromination of **293** with HBr/AcOH produced bromo derivative **294**, which was coupled with silylated thymine **295** without any catalyst to give mainly the desired β-anomer **296** along with only a trace amount of the α-anomer, which was easily removed by silica gel column chromatography or recrystallization. Clevudine (**278**) was obtained by deprotection of **296** with methanolic ammonia.[279]

Despite the success of the synthesis described above, it required rather lengthy steps and expensive L-xylose as starting material. Therefore, a more economical process was developed for the large-scale synthesis of clevudine, this time starting from L-arabinose, which is one of the most readily available L-monosaccharides. First, L-arabinose (**297**) was treated with BnOH and HCl to give benzyl β-L-arabinoside (**298**) (Scheme 40). The 3- and 4-OH groups of **298** were protected as an acetonide, and the resulting compound was then oxidized with PDC. The intermediate ketone **299** was selectively reduced with $NaBH_4$ to give the protected L-ribose intermediate **300**. Compound **300** was transformed into ribofuranose **301** by deprotection with TFA and successive treatment with HCl, pyridine, and BzCl. Finally, acetylation of **301** produced

DOI: 10.1021/acs.chemrev.5b00392
Chem. Rev. 2016, 116, 422–518

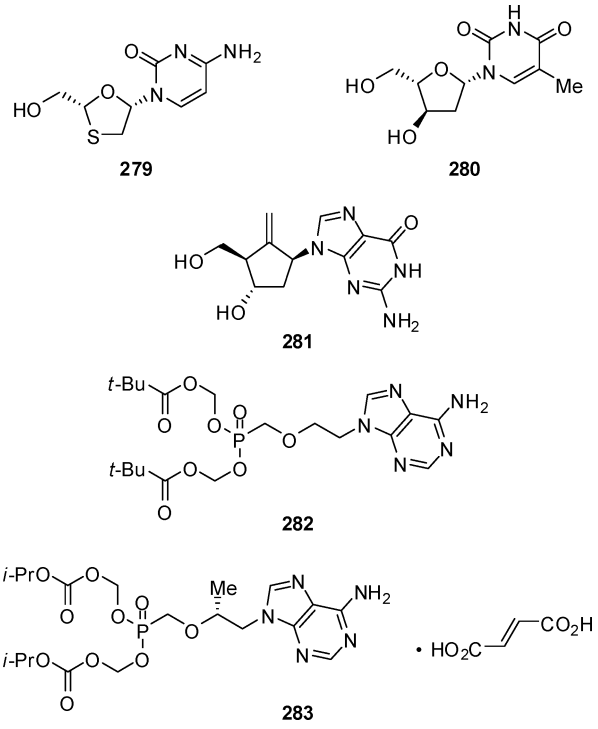

Figure 24. Structures of FDA-approved nucleoside reverse transcriptase inhibitors against HBV **279**–**283**.

synthetic intermediate **290**, whose conversion into clevudine (**278**) was performed essentially in the same manner with the previously disclosed synthesis, although the crucial fluorination step was conducted with triethylamine trihydrofluoride, a readily available and relatively noncorrosive fluorinating agent.[275]

Scheme 40. Improved Synthesis of Intermediate 290

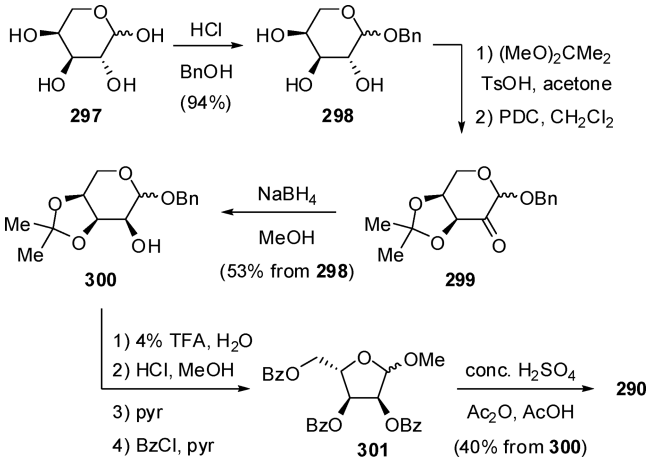

An alternative synthesis of clevudine was also reported using the electrophilic fluorination of a double bond as the key step. Acetylated bromo sugar **302** was synthesized from L-arabinose (**297**) according to a literature method (Scheme 41).[280] Compound **302** was unstable at room temperature and therefore used immediately for the next step. Treatment of **302** with Zn dust in the presence of NaOAc and $CuSO_4 \cdot 5H_2O$ gave L-arabinal **303**. Although there were several reports on the fluorination of D-arabinal, Selectfluor (**23**) was used on this occasion to give fluorinated sugar **304**. Deacetylation of **304** was performed quantitatively with NaOMe in MeOH, and was followed by treatment of **305** with H_2SO_4 in MeOH to give **306** as a 3:1 mixture of α- and β-anomers. Benzoylation of crude **306** followed by purification by flash chromatography afforded furanoside **307**. Coupling of methyl glycoside **307** with silylated thymine base **295** was carried out according to

Scheme 39. Synthetic Route to Clevudine (278)

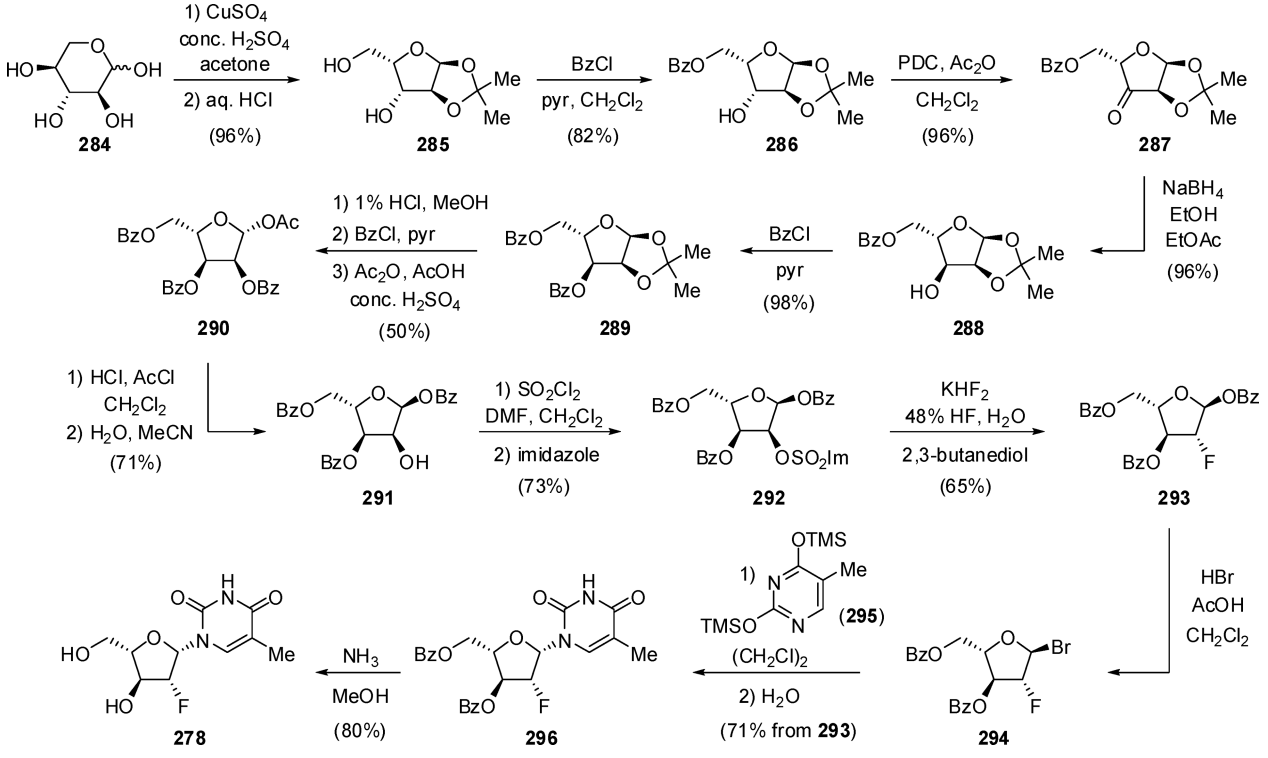

DOI: 10.1021/acs.chemrev.5b00392
Chem. Rev. 2016, 116, 422–518

Scheme 41. Alternative Synthesis of Clevudine (278)

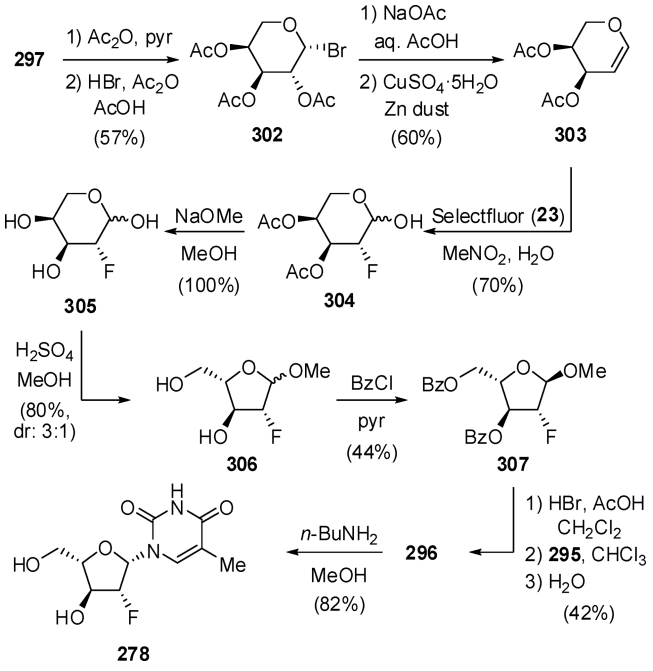

the standard protocol to give the known presursor **296**. Debenzoylation of **296** was achieved with *n*-butylamine in refluxing MeOH to furnish clevudine (**278**). Although this method provided advantages in terms of number of steps, the lack of crystalline synthetic intermediates in most of the synthetic route makes this approach less feasible for implementation on an industrial scale, in comparison to the other reported methods.[281]

2.15. Elvitegravir

Inhibitors of human immunodeficiency virus (HIV) integrase play a central role in the insertion of viral DNA into the genome of host cells via DNA processing and strand transfer.[282] This enzyme is essential for viral replication and therefore became a crucial target for anti-HIV drugs.[283] After numerous attempts to develop integrase inhibitors, raltegravir (**308**) was developed by Merck and approved by the FDA for therapeutic use as the first HIV integrase inhibitor (Figure 25).[284] Soon after, elvitegravir (GS-9137, **309**) was developed by Japan Tobacco (JT) and licensed to Gilead Sciences in the United States as a novel inhibitor of HIV type 1 (HIV-1) integrase

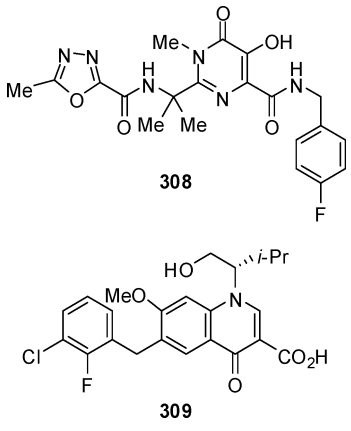

Figure 25. Structures of raltegravir (**308**) and elvitegravir (**309**).

(trade name: Vitekta). Elvitegravir was approved by the FDA in 2012 for use in adult patients starting HIV treatment for the first time as part of the fixed dose combination with two nucleoside reverse transcriptase inhibitors, emtricitabine and tenofovir disopropoxil fumarate, along with cytochrome P450 inhibitor cobicistat acting as booster.[285]

During the development of raltegravir (**308**), the diketo acid class of compounds had been most aggressively investigated, because of their remarkable antiretroviral activities.[286] Thus, the γ-ketone, α-enol, and carboxylic acid moieties were believed to be essential for the inhibitory activity, and the 4-carbamoyl-5-hydroxy-6-pyrimidinone fragment as in raltegravir was identified as a bioisostere of the keto−enol acid pharmacophore.[284,287,288] It was then discovered that the carboxylic acid in the keto−enol acid motif could be replaced by a pyridine ring.[289] In the meantime, several structures of novel quinolone HIV-1 integrase inhibitors having a monoketo acid motif had been discovered.[289,290] Thus, quinolone **310** had an IC_{50} of 1.6 μM in the strand transfer assay (Figure 26).

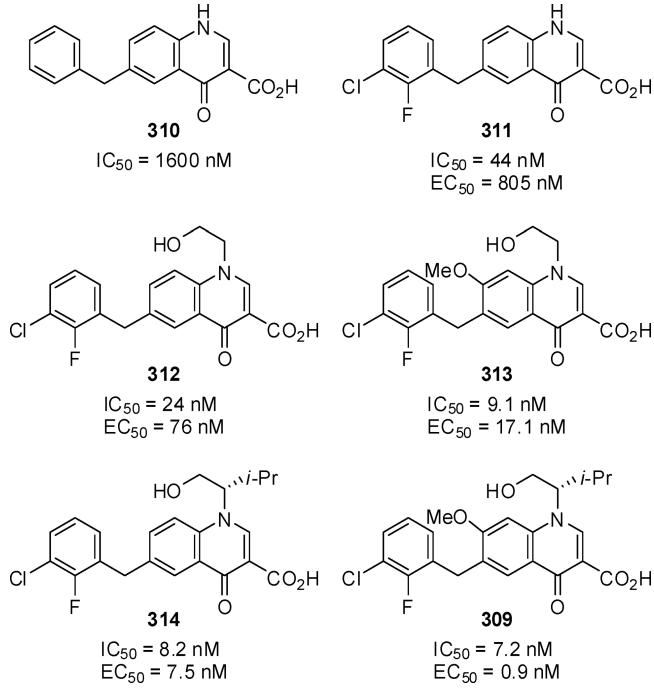

Figure 26. Evolution of the quinolone motif to elvitegravir (**309**).

Interestingly, introducing fluorine and chlorine atoms at the C-2 and C-3 positions, respectively, of the phenyl ring, as in derivative **311**, improved the inhibition of strand transfer (IC_{50} = 44 nM), while antiviral activity was also observed (EC_{50} = 805 nM). Compound **312** bearing a hydroxyethyl group at the 1-position of the quinolone was 1.8-fold more potent for strand transfer inhibition (IC_{50} = 24 nM), and showed about 11-fold stronger antiviral activity (EC_{50} = 76 nM) than **311**. Introduction of a methoxy group at the C-7 position of the quinolone ring afforded **313**, which showed a significant improvement of its inhibition of strand transfer (IC_{50} = 9.1 nM) and of antiviral activity (EC_{50} = 17 nM). Compound **314** bearing an (*S*)-configured isopropyl group at the C-1 position of the hydroxyethyl moiety was about 3-fold more potent at inhibiting strand transfer (IC_{50} = 8.2 nM) and about 10-fold stronger at inhibiting HIV replication (EC_{50} = 7.5 nM) than **312**, whereas the enantiomeric (*R*)-configured derivative could

DOI: 10.1021/acs.chemrev.5b00392
Chem. Rev. 2016, 116, 422−518

not enhance the inhibitory activity. A combined effect of both methoxy group at the C-7 position of the quinolone ring and (*S*)-isopropyl group at the C-1 position of the hydroxyethyl moiety improved the antiviral activity (EC_{50} = 0.9 nM) resulting in a novel quinolone compound, elvitegravir (**309**), as a potent integrase inhibitor.[291]

The medicinal chemistry route to elvitegravir was performed starting from 2,4-difluorobenzene carboxylic acid (**315**) (Scheme 42). Regioselective iodination of **315** was carried

Scheme 42. Medicinal Chemistry Route to Elvitegravir (309)

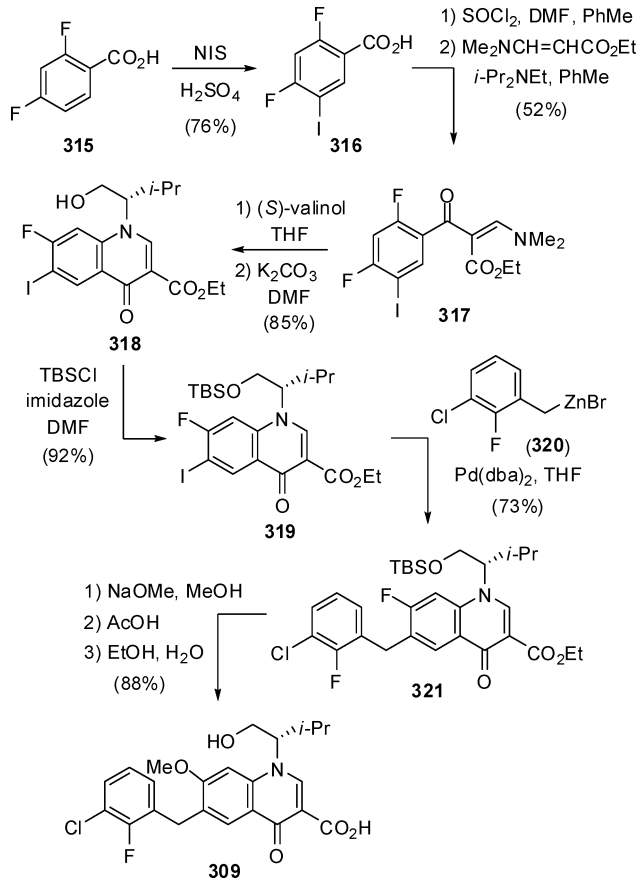

out using *N*-iodosuccinimide (NIS) in H_2SO_4 to give **316**, and its derived acid chloride was next reacted with ethyl 3-(dimethylamino)acrylate to yield acrylate **317**. Addition of (*S*)-valinol to **317** and subsequent base-mediated ring closure afforded quinolone **318**. After protection of the hydroxyl group in **318** as its corresponding TBS ether **319**, Negishi coupling with organozinc reagent **320** led to the key intermediate quinolone **321**. Final methoxylation of **321** was followed by hydrolysis to render elvitegravir (**309**).[289]

Compound **315** could be prepared starting from 2,4-dinitrotoluene (**322**) using two procedures (Scheme 43). The first one proceeded by reduction of both nitro groups in **322** followed by fluorination under Balz–Schiemann conditions to give **323**, and further oxidation with potassium permanganate produced **315**.[292] The second process for the synthesis of **315** consisted of prior oxidation of **322** to carboxylic acid **324** followed by fluorination with NaF in DMSO.[293]

3-Chloro-2-fluorobenzyl bromide (**327**) was prepared by selective fluorination[294] of 2,3-dichlorobenzaldehyde (**325**) and reduction with $NaBH_4$ followed by bromination (Scheme

Scheme 43. Preparation Methods of 2,4-Difluorobenzoic Acid (315)

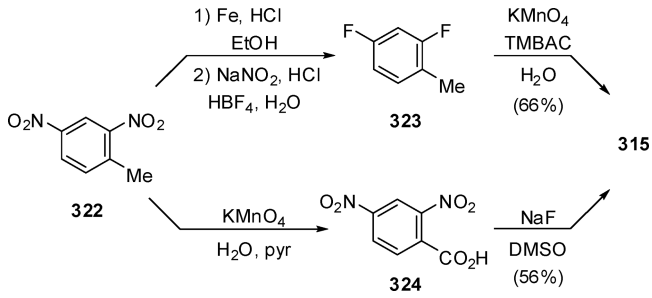

44).[295] The zinc bromide reagent **320** needed for the subsequent Negishi coupling was prepared by reaction of

Scheme 44. Preparation of Organozinc Reagent 320

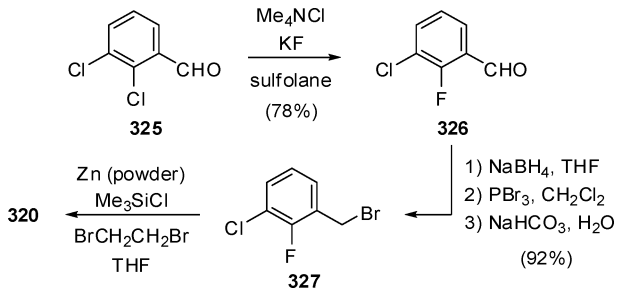

benzyl bromide **327** with Zn powder in the presence of 1,2-dibromoethane and TMSCl and used for the coupling as a THF solution.[289]

More recently, a practical process for the synthesis of elvitegravir was disclosed starting from 2,4-dibromo-5-methoxyanisole (**328**) (Scheme 45). Compound **328** was converted into the Grignard reagent **329**, which was treated with 3-chloro-2-fluoro-benzaldehyde (**326**). In situ formation of a new Grignard reagent and subsequent reaction with carbon dioxide formed acid **331** in a one-pot process from **328**. After removal of the benzylic hydroxyl group of **331** by treatment with Et_3SiH and TFA, the resulting acid **332** was amidated with CDI, which was then reacted with potassium monoethylmalonate to give the ketoester derivative **333**. Treatment of compound **333** with $Me_2NCH(OMe)_2$ gave **334**, which was then reacted without isolation with (*S*)-valinol to form **335**, after protection of the alcohol with bis(trimethylsilyl)acetamide. Cyclization of **335** followed by hydrolysis gave elvitegravir (**309**).[296]

2.16. Riociguat

Riociguat (BAY-63-2521, **336**) is a novel potent soluble guanylate cyclase (sGC) stimulator for the oral treatment of pulmonary hypertension (Figure 27).[297] sGC is a crucial signal-transduction enzyme, which is activated by nitric oxide (NO). Riociguat affects the binding and action of NO to sGC in two ways, independently and in synergy, leading to an increased generation of cyclic guanosine monophosphate (cGMP), which in turn promotes vascular endothelial function improvement. Riociguat was developed and launched by Bayer Health Care Pharmaceuticals (trade name: Adempas), being the first and only FDA-approved drug for the treatment of adults with persistent/recurrent chronic thromboembolic pulmonary hypertension (CTEPH).

DOI: 10.1021/acs.chemrev.5b00392
Chem. Rev. 2016, 116, 422–518

Scheme 45. Practical Synthesis of Elvitegravir (309)

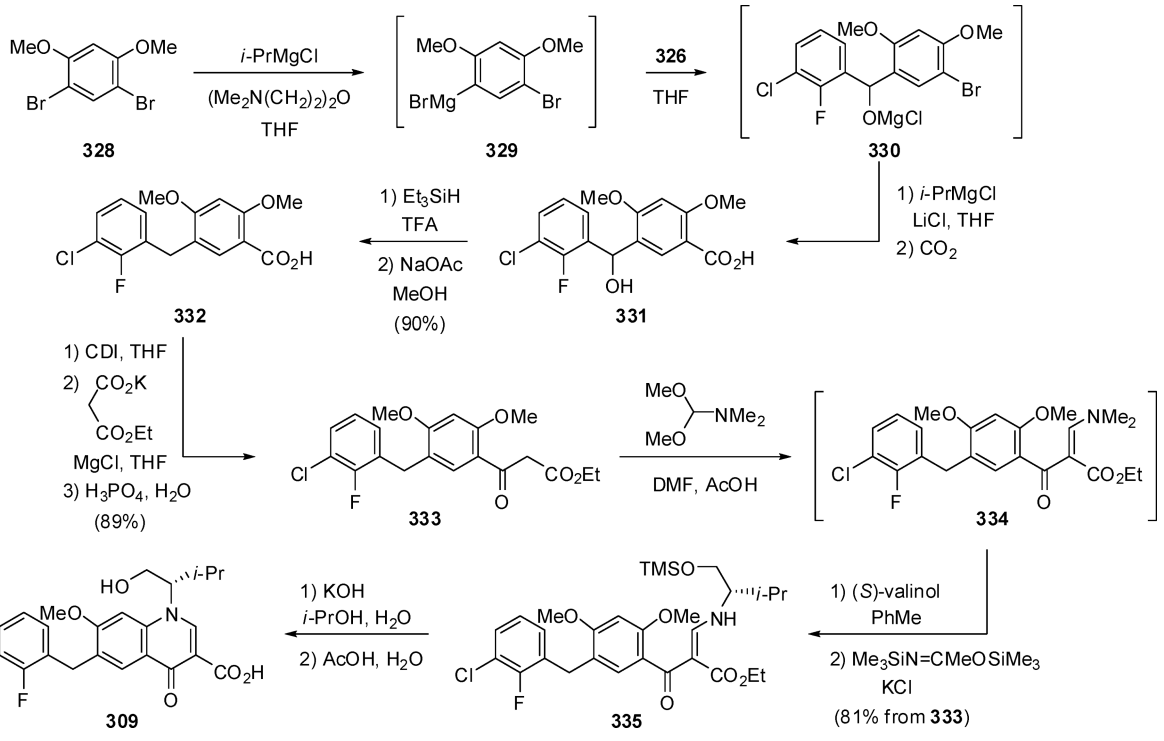

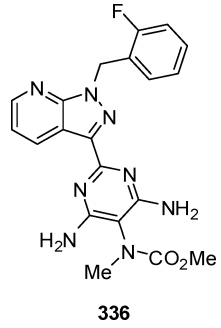

Figure 27. Structure of riociguat (**336**).

Scheme 46. Discovery of Riociguat (336)

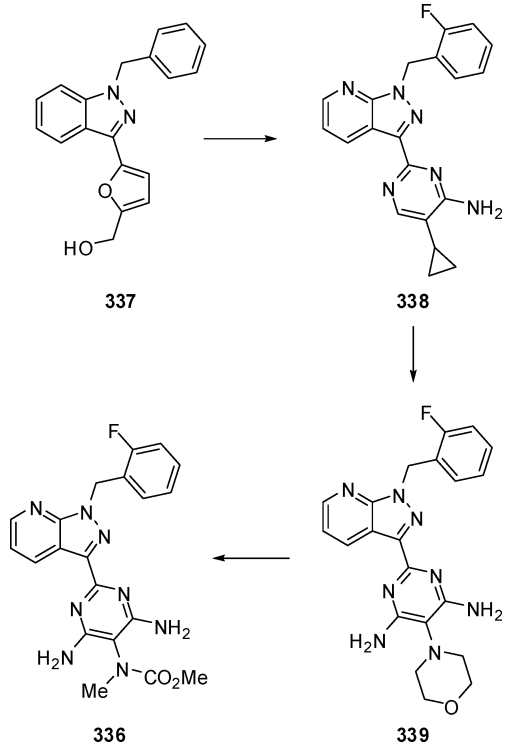

Lificiguat (YC-1, **337**), the first NO-independent sGC stimulator, was investigated in the mid-1990s (Scheme 46).[298] Using the benzylindazole scaffold of lificiguat, chemical optimization by researchers at Bayer provided compounds with a pyrazolopyridinyl pyrimidine core, such as BAY-41-2272 (**338**)[299] and BAY-41-8543 (**339**).[300] These compounds were potent sGC stimulators, with IC_{50} values of 0.1−0.3 μM in isolated rabbit aorta and mininum effective doses of 0.3−1 mg/kg in spontaneously hypertensive rats. However, these compounds were not developed further, as **338** induced and inhibited cytochrome P450 (CYP) isoenzymes, and **339** had an unfavorable pharmacokinetic profile characterized by high clearance and nondose-linear exposure.[301] To overcome these disadvantages, a wide range of derivatives of compounds **338** and **339** were investigated, varying the substituent at the C-5 position of the pyrimidine core. Finally, Bayer selected the 4,6-diamine-*N*-methylcarbamate derivative riociguat (**336**) as the lead compound.[302]

The synthetic procedure for riociguat started from 2-fluorobenzyl hydrazine (**340**) and the sodium salt of ethyl cyanopyruvate (**341**) to yield the aminopyrazole intermediate **342**, which was cyclocondensed with 3-dimethylaminoacrolein (**343**) in the presence of TFA to build the pyrazolopyridine core in compound **344** (Scheme 47). Transformation of the 3-carboxylate group into a nitrile via amide formation was accomplished using standard procedures. Next, Pinner reaction of the cyano group in **346** produced amidine **347**. The coupling of this intermediate to phenylazomalononitrile (**348**) in the presence of sodium methoxide produced pyrimidine **349**, and

DOI: 10.1021/acs.chemrev.5b00392
Chem. Rev. 2016, 116, 422−518

Scheme 47. Synthetic Route to Riociguat (336)

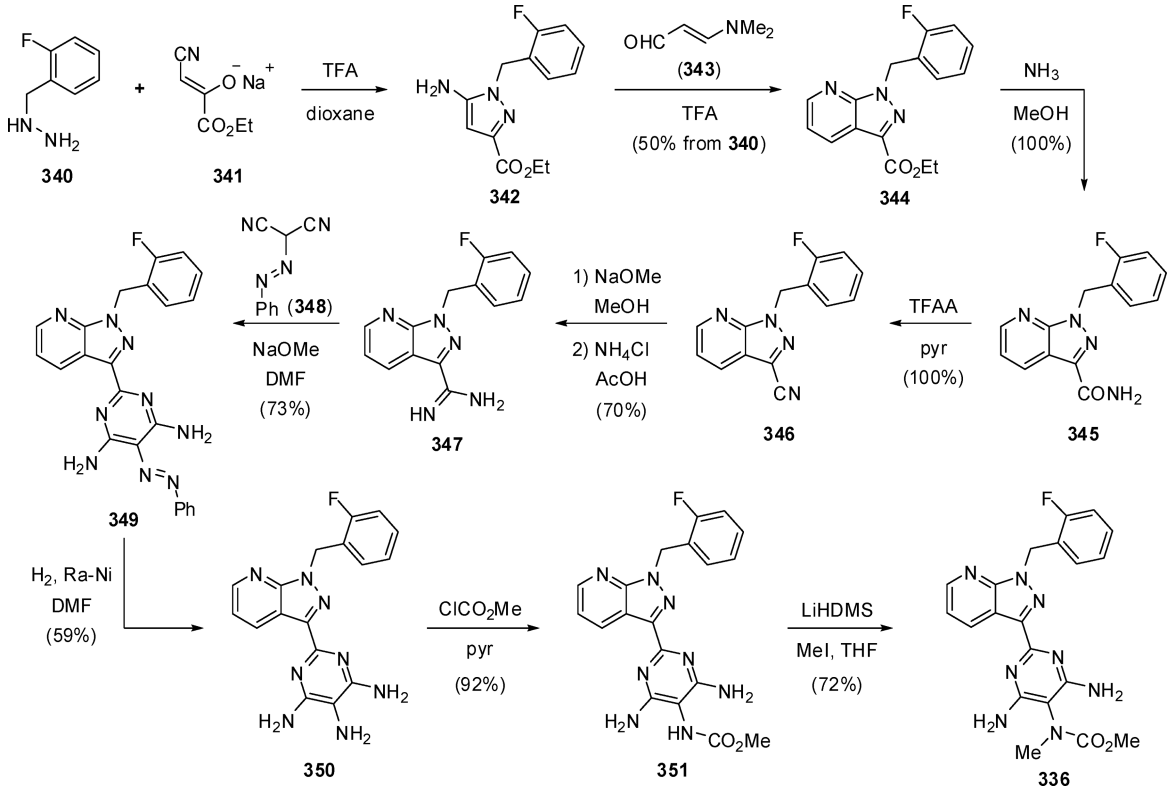

further hydrogenation of the azo group using Raney nickel furnished the corresponding triaminopyrimidine **350**. The 5-amino group was selectively converted into a carbamate moiety with methyl chloroformate, followed by *N*-methylation with iodomethane/lithium hexamethyldisilazide (LiHMDS) to yield riociguat (**336**).[302]

2.17. Setipiprant

As a G-protein-coupled receptor for prostaglandin D2 (PGD2), CRTh2 was shown to play a critical role in allergic inflammation.[303] Setipiprant (ACT-129968, **352**), a potent, selective and orally active CRTh2 antagonist, was developed by Actelion for the treatment of asthma and seasonal allergic rhinitis (Figure 28).[304] The drug inhibits the effects of PGD2 in inflammation and therefore blocks the amplification and maintenance of allergic reactions.[305] However, in 2012 the company terminated the development of setipiprant and switched attention to a more potent follow-up molecule, because the efficacy observed in previous studies was not confirmed in phase IIb and III trials. Although at least seven CRTh2 antagonists worldwide have been discontinued from clinical trials, this area will still be of great interest to the pharmaceutical companies in the next few years.[306]

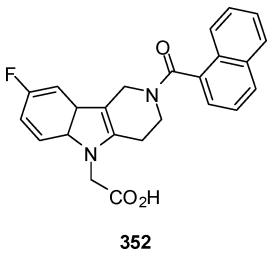

Figure 28. Structure of setipiprant (**352**).

The scaffold of setipiprant originated from the hit compound **353** (IC_{50} = 0.5 μM), discovered from high-throughput-screening (HTS) studies (Scheme 48).[307,308] Since early SAR efforts on **353** did not produce any breakthrough in improving the bioavailability or replacing the structural alerts (such as the α,β-unsaturated nitrile and the *N*-aryl amide), a scaffold hopping strategy was adopted that led to compound **354** (IC_{50} = 430 nM), in which the tetrahydropyridoindole core mimics the low energy (*s-cis*) conformation of the diene in

Scheme 48. Discovery of Setipiprant (352)

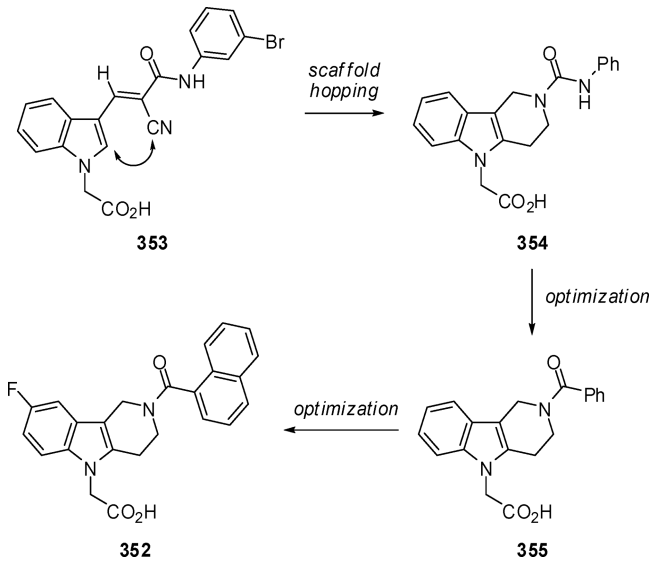

DOI: 10.1021/acs.chemrev.5b00392
Chem. Rev. 2016, 116, 422−518

compound **353** and retains the planarity of the molecule. The new scaffold was synthetically accessible, without adding stereogenic centers. The replacement of the phenylamino moiety by a phenyl group greatly enhanced the affinity and provided the new lead compound **355** (IC_{50} = 17 nM). Further optimization was concentrated in potency and oral bioavailability. Thus, introduction of substituents such as chlorine, methyl, fluorine, or trifluoromethyl at the C-8 position of the indole unit was well tolerated, while C-6 substitutions were less favorable. Given that the introduction of fluorine in *para*-position to the indole nitrogen is a commonly used modification for CRTh2 antagonists,[309] setipiprant (**352**, IC_{50} = 6 nM) with a C-8-substituted fluorine atom and a naphthoyl group was finally chosen as a candidate due to its well-balanced overall properties.[304] A study showed that setipiprant underwent moderate metabolism in humans and the tetrahydropyridoindole core remained intact in its two major metabolites,[310] so it is quite plausible to consider that the fluorine atom might block the site of oxidative metabolism on the indole unit of the molecule.

The five-step synthesis of setipiprant reported by Actelion commenced from 8-fluoro-2,3,4,5-tetrahydro-2*H*-pyrido[4,3-*b*]indole hydrochloride (**356**) (Scheme 49). *N*-Boc-protected

Scheme 49. Synthetic Route to Setipiprant (352)

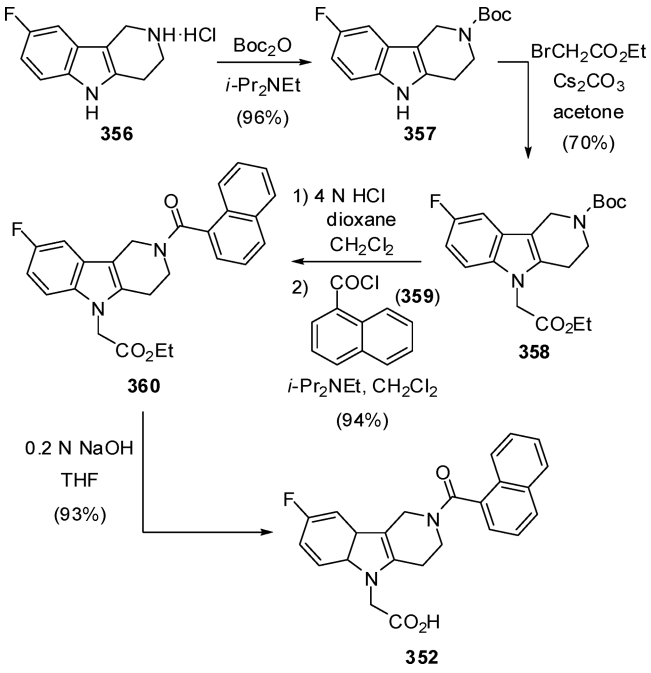

derivative **357** was treated with ethyl bromoacetate in the presence of potassium carbonate to give **358**. Deprotection of the Boc group was followed by coupling with 1-naphthoyl chloride (**359**) to provide amide **360**. Finally, saponification of the ethyl ester and subsequent chromatographic purification provided setipiprant (**352**).[304]

Although commercially available, the fluorine-containing starting material **356** can be prepared from 4-fluoro-substituted arylhydrazine **361** and 4-piperidone (**362**) by means of a thermally driven Fischer reaction (Scheme 50).[311]

2.18. Vonoprazan

Current proton pump inhibitors (PPIs), namely substituted pyridylmethylsulfinyl benzimidazole prodrugs, are a widely used

Scheme 50. Preparation of Fluorinated Tetrahydropyridoindole 356

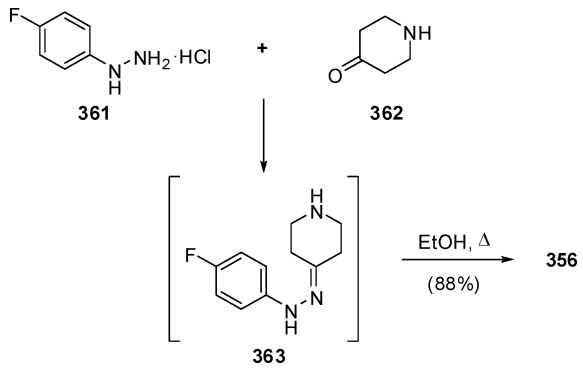

therapy for acid-related diseases.[312] However, several aspects of these drugs might be improved, such as a faster onset of pharmacological action, suppression of nighttime acid secretion, and removal of cytochrome P450 (CYP2C19) polymorphism effect.[312,313] Vonoprazan (**364**) is a new selective potassium-competitive acid blocker (P-CAB) invented by Takeda, being developed as its fumarate (TAK-438) for the oral treatment of acid-related diseases (Figure 29).[314] The drug inhibits the

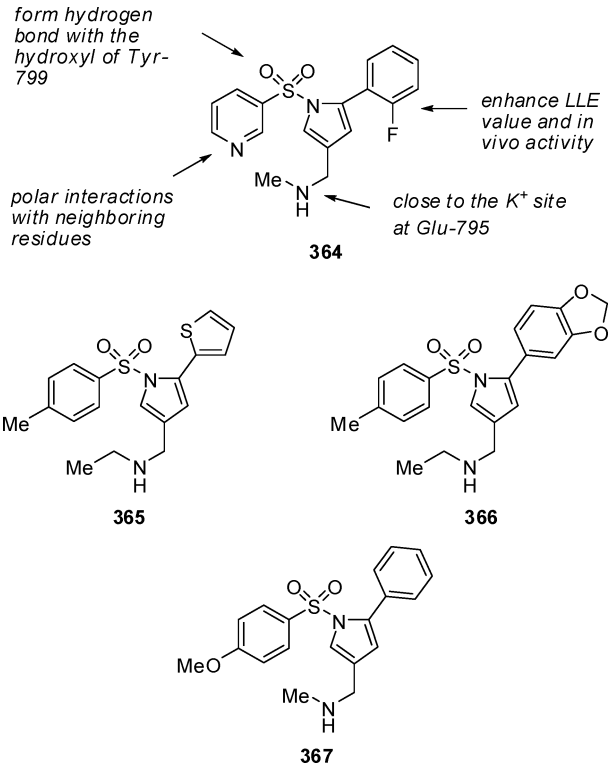

Figure 29. Structures of vonoprazan (**364**) and other pyrrole derivatives **365** and **367**.

binding of potassium ion to H^+,K^+-ATPase with slow reversibility, thus suppressing gastric acid secretion with a more strong and more sustainable effect than existing P-CABs and PPIs.[315−317] Besides, its action is unaffected by acid secretion and its metabolism is independent of CYP2C19.[316] Based on favorable results obtained from phase III trials, vonoprazan fumarate (trade name: Takecab) was approved in Japan in December 2014 for several indications including

DOI: 10.1021/acs.chemrev.5b00392
Chem. Rev. 2016, 116, 422−518

gastric ulcer, duodenal ulcer, erosive esophagitis, and *Helicobacter pylori* eradication.[318]

The discovery of vonoprazan is the result of a pursuit for more potent gastric antisecretory agents without the limitations of PPIs. Researchers at Takeda drew attention to the potassium-competitive inhibition of H^+,K^+-ATPase and identified novel pyrrole derivatives **365** and **366** by screening a low-molecular-weight compound library.[319] SAR studies based on compound **366** led to the new lead **367**, which had promising activity (IC_{50} = 30 nM) and physicochemical properties.[320] Further modifications were focused on log *D* and ligand-lipophilicity efficiency (LLE) values of the compounds. The binding model of H^+,K^+-ATPase with compound **367** suggested a small polar space near the arylsulfonyl group that can interact with the neighboring residues of the enzyme, which was confirmed by the potency and LLE benefit (7.1) of the 3-pyridylsulfonyl group. Investigation about effects of substitutions on the phenyl ring started with the fluoro derivatives. Compared with other derivatives, the 2-fluoro compound vonoprazan (**364**, IC_{50} = 19 nM) exhibited the highest LLE (7.3) and optimal inhibitory activity in vivo, while replacing the 2-fluoro by other substituents (chloro, methyl, trifluoromethyl, cyano, or hydroxymethyl) failed to make more substantial improvements.[314] Subsequent homologous modeling revealed the proximity of the positively charged *N*-methylamino group to the negatively charged group of Glu-795 and hydrogen bonds between the sulfonyl oxygens with the hydroxyl of Tyr-799, which may account for the slow dissociation rate of vonoprazan.[317]

The synthetic route to vonoprazan disclosed by Takeda is depicted in Scheme 51. Bromination of 2′-fluoroacetophenone (**368**) provided **369**, which was condensed with ethyl cyanoacetate under basic conditions to give 2-fluorophenyl derivative **370** in high yield. The central pyrrole ring was constructed by intramolecular cyclization of **370** using HCl to give 2-chloropyrrole derivative **371**, followed by reduction with H_2 over Pd/C to afford dechlorinated pyrrole **372**. The ester group of **372** was reduced to the corresponding alcohol with DIBAL, and then converted to a formyl group with TPAP and NMO to furnish aldehyde **373**. On the other hand, the pyridine building block **375** was obtained in good yield by chlorination of sulfonic acid **374** and subsequent acidification. Next, the pyrrole derivative **373** was treated with sodium hydride in THF and then sulfonylated with **375** with the aid of 15-crown-5 to give sulfonamide **376**. The methylaminomethyl moiety was formed by reductive amination of the formyl group with methylamine and sodium tetrahydroborate, and the desired product vonoprazan was isolated in crystalline form as its fumarate.[314,321]

The starting material **368** employed in the above route is commercially available, but can be also prepared from the corresponding aniline **377** via a conventional Balz–Schiemann reaction. An optimized one-pot process was conducted by using nitrosonium tetrafluoroborate and furnished **368** through the intermediate diazonium salt **378** (Scheme 52).[322] Moreover, a cost-effective method in the solid phase for the synthesis of **368** was also described. Thus, aniline **377** was diazotized and then immobilized on an *N*-benzylaminomethyl-functionalized polystyrene resin (**379**) to give resin-bonded triazene **380**. After derivatization of the resin, the fluorination step was carried out with tetrafluoroboric acid diethyl ether in the presence of perfluorohexane.[323]

Scheme 51. Synthetic Route to Vonoprazan (364)

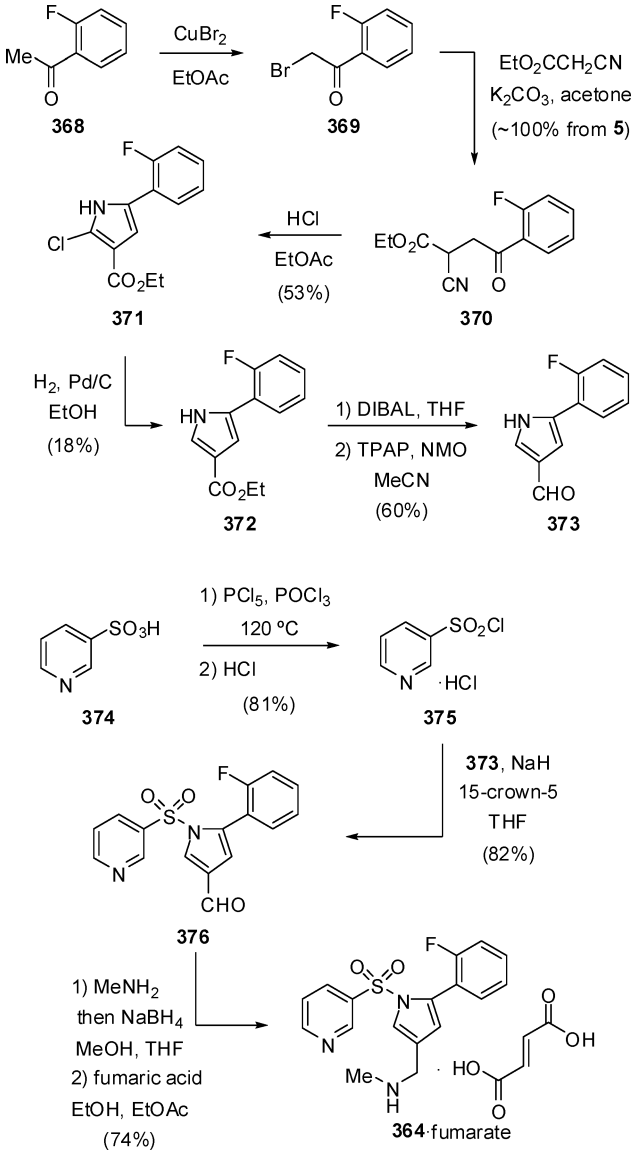

Scheme 52. Preparation of 2′-Fluoroacetophenone (368) from 2′-Aminoacetophenone (377)

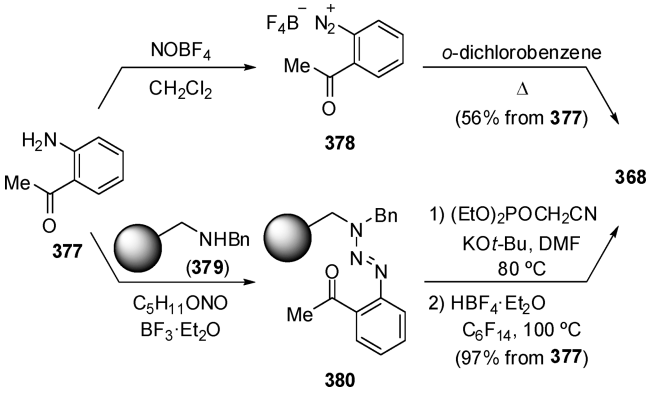

2.19. Ulimorelin

Ulimorelin (TZP-101, **381**) is an intravenous ghrelin receptor (GRLN) agonist developed by Tranzyme and Norgine for the treatment of postoperative ileus (POI) and gastroparesis

DOI: 10.1021/acs.chemrev.5b00392
Chem. Rev. 2016, 116, 422–518

(Figure 30).[324] The drug selectively activates GRLN with favorable potency, thus promoting gastric emptying in diabetic gastroparesis, alleviating the associated nausea and vomiting as well as reducing POI in a colectomy.[325] Unlike ghrelin, ulimorelin exerts a prokinetic effect without eliciting growth hormone (GH) release.[326] However, Tranzyme stopped all the new drug application (NDA) activities of ulimorelin in 2012, since no statistical differences between the drug and placebo groups were observed in two previous phase III trials in POI.[327] The company then turned to the oral GRLN agonist TZP-102, which unfortunately failed its phase IIb trial and was also aborted afterward.[328]

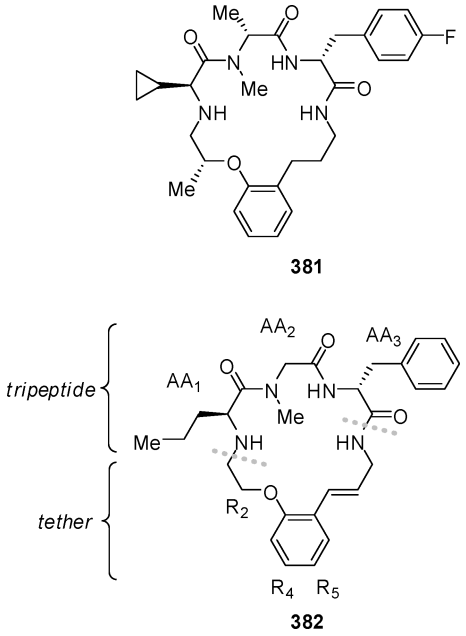

Figure 30. Structures of ulimorelin (**381**) and hit compound **382**.

The discovery of ulimorelin resulted from intensive medicinal chemistry efforts that started from the identification of the potent GRLN agonist **382** (K_i = 86 nM, EC_{50} = 134 nM), although showing poor pharmacokinetic properties, from a high-throughput screening of Tranzyme Pharma's macrocycle library. Structurally, this type of compound contained a peptidomimetic macrocycle, wherein a tether portion linked the tripeptide moiety from head to tail. The macrocyclic ring was crucial for the GRLN potency, and the double bond at the tether portion was reduced to avoid potential metabolic liability. More optimization guided by conformational design led to the structure of ulimorelin (**381**), which possesses enhanced potency (K_i = 16 nM, EC_{50} = 29 nM) and suitable PK profiles (F = 24%).[324]

SAR studies demonstrated that (*S*)-cyclopropylglycine ((*S*)-Cpg) and *N*-Me-(*R*)-Ala were preferred as AA_1 and AA_2, respectively. As to AA_3, phenyl ring substitutions enhanced potency and ligand lipophilicity efficiency (LLE) of the compounds, which may be attributed to the improved direct receptor interaction, and 4-fluoro-(*R*)-Phe was finally chosen according to the LLE trend (4-F > 4-H > 4-Cl). Notably, the fluorophenyl substitution strategy was also employed for investigating the electronic properties of the tether portion.

Scheme 53. Solution-Phase Synthesis of Ulimorelin (381)

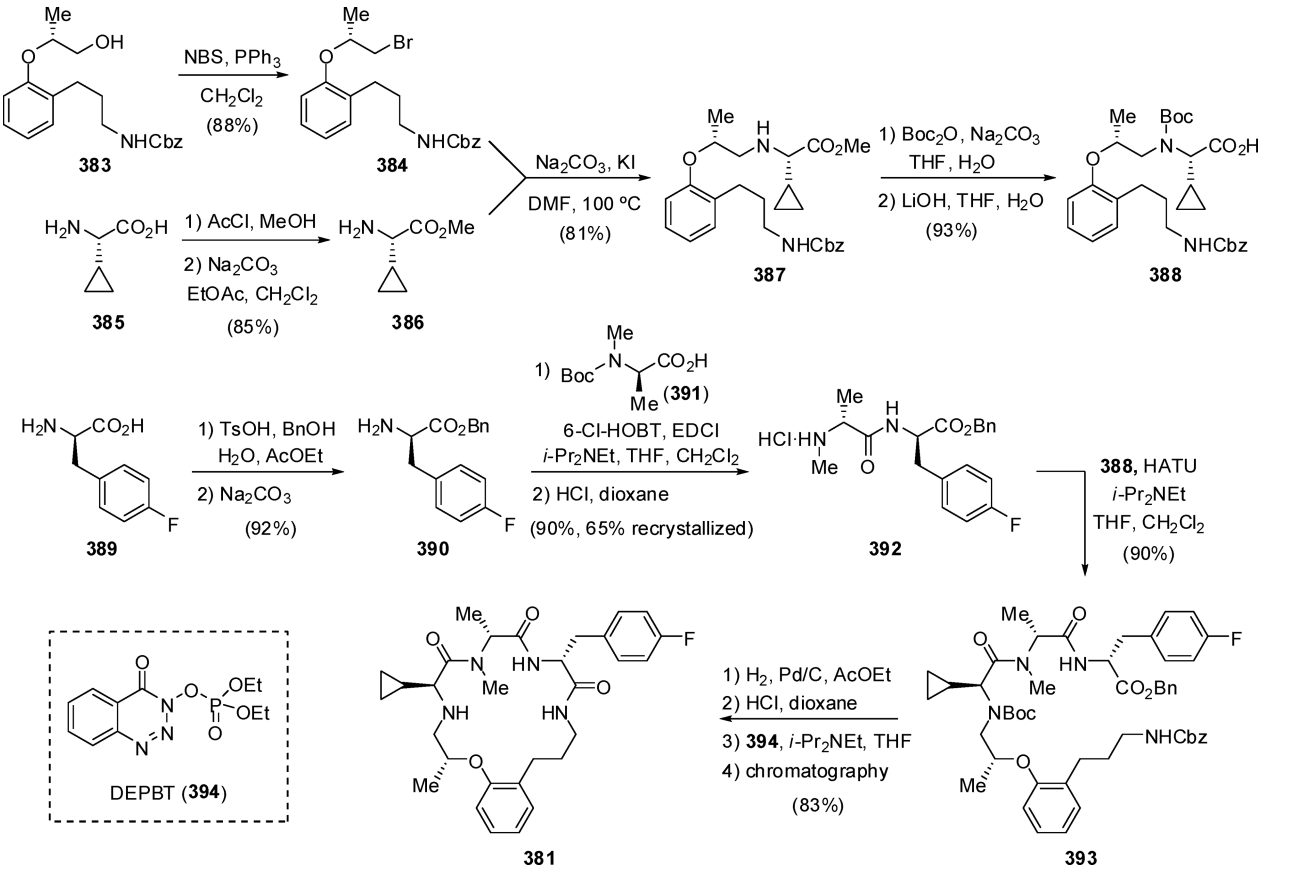

DOI: 10.1021/acs.chemrev.5b00392
Chem. Rev. 2016, 116, 422−518

Thus, structural studies demonstrated the presence of an intramolecular hydrogen bond between the NH group of AA_1 and the tether phenoxy oxygen, and the transfer of fluorine from the *p*-benzylic (R_4) to the *p*-phenoxy position (R_5) caused about 22-fold decline of the potency, because the electron withdrawing R_5-fluoro may lower the basicity of the oxygen, weaken the H-bond, and hence reduce the conformational rigidity of the molecule. Although displaying higher potency and better PK properties in rats, the R_4-fluoro derivative of ulimorelin failed to show satisfied PK profiles in monkeys. Moreover, it was proposed that a combination of the electronic effect of the cyclopropyl side chain at AA_1 and the steric shielding effect of the (*R*)-Me substituent at the R_2 position stabilized the aforementioned H-bond to offer additional rigidity, accounting for the PK cooperative effect of these two groups on ulimorelin.[324]

Ulimorelin was initially obtained through a linear route on solid phase for medicinal chemistry research.[324] Thereafter, a convergent procedure in solution was established, with amide coupling, deprotection, and macrolactamization as the key steps. The starting materials were four major building blocks, namely chiral ether **383**, (*R*)-Cpg (**385**), 4-fluoro-(*R*)-Phe (**389**), and *N*-Boc-*N*-Me-(*R*)-Ala (**391**) (Scheme 53). First, the AA_1−tether fragment was constructed by *N*-alkylation of bromide **384** with amino ester **386** to produce intermediate **387** that was further transformed into **388**. Conversely, amino ester **390** was reacted with **391** using 6-Cl-HOBt and EDCI as coupling reagents to produce AA_2−AA_3 dipeptide **392** after Boc deprotection. Then, condensation of fragments **388** and **392** proceeded uneventfully to afford acyclic derivative **393**. After removal of the protecting groups at the amino and carboxyl termini, macrocyclization was carried out in the presence of 3-(diethoxyphosphoryloxy)-1,2,3-benzotriazin-4(3*H*)-one (DEPBT, **394**) and *i*-Pr_2NEt to display optimal yield and diastereomeric purity, and ulimorelin (**381**) was finally obtained by silica gel chromatographic purification.[324,329]

Alternatively, alkylation of the *tert*-butyl ester of (*R*)-Cpg (**395**) with tether material **383** generated compound **396**, which was hydrolyzed to give **397** (Scheme 54). Without *N*-Boc-protection, fragment **397** was directly coupled with dipeptide **392** to provide acyclic precursor **398**. Prior to the macrocyclization step, both Cbz and benzyl groups in **398** were removed in one step by means of catalytic hydrogenation, thus successfully reducing the impurities derived from the Boc-deprotection step. Moreover, double crystallization procedures were adopted to purify the desired product for scale-up production, leading to the hydrated HCl salt of ulimorelin in good yield.[324,329]

4-Fluoro-(*R*)-Phe (**389**) is commercially available but relatively expensive. A favorable upstream material for the preparation of **389** is 4-fluorobenzaldehyde (**400**), which in turn can be obtained by halogen-exchange fluorination of 4-chlorobenzaldehyde (**399**) with KF in the presence of tetraphenylphosphonium bromide and 18-crown-6 (or polyethylene glycol dimethyl ether) (Scheme 55).[330−332] The reaction of **400** with hippuric acid (*N*-benzoylglycine) provided racemic *N*-benzoylamino acid **401**,[333] and eventually the optically pure amino acid is accessible by enzymatic resolution.[334,335] Alternatively, asymmetric synthesis is another approach for preparing 4-fluoro-(*R*)-Phe (**389**) from **400**.[336−339]

It should be emphasized that, in the development of ulimorelin, as well as in the discussed above idelalisib, the

Scheme 54. Scale-Up Procedure for Ulimorelin (381)

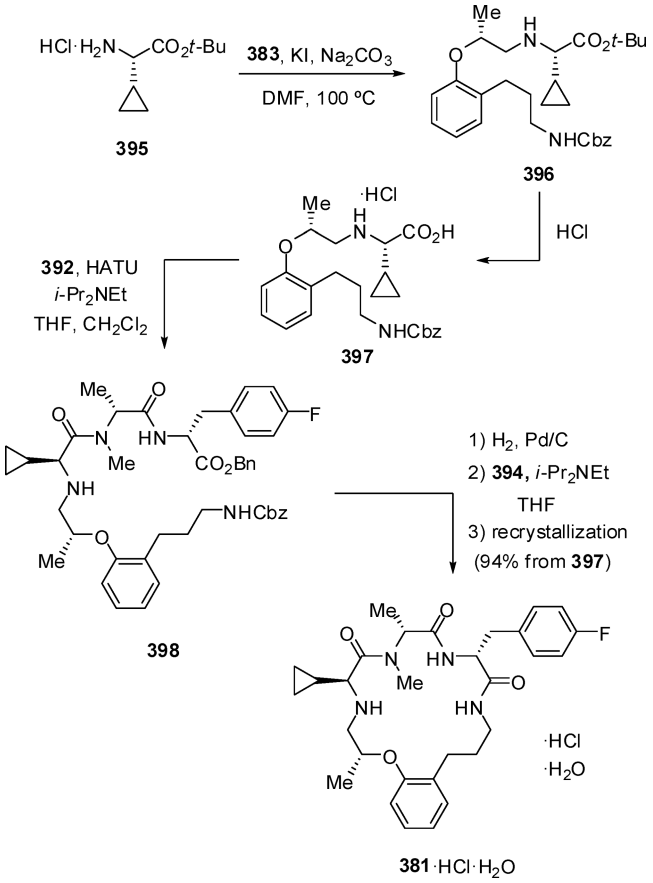

Scheme 55. Preparation of 4-Fluoro-(*R*)-Phe (389)

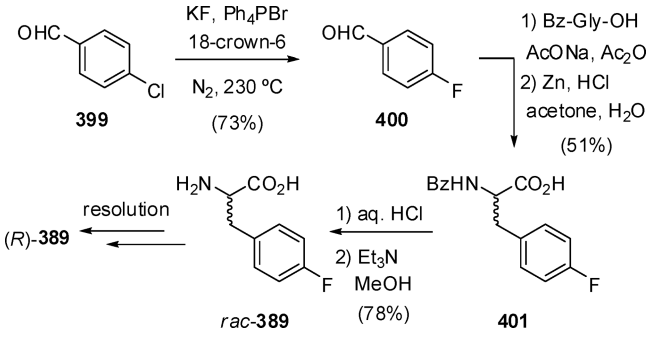

unnatural, tailor-made[340] amino acids play a rather crucial role. Their cost and availability are very important for successful structural optimization and overall cost structure. These issues are being addressed by the development of novel asymmetric approaches featuring operationally convenient conditions, simple reaction sequences, yet excellent stereochemical outcome.[341−351] In particular, chemical dynamic kinetic resolution of unprotected α-amino acids[352,353] and (*S*)/(*R*)-interconversion of natural amino acids[354−356] present some particularly practical solutions.

2.20. Ripasudil

Ripasudil (**402**), originally discovered at D. Western Therapeutics Institute (DWTI), was developed by Kowa Co. as an eyedrop formulation for the potential treatment of glaucoma and ocular hypertension (OH) (Figure 31). As a potent and selective Rho kinase (ROCK) inhibitor, ripasudil has neuro-

DOI: 10.1021/acs.chemrev.5b00392
Chem. Rev. 2016, 116, 422−518

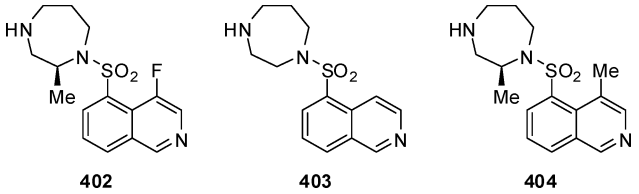

Figure 31. Structures of ripasudil (**402**), fasudil (**403**), and H-1152P (**404**).

protective effects,[357] and can reduce the intraocular pressure (IOP) by increasing the outflow of aqueous humor.[358] This unique mechanism of action suggests a promising prospect of ripasudil both as monotherapy and in combination with marketed antiglaucoma drugs.[359] Several phase III trials of the drug have been completed. In October 2013, Kowa submitted an application for approval of ripasudil hydrochloride dihydrate (K-115, trade name: Glanatec) in Japan for glaucoma and ocular hypertension, which was finally granted in September 2014.[360]

Ripasudil (**402**, IC_{50} = 0.03 μM) was developed from fasudil (**403**, IC_{50} = 0.50 μM),[361] the first protein kinase inhibitor approved for treatment of glaucoma and ocular hypertension in Japan.[362] Both of them belong to the family of isoquinolinesulfonamide derivatives. Early modifications of **403** (K_i = 0.35 μM) generated H-1152P (**404**, K_i = 1.6 nM),[363] which showed a 200-fold higher affinity than **403** for ROCK, but only 2- to 5-fold for protein kinase A (PKA).[364] According to the structure of the complex between H-1152P and ROCK, the C-4 methyl of the isoquinoline moiety limits the number of available low energy conformations and thus reduces the entropic cost during protein binding. In addition, the two extra methyl groups increase the van der Waals contacts with the protein.[365] An SAR study demonstrated that a methyl group is preferred at the C-2′ position of the 1,4-diazepane ring for its contribution to ROCK specificity, and the (*S*)-conformation displayed more potency.[362] The isoquinoline C-4 position was also crucial. Later research on the derivatives of **403** found that the incorporation of a fluorine atom at this position significantly improved the pharmacological action, which finally led to the discovery of ripasudil (**402**).[361] The crystal structure of ripasudil indicated a slight skew of the isoquinoline plane, which may be attributed to the strain induced by the bulky substituent on the sulfonyl group.[366]

Ripasudil was first synthesized using a convergent route from commercially available (*S*)-2-aminopropanol (**405**) as depicted in Scheme 56. The chiral 1,4-diazepane ring was constructed through a series of protection steps and *N*-alkylation with 3-aminopropan-1-ol (**408**) leading to acyclic precursor **410**, followed by intramolecular cyclization conducted with sodium hydride to give **411**. Removal of the Cbz protecting group afforded **412**, and its sulfonylamidation with 4-fluoroisoquinoline-5-sulfonyl chloride (**413**) in the presence of triethylamine and final deprotection using TFA furnished ripasudil (**402**).[367]

Alternatively, a multikilogram production process of ripasudil was also reported through a linear route avoiding most of the protection and deprotection steps required in the aforementioned synthetic protocol. Thus, sulfonylamidation of amino alcohol **405** with the hydrochloride salt of fluorine-containing isoquinoline **413** first provided **414** (Scheme 57). After mesylation and in situ N-alkylation with 3-aminopropan-1-ol (**408**), the product was purified using oxalic acid to give the salt **415**. Basification and subsequent intramolecular Mitsunobu

Scheme 56. Convergent Synthetic Route to Ripasudil (402)

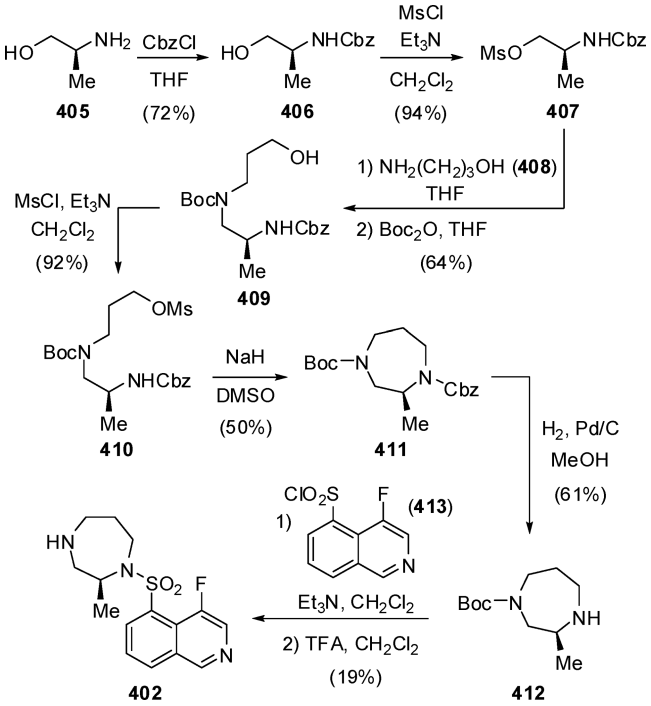

Scheme 57. Linear Synthetic Route to Ripasudil (402)

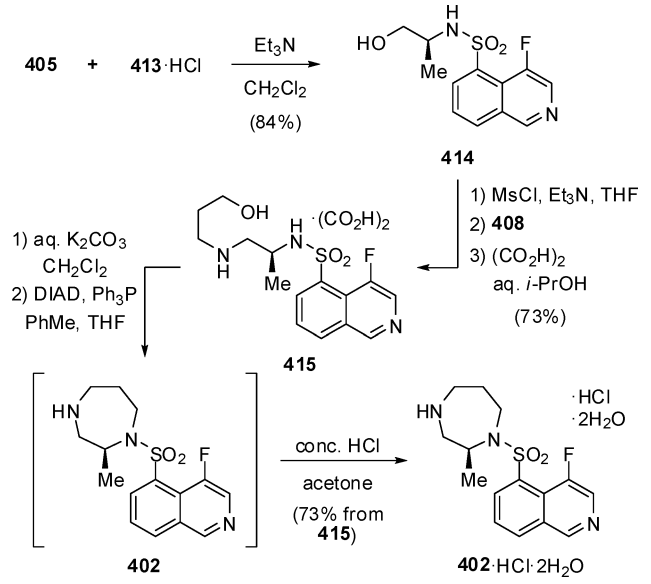

reaction closed the diazepane cycle, and ripasudil was finally obtained as its hydrochloride dihydrate salt after treatment with concentrated HCl.[361]

More recently, a practical method for the multikilogram production of ripasudil and its precursor **412** was developed. N-Nosylation of amino alcohol **405** followed by O-mesylation afforded the protected derivative **417**, which was then coupled with **408** to give **418** in good yield (Scheme 58). Fukuyama–Mitsunobu cyclization of **418** led to diazepane **419**, which was protected as its *N*-Boc derivative **420**. Next, removal of the nosyl group in **420** was conducted with thiophenol and potassium carbonate to afford intermediate **412**. Finally, sulfonamide formation by reaction between **412** and **413** yielded the protected form of ripasudil **421** that was

DOI: 10.1021/acs.chemrev.5b00392
Chem. Rev. 2016, 116, 422–518

Scheme 58. Improved Multikilogram-Scale Synthesis of 412 and Ripasudil (402)

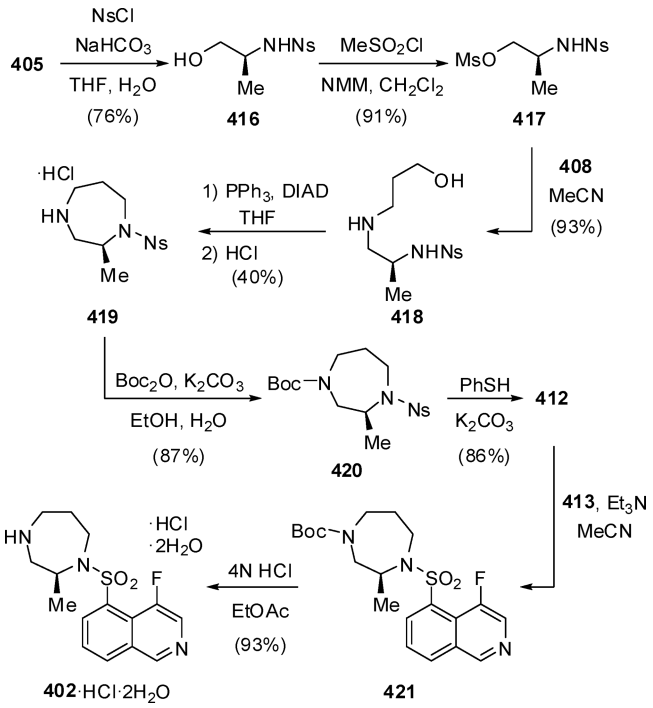

transformed into the salt **402**·HCl·2H_2O by acidic hydrolysis.[368,369]

The expensive fluorinated isoquinoline **413** can be prepared by one-pot regioselective chlorosulfonylation of 4-fluoroisoquinoline (**422**) (Scheme 59). Treatment with concentrated

Scheme 59. Preparation of Intermediate 413 by Regioselective Chlorosulfonylation

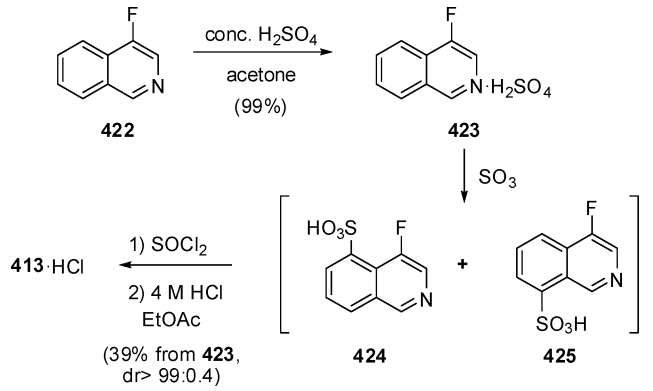

sulfuric acid in acetone yielded 4-fluoroisoquinoline sulfate (**423**), which was reacted with sulfur trioxide and then $SOCl_2$, and finally the pure salt **413**·HCl was isolated as crystals by using 4 N HCl/EtOAc.[361]

2.21. Canagliflozin and Ipragliflozin

Sodium glucose cotransporter-2 (SGLT2) is the major pathway of glucose reabsorption in the kidney.[370] Approximately 90% of renal glucose reabsorption is facilitated by SGLT2 in the S1 segment of the proximal tubules of the kidney, whereas the remaining 10% is assisted by SGLT1 in the distal S3 segment of the proximal tubules.[371] Inhibition of SGLT-2 decreases renal glucose reabsorption in the nephron, thus increasing urinary glucose excretion (UGE) and decreasing elevated circulating glucose levels in patients with type 2 diabetes mellitus (T2DM), which is a distinct mechanism of action that reduces blood glucose levels independently of insulin secretion.[372] Therefore, inhibition of SGLT2 has become an important therapeutic target for treating T2DM.[373]

Canagliflozin (JNJ-28431754, **426**) was developed and launched by Johnson & Johnson in collaboration with Mitsubishi Tanabe Pharma as an orally active potent and highly specific SGLT-2 inhibitor (Figure 32).[374] On the other

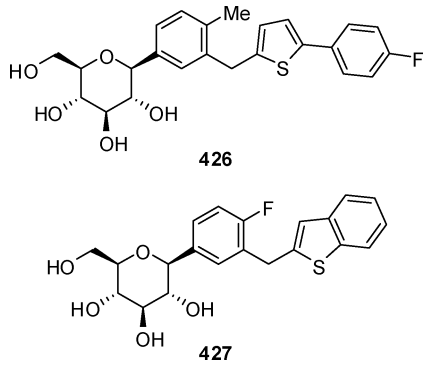

Figure 32. Structures of canagliflozin (**426**) and ipragliflozin (**427**).

hand, ipragliflozin (ASP-1941, **427**) was developed by Astellas Pharm and Kotobuki Pharmaceutical for the same goal.[375] Both inhibitors share an aryl *C*-glucoside fragment linked to a thiophene or benzothiophene moiety, also containing a fluorine atom, even if located on different positions of the scaffold. Canagliflozin (trade name: Invokana) was FDA-approved on April 2013 for the treatment of adult patients with T2DM, whereas ipragliflozin (trade name: Suglat) received approval in Japan on January 2014 for the same indication.[376] Kotobuki is also investigating ipragliflozin for the potential treatment of nonalcoholic steatohepatitis.

The structure of both canagliflozin and ipragliflozin derived from phlorizin (**428**), a natural nonselective *O*-glucoside SGLT2 inhibitor (Scheme 60).[377] Mitsubishi Tanabe Pharma disclosed the first-generation of *O*-glucoside SGLT2 inhibitors, including T-1095A (**429**) and T-1095 (**430**), that were designed to be more resistant to disaccharidases and more specific to SGLT2 than phlorizin.[378] To overcome degradation and attain sufficient stability, the second-generation SGLT2 inhibitors, such as **431**, adopted a phenyl *C*-glucoside structure. Researchers found that the linkage connecting the aromatic rings B and C could improve the activity, when it was at *meta*-position to the glycoside of the benzene ring B. In addition, the *C*-glucoside inhibitors had much better bioavailability and metabolic stability.[379] The synthesis and structure−activity relationships (SARs) of *C*-glucosides bearing various heteroaromatics as SGLT2 inhibitors were next explored, although replacing the central benzene ring with various heterocycles caused a decrease in SGLT2 inhibitory activity. However, insertion of heteroaromatics instead of the terminal benzene ring, as in structure **432**, proved to be a viable strategy, eventually leading to the discovery of canagliflozin (**426**) containing a thiophene ring as the most promising candidate of all the inhibitors studied.[380] In a parallel research, benzothiophene derivative **433** was also a potent and selective SGLT2 inhibitor, and its further optimization culminated in the discovery of ipragliflozin (**427**). The fluorine substituent in

DOI: 10.1021/acs.chemrev.5b00392
Chem. Rev. 2016, 116, 422−518

Scheme 60. Discovery of Canagliflozin (426) and Ipragliflozin (427)

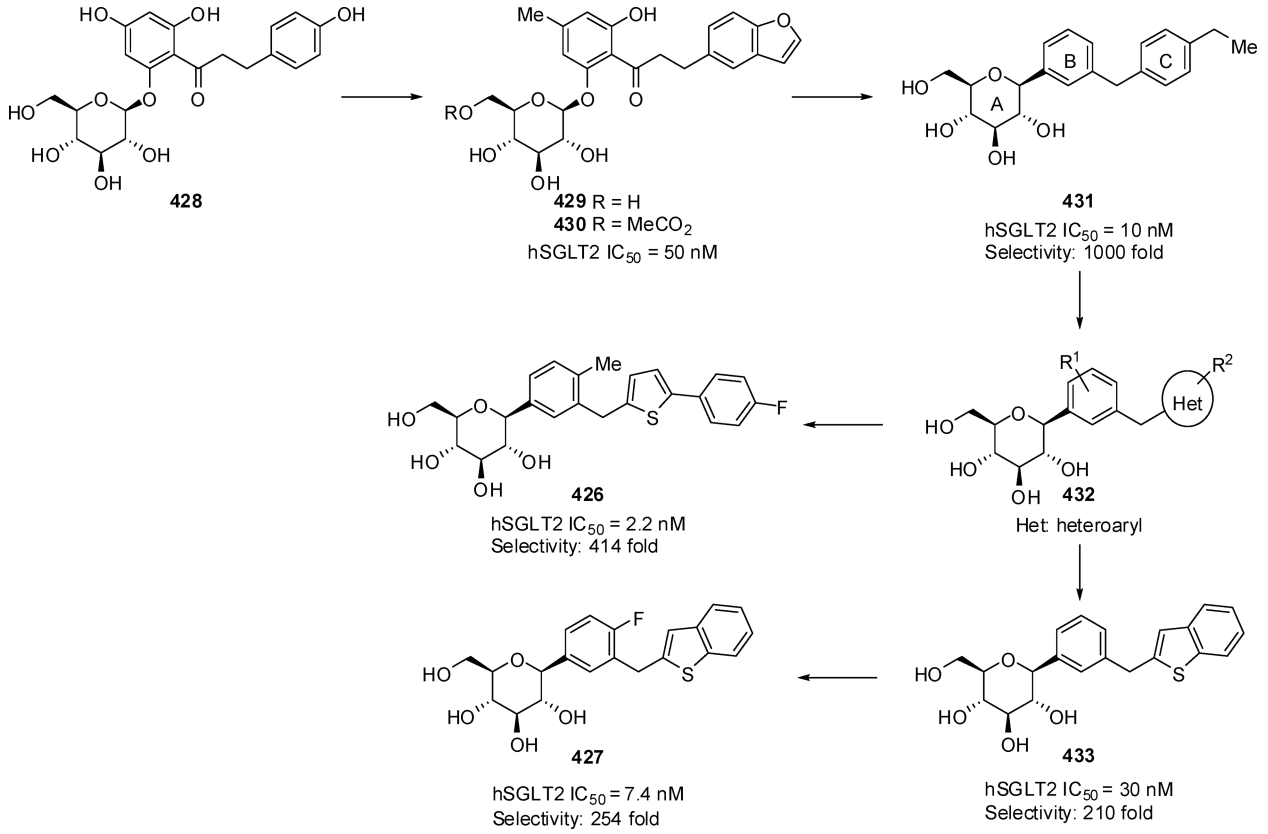

Scheme 61. Initial Synthesis of Canagliflozin (426)

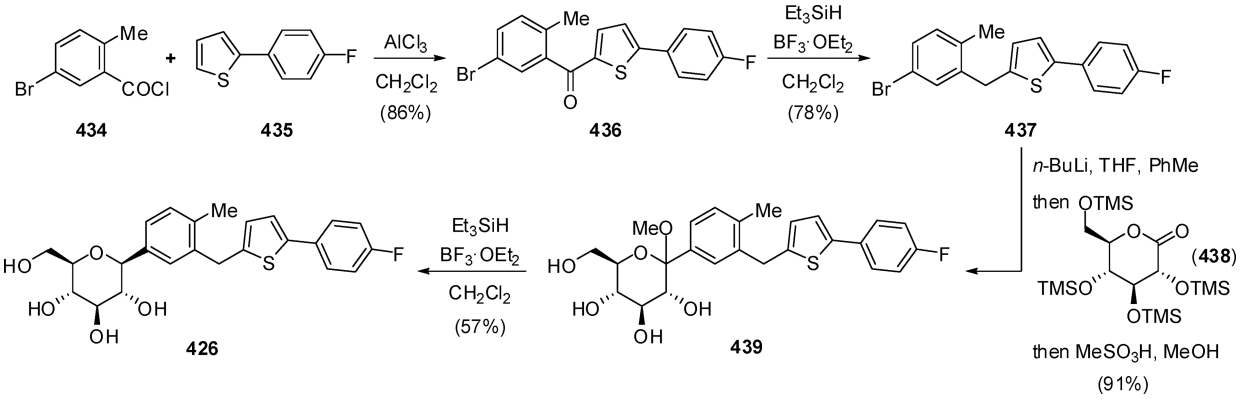

ipragliflozin enhanced SGLT2 inhibitory activity and selectivity against SGLT1 compared to the lead compound **433**.[375]

Canagliflozin reduced glycosylated hemoglobin (HbA_{1c}) levels in a dose-dependent manner.[381] The pharmacokinetics of canagliflozin are disturbed by renal function, with little reducing in renal clearance detected. No effect of renal impairment on the maximum concentration was observed. Renal impairment decreased the capability of canagliflozin to stimulate UGE.[382] During phase III studies of T2DM patients on a diversity of antihyperglycemic agents, canagliflozin significantly enhanced glycemic control, decreased body weight and blood pressure (BP), and was usually well tolerated with a low risk of hypoglycaemia.[383]

On the other hand, the safety, tolerability, pharmacokinetic, and pharmacodynamic profiles of ipragliflozin demonstrated that this novel SGLT2 inhibitor was absorbed rapidly, taking approximately 1 h to reach the maximum concentration, and the area under the concentration−time curve and maximum ipragliflozin concentration at steady state displayed dose linearity.[384−386] Ipragliflozin displayed a good pharmacokinetic profile, long half-life (3.61 h), and excellent bioavailability (71.7%) in rats.

The initial synthesis of canagliflozin is illustrated in Scheme 61. Thiophene aglycon **437** was accessed by Friedel−Crafts acylation of 2-(4-fluorophenyl)thiophene (**435**) with 5-bromo-2-methylbenzoyl chloride (**434**), followed by deoxygenation of ketone **436** with Et_3SiH and $BF_3{\cdot}OEt_2$. The aryllithium reagent derived from **437** was reacted with 2,3,4,6-tetra-*O*-(trimethylsilyl)-*β*-D-gluconolactone (**438**) to afford *C*-glucoside **439** after in situ silyl deprotection with $MeSO_3H$. Finally, reduction of the methyl ether linkage using again a combination of Et_3SiH

DOI: 10.1021/acs.chemrev.5b00392
Chem. Rev. 2016, 116, 422−518

and $BF_3{\cdot}OEt_2$ produced the target compound canagliflozin (**426**).[380]

Ipragliflozin was also synthesized using a similar approach relying on aryllithium additions followed by deoxygenation steps. First, lithiation of benzothiophene (**441**) and subsequent addition to 5-bromo-2-fluorobenzaldehyde (**440**) yielded the corresponding alcohol, which was reduced with Et_3SiH and $BF_3{\cdot}OEt_2$ to give aglycon **442** (Scheme 62). Next, lithium–halogen exchange in **442**, further addition to benzyl-protected gluconolactone **443**, and, once again, Et_3SiH-mediated deoxygenation furnished compound **444**. Successive removal of the benzyl groups in **19** afforded ipragliflozin (**427**).[375]

Scheme 62. Synthetic Route to Ipragliflozin (427)

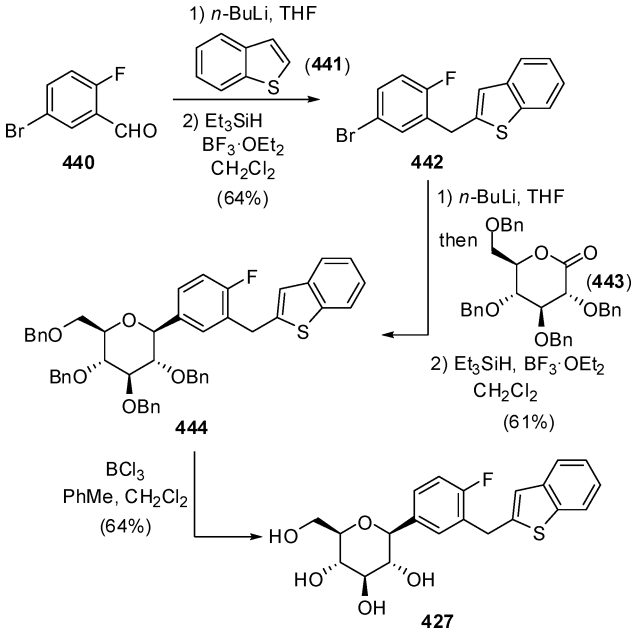

A stereoselective method for the asymmetric synthesis of β-arylated glycosides has been also applied to the preparation of canagliflozin. Thus, lithiation of aryl iodide **445** using *n*-BuLi was followed by transmetalation with $ZnBr_2$–LiBr to the reactive intermediate **447** (Scheme 63). Coupling of **447** with glycosyl bromide **448** afforded the tetrapivaloyl derivative of canagliflozin **449**, which was finally deprotected with NaOMe to the target product.[387] Very recently, a similar approach relied on the transmetalation of lithium reagent **446** with $AlCl_3$ and the further reaction of the resulting arylalane with a suitable 1,6-anhydroglucose derivative, ultimately leading to a new synthesis of canagliflozin.[388,389]

2.22. Trelagliptin

Dipeptidyl peptidase IV (DPP IV) is responsible for the degradation of the incretin peptide hormones, such as glucagon-like peptide-1 (GLP-1) and glucose-dependent insulinotropic polypeptide (GIP), to regulate blood glucose levels. Inhibition of DPP IV is a promising new approach for the treatment of type 2 diabetes mellitus (T2DM). Several classes of DPP IV inhibitors have been developed in recent years, and some of them received approval in the last years.[390−392] In this context, Takeda has developed trelagliptin (SYR-472, **450**) as a novel highly potent and selective DPP IV inhibitor, for the potential once-weekly oral treatment of T2DM (Figure 33).[393] Trelagliptin shares its pyrimidinedione-based scaffold with the nonfluorinated analogue alogliptin (**451**), a previously marketed antidiabetes drug also developed by Takeda. Trelagliptin improved glycemic control and was well tolerated in Japanese patients with T2DM in phase II studies. Once-weekly or longer acting oral antidiabetic therapies are not currently available for T2DM, and therefore trelagliptin could provide clinicians and patients with an alternative oral antidiabetic therapy.[394] In March 2014, the efficacy and safety of once-weekly administration with trelagliptin in T2DM patients was confirmed in phase III clinical trials in Japan, indicating that the once-weekly treatment with trelagliptin showed similar efficacy and safety to alogliptin once daily. Compared with placebo, both active groups had significantly reduced HbA_{1C} levels at the end of the treatment, and the frequency of adverse events was similar between active groups.[395] Very recently (March 2015), the Japanese authorities approved the use of trelagliptin succinate (trade name: Zafatek) for treating T2DM.

Scheme 63. Alternative Approach to Canagliflozin (426)

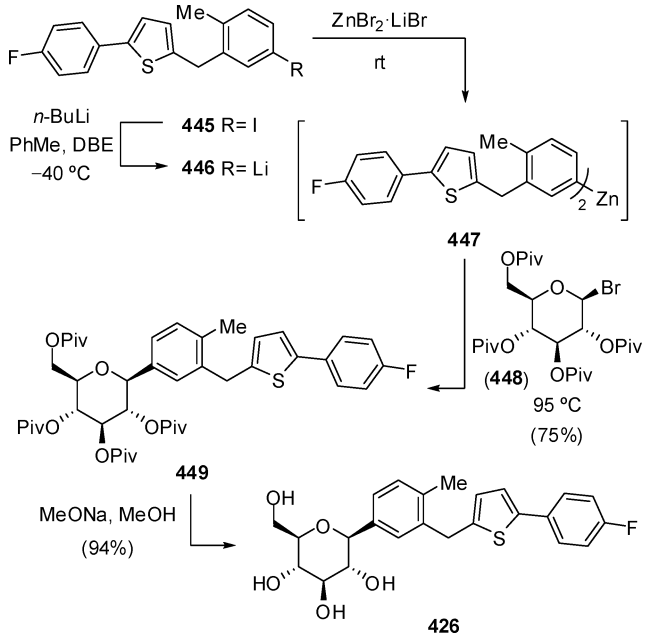

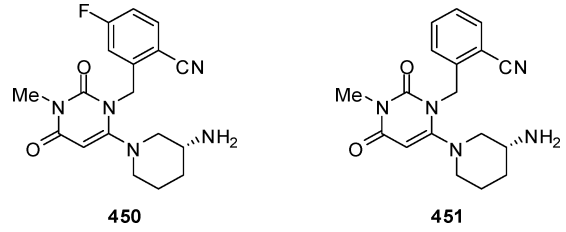

Figure 33. Structures of trelagliptin (**450**) and alogliptin (**451**).

Trelagliptin exhibited high DPP IV inhibitory activity with an IC_{50} value of 4 nM and was significantly selective for DPP IV against DPP VIII (>25000-fold). Both trelagliptin and alogliptin display similar binding modes with the DPP IV active sites. The fluorocyanobenzyl moiety occupies the hydrophobic S1 pocket and interacts with Arg-125. The amino group forms a salt bridge and hydrogen bonding interactions with Glu-205, Glu-206, and Tyr-662, respectively. Nevertheless, the introduction of the fluorine atom in the phenyl ring improved the inhibitory activity against DPP IV

DOI: 10.1021/acs.chemrev.5b00392
Chem. Rev. 2016, 116, 422−518

and lengthened the half-life. Trelagliptin exhibited good pharmacokinetic properties in dogs and monkeys with half-lives of 4.8 and 6.2 h, respectively. It enhanced glucose tolerance and postprandial plasma insulin concentrations in Zucker rats. Trelagliptin significantly reduced the HbA1c concentrations in a dose-dependent manner.

The synthetic route to trelagliptin is depicted in Scheme 64. 6-Chloro-3-methyluracil (**452**) was used a key starting material

Scheme 64. Synthetic Route to Trelagliptin (450)

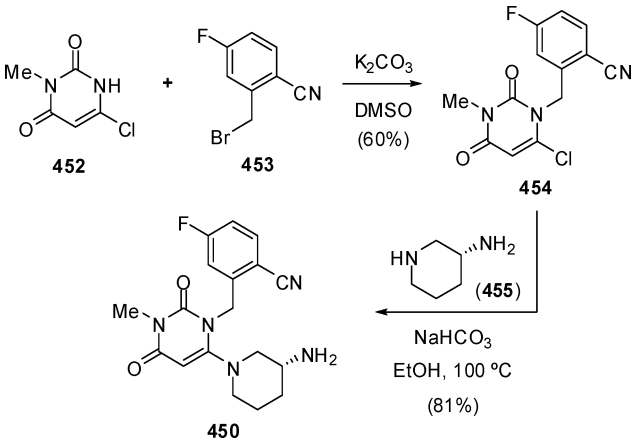

which upon N-benzylation with 2-(bromomethyl)-5-fluorobenzonitrile (**453**) gave compound **454**, which was further reacted with (*R*)-3-aminopiperidine (**455**) to afford trelagliptin (**450**).[393,396]

3. COMPOUNDS CONTAINING TWO FLUORINE ATOMS

3.1. Omarigliptin

Omarigliptin (MK-3102, **456**) is a novel potent, selective, and long-acting dipeptidyl peptidase IV (DPP IV) inhibitor for the potential once-weekly oral treatment of type 2 diabetes mellitus (T2DM). (Figure 34).[397] Omarigliptin (trade name: Marizev) was developed by Merck & Co., and very recently (September 2015) received approval from the Japanese authorities.[398]

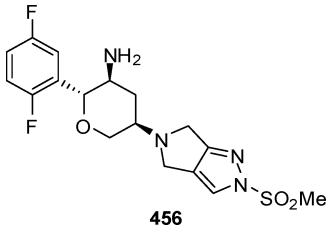

Figure 34. Structure of omarigliptin (**456**).

Sitagliptin (**7**)[399] was the first commercialized DPP IV inhibitor, approved by the FDA on Oct 17, 2006 (Scheme 65).[44] In order to prolong the half-life of sitagliptin, which is amenable for once-weekly dosing, several classes of novel DPP IV inhibitors have been developed.[390,400] The cyclohexylamine derivative **457**, which is a structurally distinct rigid analogue of sitagliptin, is also a potent and selective DPP IV inhibitor.[401] However, it blocks the human potassium channel hERG (human ether-a-go-go related gene) at low micromolar concentrations below the desired standard (IC_{50} > 30 μM),[402] resulting in QTc prolongation in a cardiovascular dog model (CV-dog). The corresponding tetrahydropyran analogue **458** has reduced basicity compared to the cyclohexylamine analogue **457** and, as a result, improved hERG selectivity. Compound **459** has excellent DPP IV inhibition activity and high hERG selectivity; however, it was unstable and led to observed undesirable circulating compound in both rats and dogs. Several attempts were made to improve the metabolic stability, and pyrrolopyrazole analogue **460** was found to be stable and no oxidation product was observed, when dosed in rats and dogs.[403] Introduction of a methylsulfonyl group led to omarigliptin (**456**), showing excellent DPP IV inhibitory activity with high hERG selectivity. Omarigliptin exhibited an attractive pharmacokinetic profile suitable for once-weekly dosing in humans. High oral bioavailability (rat, ~100; dog, ~100) and exposure [rat, 47.8 μM·h/(mg/kg); dog, 54.0 μM·h/(mg/kg)] was accompanied by a long half-life in rat and dog much better than sitagliptin (**7**). The X-ray crystal structure of fluoroomarigliptin (derivative containing the original 2,4,5-trifluorophenyl fragment) binded to DPP IV showed that the 2-F atom forms a hydrogen bond with the side chain of Arg-125, whereas the NH_2 group forms salt bridges with Glu-205 and Glu-206, and the pyrrolopyrazole moiety of omarigliptin is $\pi-\pi$ stacked against the side chain of Phe-357.[397]

The preparation of omarigliptin was designed through the prior access to pyrrolopyrazole intermediate **466** (Scheme 66). Commercially available Boc-protected ketone **461** was heated with neat *N*,*N*-dimethylformamide dimethyl acetal to form enamine **462**, which was subsequently heated with hydrazine and dehydrated by treatment with HCl. After neutralization, the free base pyrrolopyrazole **463** was obtained. Reprotection of the pyrrole nitrogen in **463** as its Boc derivative formed compound **464**, and its further condensation with methanesulfonyl chloride afforded a mixture of sulfonylated regioisomers. Final deprotection of **465** using benzenesulfonic acid produced the target methylsulfonylpyrrolopyrazole intermediate **466**.[397]

The rest of the synthetic route to omarigliptin is outlined in Scheme 67. Condensation of difluorinated aldehyde **467** with nitromethane provided nitroalcohol **468**, followed by oxidation with Dess–Martin periodinane (DMP) to form nitroketone **469**. Heating **469** with 3-iodo-2-(iodomethyl)-prop-1-ene afforded pyran **470**, which was reduced by sodium borohydride to give a 2:1 mixture of *cis* and *trans* diastereoisomers. After separation by column chromatography, the nitro group in the major product **471** was reduced using zinc and HCl, and the resulting amine was protected as its Boc derivative. The racemic material was separated by chiral HPLC to give enantiomerically pure compound **472**. Oxidation of **472** with OsO_4, followed by cleavage of the diol intermediate with $NaIO_4$, afforded ketone **473**. Reductive amination of tetrahydropyranone **473** with methylsulfonylpyrrolopyrazole **466** in the presence of $NaBH(OAc)_3$ and removal of the Boc group using H_2SO_4 afforded omarigliptin (**456**) after neutralization and recrystallization.[397]

3.2. Isavuconazole

Invasive fungal infections (IFIs) are a leading cause of illness and death in immunocompromised patients. Despite correct antifungal treatment with available agents, the morbidity and mortality rates of patients remain unacceptably high, especially due to the emergence of new pathogenic fungal species. Therefore, the development of new antifungal agents is still an urgent need.[404] Isavuconazole (BAL-4815, RO-0094815, **474**)

DOI: 10.1021/acs.chemrev.5b00392
Chem. Rev. 2016, 116, 422–518

Scheme 65. Discovery of Omarigliptin (456)

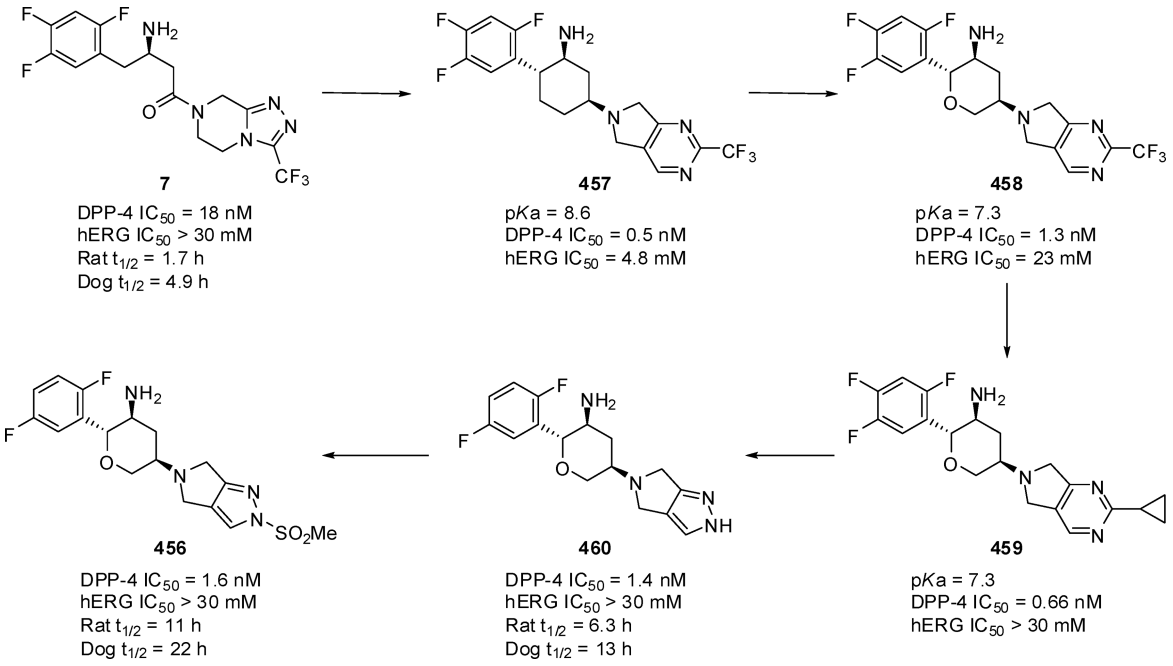

Scheme 66. Synthesis of Pyrrolopyrazole Fragment 466

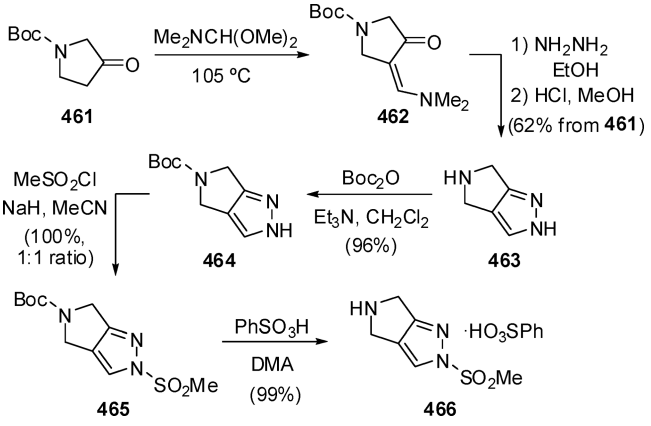

Scheme 67. Synthetic Route to Omarigliptin (456)

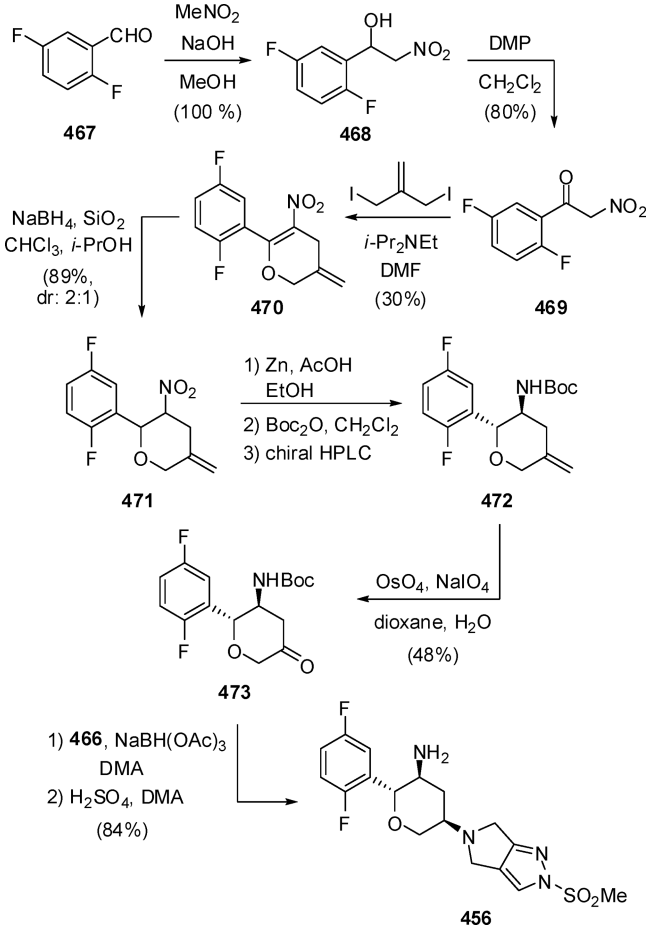

was developed by Basilea Pharmaceutica, a spin-off from Roche, in collaboration with Astellas as an inhibitor of sterol 14-α-demethylase involved in the biosynthesis of ergosterol, for the potential treatment of severe invasive and life-threatening fungal infections by disruption of fungal membrane structure and function (Figure 35).[405−407] Isavuconazole is administered as a prodrug, isavuconazonium (BAL-8557, RO-0098557, **475**), consisting of a triazolium sulfate salt. Very recently (March 2015), isavuconazonium (trade name: Cresemba) received approval by the FDA for the treatment of invasive aspergillosis and mucormycosis, while it is still in several clinical trials for other rare fungal infections.[408]

Isavuconazonium is water-soluble and can be rapidly and almost completely (>99%) metabolized by plasma esterase into the active drug isavuconazole after oral or intravenous administration.[409,410] Isavuconazole is widely distributed into tissues, with high protein binding and slow elimination. In an early study, the pharmacokinetic profile of isavuconazole has been evaluated in phase I trials in healthy volunteers with 100, 200, or 400 mg of isavuconazole. Peak plasma concentrations of isavuconazole were reached at 1.8−3 h after oral administration; the C_{max} ranged from 1.45 to 5.57 μg/mL (dose-dependent). Its AUC value increased slightly more than proportionally to the dose, and $t_{1/2}$ was very long (up to 56−77 h) with detectable drug seen in plasma up to 16 days

DOI: 10.1021/acs.chemrev.5b00392
Chem. Rev. 2016, 116, 422−518

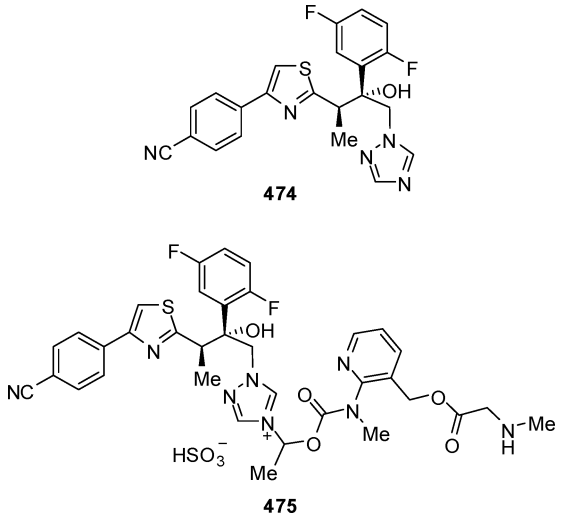

Figure 35. Structures of isavuconazole (**474**) and its prodrug isavuconazonium (**475**).

postdose, consistent with a high volume distribution and low systemic clearance.[405,411,412] Meanwhile, no significant food effect has been found with oral administration of isavuconazole, but it should not be administered with other medications which strongly inhibit the enzyme CYP3A4 due to the effect on plasma concentration.[409]

Isavuconazole is a novel broad-spectrum triazole agent that was developed to overcome some of the inherent limitations of current drugs including itraconazole and fluconazole. It demonstrated an excellent potency against a large number of clinically important invasive fungal pathogens, such as *Candida* spp., *Aspergillus*, *Cryptococcus*, and potentially the Mucorales. In vitro studies have illustrated that isavuconazole has promising antifungal activity against 118 isolates of *Aspergillus* species, such as *A. fumigatus*, *A. terreus*, *A. flavus*, and *A. niger*, including strains that were resistant to itraconazole, caspofungin, or amphotericin B. Isavuconazole was also evaluated against 296 clinical isolates of *Candida* spp. from bloodstream infections in vitro. Comparing the in vitro activity with fluconazole, itraconazole, voriconazole, and amphotericin B indicated that isavuconazole has good activity against all *Candida* species, including those that were inherently less susceptible to fluconazole (such as *C. glabrata* and *C. krusei*). Considering the minimum inhibitory concentrations (MIC) values, the activity of isavuconazole was comparable to that of amphotericin B, itraconazole, and voriconazole and superior to that of fluconazole.[410,411,413]

As shown in Scheme 68, isavuconazole could be prepared from commercially available chiral starting material (*R*)-methyl lactate (**476**). First, reacting **476** with morpholine gave amide **477**, which was further protected as its TPH derivative **478**. Addition of the Grignard reagent **479** prepared from 2-bromo-1,4-difluorobenzene afforded ketone **480**, which was subjected to a Corey−Chaykovsky epoxidation leading to a mixture of diastereomeric oxiranes **481**. Ring-opening in **481** with 1,2,4-triazole led to alcohol **482**, and after removal of the TPH group the diastereomeric mixture was separated by column chromatography. Next, intramolecular displacement on the mesylate derived from **483** produced oxirane **484**, and its nucleophilic ring-opening with TMSCN yielded chiral cyanohydrin **485**. The latter compound was reacted with diethyl dithiophosphate to afford the corresponding thioamide **486**, and finally reaction with 2-bromo-4′-cyanoacetophenone (**487**) formed the thiazole ring to produce the target product isavuconazole (**474**).[414,415]

3.3. Dolutegravir

The discovery of integrase inhibitors as a new class of human immunodeficiency virus (HIV) inhibitors has become crucial for the development of new antiretroviral drugs over the last two decades, and hence acquired immune deficiency syndrome (AIDS) is now becoming a manageable chronic disease. Based

Scheme 68. Synthetic Route to Isavuconazole (474)

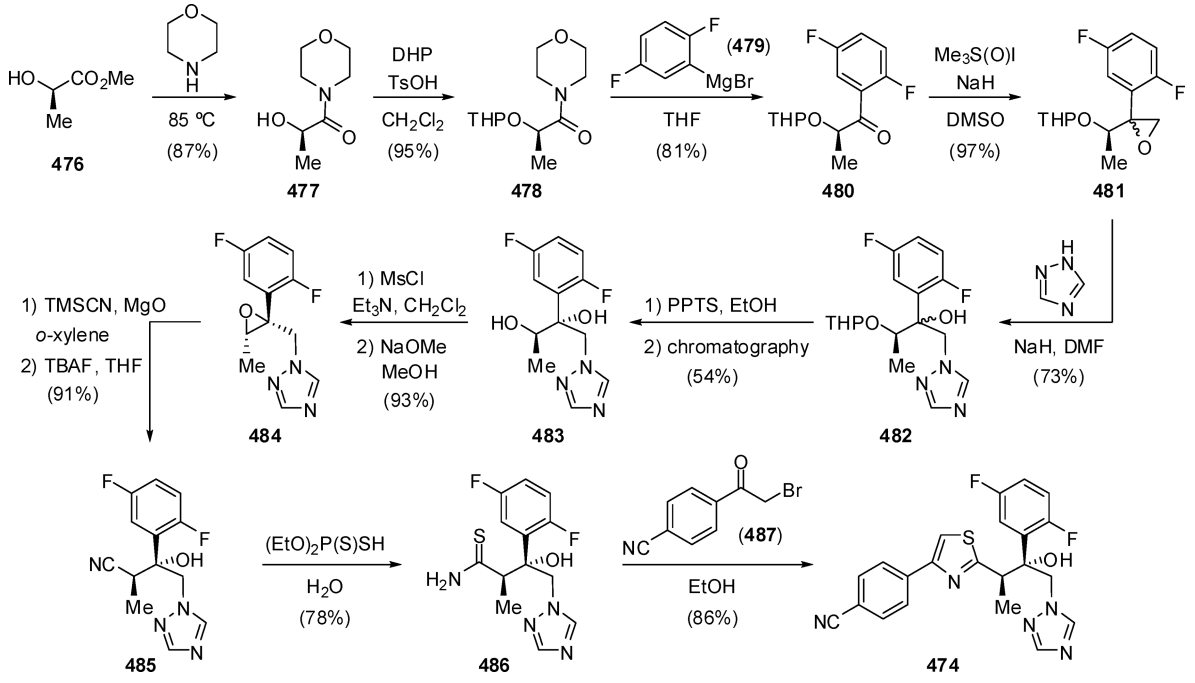

DOI: 10.1021/acs.chemrev.5b00392
Chem. Rev. 2016, 116, 422−518

on the pharmacophore, numerous two-metal chelating scaffolds were pursued, and successful examples of this approach include raltegravir (**308**) as well as elvitegravir (**309**), which have been approved as integrase inhibitors by the FDA (see section 2.15).[416] While both raltegravir and elvitegravir are valued components for combination therapy, they have some limitations and leave room for further improvements. For example, raltegravir requires a high dose of 400 mg twice daily.[417] In addition, three major mutation pathways result in substantial loss of potency of raltegravir and thereby render it ineffective against these viruses.[418,419] On the other hand, treatment with elvitegravir also showed slightly different resistance modes.[420] One big advantage of elvitegravir over raltegravir is the option for once-daily dosing. However, this requires the use of a pharmacokinetic boosting agent such as ritonavir or cobicistat to inhibit cytochrome P450 (CYP3A4).[421] In this context, Shionogi and GlaxoSmithKline (GSK) started their studies aiming at the development of more potent integrase inhibitors, which would allow once-daily doses (<100 mg) without the need for pharmacokinetic boosting, and a lack of cross-resistance to existing agents.[422] As a result, dolutegravir (S/GSK1349572, **488**) was approved by the FDA in 2013 as the third integrase inhibitor for HIV treatment (trade name: Tivicay) (Figure 36).

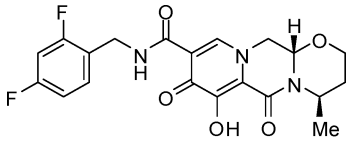

488

Figure 36. Structure of dolutegravir (**488**).

At the beginning of the study, compound **489** showed remarkable antiviral potency against wild-type HIV-1 virus with encouraging pharmacokinetic profiles from just the minimum pharmacophore elements consisting of a 2-(methoxycarbonyl)-3-hydroxy-4-pyridone moiety as a basic chelating unit and an *N*-(4-fluorobenzyl)carboxamide fragment to occupy the hydrophobic site (Figure 37).[423] Since **489** has an ester group at the C2 position to coordinate with a metal (Mg^{2+}) cofactor in the active site of the enzyme, amide modifications of **489** were expected to be useful. However, the potencies of the amide derivatives were remarkably reduced in both enzymatic and antiviral assays. Then, antiviral profiles of bicyclic and tricyclic series were examined.[424] Bicyclic derivative **490** slightly improved antiviral potencies against wild type HIV-1 virus compared to the initial compound **489**. After a series of tricyclic analogues were synthesized, compound **491** showed high antiviral potencies against wild-type virus and excellent selectivity over cytotoxicity in addition to efficacy against Q148 K mutation which was the remaining issue left for monocyclic lead compound **489**. Although the virological advances of **491** were significant, these data were based on the racemic mixture. Therefore, the enantiomers (*R*)-**491** and (*S*)-**491** were isolated by chiral chromatographic separation of the *O*-benzyl protected precursor and subsequent deprotection via hydrogenolysis. It was anticipated that the hemiaminal stability of **491** would be an issue, but no interconversion was observed with the purified enantiomers. Notably, (*R*)-**491** and (*S*)-**491** had almost identical antiviral activities but significantly different protein binding shifts against the Q148 K mutation with the

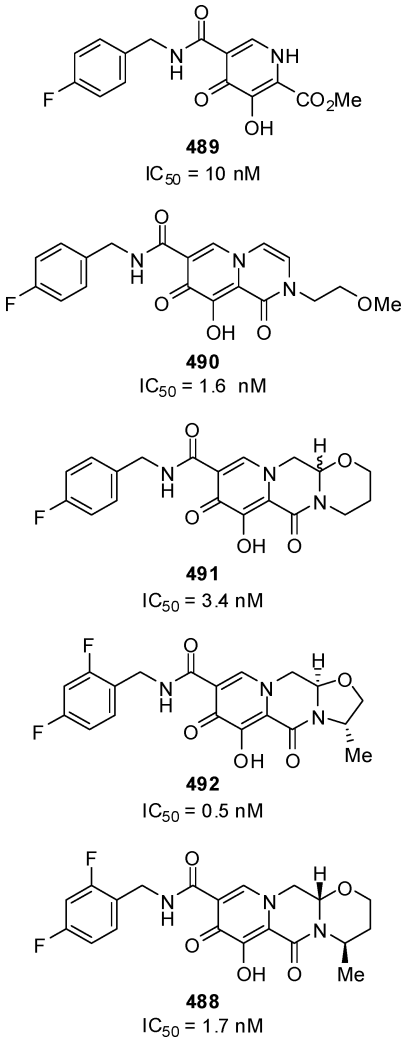

Figure 37. Evolution of the carbamoyl pyridone series to dolutegravir (**488**).

(*S*)-derivative having only a small potency change. These results led to S/GSK1265744 (**492**) and dolutegravir (**488**) by adding a chiral substituent into the system in a stereocontrolled manner and by changing the 4-fluorobenzyl group by 2,4-difluorobenzyl, since the latter was slightly more potent overall with a similar pharmacokinetic profile.[425] Both the six-membered-ring derivative **488** and the five-membered-ring derivative **492** showed high potency, robust low-dose once-daily pharmacokinetics and associated clinical efficacy, and eventually were selected as clinical candidates. Furthermore, both compounds would not require the codosing of a pharmacokinetic enhancer.

The medicinal chemistry route to dolutegravir was carried out starting with commercially available maltol (**493**), which was protected as its benzyl ether followed by treatment with ammonia to provide pyridone intermediate **494** (Scheme 69). Bromination at the C-5 position of **494** was performed with NBS and was followed by Pd-catalyzed carbonylation of bromide **495** to give methyl ester **496**. Transformation of the 2-methyl group in **496** into 2-hydroxymethyl was carried out by protection of the 4-OH group with Ac_2O, oxidation of the pyridine nitrogen with *m*-CPBA, and finally rearrangement of the resultant *N*-oxide **498** in Ac_2O to give the hydroxymethyl compound **499** after selective removal of the acetyl group with

DOI: 10.1021/acs.chemrev.5b00392
Chem. Rev. 2016, 116, 422−518

Scheme 69. Medicinal Chemistry Route to Dolutegravir (488)

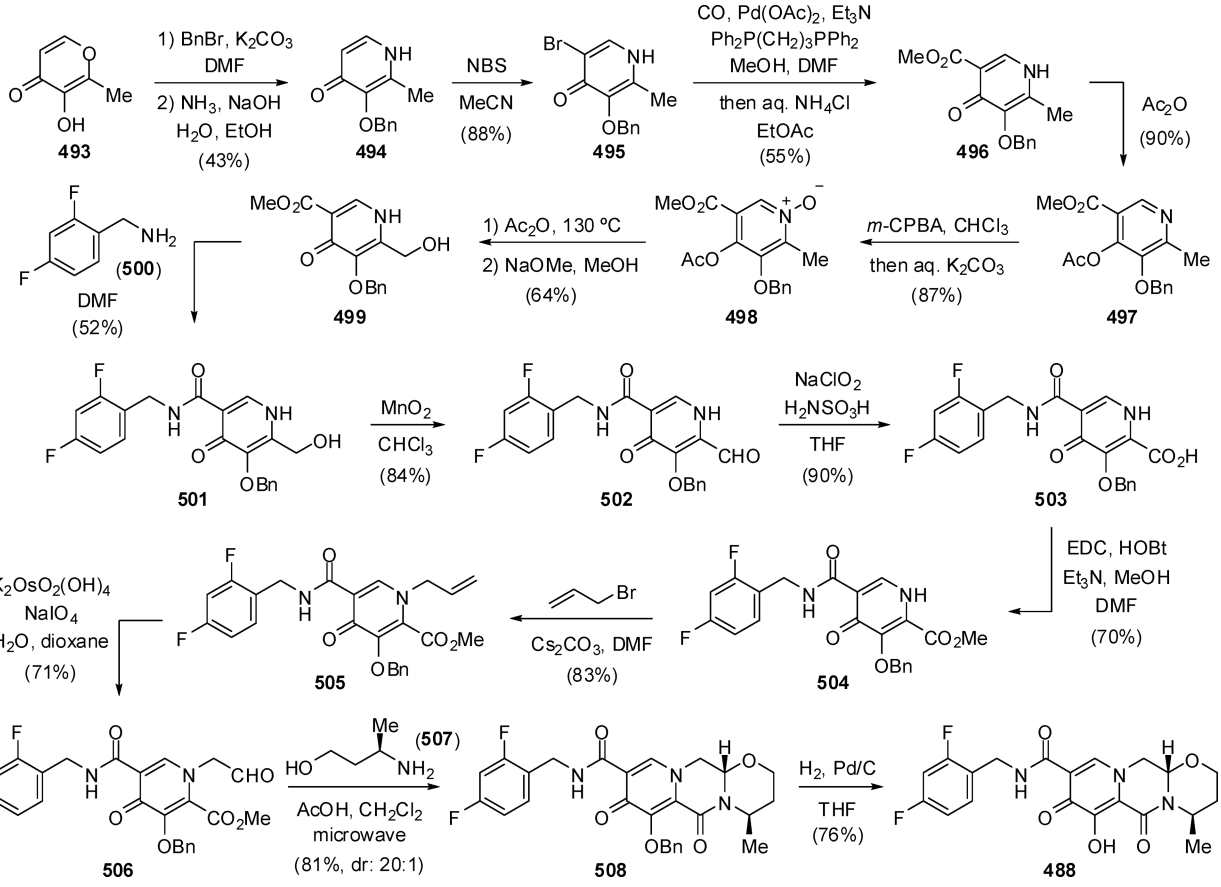

Scheme 70. Improved Synthesis of Dolutegravir (488)

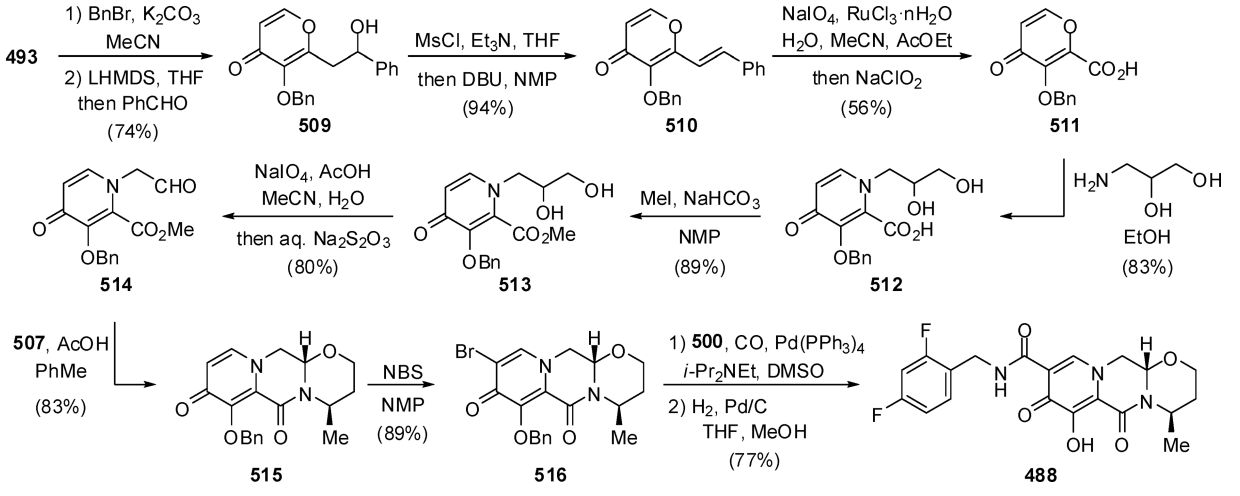

NaOMe. Next, the amide coupling of **499** with 2,4-difluorobenzylamine (**500**) afforded **501**, and the OH group was oxidized in a stepwise manner to produce the corresponding carboxylic acid **503** via aldehyde **502**. Methyl ester formation was performed by condensation of **503** with MeOH in the presence of EDCI/HOBt to give intermediate **504**. Further N-allylation of **504** and oxidative cleavage of **505** with OsO_4 and $NaIO_4$ gave the corresponding acetaldehyde intermediate **506**. Condensation of **506** with (*R*)-3-amino-butanol (**507**) took place in a microwave reaction apparatus at 140 °C for 25 min to give a 20:1 mixture of tricyclic derivatives. After purification of the major diastereomer **508** by silica gel chromatography, deprotection of the benzyl group was conducted under hydrogenolysis conditions to afford dolutegravir (**488**). Its relative and absolute stereochemistry was confirmed by single crystal X-ray analysis of the corresponding Na^+ salt.[424,425]

A more convergent synthesis of dolutegravir also started from maltol. Thus, the anion of *O*-Bn-maltol was reacted with benzaldehyde to produce intermediate **509**, followed by dehydration to give the styryl pyrone **510** in good yield (Scheme 70). Double bond cleavage in **510** was followed by

DOI: 10.1021/acs.chemrev.5b00392
Chem. Rev. 2016, 116, 422−518

further oxidation with $NaClO_2$ to give carboxylic acid **511**. Compound **511** was then reacted with 3-aminopropane-1,2-diol to convert the pyrone ring to the pyridone **512**. After esterification of **512**, oxidative cleavage of diol **513** was achieved in good yield to give the desired aldehyde **514**. The condensation reaction of aldehyde **514** with (*R*)-3-aminobutanol (**507**) afforded the chiral key intermediate **515**, which upon bromination with NBS led to compound **516**. Pd-catalyzed carbonylation with 2,4-difluorobenzylamine (**500**) and subsequent deprotection of the benzyl group provided the desired product, dolutegravir (**488**).[426,427]

Although the process shown in Scheme 70 improved much the original synthetic route, it still required lengthy steps and expensive reagents. A more concise and practical process for the synthesis of precursor **508** was reported later (Scheme 71).

Scheme 71. Practical Synthesis of Dolutegravir Precursor 508

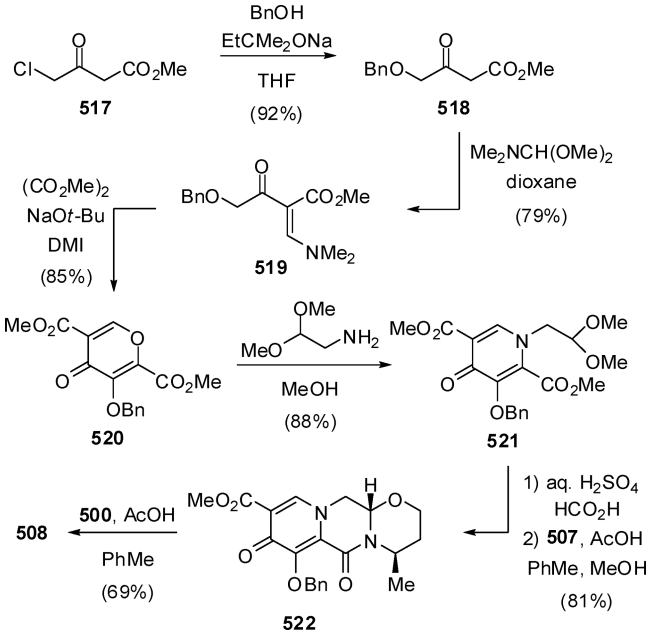

Thus, commercially available methyl chloroacetoacetate (**517**) was reacted with benzyl alcohol in the presence of sodium *tert*-pentoxide to give **518**. Condensation of **518** with dimethylformamide dimethyl acetal followed by treatment with dimethyl oxalate provided the pyrone intermediate **520**. Displacement of the oxygen of the pyrone ring was carried out with aminoacetaldehyde dimethyl acetal to give the pyridone derivative **521**. After hydrolysis of the acetal, the resulting aldehyde was reacted with (*R*)-3-aminobutanol (**507**) to provide the intermediate **522**. Amidation with 2,4-difluorobenzylamine (**500**) afforded the precursor **508**, which could be transformed into dolutegravir (**488**) in excellent yield.[428]

An alternative and attractive route to dolutegravir was also disclosed using a similar methodology, although the overall yield was somewhat lower. Condensation of ethyl acetoacetate (**523**) with dimethylformamide dimethyl acetal followed by treatment of **524** with lithium hexamethyldisilazide and ethyl oxalyl chloride provided pyrone **525** (Scheme 72). Again, conversion of the pyrone ring into a pyridone derivative was carried out by reaction with aminoacetaldehyde dimethyl acetal to give compound **526**. After bromination with NBS, acetal **527** was subjected to acidic hydrolysis and the resulting aldehyde

Scheme 72. Alternative Synthesis of Dolutegravir (488)

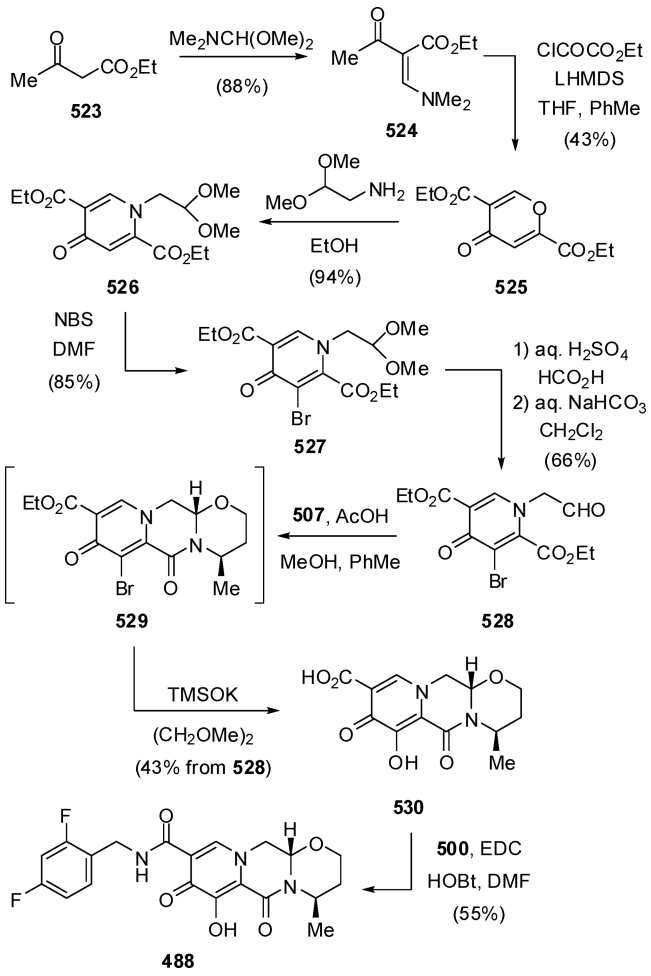

528 was reacted with (*R*)-3-aminobutanol (**507**) to provide intermediate **529**. The bromine atom was next substituted with potassium trimethylsilanolate to give **530**, which was condensed with 2,4-difluorobenzylamine (**500**) to give dolutegravir (**488**).[428]

The key starting material, 2,4-difluorobenzylamine (**500**), can be prepared from 2,4-difluorobenzonitrile (**536**) by transfer hydrogenation using a Ru catalyst in butanol (Scheme 73).[429] On the other hand, there are several known methods to produce nitrile **536**. One of the best ways involves the cyanation of 1-chloro-2,4-difluorobenzene (**534**),[430] which in turn is readily available by chlorination of 2,4-difluoronitrobenzene (**533**)[431] or oxidative chlorination of difluorobenzene (**535**).[432]

3.4. Ledipasvir

Ledipasvir (GS-5885, **539**) is an NS5A inhibitor that has the potential to be of utility in combination with direct acting antiviral agents (DAAs) of complementary mechanism in all-oral therapy for the treatment of hepatitis C virus (HCV) infection (Figure 38).[433] Ledipasvir was developed by Gilead Sciences and very recently (October 2014) received approval by the FDA coformulated with sofosbuvir (**239**) (see section 2.13) in a single tablet administered once daily (trade name: Harvoni) without interferon and ribavirin (RBV).

As described in section 2.13, the standard care for treating HCV genotype 1 (GT1) infection (both GT1a and GT1b as major subtypes) consisted of weekly pegylated interferon alfa

DOI: 10.1021/acs.chemrev.5b00392
Chem. Rev. 2016, 116, 422−518

Scheme 73. Synthesis of 2,4-Difluorobenzylamine (500)

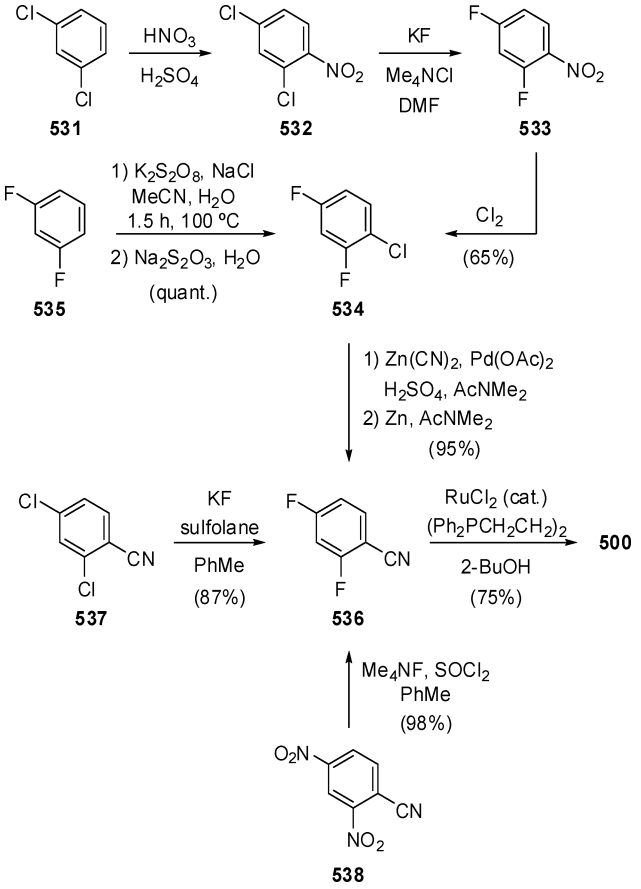

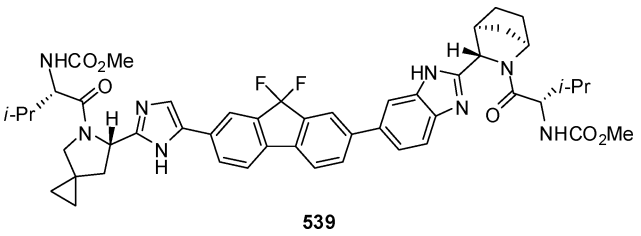

Figure 38. Structure of ledipasvir (**539**).

(PEG) injections and twice-daily oral RBV for 24 or 48 weeks (duration based on response-guided therapy).[248] However, this treatment is accompanied by considerable toxicity including flu-like symptoms, depression, and anemia.[434] Triple therapy containing PEG/RBV combined with the recently approved protease inhibitors telaprevir or boceprevir has improved the GT1 HCV sustained virologic response (SVR) rates to 66–79% for treatment of naive patients, but with increased toxicities including rash or anemia.[435] Therefore, extensive studies to identify safe oral drugs have been carried out for combination treatment of HCV infection. Research programs on NS5A inhibitors, as well as the inhibitors of NS3 protease and NS5B polymerase, were initiated at Bristol-Myers Squibb (BMS) with the goal of identifying an agent that could allow combination usage with DAAs having complementary mechanisms to achieve high SVR rates with a short-term treatment. The enzymatic activity of NS5A protein is still unknown, and the precise function of this remarkably enigmatic protein in virus replication and host cell modulation remains unclear.[436] However, the potential of NS5A as a target for HCV drug discovery attracted attention with the disclosure of the clinical efficacy of NS5A inhibitors. BMS-858 (**540**) was found by extensive screening of the GT1b replicon assay as a selective HCV inhibitor that targeted the NS5A protein (Figure 39).[437]

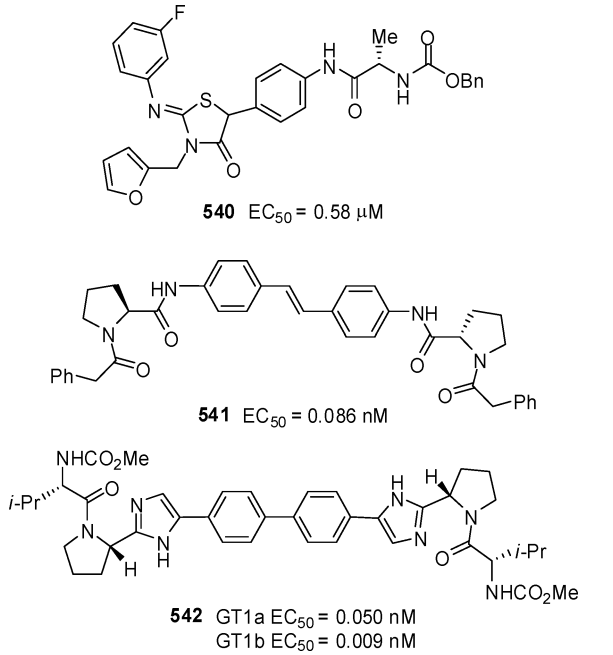

Figure 39. Evolution of NS5a inhibitors at BMS.

Enormous screening efforts led to dimeric series, which provided potent GT1b-active proline stilbenediamine diamide inhibitors, such as BMS-346 (**541**), discovered from the monomer series,[438] and highly potent GT1a- and GT1b-active bis-imidazole biphenyl inhibitors including daclatasvir (**542**) (BMS-790052, GT1a; EC_{50} = 50 pM), which achieved clinical proof-of-concept for the NS5A mechanism.[439,440] Daclatasvir is currently being studied in an ongoing phase III trial, where it is being investigated as part of an all-oral 3DAA regimen with other BMS investigational agents.

Scientists at Gilead Sciences found that an unsymmetrical core, having benzimidazole and imidazole fragments, showed a potent inhibitory effect after pursuing a number of symmetrical bis-benzimidazole cores.[433] Furthermore, in the unsymmetrical series, the fused central naphthyl ring afforded higher potency than in the symmetrical series. The importance of the lipophilicity in the linker was demonstrated by phenyl-alkyne inhibitors, and notably, the biphenyl inhibitor **543** provided the highest level of potency among many central connectors (Figure 40).[441] This prompted the study of constraint of the biphenyl to form tricyclic fused-ring systems, such as **544**–**547**. Initial SAR of central fused tricycles was carried out in a symmetric bis-imidazole series to obviate tricycle desymmetrization and simplify the synthesis. Fluorene ring-linked inhibitor **544** suffered a mild loss in potency relative to biphenyl **543**, and posed stability concerns, because the fluorene ring system readily underwent autoxidation upon standing. The oxidation product, fluorenone **545**, lost significant potency. Blocking the oxidation site with *gem*-dimethyl compound **546** caused even more loss of potency, giving some information that significant steric bulk of the fused linker is not well tolerated. Then, it was postulated that a smaller, lipophilic blocking group, such as a difluoromethylene group, might provide an optimal connector.

DOI: 10.1021/acs.chemrev.5b00392
Chem. Rev. 2016, 116, 422–518

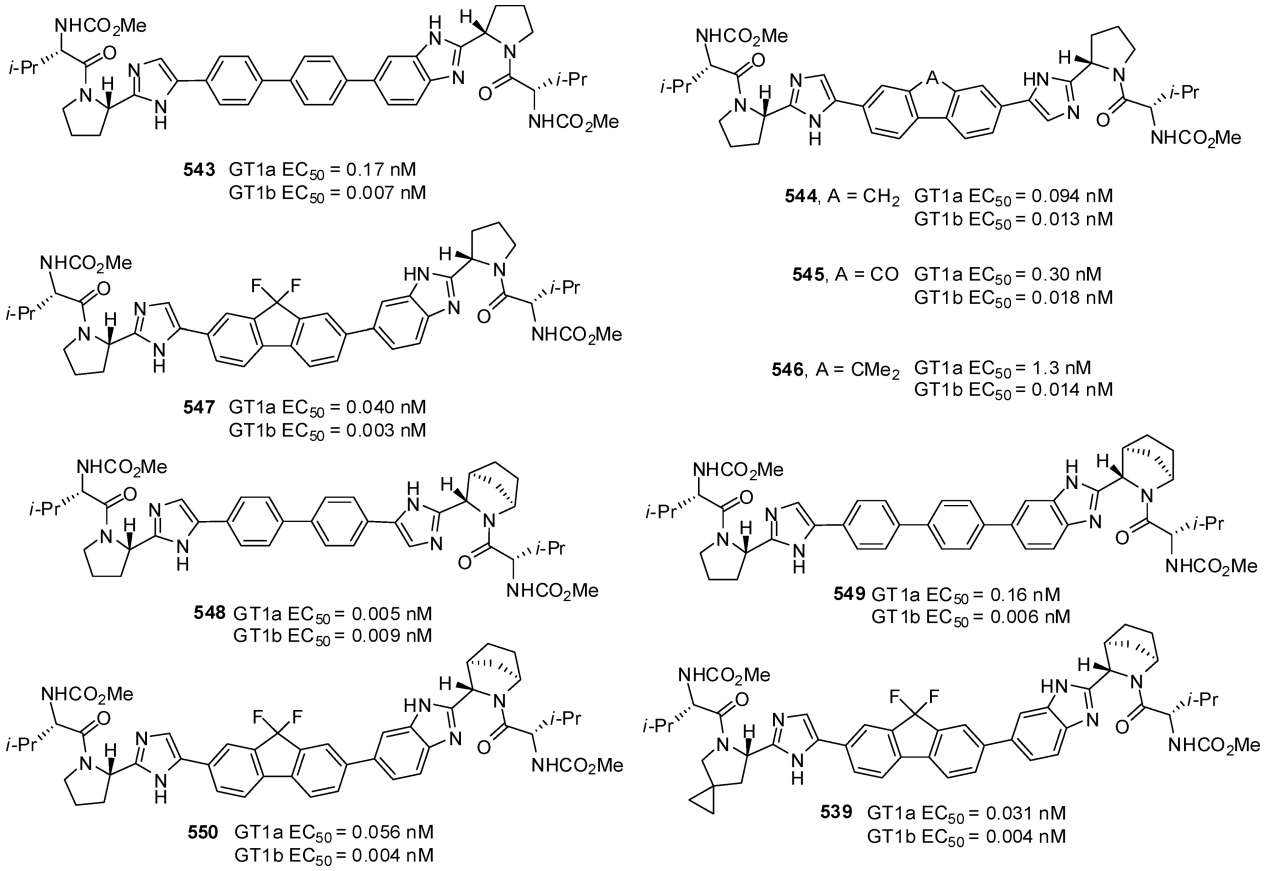

Figure 40. Discovery of ledipasvir (**539**).

This important difluoromethylene modification was directly introduced in the imidazole/benzimidazole series of interest. Use of the difluoromethylene connector produced the most potent inhibitor in the optimized unsymmetrical series, difluorofluorene **547**. The pharmacokinetics of **543** and **547** were measured in rats and dogs, and both inhibitors showed similar good half-lives in plasma, low systemic clearance (CL), and moderate volumes of distribution (Vss). Interestingly, the modest oral bioavailability (11%) of biphenyl inhibitor **543** was improved to over 35% in difluorofluorene **547**. Therefore, incorporation of a *gem*-difluoro moiety in compound **547** provided combined improvements in potency and bioavailability. Then, modifications of terminal groups were evaluated in the symmetric bis-imidazole system. It is worthy to note that [2.2.1]azabicyclic ring derivative **548** possessed a long half-life of 3 h in dog.

After finding the favorable pharmacokinetic properties of the [2.2.1]azabicyclic ring system in **548**, further studies were carried out to understand the SAR of the azabicyclic ring system in the context of an unsymmetrical core. The more synthetically accessible imidazole−biphenyl−benzimidazole core was chosen for this study. Eventually, they discovered matched and mismatched sets where the potency is remarkably better, when the [2.2.1]azabicyclic ring system is paired with the benzimidazole in compound **549**. Importantly, the extended pharmacokinetic half-life that the [2.2.1]azabicyclic ring system provided in symmetrical core inhibitor **548** was translated into unsymmetrical core inhibitor **549**; the plasma half-lives both in rat and in dog were improved in **549** over those of pyrrolidine analogue **543** having the same core. To improve the potency of **549**, biphenyl was replaced by difluorofluorene, affording inhibitor **550**. During the final optimization, replacement of the pyrrolidine in **550** by a spirocyclopropyl pyrrolidine afforded ledipasvir (**539**), the most potent inhibitor in the series. Ledipasvir has GT1a and GT1b EC_{50} values of 31 and 4 pM, respectively, and shows remarkable high potency and good pharmacokinetics and no adverse effect.[433,441] Ledipasvir was selected for clinical development in the treatment of HCV infection with a long half-life suitable for once-daily dosing.

In the initial synthesis of ledipasvir, difluorofluorene **552** was prepared by treatment of 2,7-dibromofluorenone (**551**) with Deoxo-Fluor (**21**) in good yield (Scheme 74). Stille coupling between **552** and tributyl-(1-ethoxyvinyl)-stannane provided an enol ether that was converted to bromoketone **553** upon treatment with NBS. Alkylation of Cbz-spirocyclopropyl-proline (**554a**) with **553** gave keto-ester **555**, which was cyclized to imidazole **556** upon heating in the presence of ammonium acetate. After deprotection of the Cbz group with HBr/AcOH, compound **556** was coupled with Moc-Val-OH to give intermediate **557**. Suzuki coupling of **557** with boronate **558** afforded **559** in good yield, which led to the desired ledipasvir (**539**) after deprotection of the Boc group followed by a second peptide coupling with Moc-Val-OH.[441]

One of the key intermediates, the tailor-made amino acid spirocyclic proline **554a**, was prepared from *N*-Boc-hydroxyproline (**560**) via oxidation and Wittig reaction followed by replacement of protecting group in **562** and then modified Simmons−Smith cyclopropanation and hydrolysis (Scheme 75).[442] Although *N*-Boc-4-methylene proline methyl ester is readily synthesized from 4-ketoproline methyl ester, the corresponding Wittig reaction afforded a racemic product

DOI: 10.1021/acs.chemrev.5b00392
Chem. Rev. 2016, 116, 422−518

Scheme 74. Initial Synthesis of Ledipasvir (539)

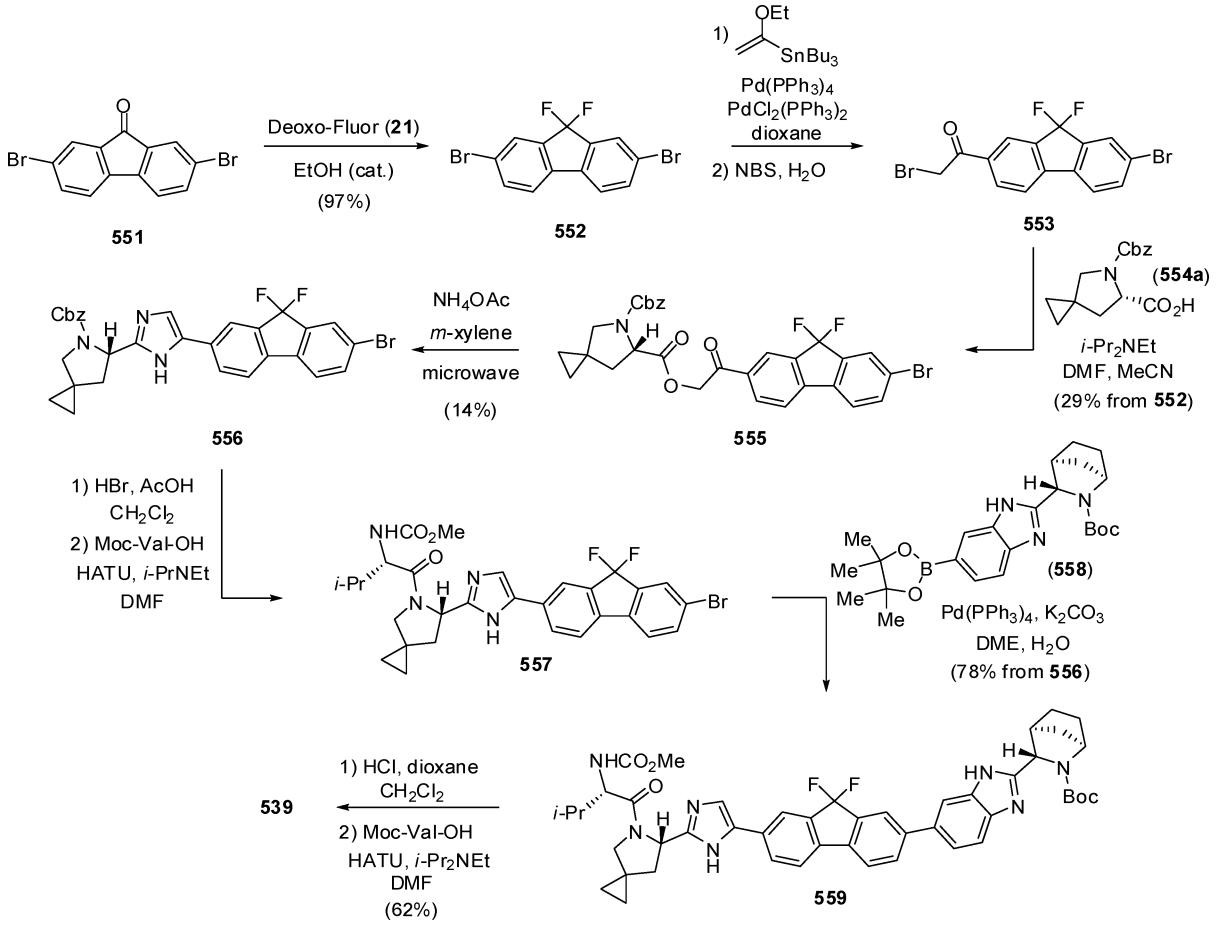

Scheme 75. Synthesis of Spirocyclopropyl Proline 554a

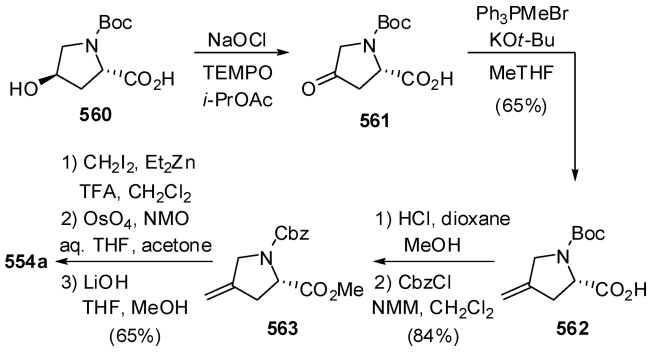

Scheme 76. Synthesis of [2.2.1]Azabicylic Intermediate 558

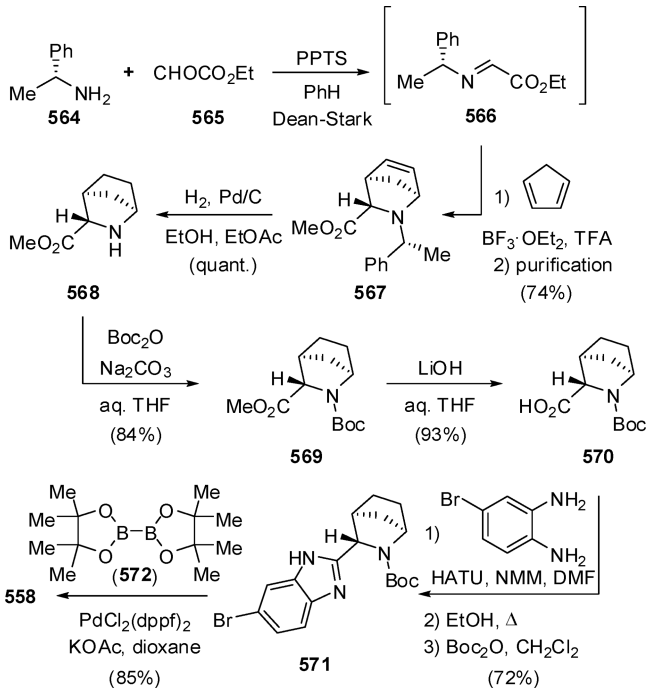

under the strong basic conditions.[443] For this reason, the Wittig reaction was carried out using 4-keto-proline in its acidic form.[444] The key importance of unnatural, tailor-made amino acids for drug design has been already highlighted in section 2.19.

Another key intermediate, boronate **558**, was prepared by condensation of 2-amino-4-bromoaniline with [2.2.1]azabicylic carboxylic acid **570**, which was synthesized via aza-Diels–Alder reaction of the optically active imine **566** with cyclopentadiene using a literature method (Scheme 76).[442,445]

In the previously discussed process, the fluorination of fluorenone **551** required an excess amount of neat Deoxo-Fluor (**21**) at elevated temperatures. Since reagent **21** is thermally unstable,[446] it might not be suitable for an industrial scale synthesis. The use of an organotin reagent should also be avoided from an environmental point of view. Furthermore, due to the lack of selectivity in the Stille reaction, the above

DOI: 10.1021/acs.chemrev.5b00392
Chem. Rev. 2016, 116, 422–518

Scheme 77. Improved Synthesis of Ledipasvir (539)

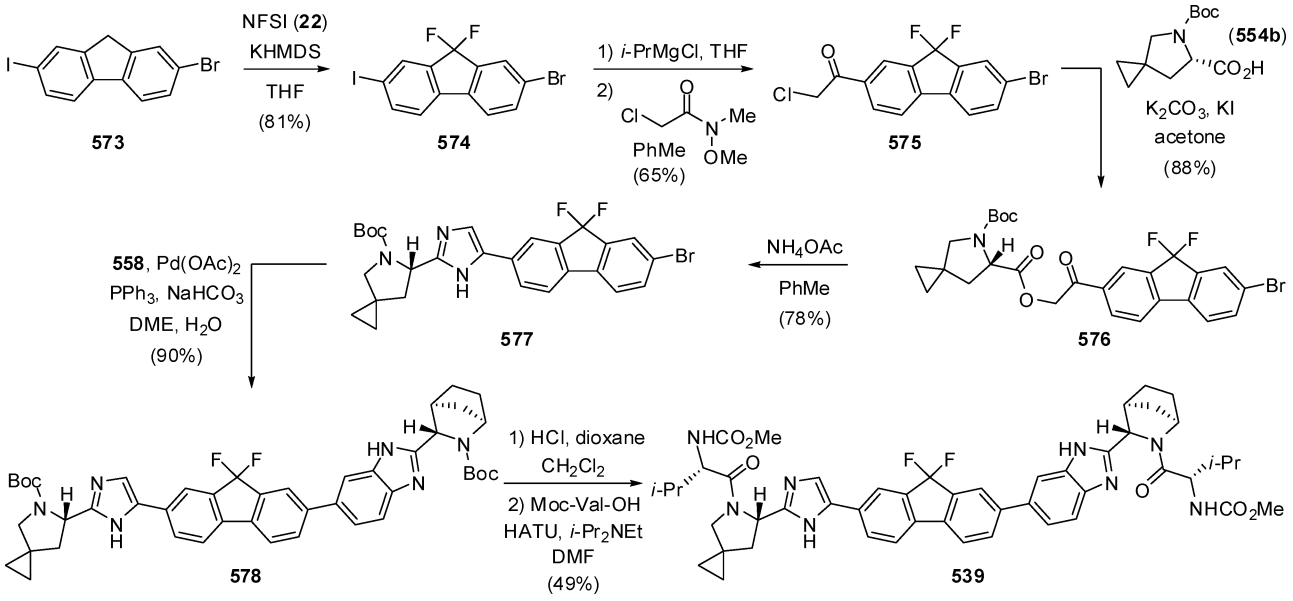

route was considered unattractive. At that point, an alternative synthesis was developed. In this novel process, fluorene **573** was difluorinated by treatment with KHMDS in the presence of NFSI (**22**)[447] to give **574** (Scheme 77). The iodine atom in **574** was selectively transmetalated by reaction with *i*-PrMgCl and converted to a single chloroketone **575** by quenching the Grignard species with the Weinreb amide, 2-chloro-*N*-methoxy-*N*-methylacetamide.[448] *N*-Boc-spirocyclopropyl proline **554b** was alkylated with **575**, and the resulting ketoester **576** was condensed to imidazole **577** upon heating with ammonium acetate. Compound **577** was subjected to the Suzuki-coupling reaction with boronate **558** using $Pd(OAc)_2/PPh_3$ as catalyst, providing late-stage intermediate **578**. Finally, Boc removal with HCl/dioxane followed by peptide coupling at both ends of the molecule with Moc-Val-OH afforded ledipasvir (**539**). Thus, the group of Gilead Sciences successfully avoided a risk of using bis(2methoxyethyl)-aminosulfur trifluoride and could overcome the low efficiency of the Stille coupling. This synthesis represents the first report on the base-promoted difluorination of the 9-position of a fluorene ring system utilizing an electrophilic source of fluorine.[449] Crucial to the success of the process was premixing the substrate and *N*-fluorobenzenesulfonimide, as well as the slow addition of base to this mixture. Additionally, the base and the fluorinating reagent are inert toward each other, and the difluorinated product is formed in high yield without isolation of the monofluorofluorene.[433]

4. COMPOUNDS CONTAINING THREE FLUORINE ATOMS

4.1. Dabrafenib

Dabrafenib (GSK-2118436, **579**) was developed by GlaxoSmithKline (GSK) as a small-molecule oral inhibitor of the mutant kinase BRAF (Figure 41).[450] By July 2013, dabrafenib (trade name: Tafinlar) had been launched in the United States for unresectable or metastatic melanoma with $BRAF^{V600E}$ mutation as detected by an FDA-approved test, and the combined use of dabrabenib and trametinib was also approved for the same indication as discussed earlier (see section 2.2).

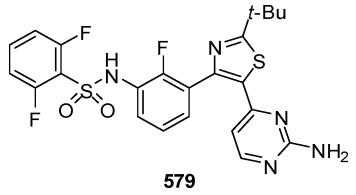

Figure 41. Structure of dabrafenib (**579**).

Furthermore, development is ongoing in other cancer indications, including non-small-cell lung cancer (NSCLC), colorectal cancer, and papillary thyroid cancer.

The discovery process of dabrafenib is depicted in Scheme 78. The hit compound **580**, identified from the oncology-directed kinase programs of GSK, exhibited good inhibitory activity against a $BRAF^{V600E}$ enzyme assay, while it lost potency in mechanistic or antiproliferative cellular assays ($BRAF^{V600E}$: IC_{50} = 9 nM; pERK: EC_{50} = >10000 nM; SKMEL28: EC_{50} = 5316 nM). After replacing the rigid imidazopyridine by a smaller thiazole core, the corresponding compound **581** displayed increased cellular potency (pERK: EC_{50} = 580 nM; SKMEL28: EC_{50} = 2753 nM).[451] Modifications of the benzamide fragment revealed that the sulfonamide analogue **582** further improved both cellular assays, and a fluorine scan in the phenyl ring demonstrated that the difluorinated derivative **583** exhibited improved metabolic stability with potent cellular activities. However, these series of compounds showed poor bioavailability with high clearance in nonrodent species. The tetrahydroisoquinoline moiety was removed in order to decrease the molecular weight and reduce the metabolic sites, although this resulted in a reduction of potency. The inhibitory activity was restored with the replacement of the isopropyl substituent by a *tert*-butyl group. Compared with the des-fluoro analogue **584**, the fluoro-substituted derivative dabrafenib (**579**) displayed dramatically improved pharmacokinetic properties with low clearance ($BRAF^{V600E}$: IC_{50} = 0.7 nM; pERK: EC_{50} = 4 nM; SKMEL28: EC_{50} = 3 nM, Cl_{Rat} = 18 h, Cl_{Dog} = 4 h).[450]

Dabrafenib was synthesized as shown in Scheme 79. Condensation of aniline **586** with benzenesulfonyl chloride

DOI: 10.1021/acs.chemrev.5b00392
Chem. Rev. 2016, 116, 422−518

Scheme 78. Discovery of Dabrafenib (579)

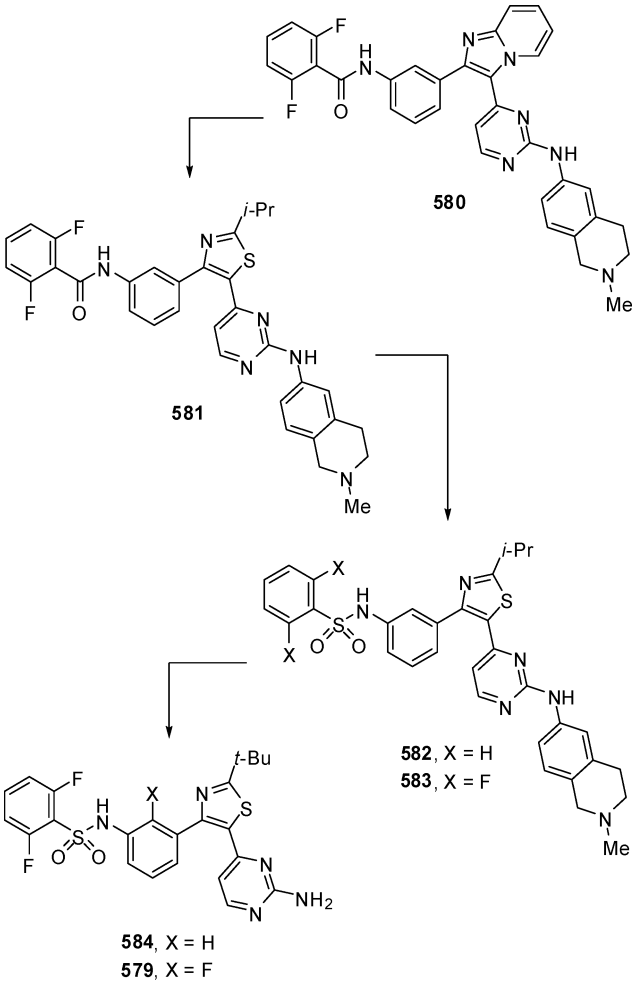

585 afforded sulfamide **587**, which underwent nucleophilic substitution with the lithium anion derived from 2-chloro-4-methylpyrimidine to give acetophenone **588**. Bromination of **588** with NBS yielded intermediate **589**, followed by in situ annulation with dimethylpropanethioamide that provided the cyclized thiazole **590**, which was then heated with ammonia to afford the targeted molecule dabrafenib (**579**).[450]

4.2. Cobimetinib

Since the KRAS and BRAF activating mutations in the ERK/MAP kinase pathway could contribute to the aberrant regulation of cell proliferation, differentiation, survival, migration, and angiogenesis, MEK inhibitors have been a very effective anticancer therapy.[154] Cobimetinib (GDC-0973, XL-518, **591**) is a potent and highly selective allosteric inhibitor of MEK1/2 (biochemical IC_{50} = 4.2 nmol/L against MEK1) for the oral treatment of solid tumors, including melanoma (Figure 42).[452] Cobimetinib (trade name: Cotellic) was developed by

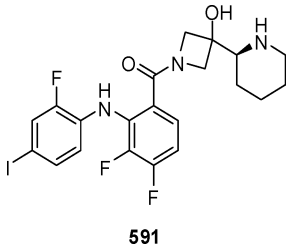

Figure 42. Structure of cobimetinib (**591**).

Exelisis and Genentech (a member of the Roche group), and is currently undergoing oncology clinical trials both as a single agent and in combination with vemurafenib or GDC-0941, a class I PI3K inhibitor,[453] receiving approval for the first combination in November 2015 in both the United States and the EU.

Cobimetinib came from the structure optimization of PD-03259012 (**592**), which was a derivative of the first MEK inhibitor, CI-1040 (**593**) (Figure 43). Obviously, the diphenyl-

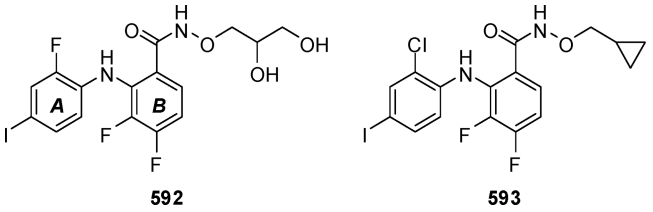

Figure 43. Structures of PD-03259012 (**592**) and CI-1040 (**593**).

amine part was the necessary pharmacophore in both cases. The introduction of fluorine at the 4-position of the B-ring

Scheme 79. Synthetic Route to Dabrafenib (579)

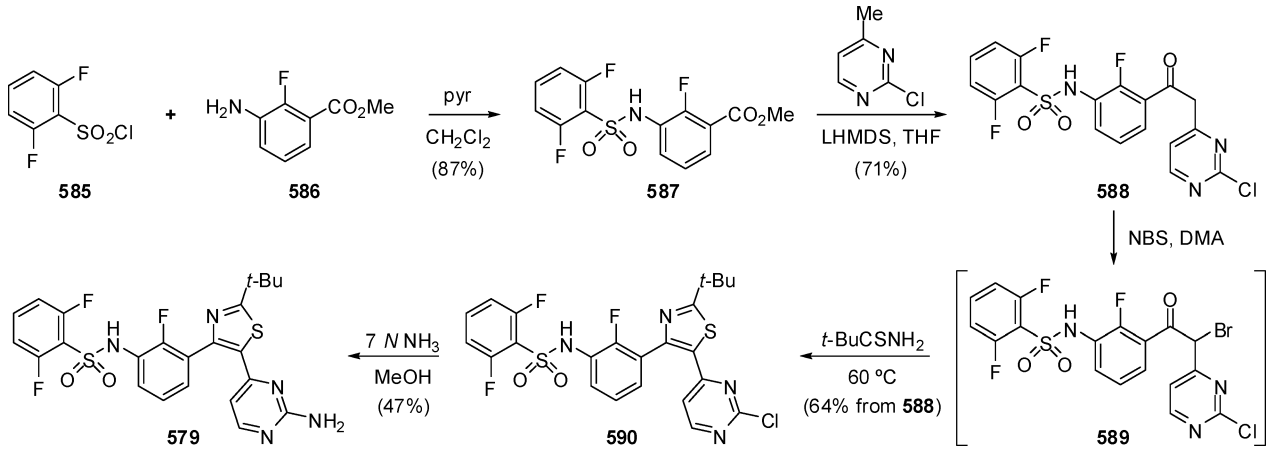

DOI: 10.1021/acs.chemrev.5b00392
Chem. Rev. 2016, 116, 422−518

improved the potency by 26-fold due to a dipolar interaction with the Ser-212 amide backbone hydrogen in the MEK1 structure.[454] Another fluorine atom on the B-ring also performed a potency-enhancing effect by 3-fold. On the other hand, substitution of chlorine by fluorine at the *ortho*-position of the A-ring in **592** gave at least 35-fold increase in colon 26 cell MEK inhibition. Besides, the fluorine on the A-ring and the (*R*)-(−)-dihydroxypropyl side chain in PD-03259012 showed a dramatic synergistic effect for both in vitro potency and ADME profiles.[455]

However, the clinical application of PD-03259012 (**592**) was limited, because of its metabolic instability and neurological side effects. Specifically, the elimination of the hydroxamate ester reduced the sustained duration of efficacy suitable for daily dosing. Moreover, the blood−brain barrier (BBB) penetration of **592** or its active metabolite suppressed the MAPK pathway in brain tissue, subsequently leading to neurological side effects related to ataxia, confusion, and syncope. To avoid these disadvantages, metabolically stable carboxamide and aminoethanol fragments were introduced to form an extra hydrogen bond with residues Asp-190 and Asn-195 to afford optimal contact with ATP γ-phosphate in the catalytic loop region of MEK1. Additionally, a piperidine ring was the ideal choice for an *N*-substituent to balance the cellular potency and oral exposure. Ultimately, the (*S*)-piperidin-2-yl isomer cobimetinib (**591**) performed over 10-fold more potency than the (*R*)-isomer and exhibited subnanomolar biochemical and cellular activity. Due to the limited brain exposure of cobimetinib and its metabolite, the risk of neurological side effects was fortunately reduced by minimizing MAPK pathway inhibition.[456]

The diaryalmino core of cobimetinib was easily prepared by coupling of 2-fluoro-4-iodoaniline (**594**) with 2,3,4-trifluorobenzoic acid (**595**) to afford acid **596**, which was subsequently converted to the corresponding benzoyl fluoride **598** with cyanuric fluoride (**597**) (Scheme 80).[456]

Scheme 80. Synthesis of Trifluorinated Acid Fluoride 598

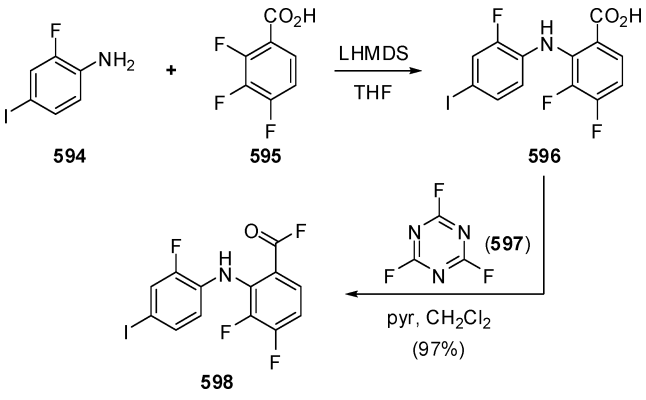

The rest of the medicinal chemistry route to cobimetinib is shown in Scheme 81. Azetidin-3-ol (**599**) was transformed into its Cbz-protected derivative **600** and then converted to the corresponding ketone **601** by Swern oxidation. Nucleophilic addition of the lithium carbanion of *N*-Boc-piperidine (**603**)[457] to ketone **601** afforded *rac*-**604**. Next, this racemic alcohol was resolved by reaction with (*R*)-(−)-α-methoxy-α-trifluoromethylphenylacetyl chloride (**605**) followed by chromatographic separation and removal of the chiral auxiliary to yield the (*S*)-isomer of **604**. Removal of the Cbz protecting group in the

Scheme 81. Synthetic Route to Cobimetinib (591)

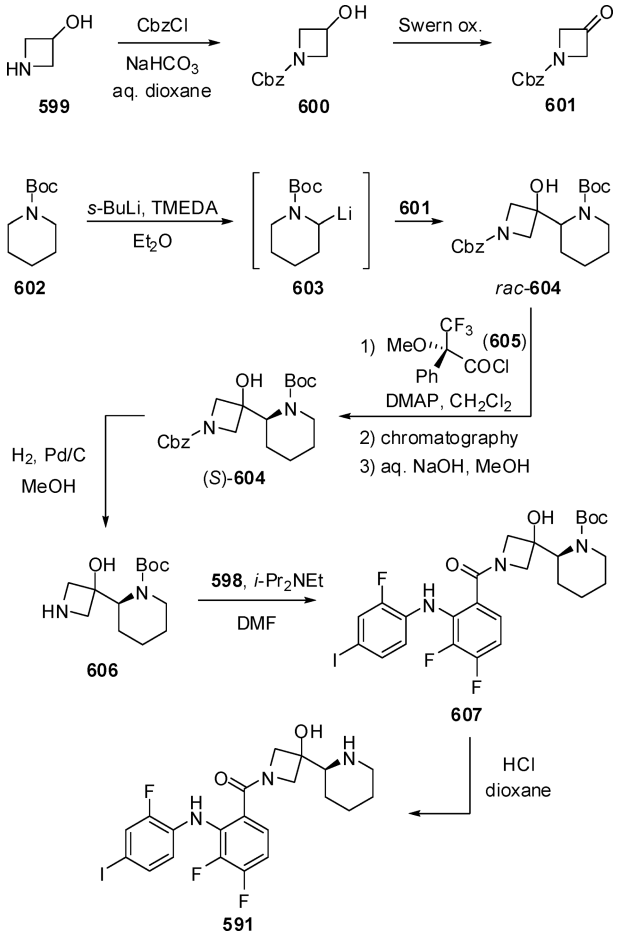

presence of Pd/C and hydrogen followed by condensation with benzoyl fluoride **598** provided amide **607**. Ultimately, cobimetinib (**591**) was easily formed by Boc deprotection.[456]

5. COMPOUNDS CONTAINING ONE TRIFLUOROMETHYL GROUP

5.1. Radotinib and Ponatinib

Since imatinib, the first generation Bcr-Abl tyrosine kinase inhibitor, was launched in 2001, Bcr-Abl tyrosine kinase has become an attractive target for the treatment of chronic myelogenous leukemia (CML). However, due to the emergence of clones expressing mutant forms of the Bcr-Abl kinase, second-generation Bcr-Abl tyrosine inhibitors have been developed to address the unmet medical need related to imatinib intolerance and imatinib resistance, with nilotinib (**608**) being an emblematic example (Figure 44).[458] In this context, radotinib (IY-5511, **609**), developed and launched by Il-yang, was approved in Korea as a second-generation oral Bcr-Abl tyrosine kinase inhibitor in January 2012 (trade name: Supect). Radotinib is used as a second-line treatment for patients with Philadelphia chromosome-positive chronic myeloid leukemia (Ph+ CML), who are refractory to existing drugs, such as imatinib, nilotinib, and dasatinib. Furthermore, phase III trials for radotinib as a first-line treatment have been conducted by Il-yang since February 2012. On the other hand, ponatinib (**610**) was developed by ARIAD Pharmaceuticals as the lead in a series of oral pan-Bcr-Abl/Src protein inhibitors. In January 2013, ponatinib (trade name: Iclusig) was launched

DOI: 10.1021/acs.chemrev.5b00392
Chem. Rev. 2016, 116, 422−518

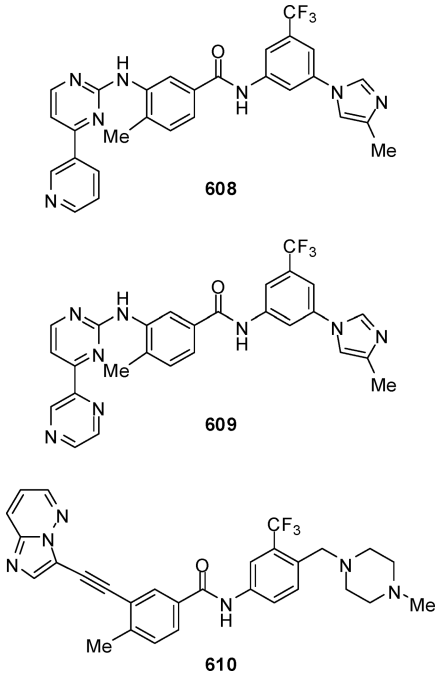

Figure 44. Structures of nilotinib (**608**), radotinib (**609**), and ponatinib (**610**).

in the United States for previously treated CML and Philadelphia chromosome-positive acute lymphoblastic leukemia (Ph+ ALL). In July 2013, ponatinib was approved in Europe for resistant or intolerant CML and Ph+ ALL.

Radotinib specifically inhibits both Bcr-Abl fusion protein (IC_{50} = 34 nM against wild-type Bcr-Abl1 kinase), an abnormal enzyme expressed in Ph+ CML cells, and platelet-derived growth factor receptor (PDGFRα, IC_{50} = 75.5 nM; PDGFRβ, IC_{50} = 130 nM), a tyrosine kinase receptor overexpressed in many tumor cell types.[459] Structurally, radotinib (**609**) is similar to nilotinib (**608**) as shown in Figure 44. In fact, the only difference is the replacement of the pyridine ring by a pyrazine. The trifluoromethyl group contributes to interactions with the hydrophobic pocket of allosteric binding region of Bcr-Abl by van der Waals interactions, thus further enhancing the selectivity and activity.[460]

Conversely, the discovery of ponatinib started from the hit compound **612**, designed as a novel "DFG-out" targeted Abl inhibitor, that was derived from the dual Src/Abl inhibitor AP23464 (**611**)[461] combined with the privileged DFG-out targeting structural fragment from nilotinib (**608**) (Scheme 82).[462] "DFG" represents three amino acids (aspartic acid, phenylalanine, and glycine) in the ATP pocket of kinases. The so-called "DFG-out" state is an unactivated conformation of kinases where the phenylalanine of the DFG motif flips "out" toward the solvent, blocking access of ATP and creating a new allosteric pocket. It is worth mentioning that this series of compounds exhibited modest potency against Bcr-Abl^{T315I} in both biochemical and cell-based assays (Abl^{T315I}: IC_{50} = 478 nM; Abl^{T315I} Ba/F3: IC_{50} = 422 nM), while nilotinib was completely inactive against this mutant, which might result in drug resistance in the treatment of CML.[463] Removal of the cyclopropanamine moiety to give compound **613** retained the potency against Bcr-Abl^{T315I}. Docking analyses of Abl^{T315I} kinase demonstrated that the less sterically demanding vinyl linkage of compounds **612** and **613** relieved the steric clash observed in the docking of nilotinib, thus indicating that the replacement of the vinyl linkage by the rigid and rod-shaped acetylenyl linkage would further reduce the undesirable steric repulsion with the mutant kinase. Compared with compound **613** (Abl^{T315I}: IC_{50} = 386 nM), the chemically and pharmacologically more stable acetylenic analogue **614**

Scheme 82. Discovery of Ponatinib (610)

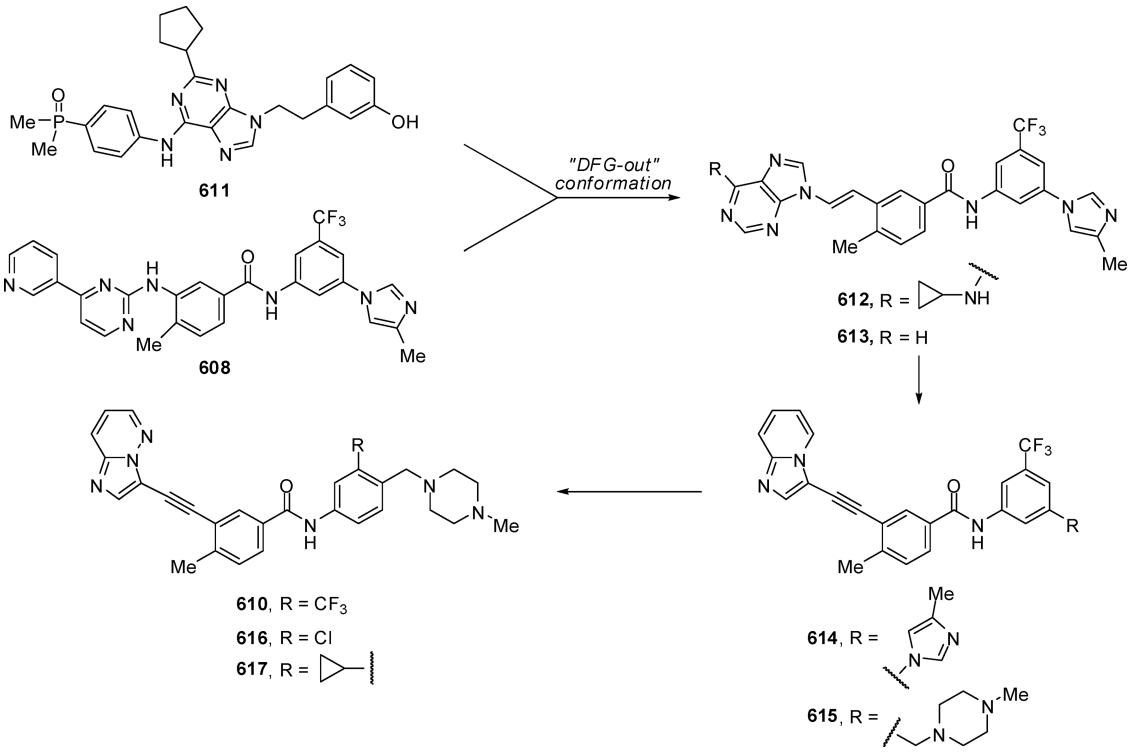

DOI: 10.1021/acs.chemrev.5b00392
Chem. Rev. 2016, 116, 422−518

exhibited 3-fold more potency against Abl^{T315I} kinase (Abl^{T315I}: IC_{50} = 102 nM; Abl^{T315I} Ba/F3: IC_{50} = 471 nM). The solubilizing piperazine fragment was incorporated into **615** to improve cell permeability and reduce lipophilicity, resulting in a dramatic increase of cellular potency (Abl^{T315I}: IC_{50} = 56 nM; Abl^{T315I} Ba/F3: IC_{50} = 26 nM). Finally, further optimization of lipophilicity with diverse heterocyclic templates led to the discovery of ponatinib (**610**) (Abl^{T315I}: IC_{50} = 40 nM; Abl^{T315I} Ba/F3: IC_{50} = 8.8 nM). Notably, replacement of the trifluoromethyl group by either chlorine or cyclopropyl in compounds **616** and **617**, respectively, remarkably reduced cellular potency against mutant T315I, which indicated the importance of the CF_3 moiety in the inhibition of Abl kinase.[464]

Radotinib was easily prepared by a three-step procedure as shown in Scheme 83. Enamino ketone **619** was obtained by

Scheme 83. Three-Step Synthesis of Radotinib (609)

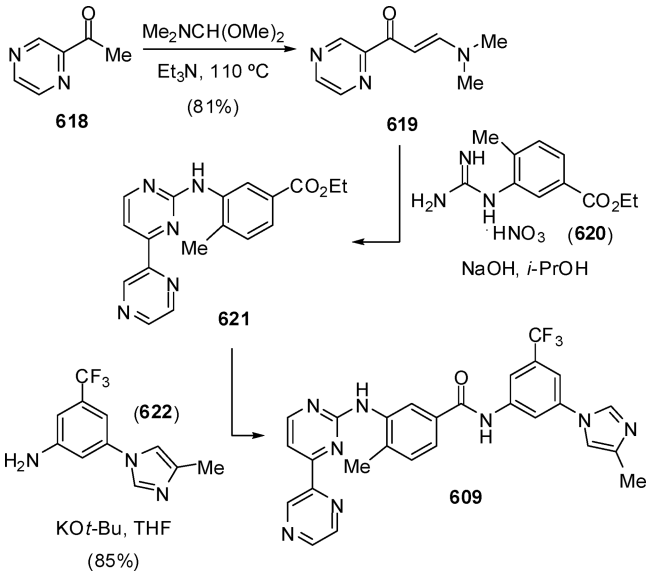

Claisen condensation of 2-acetylpyrazine (**618**) with *N*,*N*-dimethylformamide dimethylacetal. Then, ketone **619** was reacted with commercially available guanidine nitrate **620** to give aminopyridine **621** under basic conditions. Finally, radotinib (**609**) was accessed by amide formation between **621** and aniline **622**.[465,466]

Despite its commercial availability, aniline **622** can also be prepared through an Ullmann-type coupling reaction between aryl iodide **623** and 4-methyl-1*H*-imidazole (**624**) (Scheme 84). Polyethylene glycol was used as a cosolvent together with acetonitrile to improve the solubility of the reagents affording a clear reaction solution. Activation of the copper catalyst with 4,7-dimethoxy-1,10-phenanthroline not only allowed the reaction to proceed in a higher yield than using copper(I) iodide and ethylene diamine, but avoided the possible isomerization of imidazole **624** during the reaction, and ultimately led to a single regioisomer **625**. Finally, the nitro group was easily reduced in the presence of $SnCl_2{\cdot}2H_2O$ to give aniline **622**.[460]

Ponatinib was synthesized using compound **630** as a key fluorinated building block (Scheme 85). The preparation of fragment **630** has been achieved using four different approaches. First, bromination of toluene **626** yielded (bromomethyl)benzene **627**, followed by substitution with 1-methylpiperazine (**628**) and reduction of nitrobenzene **629** to

Scheme 84. Ullmann-Type Reaction as Key Step in the Synthesis of Intermediate 622

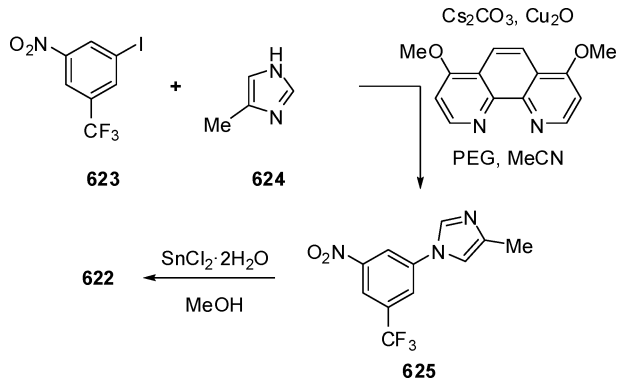

provide the intermediate **630**.[464] Alternatively, condensation of benzoic acid **631** with **628** gave amide **632**, which underwent sequential reduction of the nitro group and the amide functionality to afford compound **630**.[467] Another strategy was based on the prior protection of aniline **634** and subsequent bromination of toluene **635** to render (bromomethyl)benzene **636**, followed by substitution with **628** and deprotection to give **630**.[468] Finally, cyanide substitution of bromobenzene **638** provided benzonitrile **639**, followed by reduction with DIBAL-H and reductive amination of benzaldehyde **640** with **628** to yield building block **630**.[468]

Another key structural fragment of ponatinib, namely alkyne **643**, was obtained from heterocyclic bromide **641** via Sonogashira coupling by treatment with $Pd(PPh_3)_2Cl_2$, CuI, and ethynyltrimethylsilane to afford **642**, followed by TBAF-mediated deprotection (Scheme 86). The last remaining fragment, benzoic acid **644**, was first transformed into its derived acid chloride and then condensed with aniline **630** to yield **645**, which was then coupled with ethyne **643** through another Sonogashira-type reaction to afford ponatinib (**610**).[464]

5.2. Tasquinimod

Tasquinimod (ABR-215050, **646**) is a second-generation oral quinoline-3-carboxamide antiangiogenic agent for the treatment of castration-resistant prostate cancer, which was developed by Active Biotech and Ipsen and is currently in phase III trials (Figure 45).[469] Tasquinimod demonstrated a significant improvement in patient progression-free survival (PFS) compared with those receiving placebo (median 7.9 months versus 3.3 months, HR 0.57; P = 0.0042) in phase II trials.[470] Tasquinimod is a dual inhibitor of S100A9/TLR4 in MDSCs and HDAC4/N-CoR/HDAC3 deacetylation of hypoxia-inducible factor 1-α (HIF1-α) in both endothelial and tumor cells, which effectively leads to a significant upregulation in the expression of thrombospondin-1 (TSP-1) and down-regulation of HIF-1α and vascular endothelial growth factor (VEGF), and hence influencing tumor microenvironment to overcome tumor-associated immunosuppression and inhibiting angiogenesis, metastasis, and tumor growth.[471,472]

Structurally, tasquinimod is a derivative of the first-generation quinoline-3-carboxamide analogue linomide (**647**), being 30- to 60-fold more potent than linomide in inhibiting tumor growth in vivo.[473] Unfortunately, the phase III trial of linomide had to be discontinued, because of its unknown and unacceptable toxicity. However, preclinical studies in the Beagle-dog model indicated that linomide could induce a dose-dependent proinflammatory reaction, observed as an

DOI: 10.1021/acs.chemrev.5b00392
Chem. Rev. 2016, 116, 422−518

Scheme 85. Synthetic Approaches to Trifluoromethyl-Containing Fragment 630

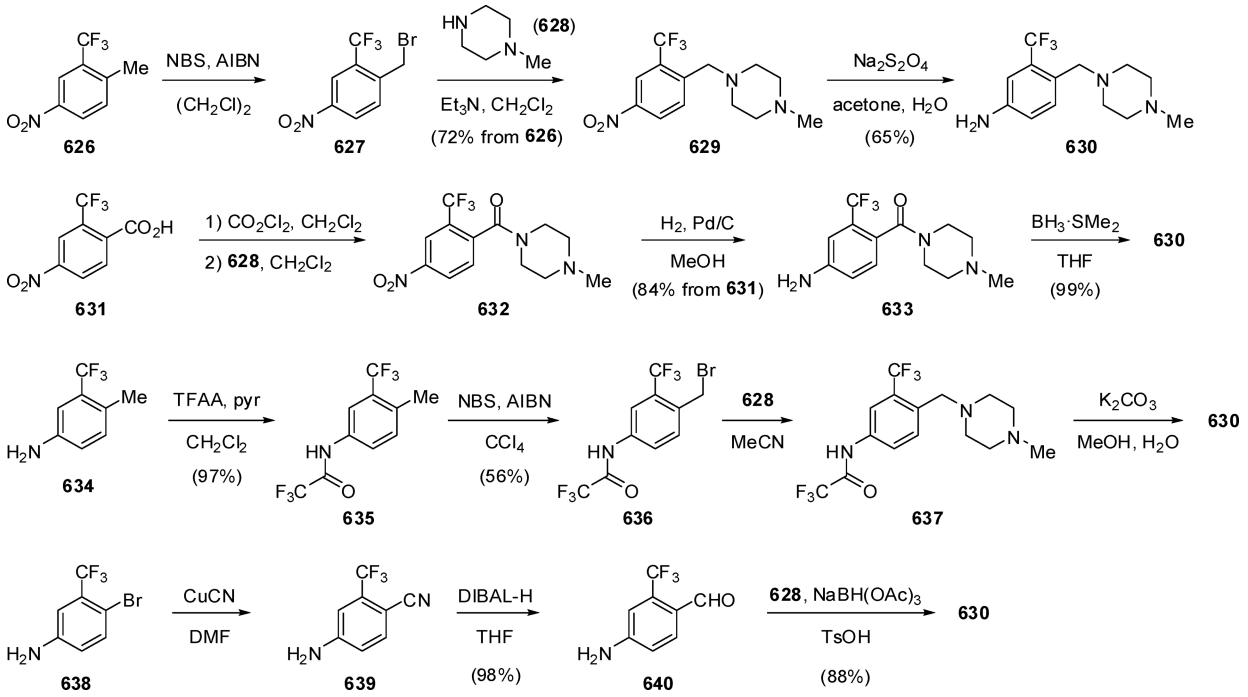

Scheme 86. Synthetic Route to Ponatinib (610)

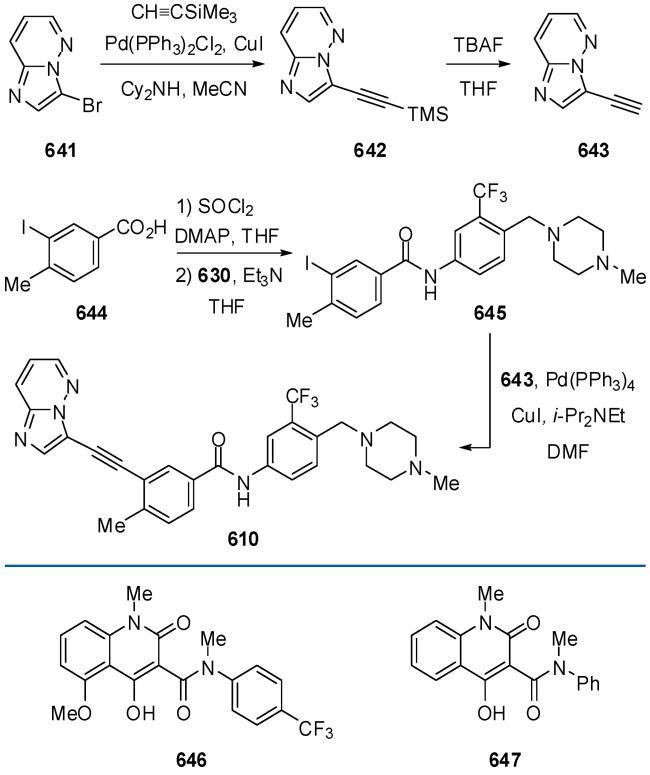

Figure 45. Structures of tasquinimod (**646**) and linomide (**647**).

increase of white blood cell (WBC) count and erythrocyte sedimentation rate (ESR). Insertion of the electron-withdrawing and stereochemically demanding[474−476] trifluoromethyl group at the *para*-position of the *N*-phenyl ring in tasquinimod prevented metabolic demethylation of the quinolinone moiety, thus decreasing the proinflammatory activities.[477]

The synthesis of tasquinimod was performed employing commercially available 2-amino-6-methoxybenzonitrile (**648**) as the starting material (Scheme 87). The corresponding

Scheme 87. Synthetic Route to Tasquinimod (646)

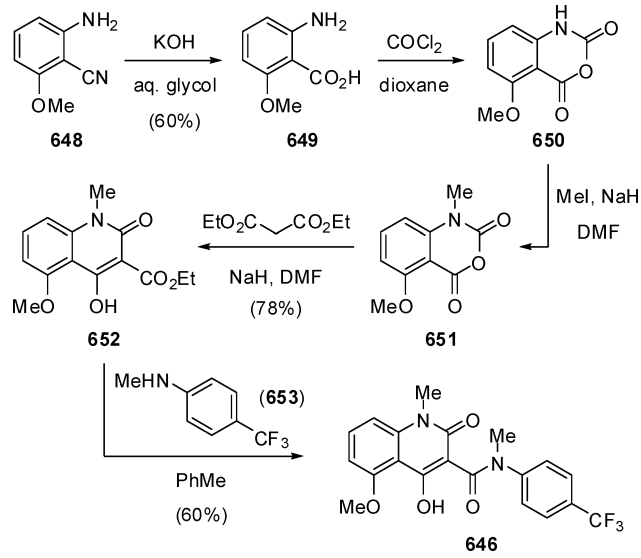

anthranilic acid (**649**) was prepared by hydrolysis of benzonitrile **648**, and then treated with phosgene to give isatoic anhydride **650**. After *N*-methylation of **650** with iodomethane in the presence of sodium hydride, condensation of **651** with ethyl malonate gave 3-quinolinecarboxylic ester derivative **652**. Finally, tasquinimod (**646**) was easily achieved by amide formation with *N*-methyl-4-(trifluoromethyl)aniline (**653**).[478]

DOI: 10.1021/acs.chemrev.5b00392
Chem. Rev. 2016, 116, 422−518

5.3. Telotristat Ethyl

Telotristat ethyl (LX-1032, LX-1606, **654**), an oral small-molecule tryptophan hydroxylase (TPH) inhibitor for the potential treatment of carcinoid syndrome, is in phase III clinical trials under the development of Lexicon Pharmaceuticals (Figure 46). Moreover, the FDA granted telotristat ethyl orphan drug status for carcinoid syndrome in March 2012.

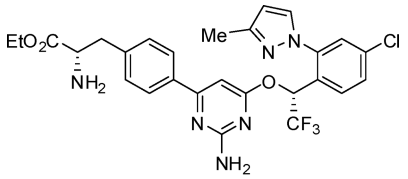

654

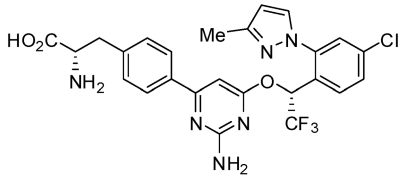

655

Figure 46. Structures of telotristat ethyl (**654**) and telotristat (**655**).

Carcinoid syndrome is believed to be partially caused by increased levels of serotonin (5-hydroxytryptamine, 5-HT). Therefore, telotristat ethyl suitably reduces the production of 5-HT by inhibiting TPH, the rate-limiting enzyme in the conversion of tryptophan to 5-HT. Actually, 5-HT is a very essential inhibitory neurotransmitter in the CNS, and hence the molecule was designed in order to avoid crossing the blood–brain barrier (BBB).[479] Telotristat ethyl is the ethyl ester prodrug of telotristat (**655**), containing a polar α-amino acid fragment to effectively avoid its penetrating the BBB and affecting CNS 5-HT synthesis. In fact, Lexicon has claimed several telotristat salts to improve its oral bioavailability, including telotristat besylate and telotristat etiprate, being the latter one the salt form used on the clinical trials.[480]

From the SAR investigation of different TPH inhibitors, it was concluded that the L-phenylalanine fragment was necessary for the in vitro TPH inhibition potency, whereas substituted phenyl rings or replacement by other heterocycles reduced the activity against TPH. The X-ray data revealed that the L-phenylalanine moiety formed three hydrogen-bond interactions, one with the carbonyl oxygen of Thr-265 and the other two with bridging water molecules. On the other hand, the phenyl ring constructed hydrophobic interactions with Pro-268 and His-272. Moreover, the pyrimidine core formed an edge-to-face $\pi-\pi$ interaction with Phe-313, and the 2-amino group built a hydrogen-bond interaction with a water molecule.[481] Furthermore, the presence of the trifluoromethyl group effectively improved the activity in the cell-based assay compared to its nonfluorinated derivative.[482]

The synthesis of telotristat ethyl is outlined in Scheme 88. Coupling of fluoride **656** and pyrazole **657** in the presence of KO*t*-Bu afforded intermediate **658** (along with 17% of the pyrazole regioisomer). Then, the trifluoroacetyl group was introduced via addition of the Grignard derived from **658** to

Scheme 88. Synthetic Route to Telotristat Ethyl (654)

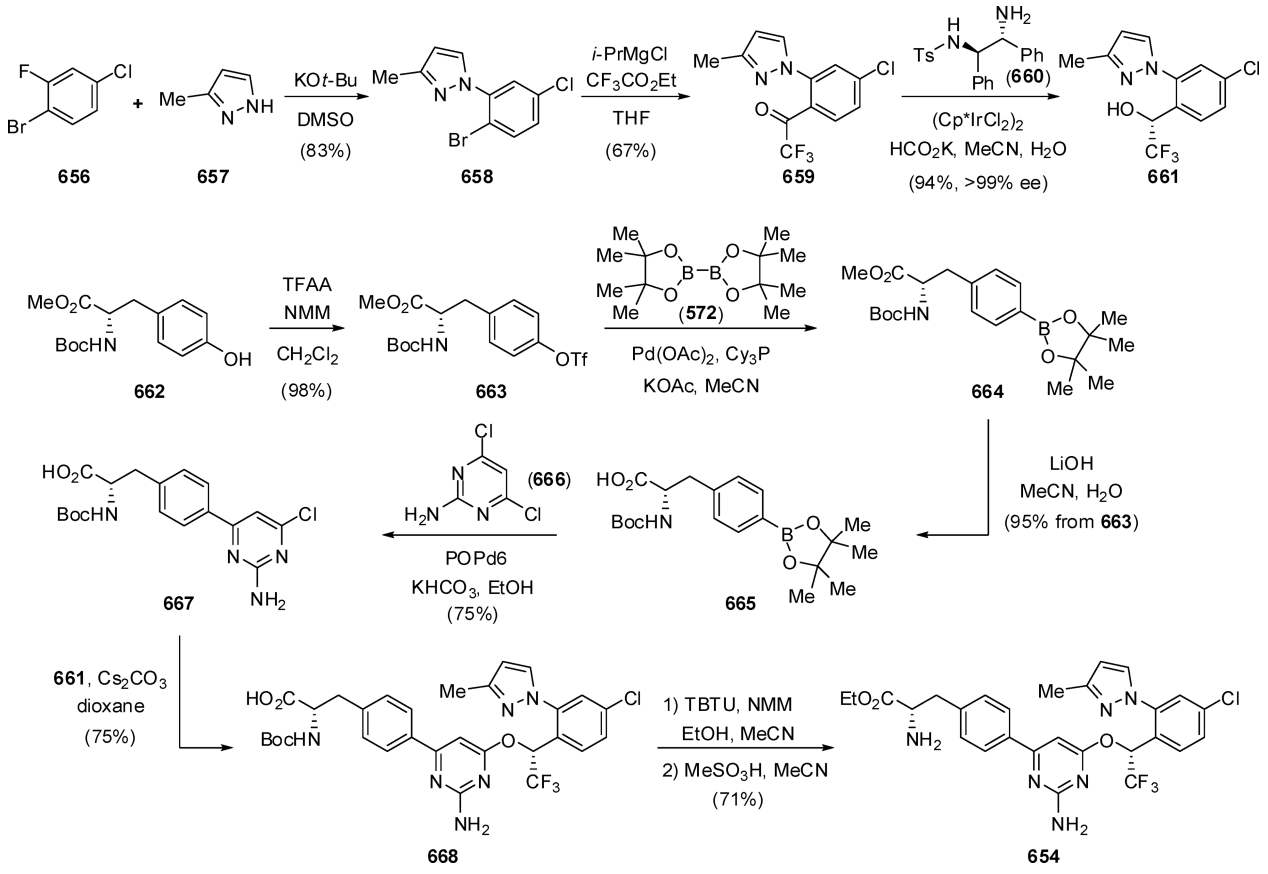

DOI: 10.1021/acs.chemrev.5b00392
Chem. Rev. 2016, 116, 422–518

ethyl trifluoroacetate, followed by asymmetric reduction of ketone **659** induced by (*R*,*R*)-TsDPEN (**660**) under Ir(III) catalysis to yield (*R*)-trifluoroethanol **661** with excellent yield and enantioselectivity (>99% ee). The other fragment of telotristat ethyl was accessed from (*S*)-Boc-Tyr-OMe (**662**) that was first initially converted into its triflate derivative **663**. Pd-mediated coupling with bis(pinacolato)diboron (**572**) afforded boronate **664**, and then hydrolysis of the methyl ester produced the corresponding carboxylic acid **665**. Suzuki coupling of acid **665** and pyrimidine **666** catalyzed by dihydrogen di-μ-chlorodichlorobis(dicyclohexylphosphinito-kp)dipalladate(2−) (POPd6) furnished compound **667**. Then, based-promoted S_NAr reaction between the two main fragments, (*R*)-trifluoroethanol **661** and chloride **667**, led to **668** and final esterification and removal of the Boc protecting group gave the target product telotristat ethyl (**654**).[483]

5.4. Buparlisib

Buparlisib (NVP-BKM-120, **669**) was developed by Novartis for the potential treatment of solid and hematological tumors, including endometrial carcinoma, glioblastoma, prostate cancer, breast cancer, melanoma, and myelofibrosis (Figure 47). As a

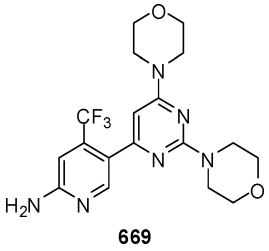

Figure 47. Structure of buparlisib (**669**).

pan class I phosphoinositide 3-kinase (PI3K)[484] inhibitor, buparlisib shows pro-apoptotic and antiangiogenic activity, and is rapidly absorbed and bioavailable after administration.[485,486] Buparlisib is currently on several clinical trials, including a phase III trial in combination with fulvestrant for advanced or metastatic breast cancer patients, and a phase II trial in combination with paclitaxel for metastatic head and neck cancer.

As shown in Scheme 89, buparlisib derived from the structure of the former PI3K inhibitor **670** (PI3Kα: IC_{50} = 0.056 μM), which was discovered from a solid phase combinatorial library of 2,4,6-trisubstituted pyrimidines.[487] While compound **670** exhibited potent in vitro activities, the in vivo potential was limited due to the presence of the phenol moiety (F = 9%, $t_{1/2}$ = 21 min, AUC_{oral} = 0.12 μM·h). For example, after replacement of the OH group by a trifluoromethyl group, the resulting compound **671** was 60-fold less active but showed improved rat PK profile (F = 71%, $t_{1/2}$ = 218 min, AUC_{oral} = 23 μM·h).[488] According to the cocrystal structure of compound **670** in PI3Kγ,[487] a variety of heterocycles at the pyrimidine C-6 position were screened in order to mimic the phenol binding interaction with Asp-841 and Tyr-867, eventually leading to the discovery of the potent PI3K inhibitor **672** with a better oral bioavailability (PI3Kα: IC_{50} < 0.002 μM, F = 89%, AUC_{oral} = 9 μM·h). However, high rodent CL values of compound **672** prevented its further development (CL = 79 mL/min/kg). Further modifications on the C-6 position showed that aminopyridine-substituted compounds exhibited a markedly reduced rat CL value, while

Scheme 89. Discovery of Buparlisib (669)

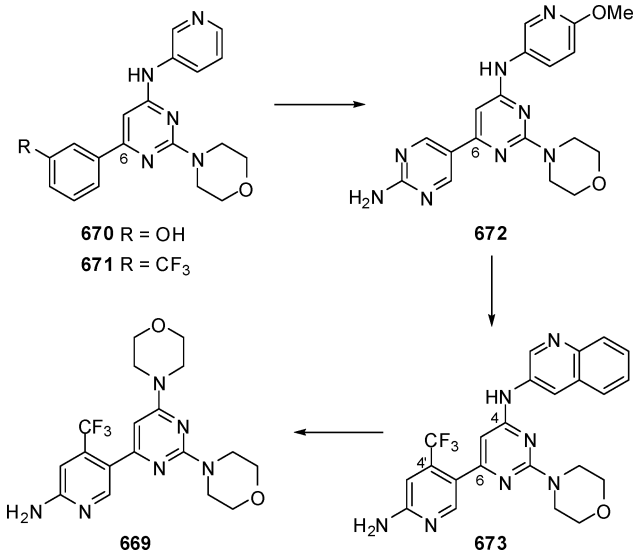

their compromised biochemical potency could be improved by introduction of electron withdrawing groups such as CN, Cl, and CF_3 at the C-4′ position. Among these series of compounds, the trifluoromethyl compound **673** showed the best PK properties with excellent PI3Kα inhibitory activity (PI3Kα: IC_{50} = 0.021 μM, CL = 8 mL/min/kg, AUC_{oral} = 114 μM·h). Finally, in order to increase the aqueous solubility and Caco-2 permeability, buparlisib (**669**) was discovered by replacing the aminoquinoline at the C-4 position by a second morpholine ring.[489]

Buparlisib was synthesized as shown in Scheme 90. Bromination of pyridine **674** with NBS afforded bromopyridine **675**, which underwent a Miyaura borylation reaction with bis(pinacolato)diboron (**572**) in the presence of KOAc as base and $Pd(dppf)_2Cl_2{\cdot}CH_2Cl_2$ as catalyst to produce boronate **676**. On the other hand, dimorpholine-pyrimidine **678** was obtained by nucleophilic substitution of 2,4,6-trichloropyrimidine (**677**) with morpholine. Then, Suzuki coupling of boronate **676** and chloropyrimidine **678** provided buparlisib (**669**) using the combination of $Pd(dppf)_2Cl_2{\cdot}CH_2Cl_2$ as catalyst and Na_2CO_3 as base.[489]

5.5. Enobosarm

The androgen receptor (AR) is essential for the maintenance of the function of several organs including primary and secondary sexual organs, skeletal muscle, and bone, making it a desirable therapeutic target. Selective androgen receptor modulators (SARMs) bind to the AR and show osteo- and myo-anabolic biological effects, and do not stimulate growth on prostate and other secondary sexual organs. Therefore, SARMs provide ideal therapeutic opportunities in numerous disorders associated with muscle wasting, osteoporosis, cancer cachexia, or end-stage renal disease and hypogonadism.[490,491] Enobosarm (GTx-024, MK-2866, **679**) was developed by GTx (initially in collaboration with Merck) as a SARM for the potential treatment of disorders associated with muscle wasting and osteoporosis (Figure 48). At present, enobosarm (trade name: Ostarine) is in phase III clinical trials for cachexia and phase II for metastatic breast cancer and sarcopenia and testosterone defficiency.

As shown in Scheme 91, enobosarm is an aryl propionamide that originated from bicalutamide (**680**), which was unexpect-

DOI: 10.1021/acs.chemrev.5b00392
Chem. Rev. 2016, 116, 422−518

Scheme 90. Synthetic Route to Buparlisib (669)

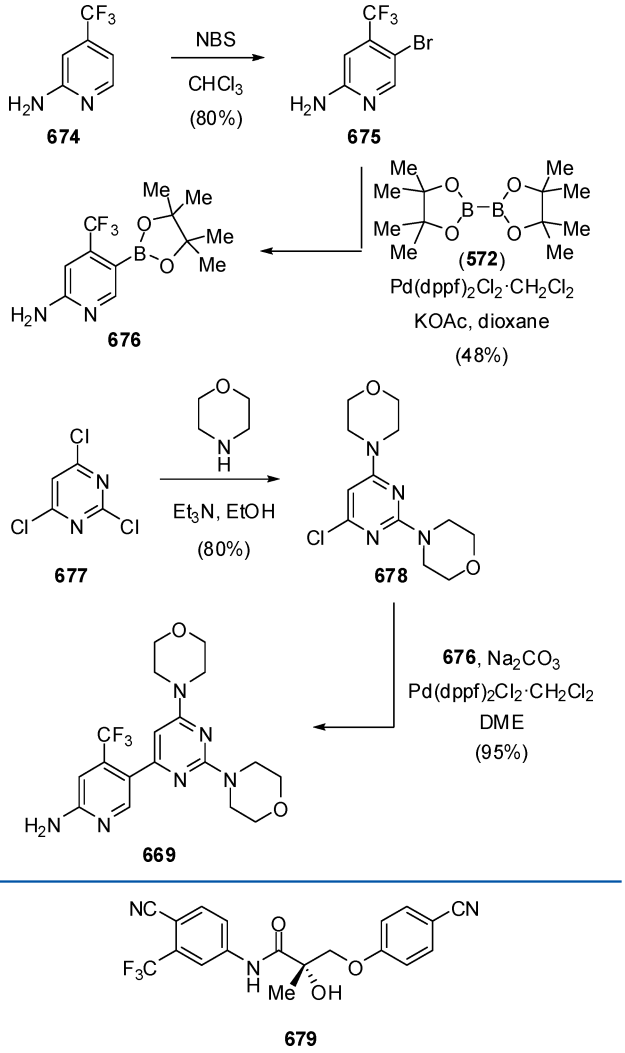

Scheme 91. Discovery of Enobosarm (679)

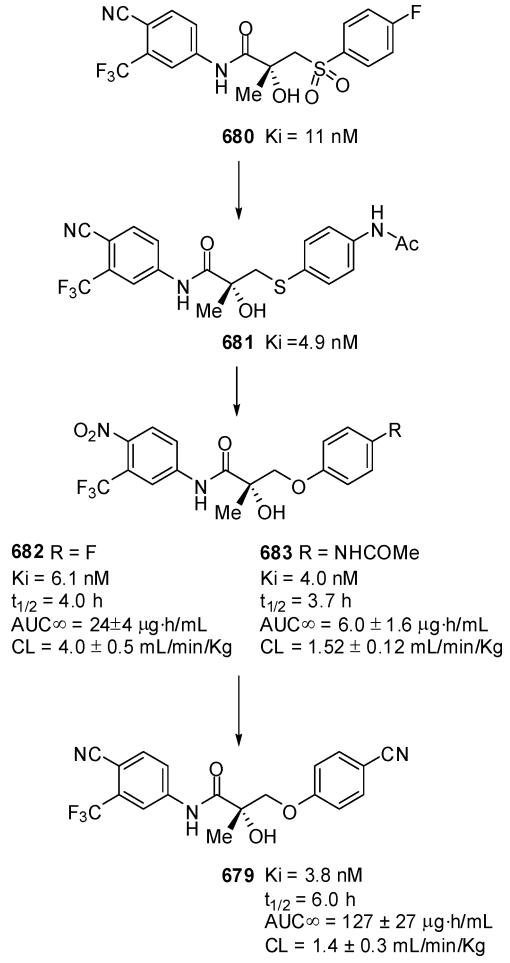

Figure 48. Structure of enobosarm (**679**).

edly discovered with the ability to fully stimulate in vitro AR-dependent transcriptional activation.[490] Replacement of the sulfonyl linker and the *p*-fluoro substituent of bicalutamide by a thioether linker and an acetamide group, respectively, gave the early lead compound thioacetolutamide (**681**) with an improved in vitro agonist activity.[492,493] However, the thioether-linked compound **681** suffered from the lack of the expected pharmacological activity in vivo, owing to metabolic oxidation of the thioether group to the corresponding sulfoxide or sulfone with little or no agonistic potency. Further optimization consisted of the replacement of the thioether moiety by an ether bond leading to the discovery of two new key lead compounds, S-1 (**682**) and S-4 (also known as GTx-007 and andarine, **683**), with high affinity for the androgen receptor, tissue selectivity in animal models, and an improved PK profile,[491,494,495] which indicated that these compounds would be good candidates for further development.[490,496]

Based on the established SAR and metabolic profiles, the second generation of aryl propionamides was subsequently developed, in which the ether bond was kept to maintain the agonist activity, and different substituents were introduced into the two aromatic rings in order to obtain different intrinsic activities and ameliorate the metabolic profiles. Among the resulting compounds, enobosarm (**679**), with two cyano groups and one trifluoromethyl group, eliminated the metabolically labile sites of previous analogues and held the tissue-selective bioactivity. Since the cyano group did not undergo reduction as the nitro group does, the $t_{1/2}$ of enobosarm in rat was prolonged to 6 h.[491] The lower CL value (1.4 ± 0.3 mL/min/kg) and the highest AUC_{∞} value (127 ± 27 μg·h/mL) indicated that enobosarm may have the most promising in vivo bioactivities. In fact, enobosarm showed the most potent in vivo androgenic and anabolic activity of any AR nonsteroidal agonist determined to date. Nonlinear regression analysis of dose–response relationships for enobosarm showed that the ED_{50} values were 0.12 ± 0.05, 0.39 ± 0.15, and 0.03 ± 0.01 mg/day in prostate, seminal vesicles, and levator ani muscle, respectively.[497]

Enobosarm was prepared via an asymmetric process according to Scheme 92. The key chiral intermediate (*R*)-3-bromo-2-hydroxy-2-methylpropionic acid (**688**) was synthesized from (*R*)-proline (**684**) and methacryloyl chloride (**685**) through several simple operations including condensation, bromination, and removal of the chiral auxiliary using 24% HBr solution. Then, activation of **688** with $SOCl_2$ and further condensation with 4-amino-2-(trifluoromethyl)benzonitrile (**639**) gave amide **689**, and final ether formation by reaction with 4-cyanophenol afforded enobosarm (**679**) isolated as a colorless solid.[498]

DOI: 10.1021/acs.chemrev.5b00392
Chem. Rev. 2016, 116, 422–518

Scheme 92. Synthetic Route to Enobosarm (679)

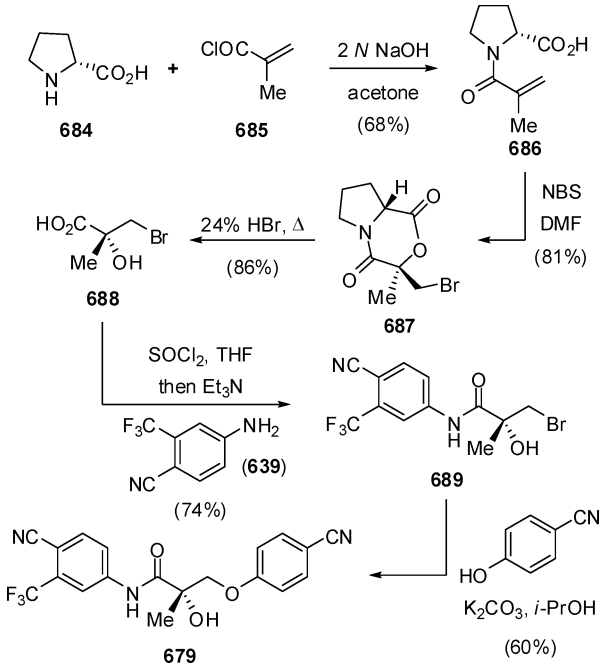

5.6. Siponimod

Novartis is developing siponimod (BAF-312, **690**) as a next-generation sphingosine-1-phosphate receptor (S1P) modulator for treating multiple sclerosis (MS) and related disorders (Figure 49).[499] As a potent and selective $S1P_{1/5}$ agonist (EC_{50} = 0.39 and 0.98 nM, respectively) with relatively fast washout, the drug elicits a significant but rapidly reversible suppression of lymphocyte trafficking by internalizing the $S1P_1$ receptor.[500] Results of an adaptive dose-ranging phase II study suggested an up to 80% reduction of brain MRI lesions and a significant reduction of annualized relapse rate in relapsing−remitting MS by taking siponimod compared to placebo.[501] In November 2013, siponimod was granted orphan designation by the U.S. FDA for the treatment of polymyositis. Siponimod is currently undergoing a phase III clinical trial in secondary progressive MS and a phase II trial in polymyositis as an oral formulation.

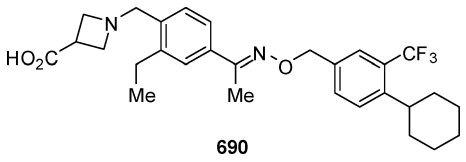

Figure 49. Structure of siponimod (**690**).

Structurally, siponimod contains an alkoxyimino function bridging a hydrophilic head and a hydrophobic tail. It was discovered through a de novo design, based on the structure of fingolimod (**691**), an oral S1P agonist launched by Novartis in 2010 (Scheme 93).[502] Fingolimod is metabolized in vivo to its phosphate derivative **692** to exert the immunosuppressive effect. To achieve selectivity against $S1P_3$ and avoid $S1P_3$-induced bradycardia, more rigidity was introduced into the molecule by replacing the *n*-octyl chain by substituted benzyloxy oximes. On the other hand, various amino carboxylic acids were employed to mimic the amino phosphate moiety in **692**, avoiding nonspecific binding to lipoproteins in tissues and

Scheme 93. Discovery of Siponimod (690)

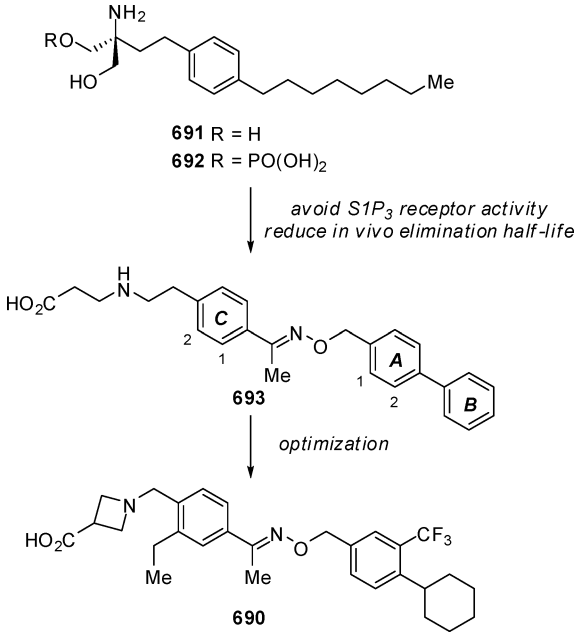

shortening the elimination half-life. These modifications pointed to the new lead **693** for further optimization.[499]

According to molecular modeling studies, compound **693** binds to $S1P_1$ through the amino carboxylic acid head by means of several strong electrostatic interactions, while the biphenyl tail is located into a large hydrophobic cavity of the protein. Substitution at the C-1 position of the A ring with fluorine or a trifluoromethyl group was detrimental in the biological activity of the resulting molecules due to much less efficient interactions with the receptor. Although introduction of a fluorine atom at C-2 enhanced the potency by forming an extra hydrophobic interaction, the presence of a bulkier CF_3 in the C-2 position greatly improved the nonpolar interactions with residues Leu-276 and Leu-272, also compelling the biphenyl moiety to adopt a near-perpendicular conformation with improved van der Waals interactions. SAR studies also showed that a cyclohexyl group as the B ring greatly enhanced the $S1P_1$ activity, and the insertion of an ethyl group at the C-2 position of the C ring conferred weaker agonism at $S1P_3$. Ultimately, optimal combinations of hydrophilic headgroup and hydrophobic tail led to the discovery of siponimod (**690**).[499]

The first synthetic route to siponimod used commercially available acetophenone **694** and trifluoromethylbenzene **698** as starting building blocks (Scheme 94). Benzylic bromination of **694** with NBS and AIBN and further reaction with $CaCO_3$ afforded primary alcohol **695**. Next, Suzuki coupling of **695** with dibutyl vinylboronate gave olefin **696**, which was hydrogenated over Pd/C to give saturated ketone **697**. On the other hand, trifluoromethyl-containing derivative **698** was first condensed with ethyl *N*-hydroxyethanimidoate (**699**) to give **700**, and then coupled with cyclohexyl magnesium chloride in the presence of $ZnCl_2$ and $Pd(t\text{-}Bu_3P)_2$ to provide alkoxyamine precursor **701**. Hydrolysis of **701** with HCl and in situ condensation with fragment **697** afforded (*E*)-imine **702**, and then oxidation with MnO_2 followed by reductive amination with azetidine-3-carboxylic acid (**703**) furnished siponimod (**690**).[499,503−506]

A different synthesis of intermediate **697** commenced with the diazotization of 4-amino-3-ethylbenzonitrile (**704**)

DOI: 10.1021/acs.chemrev.5b00392
Chem. Rev. 2016, 116, 422−518

Scheme 94. Synthetic Route to Siponimod (690)

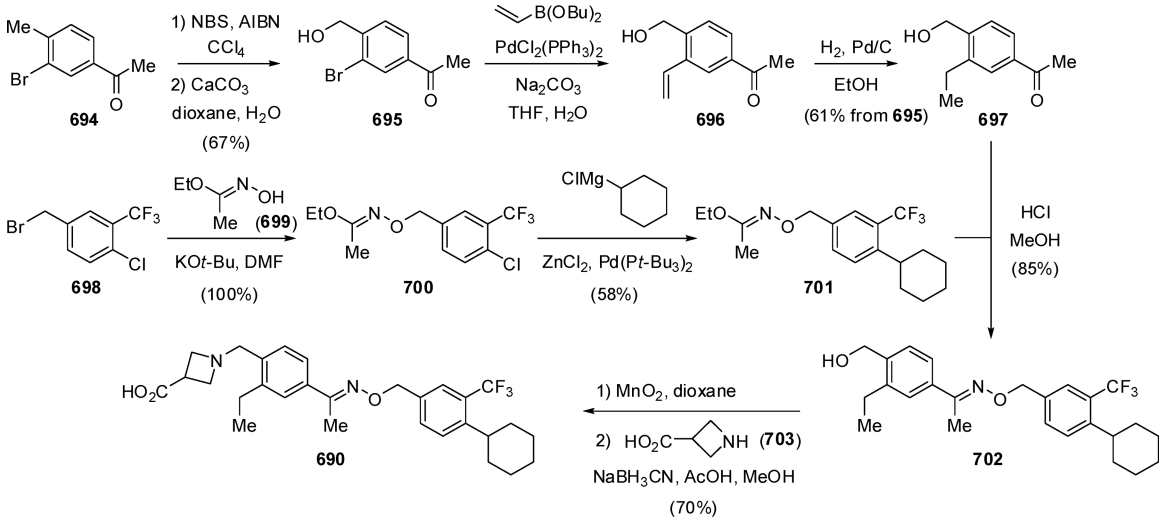

(Scheme 95). The resulting diazonium chloride **705** then reacted with formaldoxime trimer hydrochloride (**706**) in the presence of $CuSO_4$, Na_2SO_3, and NaOAc, and was subsequently treated with HCl to afford aldehyde **707**. The corresponding alcohol **708** was accessed by reduction of **707** with $NaBH_4$, and then reacted with MeMgBr in refluxing THF, followed by hydrolysis with HCl to provide the desired ketone **697**.[503]

Scheme 95. Alternative Synthesis of Intermediate 697

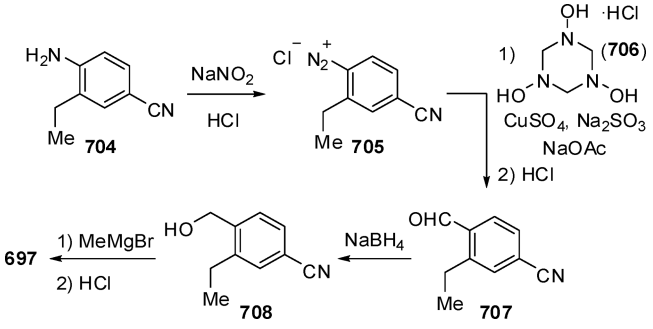

Novartis has disclosed alternative approaches (without chemical yield) for the large-scale production of intermediate **701**, by coupling the phenyl and cyclohexyl rings prior to the condensation with imidoate **699**. Thus, Grignard reaction between 1-bromo-2-(trifluoromethyl)benzene (**709**) and cyclohexanone followed by dehydration using H_2SO_4 and hydrogenation over Pd/C provided cyclohexane derivative **712** (Scheme 96). Bromination of **712** with 1,3-dibromo-5,5-dimethylhydantoin (DBDH) and H_2SO_4 gave bromobenzene

Scheme 96. Alternative Processes for Preparing Intermediate 701

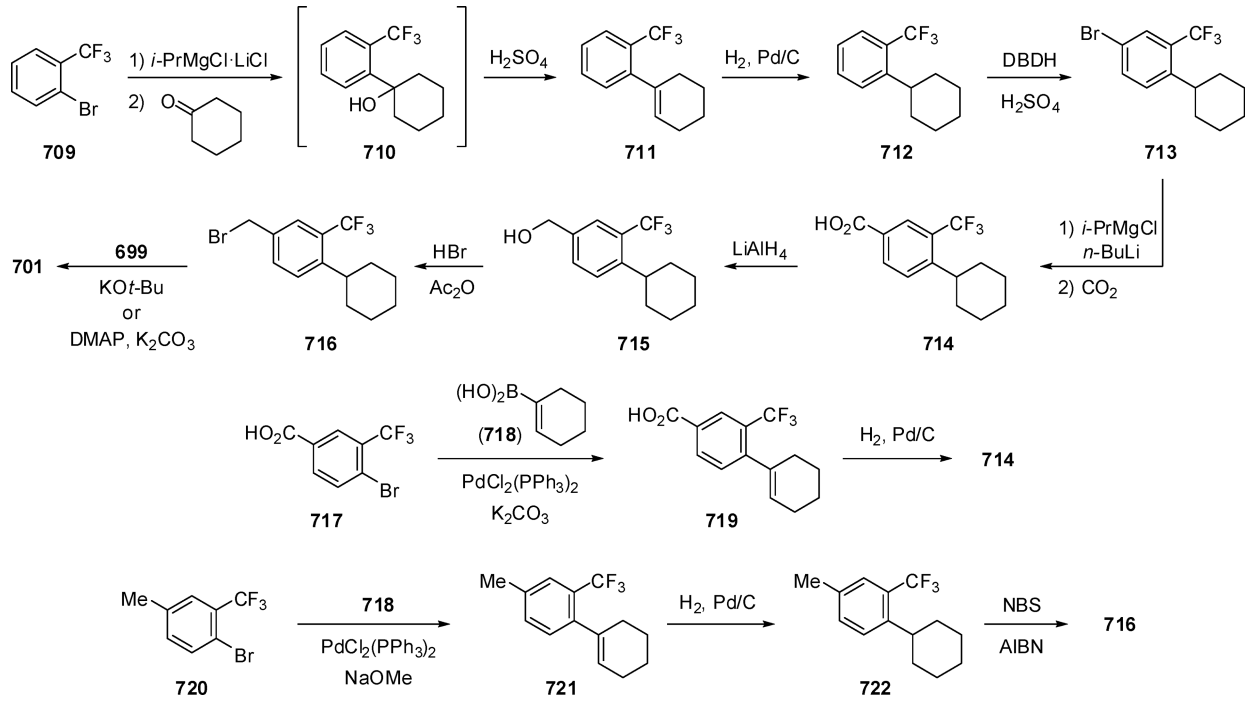

DOI: 10.1021/acs.chemrev.5b00392
Chem. Rev. 2016, 116, 422−518

713, which was metalated with *i*-PrMgCl and *n*-BuLi and carboxylated with CO_2 to give acid **714**. Reduction with $LiAlH_4$ and subsequent bromination with HBr and Ac_2O furnished benzyl bromide derivative **716**, which then reacted with **699** to yield intermediate **701**. Alternatively, compound **714** also was prepared from acid **717** in two steps involving Suzuki coupling with 1-cyclohexen-1-ylboronic acid (**718**) and subsequent hydrogenation over Pd/C. Similarly, toluene derivative **720** was converted into cyclohexane **722**, which upon bromination with NBS and AIBN afforded benzyl bromide derivative **716**.[507]

Several approaches have been considered to access the readily available fluorine containing material **709**. Introduction of a trifluomethyl group into bromobenzene (**723**) by using CF_3 sources like trifluoroacetic anhydride,[508] CF_3I,[509] or CF_3TeCF_3[510] led to **709** in moderate yields (Scheme 97).

Scheme 97. Preparation of Fluorine-Containing Building Block 709

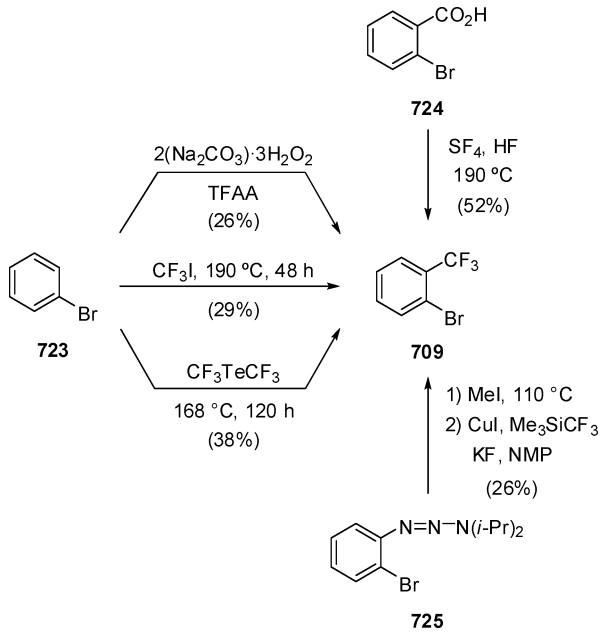

Additionally, 2-bromobenzoic acid (**724**) reacted with SF_4 and HF at 190 °C to furnish **709**.[511] Moreover, **709** can also be synthesized via a two-step, one-pot reaction from triazene **725** (derived from the corresponding aniline) and the Ruppert–Prakash reagent (Me_3SiCF_3) as CF_3 source. Thus, **725** was first treated with methyl iodide and then reacted with Me_3SiCF_3 in the presence of CuI and KF.[512]

5.7. Teriflunomide

Sanofi has developed and launched the oral immunomodulator teriflunomide (A77 1726, **726**) for the treatment of relapsing forms of multiple sclerosis (MS) (Figure 50). As a primary metabolite of the rheumatoid arthritis drug leflunomide (**727**), teriflunomide potently inhibits the mitochondrial enzyme

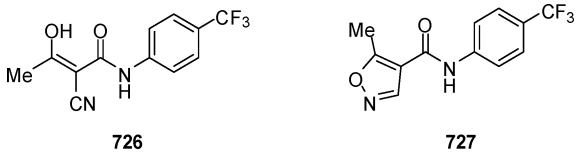

Figure 50. Structures of teriflunomide (**726**) and leflunomide (**727**).

dihydroorotate dehydrogenase (DHODH) and blocks the fourth step of de novo pyrimidine biosynthesis, therefore suppressing the proliferation of human B and T cells.[513] Teriflunomide was approved by the FDA in September 2012 and was launched in the United States shortly afterward. In August 2013 the drug was approved in the EU, and by November 2013, it had been licensed in other six countries worldwide. Sales for the marketed drug (trade name: Aubagio) in 2014 were up 160.8% from 2013, reaching $487 million.

In the 1970s Hoechst Marion Roussel AG disclosed a series of 5-methylisoxazole-4-carboxylic acid anilides possessing antiphlogistic and analgesic actions.[514] Subsequent investigations displayed that derivatives with a trifluoromethyl group at the 4-position of the phenyl ring outperform the other compounds in activity, therapeutic range, and pattern of action, which led to the discovery of leflunomide (**727**).[515] In vivo, the isoxazole moiety of leflunomide is rapidly converted to a (*Z*)-enol as in teriflunomide (**726**) whose target for action was identified as DHODH.[516] Crystal structures of human DHODH in complex with teriflunomide revealed that the binding site of the drug is located in a tunnel leading to the flavin mononucleotide (FMN) binding cavity inside the enzyme. The hydrophilic head forms hydrogen bonds with Arg-136 (mediated by a water molecule) and Tyr-356, while the 4-(trifluoromethyl)phenyl moiety is involved in multiple hydrophobic interactions with residues in the tunnel.[517]

The earliest synthetic route to teriflunomide involved condensation of 5-methylisoxazole-4-carbonyl chloride (**729**) (obtained from acid **728** by chlorination) with 4-(trifluoromethyl)aniline (**730**) to give the prodrug **727**, and the isoxazole ring was then opened by using NaOH in refluxing MeOH to furnish the target molecule teriflunomide (**726**) (Scheme 98).[518] In a similar, more recent example, acid **728**

Scheme 98. Synthesis of Teriflunomide (726) through Isoxazole Ring-Opening

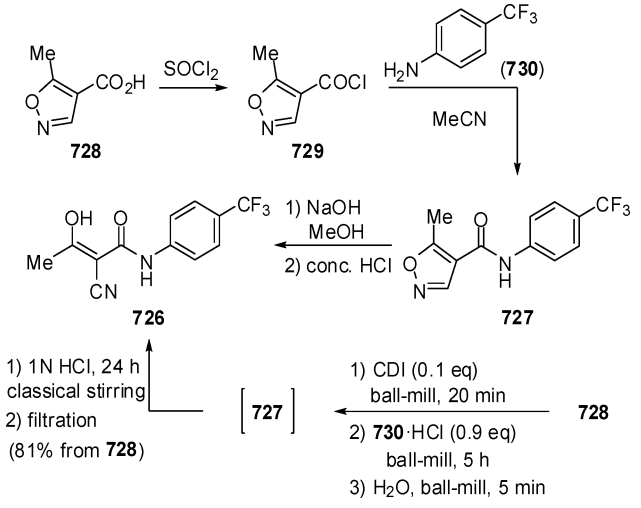

was first treated with CDI without solvent and then coupled with 4-(trifluoromethyl)aniline hydrochloride (**730**·HCl), and finally concentrated HCl was employed to open the ring and afford **726**.[519]

Alternatively, teriflunomide was prepared from ethyl cyanoacetate (**731**) or cyanoacetic acid (**732**) (Scheme 99). Ethyl cyanoacetate (**731**) condensed with aniline **730** at 180 °C to give amide **733**, which was treated with NaH and then

DOI: 10.1021/acs.chemrev.5b00392
Chem. Rev. 2016, 116, 422–518

Scheme 99. Alternative Synthesis of Teriflunomide (726)

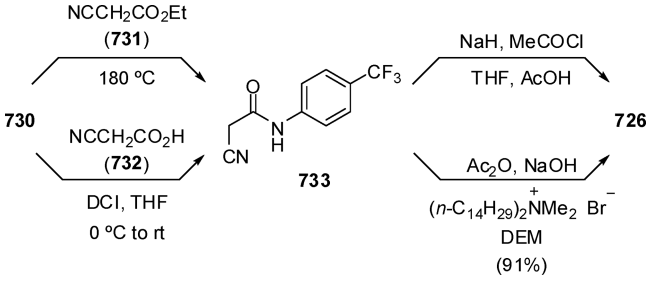

condensed with acetyl chloride to provide teriflunomide (**726**).[520] On the other hand, reaction of cyanoacetic acid (**732**) with aniline **730** in the presence of 1,3-diisopropylcarbodiimide (DCI) also yielded the key intermediate **733**.[521] For improved yield and purity, amide **733** reacted with acetic anhydride in the presence of dimethylditetradecylammonium bromide and NaOH to afford **726** in 91% yield (HPLC purity 99.0%).[522]

For scale-up purposes, a convenient process free of chromatographic purifications consisted in the preparation of (*Z*)-enol ester **734** from ethyl cyanoacetate (**731**) and acetic anhydride using K_2CO_3 as base (Scheme 100). Compound **734** was next coupled with aniline **730** in refluxing xylene to give teriflunomide (**726**).[523]

Scheme 100. Two-Step Preparation of Teriflunomide (726)

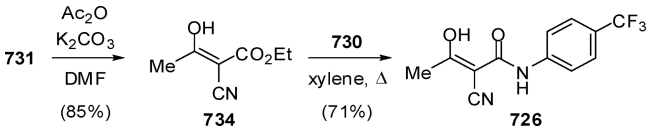

Later on, a route using ethyl acetoacetate (**735**) and aniline **730** as starting materials was developed (Scheme 101).

Scheme 101. Synthesis of Teriflunomide (726) from Ethyl Acetoacetate (735)

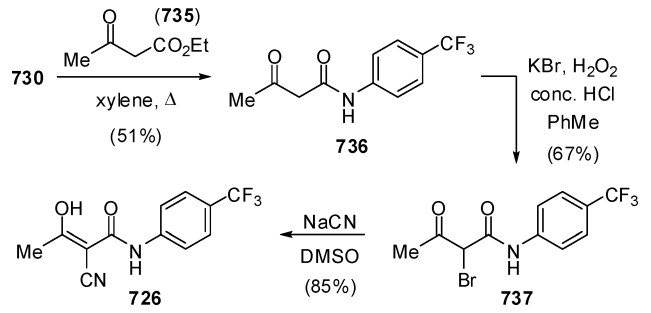

Condensation of **730** and **735** in refluxing xylenes provided acetoamidate **736**, followed by bromination with H_2O_2, KBr, and concentrated HCl to give bromide **737**. Then, displacement with cyanide furnished teriflunomide (**726**). However, column chromatography was required to purify the products of the first two steps.[524]

More recently, a new method for preparing amide **733** was disclosed. Cyanoacetic anhydride (**738**) was prepared from cyanoacetic acid (**732**) in refluxing toluene or by reaction with P_2O_5, and then condensed with aniline **730** in the presence of H_2SO_4 to afford amide **733** (Scheme 102). Finally, conventional condensation with acetyl chloride led to teriflunomide (**726**).[525]

Scheme 102. A New Approach to Amide 733 and Teriflunomide (726)

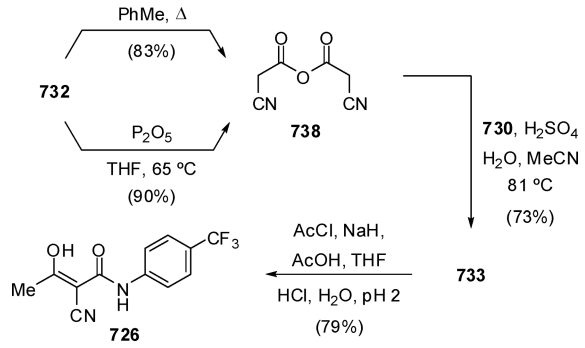

4-(Trifluoromethyl)aniline (**730**) can be accessed by fluorination of 4-trichloromethylphenylisocyanate (**741**) with HF, followed by treatment with water (Scheme 103).[526] The

Scheme 103. Preparation of 4-(Trifluoromethyl)aniline (730)

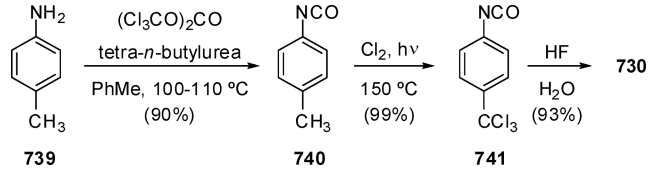

precursor **741** can be smoothly obtained by chlorination of toluene derivative **740** initiated by ultraviolet radiation,[527] while isocyanate **740** can be prepared in good yield by treating readily available 4-methylaniline (**739**) with triphosgene in the presence of tetra-*n*-butylurea.[528]

5.8. Pradigastat

Inhibitors of diacylglycerol acyl transferase-1 (DGAT1) are promising candidates for treating a wide variety of metabolic disorders,[529,530] among then familial chylomicronemia syndrome (FCS), an uncommon genetic disease that may lead to pancreatitis due to high levels of triglycerides in blood. Pradigastat (LCQ-908, **742**), developed by Novartis, is a potent and specific orally available DGAT1 inhibitor, which is currently in phase III clinical trials for treating FCS (Figure 51).

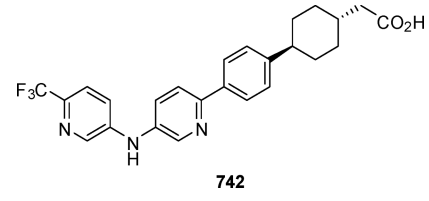

Figure 51. Structure of pradigastat (**742**).

Preclinical models indicated that pradigastat could decrease hyperglycemia, modulate dyslipidemia, and reduce body weight gain.[531] The development for other indications is ongoing, including nonalcoholic fatty liver disease (NAFLD), diabetes, hypertriglyceridemia, and hepatitis C virus (HCV) infection.[532] Clinical studies indicated that pradigastat decreases triglyceride levels in patients with FCS, decreases chylomicron secretion,

DOI: 10.1021/acs.chemrev.5b00392
Chem. Rev. 2016, 116, 422−518

Scheme 104. Synthetic Route to Pradigastat (742)

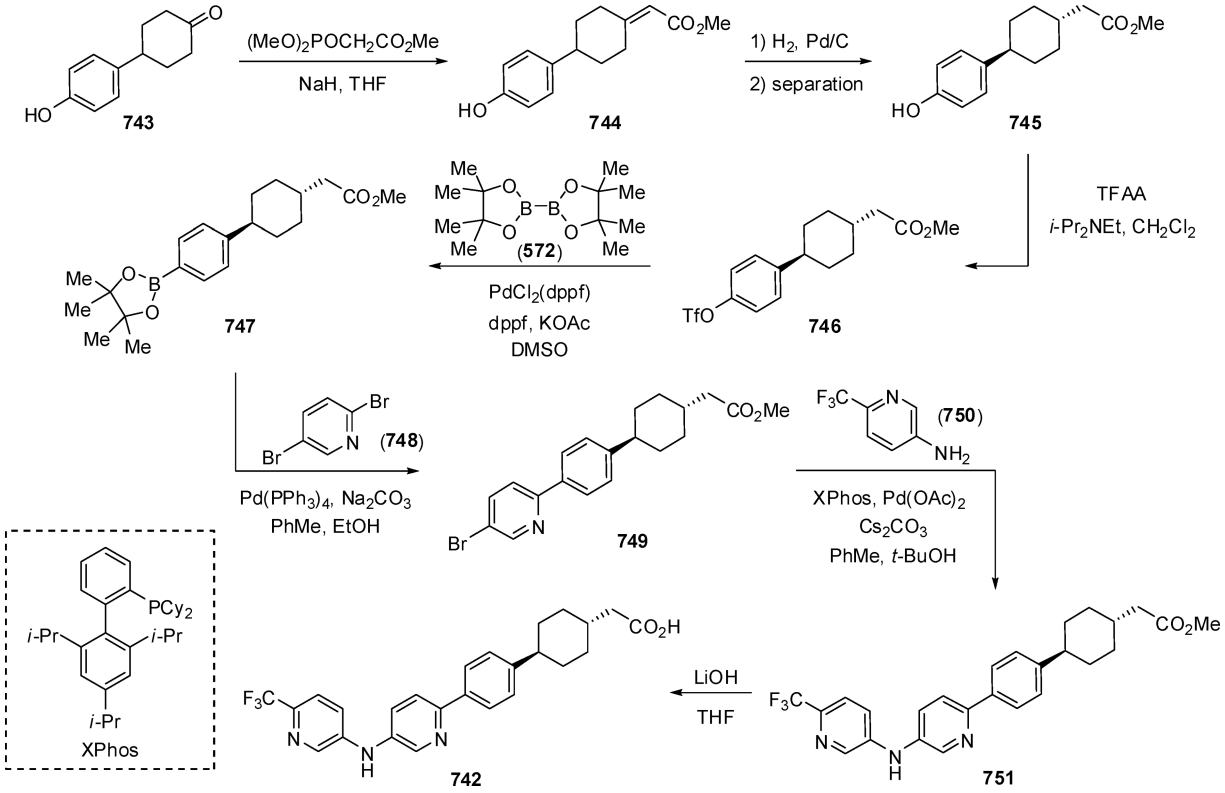

and prevents postprandial triglyceride elevation in humans.[533] In March 2011, the FDA awarded pradigastat orphan status for FCS.

DGAT1 is found mainly in the gastrointestinal (GI) tract, and hence its selective inhibition would diminish the requirements for plasma exposure in vivo. The design of pradigastat derived from a previous series of DGAT1 inhibitors with a benzimidazole carboxamide structure, which were studied to reduce plasma exposure in vivo after oral administration.[534] It was assumed that the trifluoromethyl moiety would increase the metabolic stability and modulate the physicochemical properties of the molecule. Furthermore, in vivo data exhibited by pradigastat showed its efficiency in postprandial plasma triglyceride (PPTG) assays in monkey and dog at 1 mg/kg dose.

The only synthesis of pradigastat described thus far is shown in Scheme 104, although reaction yields were not reported. Horner−Wadsworth−Emmons olefination of ketone **743** produced enoate **744**, and further hydrogenation afforded a mixture of *trans*- and *cis*-cyclohexane isomers, which were separated by chromatography. The *trans*-isomer **745** was transformed into triflate **746**, which upon reaction with bis(pinacolato)diboron (**572**) gave boronate **747**. Suzuki coupling between **747** and 2,5-dibromopyridine (**748**) formed intermediate **749**, which was further coupled with 6-(trifluoromethyl)pyridin-3-amine (**750**) under Buchwald−Hartwig conditions to yield compound **751**. Finally, base-mediated ester hydrolysis and acidification furnished the target compound pradigastat (**742**).[532,535]

5.9. Delamanid

Tuberculosis (TB) is an infectious disease caused by *Mycobacterium tuberculosis* that primarily affects the lungs and is still a leading cause of death worldwide. Approximately 32% of the world population is infected with TB bacillus, being the infection by human immunodeficiency virus (HIV) one of the major reasons for the current expansion of TB. Especially the emergence of multidrug-resistant strains of *M. tuberculosis* that are resistant to the two major first-line drugs, rifampicin and isonicotinic acid hydrazide, has further deteriorated the current situation. Therefore, it is very urgent to develop new and potent antituberculosis drugs with low toxicity that are effective against both drug-susceptible and drug-resistant strains of *M. tuberculosis*. Delamanid (OPC-67683, **752**), developed by Otsuka Pharmaceutical, is a nitroimidazo-oxazole derivative that acts by inhibiting the biosynthesis of mycobacterial cell wall components, methoxy mycolic acid, and ketomycolic acid, for the treatment of multidrug resistant tuberculosis (MDR-TB) infection (Figure 52).[536−538] Currently, delamanid (trade name: Deltyba) is approved in Japan and the EU for use as part of an appropriate combination regimen in adults with MDR-TB infection.[539]

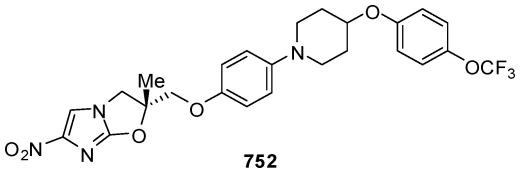

Figure 52. Structure of delamanid (**752**).

Delamanid is a prodrug that requires a bioreduction of its nitro moiety by the deazaflavin dependent nitroreductase to afford the reactive metabolite, which likely plays a vital role in the inhibition of mycolic acid production for the treatment of tuberculosis.[536,539] The structural design of delamanid was initiated from bicyclic compound CGI-17341 (**753**), which was

DOI: 10.1021/acs.chemrev.5b00392
Chem. Rev. 2016, 116, 422−518

discovered at Ciba-Geigy showing favorable in vitro activity and in vivo efficacy against tuberculosis, although its mutagenicity prevented its further development (Scheme 105).[540] Another

Scheme 105. Discovery of Delamanid (752)

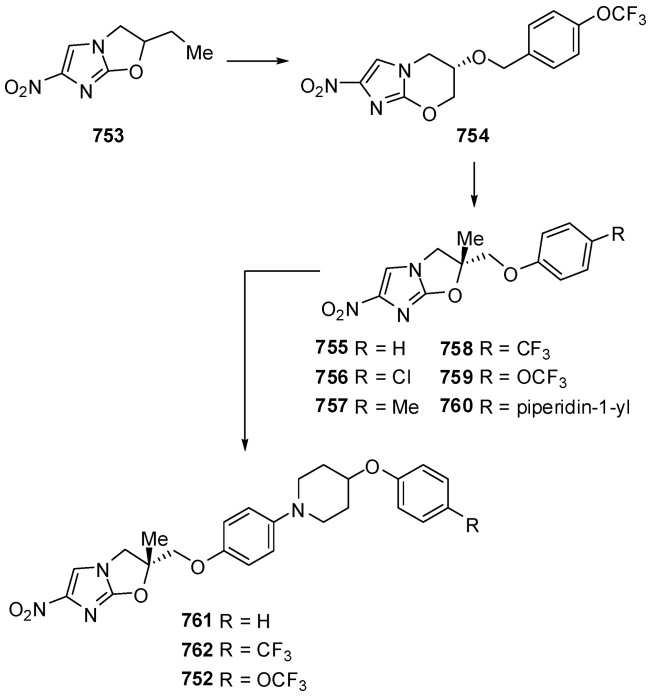

bicyclic compound, nitroimidazopyran PA-824 (**754**), containing a trifluoromethoxy group, was subsequently developed by PathoGenesis Corp., demonstrating potent activity against MDR *M. tuberculosis* and favorable oral activity in animal infection models.[541,542] Based on these findings, researchers at Otsuka Pharmaceutical studied the substitution patterns at the C-2 position of 6-nitro-2,3-dihydroimidazo[2,1-*b*]oxazoles in order to enhance antituberculosis activity and eliminate mutagenicity, initially leading to derivatives **755**–**760** that did not exert mutagenicity. For instance, introduction of fluorine atoms as in compounds **758** and **759** resulted in a loss of in vitro activity, but they exhibited more potent in vivo efficacy than unsubstituted analogue **755**. A hydrophilic piperidine group was also tested in order to improve the bioavailability, but compound **760** showed a poor efficacy in vitro and in vivo. However, further inclusion of lipophilic phenoxy groups to the C-4 position of the piperidine ring (compounds **761** and **762**) increased antituberculosis activity. In particular, the introduction of a trifluoromethoxy moiety in delamanid (**752**) afforded the highest in vitro and in vivo antibacterial activity against drug-susceptible and drug-resistant strains of *M. tuberculosis* among all synthesized compounds.[543]

In addition, delamanid demonstrated a high and dose-dependent activity against intracellular *M. tuberculosis* H37Rv, with activity superior to the first-line drug rifampicin. Administration of delamanid in combination with rifampicin and pyrazinamide also exhibited a much faster eradication (by at least 2 months) of viable TB bacilli in the lung, in comparison to the use of rifampicin/pyrazinamide alone. More important, delamanid did not affect the activity of liver microsome enzymes, indicating that it could be used in combination with some antiretroviral drugs.[544] After oral administration, the C_{max} of delamanid for the different dosage groups was observed at 4–5 h. Its exposure did not increase in a dose-dependent fashion, needing 10–14 days to reach the steady state concentration.[536,545]

Delamanid was synthesized according to the strategy depicted in Scheme 106. First, compound **765** was prepared from the starting materials TPH-protected phenol **763** and 4-(4-(trifluoromethoxy)phenoxy)piperidine (**764**) via a simple palladium-catalyzed Buchwald–Hartwig coupling followed by deprotection with pyridinium *p*-toluenesulfonate (PPTS). On the other hand, imidazole **766** was reacted with chiral epoxide **767** in the presence of Et_3N to give intermediate **768**, which was further converted into diol **769** by hydrolysis of the *p*-nitrobenzoate moiety. Diol **769** was selectively activated as its primary mesylate **770** and then further transformed into the key (*R*)-epoxide **771** by reaction with DBU. Finally, nucleophilic ring-opening of **771** by reaction with the sodium

Scheme 106. Synthetic Route to Delamanid (752)

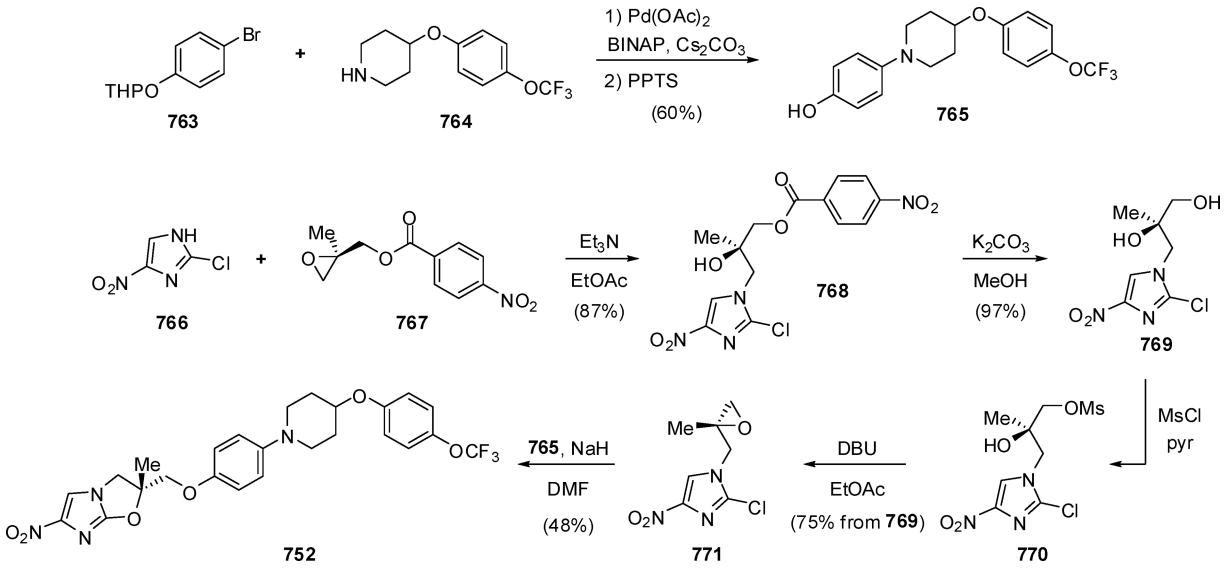

DOI: 10.1021/acs.chemrev.5b00392
Chem. Rev. 2016, 116, 422–518

phenoxide derived from **765** and in situ ring-closure afforded the target product delamanid (**752**).[543]

6. COMPOUNDS CONTAINING TWO TRIFLUOROMETHYL GROUPS

6.1. Netupitant and Rolapitant

The neurokinin-1 (NK_1) receptor is a G-protein coupled receptor widely found in the mammalian central and peripheral nervous system.[546] The endogenous ligand of NK_1 receptor is substance P, a neuropeptide composed of 11 amino acids that induces vomiting by binding to NK_1 receptor.[547] Therefore, NK_1 receptor antagonists may prevent the vomiting reflex by blocking the action of substance P existing in the vomiting center of the brainstem. As a result, these antagonists have an important therapeutic value in treating chemotherapy-induced nausea and vomiting (CINV) or postoperative nausea and vomiting (PONV) in patients with cancer,[548,549] as well as in a large number of both central and peripheral diseases, such as pain and migraine, mood and anxiety levels, etc.[550−552] Remarkably, a 3,5-bis(trifluoromethyl)phenyl moiety is shared in a number of structurally unrelated series of NK_1 receptor antagonists such as aprepitant (**772**), developed by Merck, which was approved by the FDA for the treatment of CINV in 2003 (Figure 53).[553] More recently, netupitant (R-1124, Ro-7-

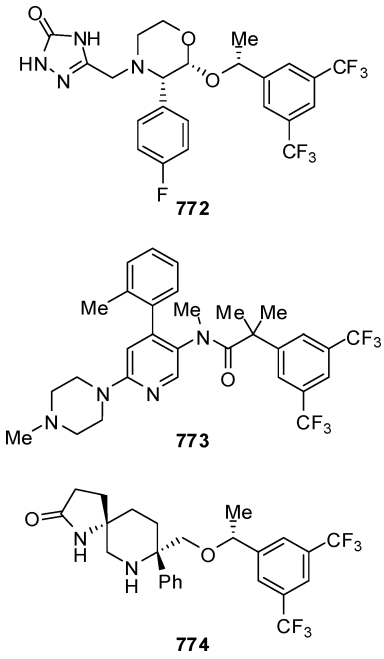

Figure 53. Structures of aprepitant (**772**), netupitant (**773**), and rolapitant (**774**).

3189, **773**) was originally discovered by Roche as a highly selective NK_1 receptor antagonist for the potential treatment of CINV and overactive bladder, and subsequently licensed to Helsinn Healthcare. In 2010, the phase III trials for netupitant were initiated for treating CINV, and its combination with palonosetron, a 5-HT_3 receptor antagonist approved in 2008, received authorization by the FDA on October 10, 2014 (trade name: Akynzeo) to treat nausea and vomiting in patients undergoing cancer chemotherapy.[554]

Similarly, rolapitant (SCH-619734, **774**) is an oral NK_1 receptor antagonist for the potential prevention of CINV/PONV and the treatment of cough.[555,556] Rolapitant originated from Schering-Plough, but was licensed successively to OPKO Health and Tesaro Inc. In October 2012, Tesaro initiated a phase III trial to assess the safety and efficacy of rolapitant administered in patients receiving highly emetogenic chemotherapy. The final phase III study was finished in June 2014, followed by submitting an NDA to the FDA for the treatment of CINV. Rolapitant (trade name: Varubi) was recently (September 2015) approved by the FDA.[557]

The discovery of netupitant at Roche began from the lead compound **775**, obtained through a screening of their corporate compound library, and displaying a moderate affinity at the human NK_1 receptor (Scheme 107). In the initial optimization,

Scheme 107. Discovery of Netupitant (773)

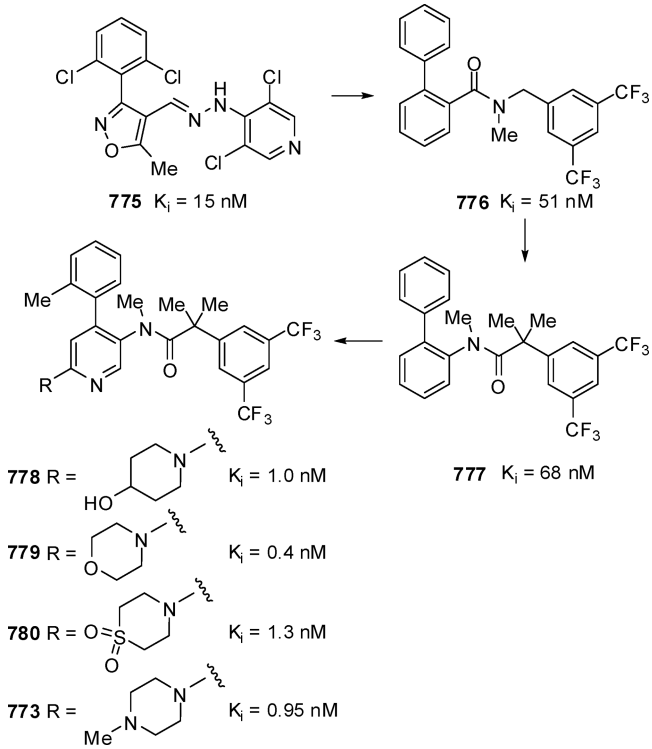

the isoxazole moiety was replaced by a simple benzene ring, and the potentially toxic *N*-(4-pyridyl)-hydrazone was also substituted by an amide fragment containing the familiar 3,5-bis(trifluoromethyl)phenyl group to allow a better penetration of the blood−brain barrier (BBB), affording compound **776**. Further modifications focused on the linker between both aromatic subunits, and hence replacement of the *N*-methyl carboxamide of **776** by the inverse amide linker led to a similar potent binding affinity in compound **777**. The final optimization preserved the fluorinated part of the molecule, and consisted of the introduction of heterocycles into the biaryl scaffold. In this manner, a significant increase in binding affinity against the NK_1 receptor was observed in compounds **778**−**780** and netupitant (**773**). Moreover, these compounds were highly selective (more than 100-fold) in their binding toward NK_2 and NK_3 subtype receptors, and in vivo excellent oral antagonist activities were also accomplished in studies in gerbils.[558]

Meanwhile, rolapitant was initially developed by a Schering-Plough (now Merck) group during the search for NK_1 receptor antagonists, such as racemic 2,2-disubstituted piperidine **781**

DOI: 10.1021/acs.chemrev.5b00392
Chem. Rev. 2016, 116, 422−518

(Scheme 108).[559] Another active lead compound **782** was designed from **781** by keeping the 3,5-bis(trifluoromethyl)-

Scheme 108. Discovery of Rolapitant (774)

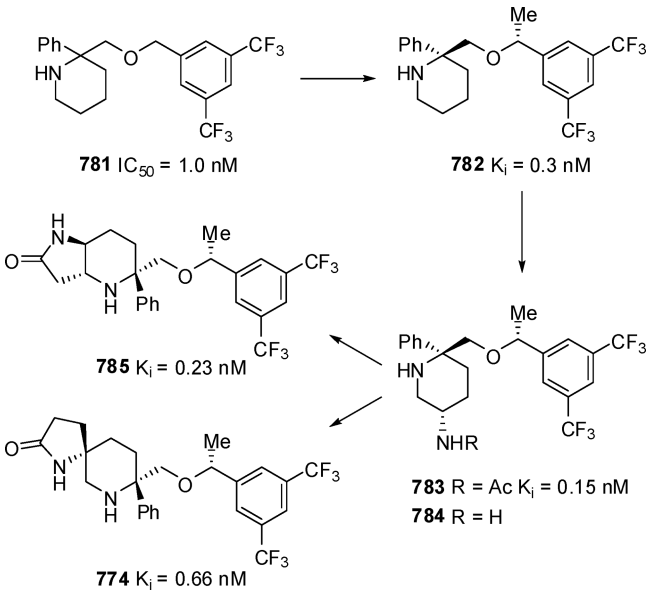

phenyl group and introducing a chiral carbon center.[560] Further SAR investigation from compound **782** was undertaken in order to improve its overall biological profile, and their efforts provided a series of potent, orally active NK_1 antagonists represented by compound **783**. However, detailed studies found that **783** could be metabolized to deacetylation product **784**, which is susceptible to produce phospholipidosis by attaching its diamino function to the lipid bilayer. Therefore, a cyclization strategy was pursued to circumvent this undesirable adverse effect, generating bicyclic lactam structures such as L-00400882 (**785**)[561] and rolapitant (**774**),[562] the latter showing a high affinity in vitro for the human NK_1 receptor, as well as high selectivity (>1000-fold) over the human NK_2 and NK_3 subtypes. In addition, rolapitant has high CNS penetrance, with an exceptionally long $t_{1/2}$ of approximately 180 h after oral administration. Furthermore, its efficacy in various animal models of emesis was demonstrated.[563]

The initial synthesis of netupitant, achieved during its early development at Roche, utilized 2-chloro-5-nitropyridine (**786**) as the starting material (Scheme 109). Nucleophilic substitution in **786** with *N*-methylpiperazine (**787**) afforded **788**, which was further hydrogenated to aminopyridine **789**. After protection of the amino group, regioselective deprotonation and trapping with iodine produced **791**. Next, Suzuki cross-coupling with *o*-tolylboronic acid furnished biaryl derivative **792**. The amide protecting group was then removed and the carbamate **794** was next formed by reaction of **793** with trimethyl orthoformate. Reduction of **794** yielded methylamine **795**, and final amide bond formation by reaction with acid chloride **796** led to netupitant (**773**).[558]

However, the above synthesis had some weaknesses that precluded its implementation on a larger scale, namely the low temperature (−78 °C) required in the lithiation of intermediate **790**, and the relatively expensive *o*-tolylboronic acid as the Suzuki coupling substrate. Therefore, an alternative route was pursued that could provide larger quantities of netupitant for clinical evaluation. As shown in Scheme 110, *tert*-butylamide **798** was prepared using 6-chloronicotinic acid (**797**) as the starting material. The 4-aryl substituent of the pyridine ring was introduced by 1,4-addition of *o*-tolylmagnesium chloride followed by dihydropyridine oxidation mediated by DDQ. Then, the resulting intermediate **799** was coupled with piperazine **787** to afford amide **800** after deprotection with $MeSO_3H$. Compound **800** was subjected to a Hofmann rearrangement with in situ generated sodium hypobromite to form the corresponding methyl carbamate **794**, which was reduced with excess Red-Al to the methylamine **795**. As before, coupling of **795** with acid chloride **796** gave the target product netupitant (**773**).[564]

An efficient synthesis of bis(trifluoromethyl)-containing acid chloride **796** was described starting from 1-bromo-3,5-bis(trifluoromethyl)benzene (**801**) (Scheme 111). The Grignard

Scheme 109. Medicinal Chemistry Route to Netupitant (773)

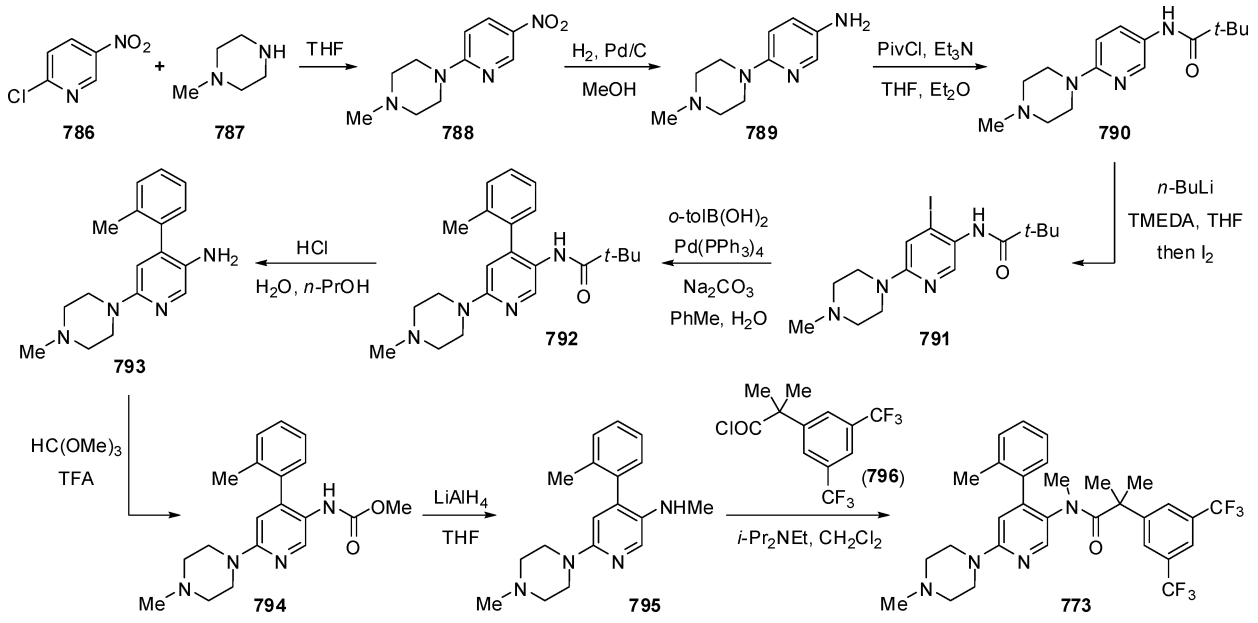

DOI: 10.1021/acs.chemrev.5b00392
Chem. Rev. 2016, 116, 422−518

Scheme 110. Improved Synthesis of Netupitant (773)

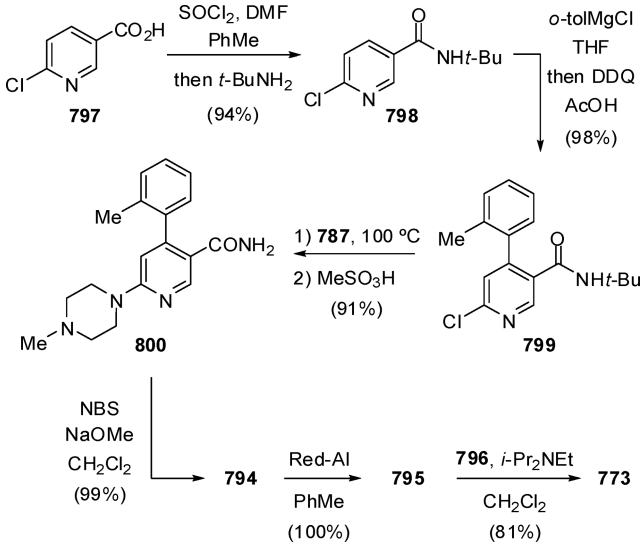

Scheme 111. Preparation of Acid Chloride 796

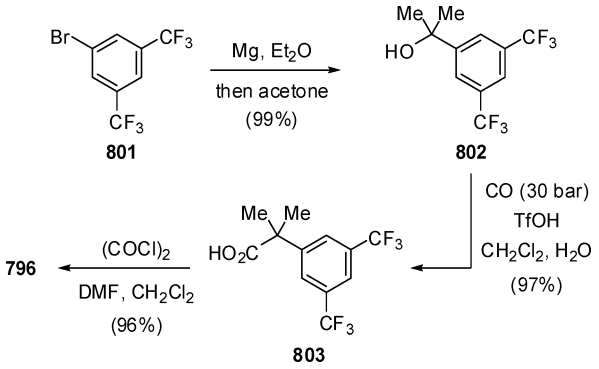

reagent derived from **801** reacted with acetone, and the resulting intermediate **802** was then carbonylated at high pressure to afford carboxylic acid **803**. Finally, acid chloride formation furnished **796**.[564]

Still, the use of the relatively expensive nicotinic acid **797** was circumvented in an advanced synthetic approach using readily available starting materials. Thus, 2-methylbenzaldehyde (**804**) was reacted with methyl cyanoacetate to produce ester **805**, which was mixed with pyridinium salt **807** (in situ prepared from pyridine and 2-chloroacetamide (**806**)) to give intermediate **808** that evolved to the isolable pyridinium inner salt **809** in high yield (Scheme 112). Removal of the pyridinium moiety with $POCl_3$ afforded dichloropyridine **810**. Displacement of one chlorine atom by morpholine **787** proceeded with high regioselectivity, and finally removal of the remaining chlorine in **811** by hydrogenation and hydrolysis of the nitrile function furnished amide intermediate **800**.[565]

The only synthesis of rolapitant described thus far is depicted in Scheme 113. Chiral oxazolidinone **812** was alkylated with bromide **813** to produce compound **814**. Reduction to lactol **815** was followed by a Wittig reaction with phosphonium salt **816** to afford olefin **817**. Double bond hydrogenation and acid-mediated cyclization led to enamide **818**, which was converted into ketone **819** by hydroboration and subsequent Swern oxidation. Next, reaction of **819** with ammonium carbonate and potassium cyanide yielded hydantoin **820**, and its hydrolysis furnished cyclic amino acid **821**. Reduction to amino alcohol

Scheme 112. Process Synthesis of Intermediate 800

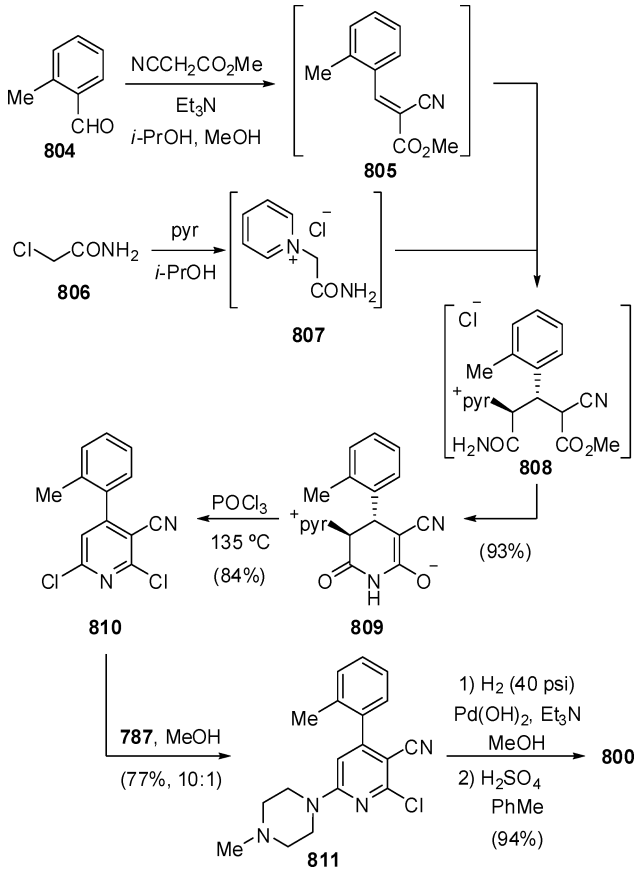

822 was carried out by activation with triphosgene and further reaction with $LiBH_4$, and then **822** was oxidized and subjected to a Horner–Wadsworth–Emmons olefination to give enoate **823**. Finally, hydrogenation and lactam formation gave rise to a mixture of spirocyclic compounds, from which rolapitant (**774**) was isolated by separation on a chiral stationary phase.[562] Due to the multistep character of this synthetic route, some modifications have been further disclosed based on the key intermediate **818**, which shorten the synthetic steps, lessen undesirable isomers, and improve the chemical yields.[566,567]

6.2. Evacetrapib

Cholesteryl ester transfer protein (CETP) is a glycoprotein that regulates the equilibrium between plasma lipoprotein particles, high-density lipoprotein (HDL), and low-density lipoprotein/very-low-density lipoprotein (LDL/VLDL) by facilitating the transfer of cholesteryl ester and triglycerides. Plasma CETP mass and activity are elevated in cardiovascular disease (CVD) patients, resulting in decreased HDL and increased LDL.[568] However, epidemiological studies suggest that both high LDL-cholesterol (LDL-C) levels and low HDL-cholesterol (HDL-C) levels are positive predictors of CVD. Therefore, CETP inhibitors are gaining substantial research interest for the treatment of coronary heart disease.[569] Evacetrapib (LY2484595, **824**), a novel benzazepine-based CETP inhibitor, was developed by Eli Lilly for the potential treatment of hypercholesterolemia and dyslipidemia, and to prevent atherosclerosis (Figure 54).[570,571] Phase III trials of evacetrapib are still in progress for the indications of high-risk CVD.

Torcetrapib (**825**) was the first CETP inhibitor (in vivo IC_{50} = 13 ± 2.7 nM) that underwent large phase III trials supported

DOI: 10.1021/acs.chemrev.5b00392
Chem. Rev. 2016, 116, 422–518

Scheme 113. Synthetic Route to Rolapitant (774)

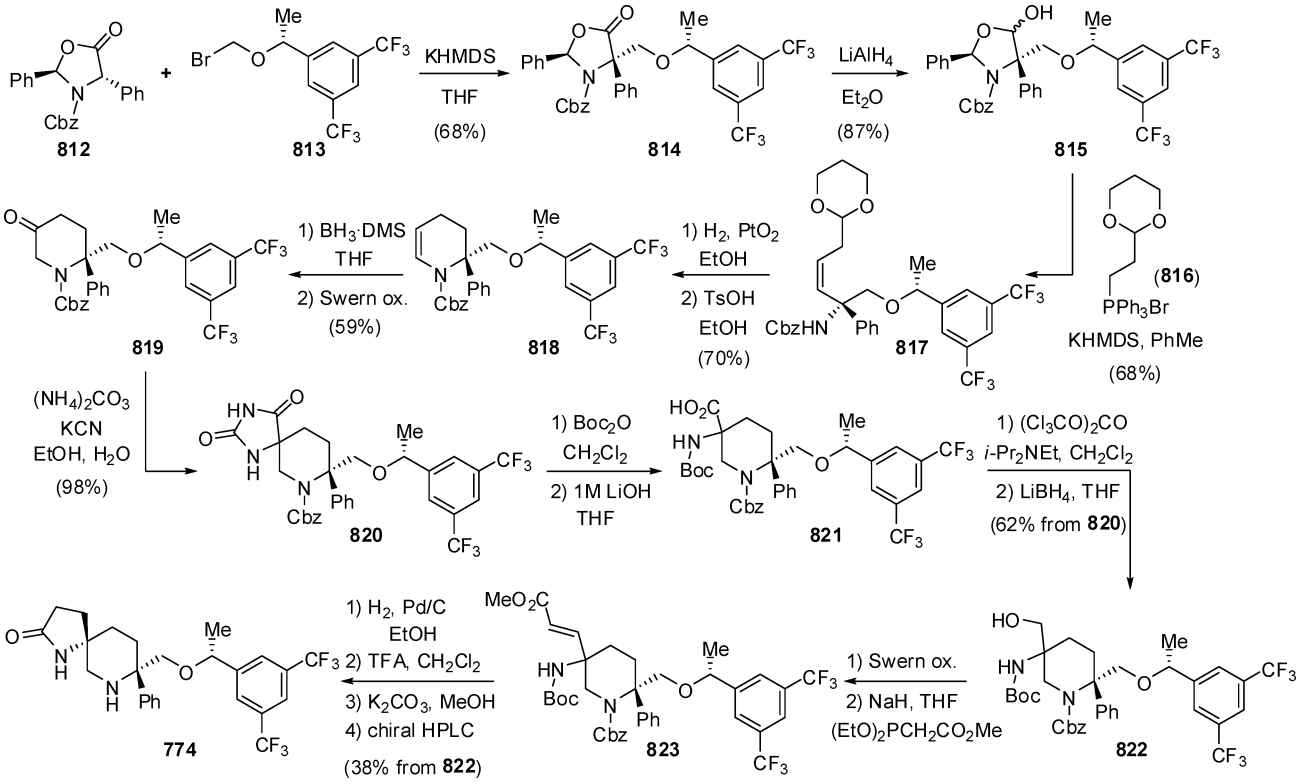

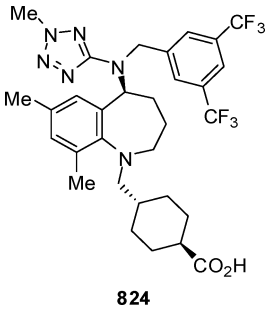

Figure 54. Structure of evacetrapib (**824**).

Scheme 114. Evolution from Torcetrapib (825) to Evacetrapib (824)

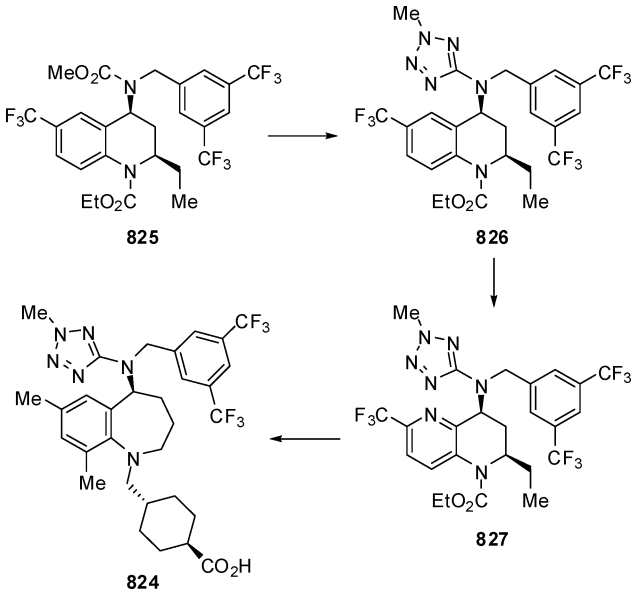

by Pfizer, and gave researchers at Eli Lilly the ideas for structural transformations in the search for new inhibitors (Scheme 114). They attempted the heterocyclic replacement of the 4-carbamate of torcetrapib, and the resulting 2-methyltetrazole analogue **826** exhibited a significant potency of CETP inhibition (plasma CETP IC_{50} = 13 nM). Tetrahydronaphthyridine analogues were also part of the investigation, and the most potent compound was the (2*R*,4*S*)-enantiomer **827**, with the same substitution pattern as in **826**, and displaying a CETP IC_{50} of 23 nM in plasma. Subsequently, the tetrahydronaphthyridine core was replaced by a benzazepine system, where the substituents were optimized for potency and bioavailability to ultimately provide evacetrapib (**824**, IC_{50} = 26 nM).[572] Noticeably, the trifluoromethyl groups in evacetrapib that enhanced significantly the potency were inherited from torcetrapib. In addition, evacetrapib circumvented some of the side effects associated with the use of torcetrapib, essentially an increase in blood pressure, because of adrenal synthesis of aldosterone or cortisol.[569]

Eli Lilly's preparation of evacetrapib is illustrated in Scheme 115. The crucial steps of the synthesis involved the highly effective construction of the three chiral centers. Boc protection of the commercially available 2-amino-3,5-dimethylbenzoic acid (**828**) was followed by methyl esterification to obtain **829**, which was alkylated with ethyl 4-bromobutyrate to give intermediate **830**. Dieckmann condensation of **830** afforded a mixture of methyl and ethyl ketoesters **831** that were decarboxylated in acidic media to get seven-membered ring bearing compound **832**. After protection of the amino group with benzyl chloroformate, construction of the first chiral center started from the condensation of intermediate **833** and

DOI: 10.1021/acs.chemrev.5b00392
Chem. Rev. 2016, 116, 422−518

Scheme 115. Synthetic Route to Evacetrapib (824)

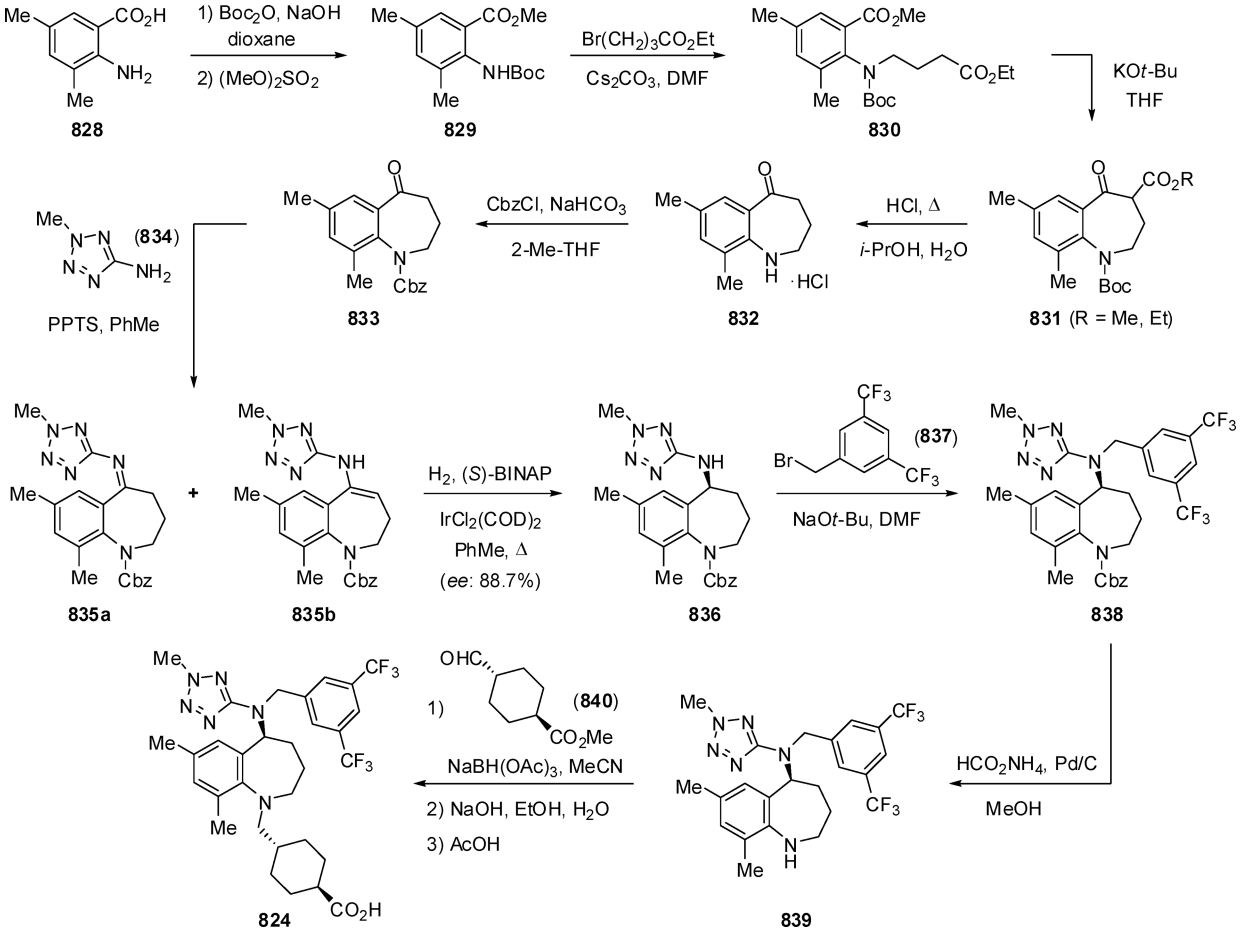

5-amino-2-methyltetrazole (**834**) to give two different intermediates, imine **835a** and enamine **835b**. A mixture of both substrates was then subjected to an asymmetric hydrogenation using (*S*)-BINAP as chiral auxiliary to get chiral amine **836** in moderate enantiomeric excess. The introduction of the bis(trifluoromethyl)-containing fragment was achieved by alkylation of **836** with bromide **837**, and then the protecting group was removed to yield compound **839**. It should be noted that an alternative approach may involve using 3,5-bis-(trifluoromethyl)benzylamine, which can be conveniently prepared by biomimetic transamination.[573] The remaining prochiral centers both derived from the raw material, methyl *trans*-4-formylcyclohexanecarboxylate (**840**), which was reacted with **839** through a reductive amination reaction, and finally evacetrapib (**824**) was easily accessed by converting the ester group to a carboxylic acid.[574] More recently, a hydrogenative reductive amination protocol for the coupling of **839** and **840** was described, avoiding the use of the relatively expensive $NaBH(OAc)_3$ and minimizing the risk of epimerization of aldehyde **840** by addition of a small amount of water.[575]

7. COMPOUNDS CONTAINING BOTH TRIFLUOROMETHYL GROUPS AND FLUORINE ATOMS

7.1. Enzalutamide

Androgen-deprivation therapy (ADT) has been the basic treatment for advanced and metastatic prostate adenocarcinoma since the 1940s. Although the disease is initially sensitive to ADT, clinical resistance will eventually arise after using first-generation androgen receptor (AR) antagonists, such as bicalutamide (**680**) (see section 5.5), leading to metastatic castration-resistant prostate cancer (mCRPC) due to AR overexpression, AR mutation, and upregulation of the enzymes associated with androgen biosynthesis (Figure 55).[576] Since the AR signaling remains active in patients with mCRPC, a great

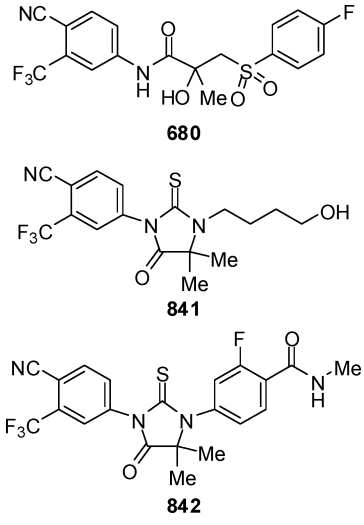

Figure 55. Structures of bicalutamide (**680**), RU 59063 (**841**), and enzalutamide (**842**).

DOI: 10.1021/acs.chemrev.5b00392
Chem. Rev. 2016, 116, 422−518

deal of effort was invested in screening derivatives of the nonsteroidal AR antagonist RU 59063 (**841**), that culminated in the discovery of enzalutamide (MDV3100, **842**), a novel oral AR signaling competitive antagonist with no agonism activity.[577] Enzalutamide was developed by Medivation in collaboration with Astellas, and received approval by the FDA in September 2012 indicated for patients with mCRPC who have been previously treated with docetaxel.[578] Sales of the marketed drug (trade name: Xtandi) reached $71.5 million in 2012.

Structurally, 1,3-diarylthiohydantoin analogues with electron-withdrawing groups attached directly to the phenyl ring, such as an *N*-methylamide, can effectively avoid oxidative metabolism in order to increase the serum concentration. The introduction of a fluorine atom at the 3-position of the phenyl ring not only enhanced the antitumor activity (IC_{50} = 122 nM), but also gave a better pharmacokinetic (PK) profile, compared with bicalutamide (IC_{50} = 1000 nM).[579]

Enzalutamide demonstrated a significant improvement in patient overall survival (OS) compared with those receiving placebo (median 18.4 months versus 13.6 months, HR 0.63; $P < 0.001$).[580] The potent antitumor activity of enzalutamide probably results from its multifold mechanisms in the AR signaling pathway. First of all, enzalutamide shows higher affinity to AR compared with testosterone and the first-generation AR antagonists, and also inhibits AR-testosterone nuclear translocation and DNA transcription. In addition, enzalutamide induces a conformational change of AR to impair the binding to DNA and cofactor recruitment, resulting in apoptosis of prostate cancer cells.[581]

The initial medicinal chemistry route to enzalutamide relied on the late condensation of isothiocyanate **843** and benzamide **848** to form the thiohydantoin ring (Scheme 116). Isothiocyanate **843** was easily obtained by reacting benzonitrile **639** with thiophosgene. On the other hand, benzamide **848** was prepared from commercially available 2-fluoro-4-nitrotoluene (**844**), which was initially oxidized to carboxylic acid **845**. The corresponding acid chloride reacted with methylamine to afford benzamide **846**, and then the nitro group was reduced to give aniline **847**. Subsequent condensation with acetone cyanohydrin was followed by final coupling between **843** and **848** to furnish enzalutamide (**842**).[579]

An improved, multigram synthesis of enzalutamide was performed using a similar approach starting from 4-bromo-2-fluorocarboxylic acid (**849**) (Scheme 117). The derived benzamide **850** reacted with aminoisobutyric acid using copper(I) catalysis to yield acid **851**, which was subsequently esterified and finally converted into enzalutamide (**842**) by reaction with trifluoromethyl-containing isothiocyanate **843**.[582]

7.2. Regorafenib

Regorafenib (BAY 73-4506, **853**), as a novel oral multikinase inhibitor, was developed and launched by Bayer in collaboration with Onyx Pharmaceuticals for the potential treatment of metastatic colorectal cancer (CRC) (Figure 56).[583,584] Regorafenib (trade name: Stivarga) was approved for metastatic CRC and gastrointestinal stromal tumor (GIST) in the United States and the EU in 2013. This drug was also launched in Japan for unresectable, advanced/recurrent CRC in May 2013. In addition, regorafenib has been in phase III clinical trials since May 2013 as a second-line therapy in advanced hepatocellular carcinoma (HCC).

Scheme 116. Medicinal Chemistry Route to Enzalutamide (842)

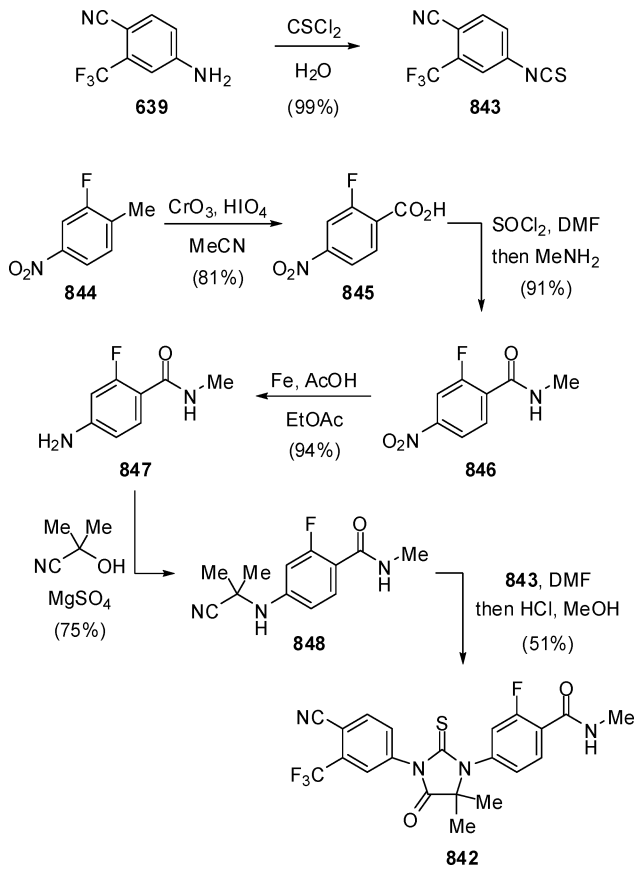

Scheme 117. Scaled-Up Process to Enzalutamide (842)

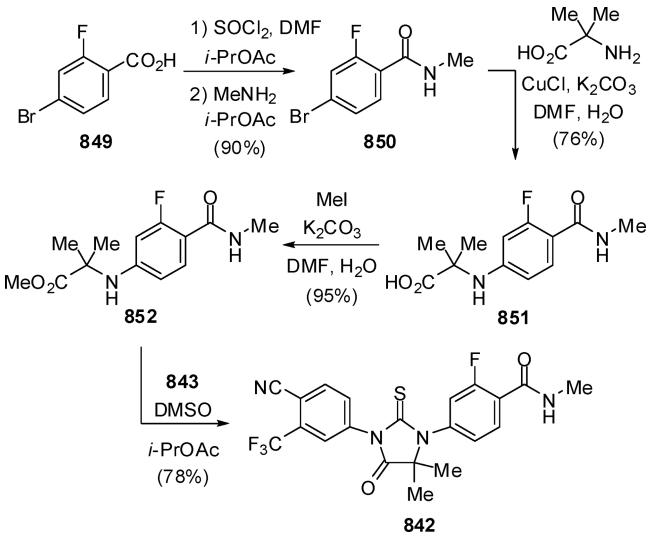

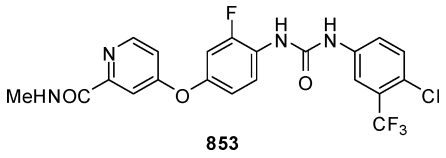

Figure 56. Structure of regorafenib (**853**).

DOI: 10.1021/acs.chemrev.5b00392
Chem. Rev. 2016, 116, 422−518

Regorafenib is a monofluorinated derivative of the previously marketed anticancer drug sorafenib (**859**) (Scheme 118). The

Scheme 118. Discovery of Regorafenib (853)

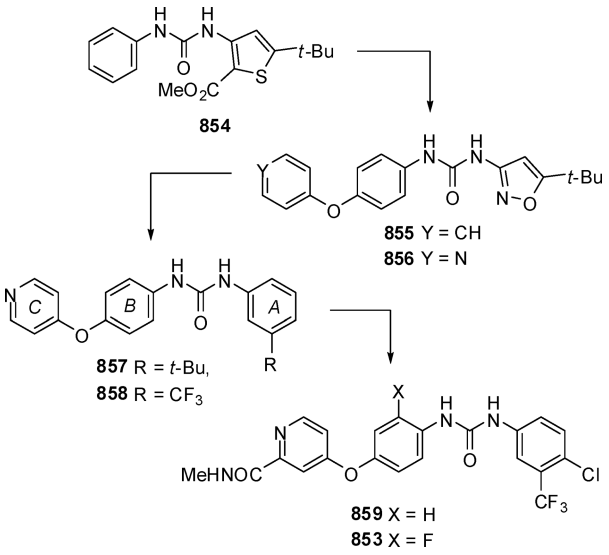

structural design of both sorafenib and regorafenib started from the hit compound **854**, identified from high-throughput screening by Bayer and Onyx Pharmaceuticals, exhibiting moderate inhibition against Raf-1 kinase (Raf-1: IC_{50} = 17 μM).[585] A series of urea derivatives were synthesized by means of a combinatorial chemistry approach to explore the SAR preliminarily, which led to the identification of derivatives **855** and **856** with improved potency (Raf-1: IC_{50} = 1.1 and 0.23 μM, respectively).[586] While the essential pyridine fragment was retained, a phenyl ring was introduced instead of the isoxazole moiety for further facile modification to afford compound **857** with slightly decreased potency (Raf-1: IC_{50} = 0.87 μM).[587] It was noteworthy that the inhibitory potency was considerably improved by replacement of the *tert*-butyl group in **857** by substituents, such as a trifluoromethyl group, to give compound **858** (Raf-1: IC_{50} = 0.46 μM). Further elaboration at rings A and C led to the discovery of sorafenib (**859**), followed by the incorporation of fluorine at the ring B to afford regorafenib (**853**). Interestingly, regorafenib demonstrated a better pharmacological potency compared with sorafenib, but with a similar but distinct in vitro inhibitory profile.[584,588]

Regorafenib was synthesized as shown in Scheme 119. Picolinic acid (**860**) was heated in the presence of the Vilsmeier reagent, and the corresponding acyl chloride was treated directly with methylamine to provide **861** without additional purification. Substitution of **861** with iminophenol **862** (prepared from the corresponding aniline) in the presence of potassium *tert*-butoxide gave intermediate **863**, and final reaction with isocyanate **864** formed the urea function of regorafenib (**853**).[589]

7.3. Bitopertin

Bitopertin (RG1678, **865**) was developed by Roche and its subsidiary Chugai for the potential treatment of schizophrenia, including negative symptoms and suboptimally controlled positive symptoms (Figure 57).[590] As an oral small molecule glycine transporter-1 (GlyT1) inhibitor,[591] administration of bitopertin could enhance *N*-methyl-D-aspartate (NMDA) receptor activity by elevating extracellular levels of glycine in

Scheme 119. Synthetic Route to Regorafenib (853)

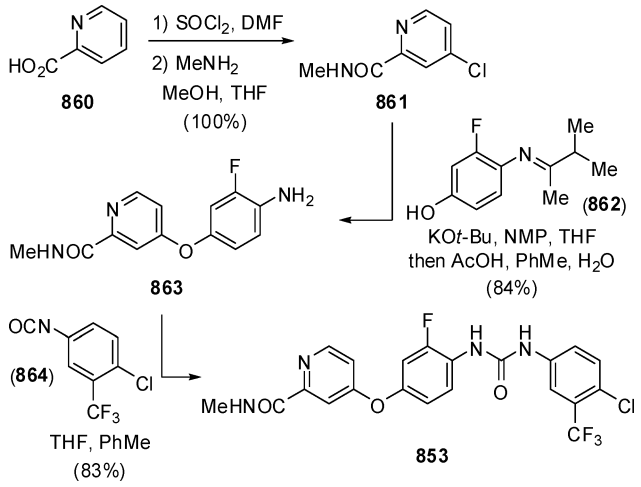

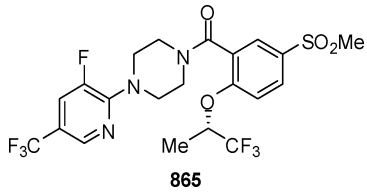

Figure 57. Structure of bitopertin (**865**).

the brain.[592] By November 2010, a global phase III program had been initiated in the United States, including three trials in patients with suboptimally controlled positive symptoms and three in patients with negative symptoms with all patients already stable on antipsychotic therapy.

The discovery of bitopertin originated from benzoylpiperazine hit **866**, identified as one of non-amino-acid chemotypes of GlyT1 inhibitors by screening of the Roche compound collection, and showing a selectivity higher than 300-fold against the type 2 isoform with a potent inhibitory activity (GlyT1: EC_{50} = 0.015 μM; GlyT2: EC_{50} = 4.8 μM) (Scheme 120).[593] However, the nitro group in compound **866** had to be removed, because of potentially serious safety issues.[594] After replacements with various groups, potent activity was only obtained with the introduction of polar electron-withdrawing groups at position 4, such as methylsulfone **867** (GlyT1: EC_{50} = 0.07 μM). Further modifications at position 2 of the benzoyl motif and position 4′ of piperazine-benzene led to the discovery of the cyclopropylmethylenoxy analogue **868**, which exhibited high in vitro potency and good physicochemical properties [GlyT1: EC_{50} = 0.016 μM, *c* Log *P* = 1.83, aqueous solubility 31 μg/mL (pH 6.5), membrane permeability Pe(PAMPA) 3.2]. However, compound **868** could cause heart problems, due to a pronounced inhibitory activity measured at the hERG channel (IC_{50} = 0.6 μM) and demonstrated suboptimal CNS penetration (brain/plasma = 0.10).[595] During the investigations of a series of alkoxy residues at the position 2, shorter substituents, such as isopropyloxy or trifluoroisopropyloxy in derivatives **869** and **870**, respectively, significantly decreased hERG inhibitory activity (**869**: IC_{50} = 3.3 μM; **870**: IC_{50} = 3.0 μM). Compared with the methyl group, the trifluoromethyl group in compound **870** slightly improved CNS penetration (brain/plasma = 0.25).[596] After detailed SARs at position 4′ of the aniline moiety, trifluoromethyl derivative **871**, which maintained high affinity (GlyT1: EC_{50} = 0.013 μM), proved

DOI: 10.1021/acs.chemrev.5b00392
Chem. Rev. 2016, 116, 422−518

Scheme 120. Discovery of Bitopertin (865)

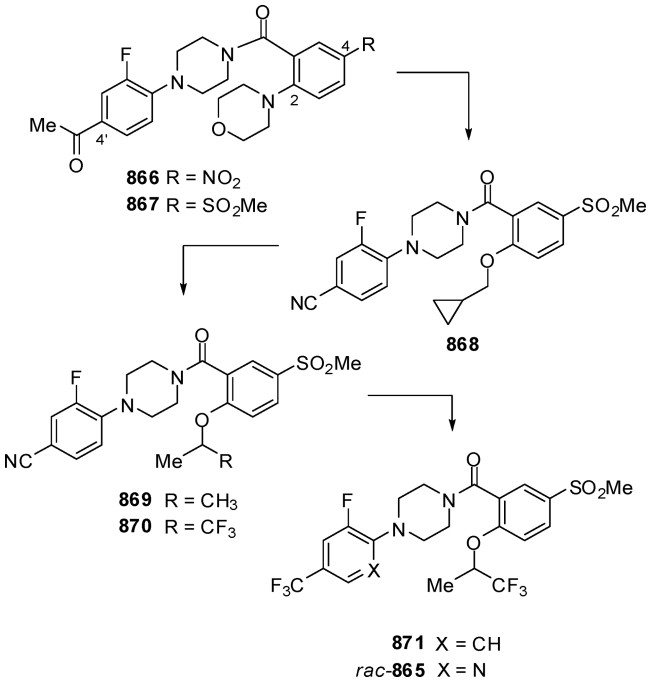

to be more favorable than nitrile analogue **870**, because of superior CNS penetration (brain/plasma = 1.15) and significantly lower inhibitory activity at the hERG channel (IC_{50} = 6.9 μM). The hERG selectivity profiles were further improved by exchanging the *N*-phenyl ring of **871** by heteroaromatic systems for increased polarity and reduced lipophilicity. During the modifications, pyridine derivative *rac*-**865** showed exceptional hERG selectivity (IC_{50} = 20 μM) combined with very good CNS penetration and in vivo potency, while its (*S*)-enantiomer **865** (bitopertin) demonstrated more favorable profiles than the (*R*)-enantiomer (**865**: GlyT1: EC_{50} = 0.030 μM; hERG: IC_{50} = 17 μM, brain/plasma = 0.50).[590,596]

The synthetic route of bitopertin is illustrated in Scheme 121. Pyridine-piperazine **874** was prepared via nucleophilic substitution of pyridine **872** with *N*-Boc-piperazine (**873**) and sequential cleavage of the Boc group with TFA. Correspondingly, 2-fluorobenzoic acid (**875**) was heated with chlorosulfonic acid to give chlorosulfonyl benzene **876**, which was transformed into the corresponding sulfinobenzoic acid **877** under reductive conditions. Treatment of **877** with MeI and Na_2CO_3 yielded methylsulfonylbenzene **878**, which was then hydrolyzed by LiOH. The resulting fluorobenzene **879** was heated with (*S*)-alcohol **880** under basic conditions to afford the trifluoromethyl analogue **881**, which underwent condensation with piperazine **874** to furnish bitopertin (**865**) by treatment with *O*-(benzotriazol-1-yl)-*N*,*N*,*N*′,*N*′-tetramethyluronium tetrafluoroborate (TBTU) and Hünig's base.[590]

7.4. Elagolix

Elagolix (NBI-56418, ABT-620, **882**) was developed by Neurocrine Biosciences in collaboration with AbbVie for the potential treatment of hormone-dependent diseases, such as endometriosis and uterine fibroids (Figure 58).[597] As an oral bioavailable nonpeptidic gonadotropin releasing hormone (GnRH) receptor antagonist, elagolix may provide flexibility for a greater control over the degree of pituitary suppression compared to current treatments consisting of peptide

Scheme 121. Synthetic Route to Bitopertin (865)

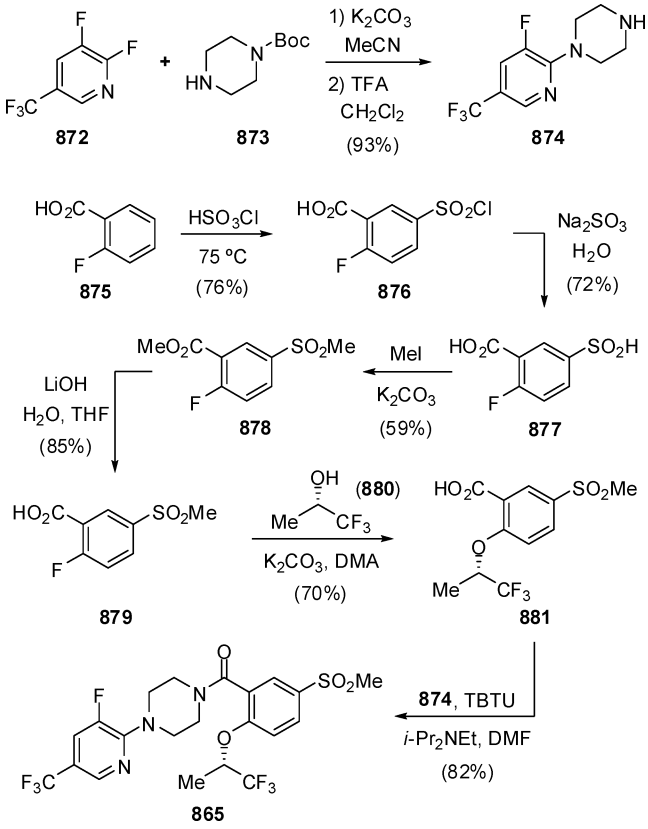

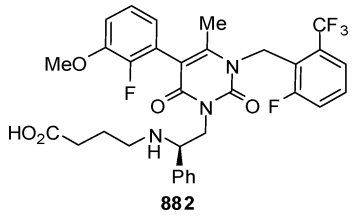

Figure 58. Structure of elagolix (**882**).

depots.[598] Several phase III trials for endometriosis have been conducted, and an NDA filing is expected in 2016.

As shown in Scheme 122, the scaffold of elagolix derived from the structure of potent antagonists of human GnRH receptor, such as pyrazolopyrimidone **883**[599,600] and imidazolopyrimidone **884**.[601] Structure–activity relationship (SAR) results showed that a large portion of compound **884** might not be necessary for binding, and thus a series of much smaller monocyclic compounds, especially with uracil core structures, were synthesized.[602−604] While uracil compounds with tertiary amines, such as **885** (K_i = 0.5 nM), maintained excellent potency against the human GnRH receptor,[605] their major metabolites, such as the N-dealkylation products, possessed low binding affinity. In order to reduce the oxidative cleavage of C–N bonds and improve the oral bioavailability, the benzylic moiety was moved from the nitrogen to the stereogenic carbon of the 2-aminoethyl side chain, which led to the discovery of the orally active antagonist NBI-42902 (**886**, K_i = 0.56 nM; C_{max} = 737 ng/mL, AUC = 2392 ng/mL·h at a 10 mg/kg dose, *F* = 16%).[606] However, this drug candidate may raise potential risk of drug–drug interaction for its high CYP3A4 inhibition (CYP3A4: IC_{50} = 0.70 μM),[607] which was relieved by

DOI: 10.1021/acs.chemrev.5b00392
Chem. Rev. 2016, 116, 422–518

Scheme 122. Discovery of Elagolix (882)

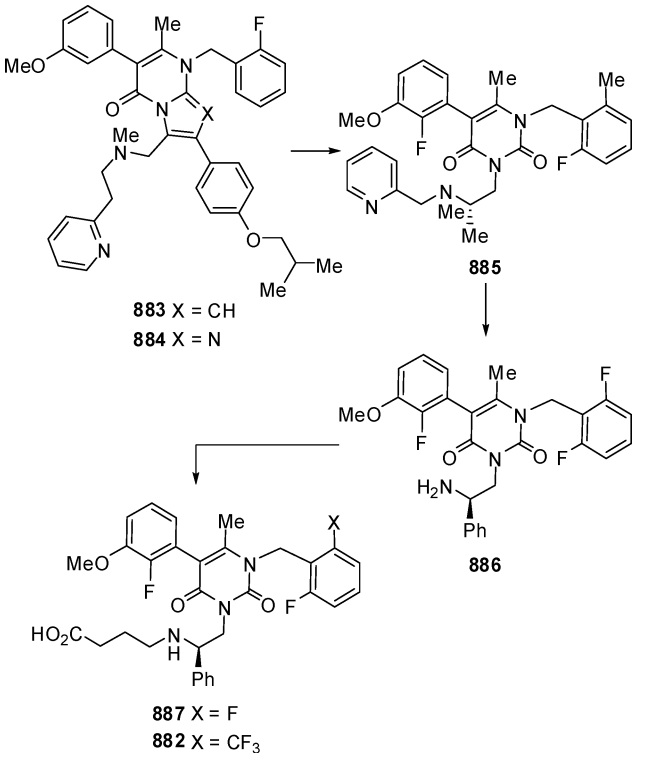

incorporating a carboxylic acid function as in compound **887** (hGnRH-R IP: IC_{50} = 27 nM; CYP3A4: IC_{50} = 135 μM). Detailed SAR studies revealed that the binding affinity of these compounds could be further improved, when one of the two fluorine groups at the 1-benzyl group was replaced by a bulkier substituent, such as a trifluoromethyl group. The corresponding structure, elagolix (**882**, hGnRH-R IP: IC_{50} = 1.5 nM; CYP3A4: IC_{50} = 56 μM), was 18-fold more potent and had higher plasma concentrations than the parent compound **887**.[597]

The synthetic route to elagolix is illustrated in Scheme 123. Benzylamine **888** and urea were refluxed in HCl/water solution to form the benzyl urea **889**, which was cyclized with diketene by treatment with TMSCl and NaI. The resulting uracil **890** was brominated in acetic acid to give **891**, which was alkylated at the N-3 position with *N*-Boc-(*S*)-2-amino-1-phenylethanol (**892**) under Mitsunobu conditions (PPh_3/di-*tert*-butyl azodicarboxylate, DBAD). Next, bromouracil **893** underwent a Suzuki cross-coupling with benzeneboronic acid **894**. After removal of the Boc group, alkylation of amine **895** with ethyl 4-bromobutyrate followed by ester hydrolysis afforded elagolix (**882**).[597]

7.5. Odanacatib

Odanacatib (MK-0822, **896**) was developed by Merck & Co. for the potential oral once-weekly treatment of osteoporosis in postmenopausal women, as a selective inhibitor of cathepsin K (Cat K) that leads to an increase in bone mineral density (BMD) (Figure 59).[608] In September 2007, a phase III clinical trial evaluating fracture risk in postmenopausal osteoporosis was initiated; in July 2012, the trial was stopped early following a data review, which found that the trial had met its primary end point. However, in February 2013, the company concluded that review of additional data from an ongoing extension study was warranted, and would delay regulatory filing until 2014.

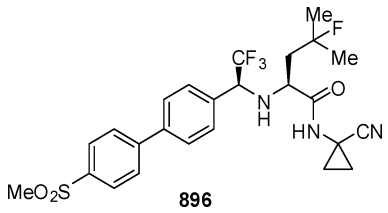

Figure 59. Structure of odanacatib (**896**).

As shown in Scheme 124, odanacatib derived from the structure of the former Cat K inhibitor L-006235 (**897**). X-ray crystallography of compound **897** with Cat K showed that the

Scheme 123. Synthetic Route to Elagolix (882)

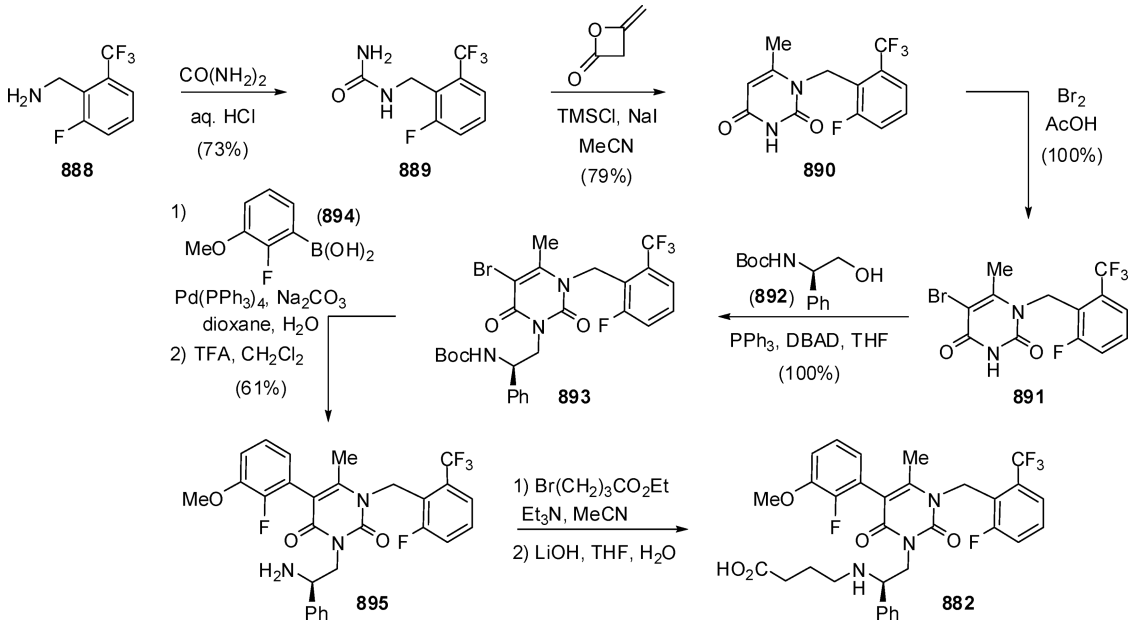

DOI: 10.1021/acs.chemrev.5b00392
Chem. Rev. 2016, 116, 422−518

Scheme 124. Discovery of Odanacatib (896)

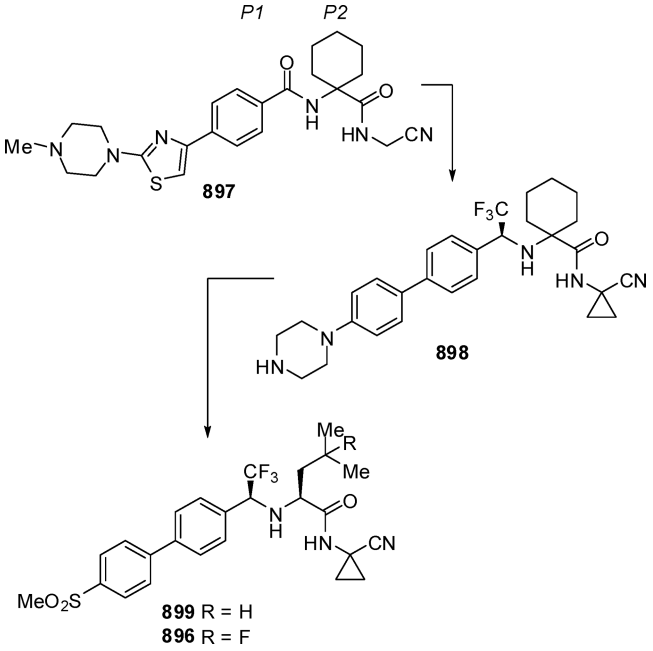

P1−P2 amide bond forms only one hydrogen bond with Gly-66, while the N−H and the carbonyl project into solution.[609] At this point, it was envisioned to replace the P1−P2 amide by a trifluoromethyl group, since the CH(CF_3)−NH−CH backbone angle is close to 120° and a C−CF_3 bond is markedly isopolar with the carbonyl, maintaining a neutral NH group.[610] The resulting compound **898** (IC_{50} = 5.0 nM) was less active than the corresponding amide derivative (IC_{50} = 0.4 nM), which could be explained by the steric clash between the CF_3 group and the cyclohexyl ring, indicating that only a single substituent would be tolerated at P2.[611] The later SAR research on the scaffold of (*S*)-1-(biphenyl-4-yl)-2,2,2-trifluoro-ethanamine led to the discovery of L-873724 (**899**, IC_{50} = 0.2 nM), of which metabolic liabilities ($t_{1/2}$ = 2 h) prevented its further development.[612] Subsequent blocking of the key metabolic sites with fluorine resulted in the identification of odanacatib (**896**, IC_{50} = 0.2 nM, $t_{1/2}$ = 18 h). The pharmacokinetics of odanacatib, which was evaluated in several preclinical species, showed that the half-lives were long in all species and its oral bioavailability was highly dependent on vehicle, dosage, and sample preparation.[613]

Odanacatib was first synthesized as shown in Scheme 125. Reduction of the aspartic acid derivative **900** and treatment with tosic anhydride afforded cyclic carbamate **901**. Methyl Grignard addition to the benzyl ester followed by fluorination with DAST provided fluoride **902**, which was hydrolyzed with barium hydroxide to fluorinated amino alcohol **903** in quantitative yield. After silylation of alcohol **903** with TBSCl to facilitate isolation, condensation with trifluoroacetaldehyde hemiacetal gave imine **904**, followed by addition of bromophenyllithium and desilylation giving rise to trifluoroethylamine **905** as a 10:1 mixture of (*S*,*S*) and (*R*,*S*) diastereomers. Oxidation of alcohol **905** with periodic acid led to the carboxylic acid **906** in >99% diastereomeric excess after recrystallization. Amide formation with 1-aminocyclopropanecarbonitrile hydrochloride (**907**) gave amide **908**, which was coupled with boronic acid **909** and then oxidized with hydrogen peroxide to afford odanacatib (**896**).[613]

In the above route, the critical step was the construction of the trifluoromethyl-containing stereocenter, and this inspired a large amount of work at Merck[614,615] and academia[94,98,117,616−619] for the synthesis of chiral trifluoromethylamines that culminated in an advanced, chromatography-free preparation method of odanacatib. Thus, reduction of trifluoromethyl ketone **910** in the presence of a chiral oxazaborolidine proceeded in high enantioselectivity (Scheme 126). The resulting alcohol **911** was activated as its triflate derivative **912** and subjected to a nucleophilic substitution with amino ester **913** to form intermediate **914** as a mixture of diastereomers as a consequence of a small racemization of the CF_3 substituent. The ensuing Suzuki cross-coupling was performed with sulfone-derived boronic acid **915**, and was

Scheme 125. Synthetic Route to Odanacatib (896)

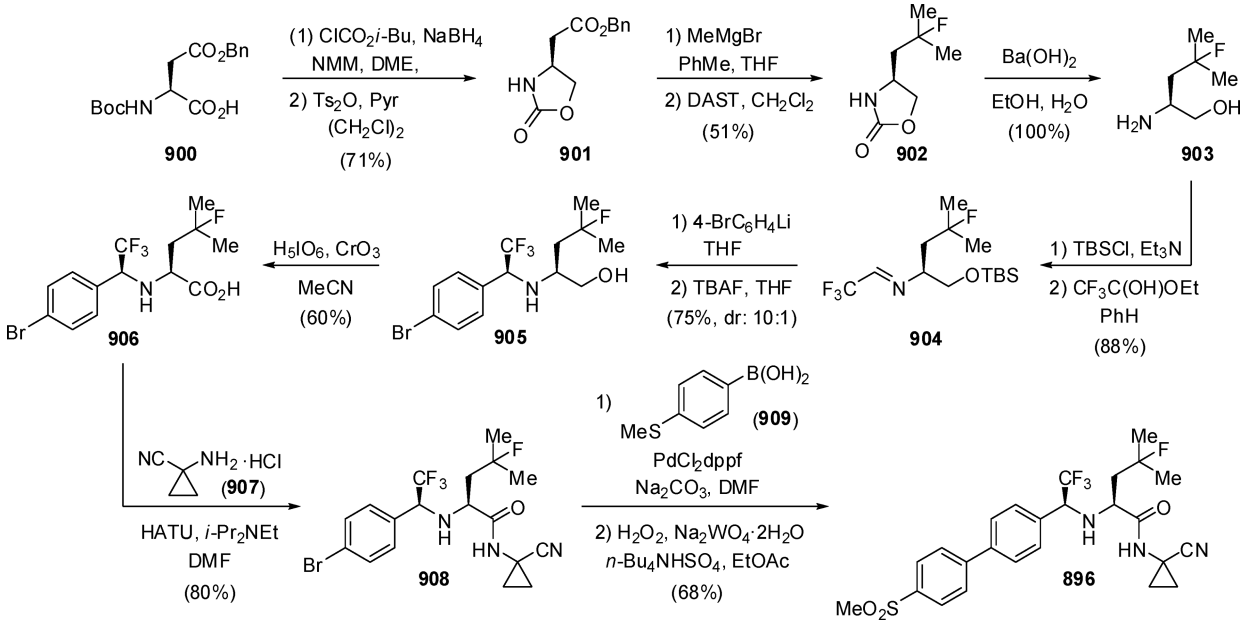

DOI: 10.1021/acs.chemrev.5b00392
Chem. Rev. 2016, 116, 422−518

Scheme 126. Improved Synthesis of Odanacatib (896)

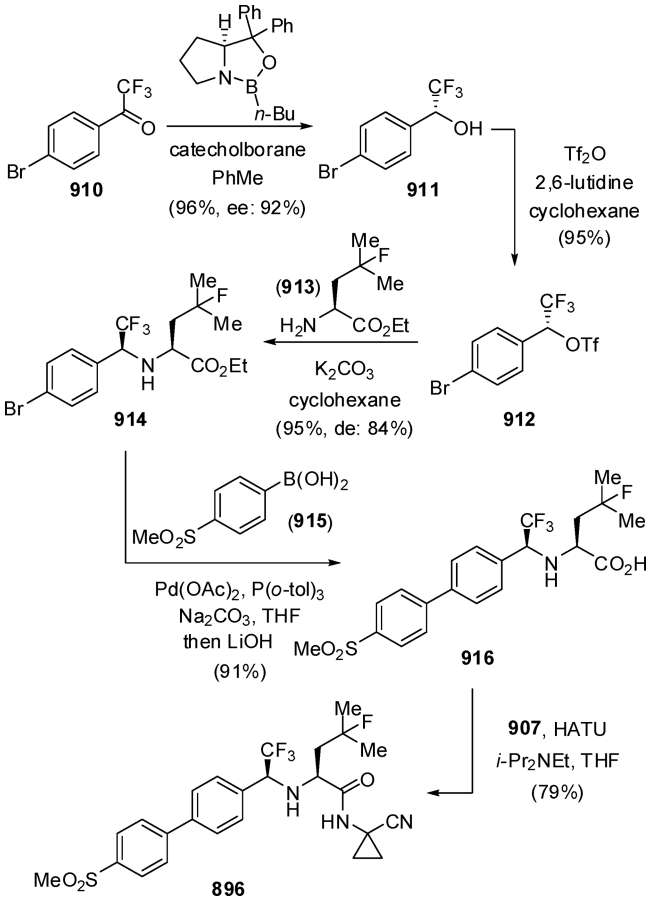

followed by in situ hydrolysis of the ester group with LiOH. Final amide bond formation between carboxylic acid **916** and amine **907** afforded odacanatib (**896**) in high optical purity after recrystallization.[620]

7.6. Anacetrapib

Merck & Co. developed anacetrapib (MK-0859, **917**), a small oxazolidinone molecule, as a treatment for atherosclerosis, hypercholesterolemia, and mixed dyslipidemia (Figure 60). As an oral selective cholesterol ester transfer protein (CETP) inhibitor, anacetrapib increases high-density lipoprotein cholesterol (HDL-C) and apolipoprotein A1, while reduces low-density lipoprotein cholesterol (LDL-C) and apolipoprotein B.[621] From April 2008 several phase III clinical trials have been conducted, and an NDA filing in the United States is expected after 2015. Results from the clinical trials anticipated that anacetrapib had no effect on blood pressure or plasma aldosterone, in contrast to previously discontinued CETP inhibitors, such as torcetrapib.[622]

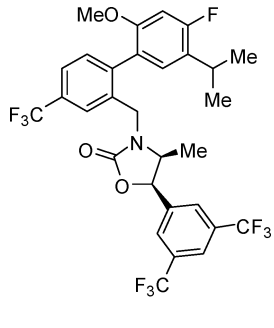

Figure 60. Structure of anacetrapib (**917**).

Similarly as in the case of evacetrapib (see section 6.2), the structure of anacetrapib derived from the CETP inhibitor described by Pfizer torcetrapib (**825**) (Scheme 127).

Scheme 127. Discovery of Anacetrapib (917)

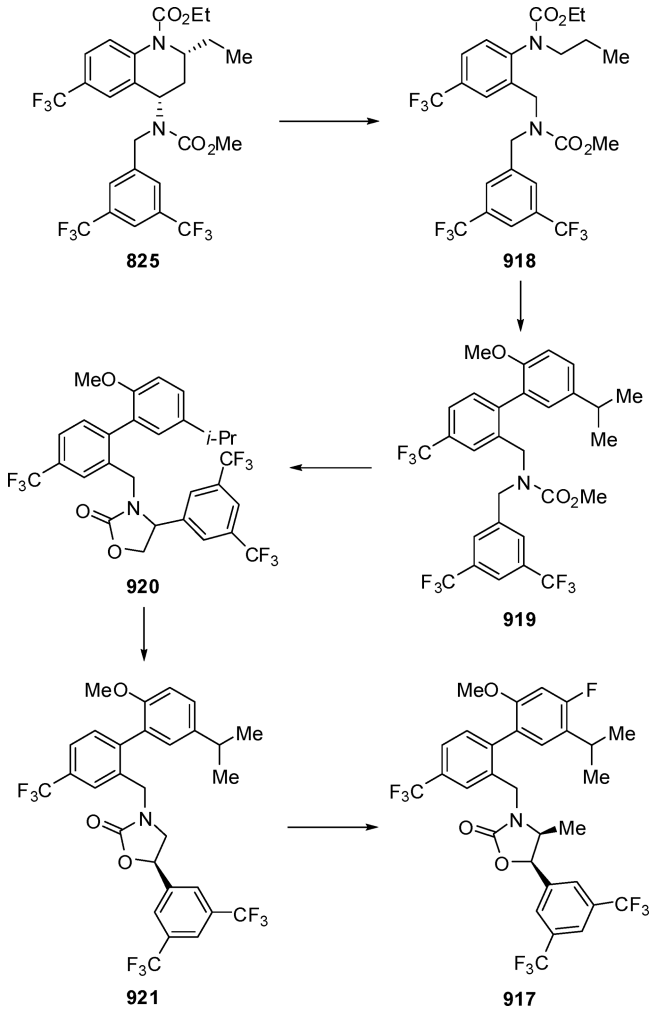

Researchers at Merck envisioned that opening the tetrahydroquinoline ring of torcetrapib would result in molecules, such as **918**, more synthetically accessible because of the lack of stereocenters. In this regard, the most active molecules in this series contained a 2,5-disubstituted phenyl ring as in compound **919**, since those substituents were oriented in a comparable manner as the pendant groups of torcetrapib.[623] The next strategy consisted in the restriction of the conformational flexibility through cyclization of the carbamate moiety into an oxazolidinone ring. However, the inhibitory activity of the corresponding racemic compound **920** was much lower compared to the open-chain derivative **919**. In contrast, the regioisomeric, optically active oxazolidinone **921** resulted in a much more potent inhibitor.[624] Ultimately, the inhibition of CETP and the pharmacokinetic properties were improved by incorporation of fluorine into the anisole ring, as well as adding a methyl substituent into the oxazolidinone, leading to the discovery of anacetrapib (**917**).[625] It should be mentioned that

DOI: 10.1021/acs.chemrev.5b00392
Chem. Rev. 2016, 116, 422−518

inclusion of other small substituents in place of the CF_3 group located in the central aromatic ring preserved the in vitro activity, but the in vivo properties of those analogues were poorer compared to anacetrapib.[626] In fact, the oral absorption of anacetrapib in humans is low to moderate, being further metabolized by a CYP3A4-catalyzed oxidative pathway and excreted through the biliary−fecal route.[627,628] Interestingly, anacetrapib is orally bioavailable although it contravenes some rules that are considered as mandatory for drugability, such as molecular weight and permeability.[629]

Anacetrapib was synthesized through a convergent route that sequentially linked the different subunits of the molecule. For the synthesis of the oxazolidinone-containing moiety, *N*-Cbz-Ala-OH (**922**) was converted into its derived Weinreb amide **923**, which was successively treated with *i*-PrMgCl and the Grignard reagent **924** (prepared in turn from the corresponding iodobenzene) to yield ketone **925** (Scheme 128). Next, silane-mediated diastereoselective reduction of ketone **925** afforded *syn*-alcohol **926**, and further cyclization, by reaction with aqueous NaOH, gave *cis*-oxazolidinone **927**.[625]

Scheme 128. Synthesis of Oxazolidinone-Containing Fragment 927

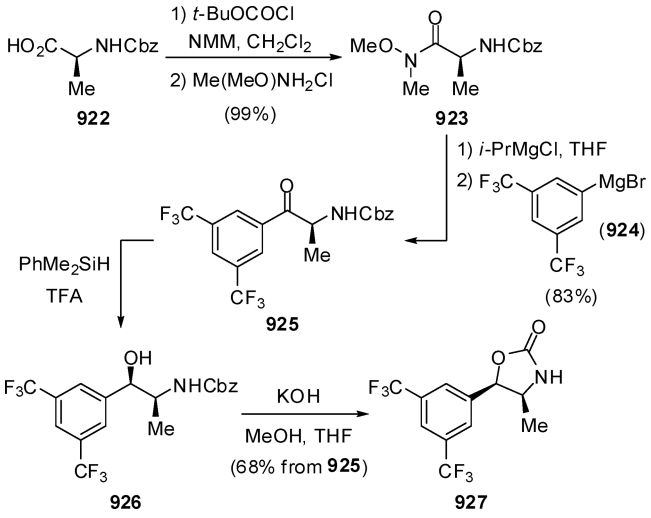

Correspondingly, addition of MeMgBr to acetophenone **928** gave tertiary alcohol **929**, and elimination reaction to styrene **930** was carried out by treatment with MsCl (Scheme 129). Direct formation of **930** was also feasible via a Wittig reaction of acetophenone **928** with the ylide derived from methyltriphenylphosphonium bromide. Hydrogenation of alkene **930** over Pd/C and further regioselective iodination of the aromatic ring furnished iodide **931**, which was transformed into boronic acid **932** by metalation with *n*-BuLi and trapping with trimethyl borate.[625]

The central aromatic ring of anacetrapib originated from benzonitrile **933**, which was hydrolyzed to carboxylic acid **934** with KOH (Scheme 130). This acid was next reduced with borane to give alcohol **935** and then brominated to compound **936**. Alkylation of oxazolidinone **927** with bromide **936** afforded intermediate **937**, and Suzuki cross-coupling with boronic acid **932** completed the synthesis of anacetrapib (**917**).[625]

The access to the biaryl core of anacetrapib has also been described via a ruthenium-catalyzed arylation reaction as the key step. Starting from 1-bromo-2,4-difluorobenzene (**938**), a

Scheme 129. Synthesis of Fluorine-Containing Boronic Acid 932

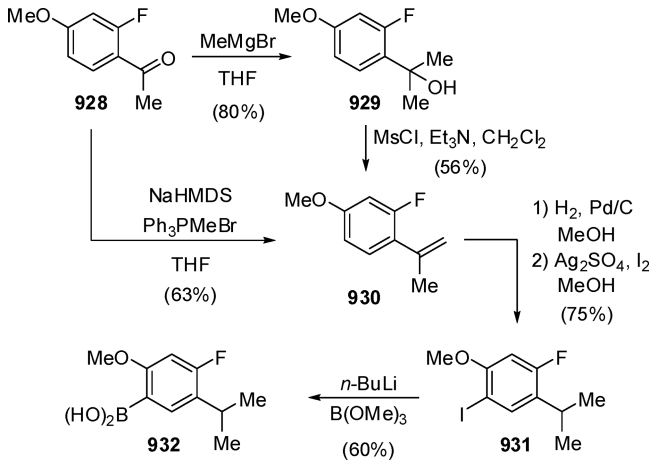

Scheme 130. Synthetic Route to Anacetrapib (917)

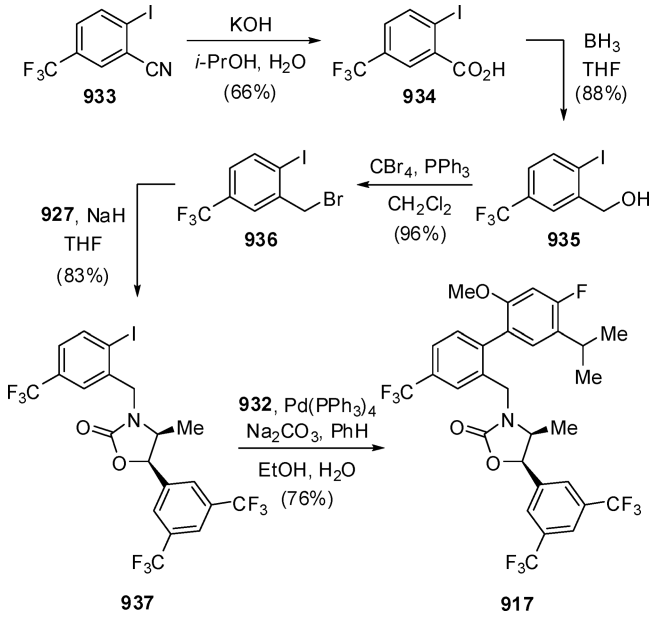

highly regioselective substitution with KOMe afforded anisole derivative **939**, followed by a Friedel−Crafts acylation to give acetophenone **940** (Scheme 131). The acetyl group was transformed into isopropyl by addition of MeMgBr to ketone **940** and then tetramethyldisiloxane-assisted deoxygenation of tertiary alcohol **941** produced fragment **942**. The second aromatic ring was elaborated from 3-(trifluoromethyl)-benzonitrile (**943**) by conversion into oxazoline **944**. Next, coupling between **942** and **944** proceeded in very high yield to furnish biaryl derivative **945**. It is interesting to note that the success of the reaction depended on the amount of an impurity, γ-butyrolactone, found on the solvent employed, *N*-methyl-2-pyrrolidone (NMP). Therefore, potassium acetate was employed as additive to ensure the reproducibility of the reaction. Finally, alcohol **946** was obtained from **945** by opening the oxazoline ring with methyl chloroformate and in situ reduction of the *N*-acylcarbamate intermediate. Overall, the synthetic route was easily scalable and did not need any chromatographic purification.[630]

DOI: 10.1021/acs.chemrev.5b00392
Chem. Rev. 2016, 116, 422−518

Scheme 131. Scaled-Up Synthesis of the Biaryl Fragment 946

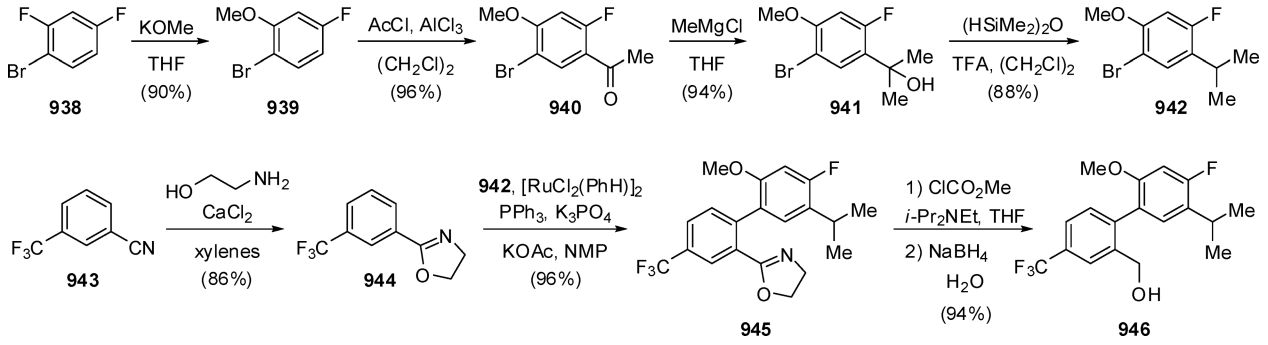

Finally, a catalytic asymmetric nitroaldol reaction served to build the chiral oxazolidinone core of anacetrapib. Thus, aldehyde **947** was reacted with nitroethane in the presence of a heterobimetallic (Nd−Na) catalyst containing chiral ligand **948** (Scheme 132). Most importantly, this catalytic system worked much better, when confined into a carbon nanotube network, and hence nitroalcohol **949** was obtained in excellent yield and enantiomeric excess. This also allowed reusing the catalyst after a simple filtration of the crude mixture. From compound **949**, reduction of the nitro group with zinc and HCl in cyclopentyl methyl ether (CPME) was followed by reaction with triphosgene to access oxazolidinone **950**. Next, displacement of both iodine atoms with the Ruppert−Prakash reagent (Me_3SiCF_3) led to intermediate **927**, and its further alkylation with benzyl chloride **951** (derived from alcohol **946**) provided anacetrapib (**917**).[631]

Scheme 132. Enantioselective Synthesis of Anacetrapib (917)

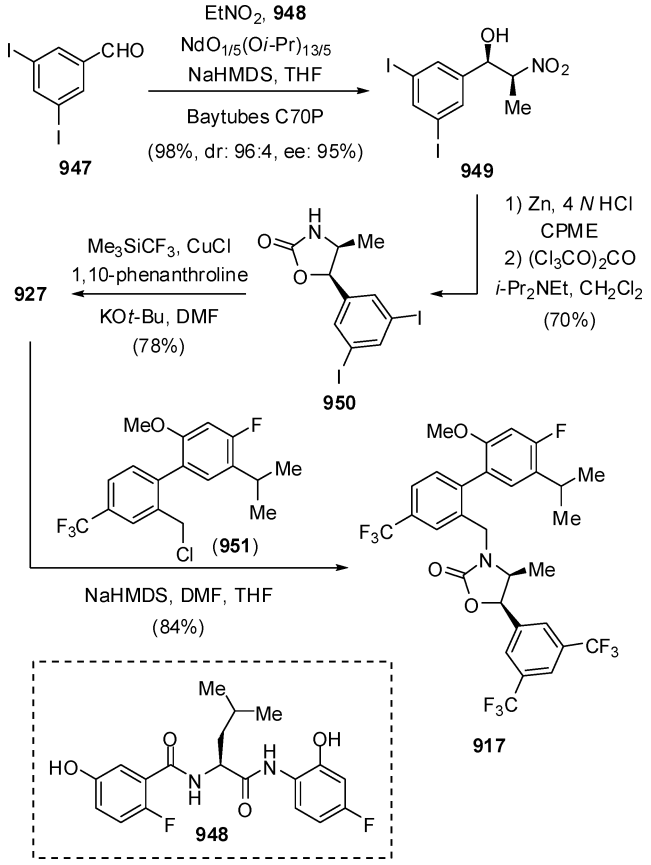

7.7. Darapladib

Lipoprotein-associated phospholipase A2 (Lp-PLA_2) is recognized as a pro-atherogenic enzyme regulating lipid metabolism and inflammatory response. It is responsible for the hydrolysis of oxidized low density lipoprotein (LDL) into lysophosphatidylcholine (lyso-PtdCho) and oxidized nonesterified fatty acids (oxNEFAs), which play essential roles in atherogenesis.[632] The design of selective inhibitors of Lp-PLA_2 over other types of phospholipases may provide useful drug candidates for the treatment of inflammatory diseases.[633] Darapladib (SB-480848, **952**), under development by GlaxoSmithKline (GSK), is an oral selective inhibitor of Lp-PLA_2 used for the treatment of atherosclerosis, coronary artery disease (CAD), and diabetic macular edema (DME) by the mechanism of targeting the active-site serine residue of Lp-PLA_2 (Figure 61).[634] Phase III clinical trials of darapladib are now in progress for the first two indications, while the trials of DME are still in phase II.

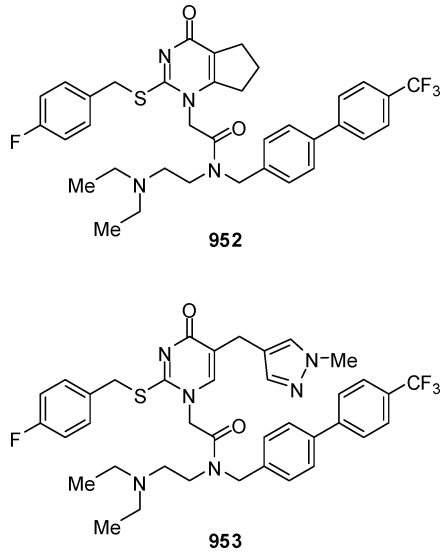

Figure 61. Structures of darapladib (**952**) and SB-435495 (**953**).

During the course of the optimization of pyrimidinone derivatives as inhibitors of Lp-PLA_2, such as SB-435495 (**953**, IC_{50} = 0.06 nM, permeability = 0.017 cm/h), initial SAR analysis proved that the substituents larger than fluoro on the *S*-benzyl group caused a marked reduction in potency.[635] On the other hand, a 4-substituted biphenyl fragment was an essential contributor for whole-cell activity, although mostly two

DOI: 10.1021/acs.chemrev.5b00392
Chem. Rev. 2016, 116, 422−518

Scheme 133. Synthetic Route to Darapladib (952)

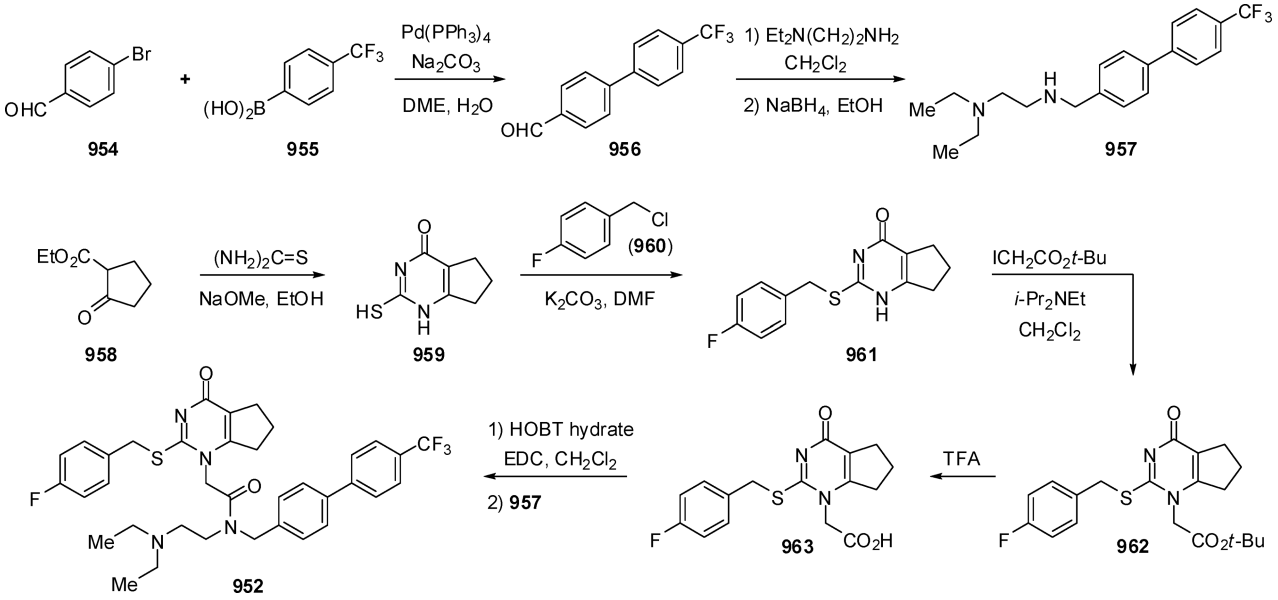

different substituents on the biphenyl, CF_3 or Cl, were investigated.[636] In general, a trifluoromethyl substituent gave molecules with a superior cytochrome P450 (CYP450) profile (lesser risk of potential drug−drug interactions), compared to compounds containing a chlorine atom.[637] The structure of darapladib (**952**) finally emerged by simplification of the pyrimidinone core, replacing the 5-substituent by a fused cyclopentane ring, and resulting in somewhat lower inhibitory activity (IC_{50} = 0.25 nM) but with enhanced permeability (0.10 cm/h), whereas the corresponding cyclohexyl analogue showed a weak CYP450 interaction with the key isozymes 2D6 and 3A4.[638]

The synthetic route to darapladib developed by GSK is outlined in Scheme 133. Starting from the Suzuki coupling between 4-bromobenzaldehyde (**954**) and 4-(trifluoromethyl)-benzeneboronic acid (**955**), biaryl derivative **956** was obtained. Intermediate **957** was next prepared from aldehyde **956** through a reductive amination reaction with *N*,*N*-diethylethylenediamine. The second main fragment, pyrimidinone **963**, derived from the condensation between 2-(ethoxycarbonyl)-cyclopentanone (**958**) and thiourea, followed by benzylation of the thiol with 4-fluorobenzyl chloride (**960**). The subsequent alkylation of **961** with *tert*-butyl iodoacetate formed ester **962**, which was converted into carboxylic acid **963** by ester deprotection with TFA. The completion of the synthesis of darapladib (**952**) involved the easy formation of the amide bond between intermediates **957** and **963**.[638,639]

More recently, another process for the preparation of pyrimidinone compounds was applied to the synthesis of intermediate **963** (Scheme 134). 2-(Methoxycarbonyl)-cyclopentanone (**964**) reacted with the sodium salt of glycine, and without isolation enamino ester **965** was treated with sodium thiocyanate and TMSCl to give thiopyrimidinone **966**. Further N-alkylation of **966** with benzyl chloride **960** furnished darapladib precursor **963**.[640]

Although 4-(trifluoromethyl)benzeneboronic acid (**955**) is a commercial reagent, it was also accessed using a convenient and highly efficient one-pot method for the synthesis of functionalized arylboronic acids. The aryl Grignard reagent **968** was prepared from the readily available 1-bromo-4-

Scheme 134. Improved Preparation Method of Intermediate 963

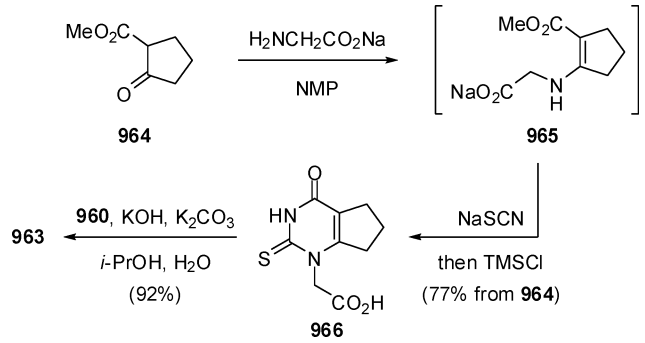

(trifluoromethyl)benzene (**967**) by metal/halogen exchange or by direct insertion of magnesium into the C−Br bond (Scheme 135). Boronic acid **955** was thus obtained after in situ reaction of Grignard **968** with trimethyl borate.[641]

Scheme 135. One-Pot Access to 4-(Trifluoromethyl)benzeneboronic Acid (955)

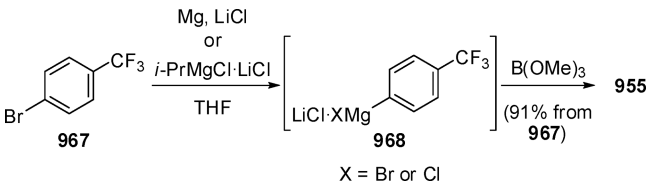

8. SUMMARY OF THERAPEUTIC AREAS AND DRUG INDICATIONS

As suggested by one of the reviewers, we provide here a table summarizing the types of diseases and compounds profiled in this review (Table 1). We believe it could be very useful for a quick overview of the biological activities targeted by the new types of fluorine-containing drugs.

DOI: 10.1021/acs.chemrev.5b00392
Chem. Rev. 2016, 116, 422−518

Table 1. List of Therapeutic Areas, Indications, Mechanisms of Action, and Legal Status of the Drugs or Drug Candidates

therapeutic area	indication	mechanism of action	compound	status
oncology	non-small-cell lung cancer	tyrosine kinase inhibitor	afatinib (**49**)	approved (U.S., EU, and Japan)
			dacomitinib (**50**)	phase III
			cediranib (**105**)	discontinued[a]
	melanoma	tyrosine kinase inhibitor	trametinib (**73**)	approved (U.S.)
			dabrafenib (**579**)	approved (U.S.)
			cobimetinib (**591**)	approved (U.S. and EU)
	ovarian cancer	poly ADP ribose polymerase inhibitor	olaparib (**85**)	approved (U.S. and EU)
	medullary thyroid cancer	tyrosine kinase inhibitor	cabozantinib (**98**)	approved (U.S.)
	hepatocellular carcinoma	tyrosine kinase inhibitor	brivanib alaninate (**106**)	phase III
	chronic lymphocytic leukemia, follicular B-cell lymphoma, and small lymphocytic lymphoma	phosphatidylinositol 3-kinase inhibitor	idelalisib (**134**)	approved (U.S.)
	Philadelphia chromosome-positive chronic myeloid leukemia	tyrosine kinase inhibitor	radotinib (**609**)	approved (South Korea)
			ponatinib (**610**)	approved (U.S. and EU)
	castration-resistant prostate cancer	hypoxia-inducible factor 1-α inhibitor	tasquinimod (**646**)	phase III
		androgen receptor antagonist	enzalutamide (**842**)	approved (U.S.)
	carcinoid syndrome	tryptophan hydroxylase inhibitor	telotristat ethyl (**654**)	phase III
	breast cancer	phosphatidylinositol 3-kinase inhibitor	buparlisib (**669**)	phase III
	cancer cachexia	selective androgen receptor modulator	enobosarm (**679**)	phase III
	metastatic colorectal cancer and advanced gastrointestinal stromal tumor	tyrosine kinase inhibitor	regorafenib (**853**)	approved (U.S., EU, and Japan)
central nervous system	attention deficit hyperactivity disorder and major depressive disorder	norepinephrine reuptake inhibitor	edivoxetine (**140**)	discontinued
	schizophrenia	serotonin and dopamine receptors antagonist	blonanserin (**150**)	approved (Japan and South Korea)
		glycine transporter-1 inhibitor	bitopertin (**865**)	phase III
	chemotherapy-induced nausea and vomiting	NK_1 receptor antagonist	netupitant (**773**)	approved (U.S.)
			rolapitant (**774**)	approved (U.S.)
cardiovascular system	acute coronary syndrome	thrombin receptor antagonist	vorapaxar (**158**)	approved (U.S.)
	cardiovascular disease	cholesteryl ester transfer protein inhibitor	evacetrapib (**824**)	phase III
			anacetrapib (**917**)	phase III
	atherosclerosis and coronary artery disease	lipoprotein-associated phospholipase A2 inhibitor	darapladib (**952**)	phase III
infectious diseases	acute bacterial skin and skin structure infections	binding to 50S subunit of ribosome	tedizolid phosphate (**178**)	approved (U.S.)
	chronic obstructive pulmonary disease and pneumonia	DNA gyrase and topoisomerase IV inhibitor	zabofloxacin (**201**)	phase II–III
	community-acquired bacterial pneumonia	binding to 50S subunit of ribosome	solithromycin (**219**)	phase III
	hepatitis C	RNA polymerase inhibitor	sofosbuvir (**239**)	approved (U.S. and EU)
		NS5A protein inhibitor	ledipasvir (**539**)	approved (U.S.)
	hepatitis B	DNA polymerase inhibitor	clevudine (**278**)	approved (South Korea and Philippines)
	HIV infection	HIV integrase inhibitor	elvitegravir (**309**)	approved (U.S.)
			dolutegravir (**488**)	approved (U.S. and EU)
	invasive aspergillosis and mucomycosis	sterol 14-α-demethylase inhibitor	isavuconazole (**474**)	approved (U.S.)
	multidrug resistant tuberculosis	inhibitor of mycolic acid synthesis	delamanid (**752**)	approved (EU and Japan)
respiratory system	pulmonary hypertension	stimulator of soluble guanylate cyclase	riociguat (**336**)	approved (U.S.)
immunology	asthma and seasonal allergic rinitis	prostaglandin D_2 receptor antagonist	setipiprant (**352**)	discontinued
	multiple sclerosis	sphingosine-1-phosphate receptor modulator	siponimod (**690**)	phase III

DOI: 10.1021/acs.chemrev.5b00392
Chem. Rev. 2016, 116, 422–518

Table 1. continued

therapeutic area	indication	mechanism of action	compound	status
gastrointestinal tract	gastric ulcer, duodenal ulcer, and erosive esophagitis	proton pump inhibitor	vonoprazan (**364**)	approved (Japan)
	postoperative ileus and gastroparesis	ghrelin receptor antagonist	ulimorelin (**381**)	discontinued
eye care	glaucoma and ocular hypertension	rho kinase inhibitor	ripasudil (**402**)	approved (Japan)
diabetes	type 2 diabetes mellitus	sodium glucose cotransporter-2 inhibitor	canagliflozin (**426**)	approved (U.S.)
			ipragliflozin (**427**)	approved (Japan)
		dipeptidyl peptidase IV inhibitor	trelagliptin (**450**)	approved (Japan)
			omarigliptin (**456**)	approved (Japan)
		dihydroorotate dehydrogenase inhibitor	terifluonomide (**726**)	approved (U.S. and EU)
endocrine system	familial chylomicronemia syndrome	diacylglycerol acyl transferase-1 inhibitor	pradigastat (**742**)	phase III
obstetrics/ gynecology	endometriosis	gonadotropin releasing hormone receptor antagonist	elagolix (**882**)	phase III
musculoskeletal	osteoporosis	cathepsin K inhibitor	odanacatib (**896**)	phase III

[a]Cediranib is currently in phase II trials for other indications.

9. CONCLUSIONS

In the last 10 years, the amount of fluorine-containing drugs covers 27% of all approved small molecule drugs (excluding biopharmaceuticals), and this percentage has increased to 36% in the last 3 years. Most importantly, about 40% of the new chemical entities entering phase III trials in 2012 and 2013 (no data for 2014) are fluoroorganic compounds. This review profiles 51 fluorine-containing drugs that were either just recently approved (after 2011), or are currently in the latest (phase II/III) stages of clinical studies. Taken in conjunction with our previous projects,[33−35] the present work provides a complete and most comprehensive treatment of ∼100 fluorine-containing pharmaceuticals—the fastest growing area of current chemical/medicinal/clinical sciences with extraordinary social impact. In fact, while from 2001 to 2011 there were ∼40 new fluorine-containing drugs introduced to the pharmaceutical market, during the past few years (2011−2013) we have witnessed ∼60 new structures, most, if not all, of which will be in medicinal use anytime soon. This trend presents a 150% growth, a truly unparalleled socioscientific fact that still has to be rationalized. There is also a growing perception that, in principle, any given drug molecule can be improved by introducing fluorine. This assumption is strongly supported by the current data showing that fluorine substitution can be reliably used to increase the drug biological stability by blocking metabolically labile positions. Most likely, these trends on increasing number of fluorine-containing drugs will continue to hold in the future.

For each and every drug profiled in this review we did our best to find and discuss the chemical source of fluorine, the modes of biological action, and the difference in pharmaceutical properties between fluorinated and fluorine-free compounds. However, in most cases, including other projects,[33−35] we noticed a lack of relevant data on the metabolism of fluorine-containing molecules. One should keep in mind that fluorine (fluoride) is xenobiotic from the standpoint of biological evolution, and does not play virtually any role in the living processes. Accordingly, we believe that it is very important to highlight that effects of water-soluble/organic fluorine on the biosphere in general, and processes essential to human life and health, have never been systematically studied. Considering the trends discussed here, as well as similarly essential and ever-growing impacts of fluorine on the design and development of modern agrochemicals,[21,22] the obvious lack of research into the biological metabolism of fluorinated compounds is rather alarming. Therefore, the modern pharmaceutical and agrochemical industries vs human fluoride overload seems to be a timely and vital area of research to ensure that fluorine-containing organics do not cause any adverse long-term effects.

Another critical issue we would like to highlight in these conclusions is a persistent unawareness of the research community in the phenomenon of self-disproportionation of enantiomers (SDE).[642,643] SDE is virtually always observed in the case of nonracemic compounds and causes a spontaneous separation of racemate from the excess enantiomer under totally achiral conditions. Many routinely used conditions in laboratory practice include achiral chromatography,[644−647] evaporation/distillation,[648,649] and drying compounds in a vacuum.[650−654] The growing amount of data on SDE undoubtedly suggests that fluorine is a uniquely SDE-enabling element and fluorine-containing compounds are particularly prone to the SDE under any physicochemical phase transitions.[655−659] Thus, fluorine and fluorine-containing groups have strongly polarizing effects on chemical bonds leading to enhanced intermolecular homo/heterochiral interactions (dipole−dipole or H-bonding) and therefore high magnitude of the SDE. A general problem associated with the ignorance about the SDE is an incorrect determination of the enantiomeric purity of a drug sample and can cause marketing a compound of less than specified enantiomeric purity. Of course, these problems can be avoided if appropriate precautions are made including the SDE test.

Having pointed out some overlooked aspects of current research, we would like to emphasize the greater importance of fluorine. It is rather obvious that the pronounced success of fluorine-containing drugs has to do with their superior potency and therapeutic value, even though introduction of fluorine renders drugs more expensive. Therefore, the development of fluoroorganic methodology should be encouraged by the science funding agencies, which so far have miserably failed to do so. However, we are confident that this review, providing an outlook on the structural types of current and future pharmaceuticals, will further encourage creative ingenuity and

DOI: 10.1021/acs.chemrev.5b00392
Chem. Rev. 2016, 116, 422−518

research focused on discovering better fluorine methodology for overall benefits of our society.

AUTHOR INFORMATION

Corresponding Authors

*E-mail: jose.acenna@uam.es.
*E-mail: vadym.soloshonok@ehu.es.
*E-mail: kunisuke-izawa@hamari.co.jp.
*E-mail: hliu@mail.shcnc.ac.cn.

Notes

The authors declare no competing financial interest.

Biographies

Yu Zhou graduated from Shenyang Pharmaceutical University in 2003 and received his Ph.D. degree in medicinal chemistry from Shenyang Pharmaceutical University in 2008 under the supervision of Prof. Linxiang Zhao. After two year's postdoctoral training with Prof. Hualiang Jiang and Prof. Hong Liu at Shanghai Institute of Materia Medica, he joined Prof. Liu's group at the Shanghai Institute of Materia Medica and was promoted to associate professor in 2010. His research interests focus on the development of highly effectively synthetic methods to construct drug-like compound libraries for the discovery of drug candidates of some serious diseases, such as Alzheimer's disease, depressive disorder, and benign prostatic hyperplasia.

Jiang Wang received her Ph.D. in medicinal chemistry under the supervision of Prof. Hong Liu at the Shanghai Institute of Materia Medica. In 2011, she worked as a postdoctoral fellow in Prof. Hualiang Jiang's group at the Shanghai Institute of Materia Medica. Her research interests are focused on the research of drug design, synthesis, and biological evaluation to treat diabetes disease and HIV infection, as well as application of nickel(II) complexes to the asymmetric synthesis of a variety of chiral non-natural amino acids.

Zhanni Gu received her bachelor's degree in pharmacy from China Pharmaceutical University in 2013. Since then she has been pursuing a Ph.D. degree under the supervision of Prof. Hong Liu. Her major field of research is medicinal chemistry.

Shuni Wang received her bachelor's degree in pharmaceutical science at Sun Yat-Sen University, Guangzhou, China. In 2013, she started to study for a Ph.D. degree under the supervision of Prof. Hong Liu at the Shanghai Institute of Materia Medica. Her research interests are focused on the discovery and synthesis of pharmacologically active molecules acting on targets related to epigenetics for the treatment of cancers, and applications of nickel(II) complexes in dynamic resolution of amino acids.

Wei Zhu received his bachelor's degree in pharmaceutical engineering at East China University of Science and Technology, Shanghai, China. In 2011, he started to study for a Ph.D. degree in Prof. Hong Liu's group at the Shanghai Institute of Materia Medica. His research interests are focused on the discovery and optimization of anticancer compounds and the synthesis of bioactive heterocyclic molecules by copper-mediated C−H activation strategy.

José Luis Aceña was born in Madrid, Spain, in 1968. He studied chemistry at the Complutense University (Madrid), where he obtained his B.Sc. in 1991 and Ph.D. in 1996. He then carried out postdoctoral studies for nearly three years at the University of Cambridge (U.K.), under the supervision of Prof. Ian Paterson. After working for four years in the pharmaceutical industry, in 2005 he joined the group of Prof. Santos Fustero at the Príncipe Felipe Research Center (Valencia). Since January 2012 he has been working as a research associate at the University of the Basque Country in San Sebastián, in Prof. Vadim Soloshonok's group, and currently he holds a position as interim professor at the Autónoma University (Madrid). His research interests are the design and synthesis of peptidomimetics and biologically active molecules, organofluorine chemistry, and total synthesis of natural products.

Vadim A. Soloshonok graduated from Kiev State University in 1983 and received his Ph.D. in 1987 from the Ukrainian Academy of Sciences. He continued his education in the area of asymmetric synthesis in collaboration with Prof. Y. Belokon (Moscow, USSR, 1987−1990), Prof. P. Bravo (Milan, Italy, 1993), Prof. T. Hayashi (Sapporo, Japan, 1994−1995), and Prof. V. Hruby (Tucson, AZ, USA, 1998−2000). In 1987 he joined the Institute of Bioorganic Chemistry, Kiev, Ukraine, where he worked until 1995. From 1995 through 1999 he was senior researcher at the National Industrial Research Institute, Nagoya, Japan, and from 2001 to 2010 professor of chemistry at the University of Oklahoma, USA. Currently he is the Ikerbasque Research Professor at the University of the Basque Country, San Sebastián, Spain. He is currently serving as a member of the international advisory editorial board of the *Journal of Fluorine Chemistry* (2003−present) and as Synthesis Field Editor of *Amino Acids* (2009−present). He is also Past-Chair of the ACS Fluorine Division (2010), author of over 250 research papers, 11 book chapters, and 10 patents, and editor of 13 books/special issues of many international journals. His publications have generated over 6800 citations with an *h*-index of 57. Since 2005 he has been invited to give more than 250 keynote lectures and invited talks at international meetings, at universities, and for industry. His major current research interests are fluorine chemistry, asymmetric synthesis, and self-disproportionation of enantiomers.

Kunisuke Izawa received his Ph.D. from Osaka University in 1973, and joined Ajinomoto Co. to develop a new catalytic process for amino acid synthesis. After carrying out postdoctoral research at MIT for two years (1979−1981), he returned to the same company aiming at discovery of new methodology for pharmaceuticals. In 1990, he moved to the Process Research as a general manager. Since then, he engaged in the process development of pharmaceutical fine chemicals in Ajinomoto. In 1999, he became a corporate executive fellow for 7 years and then served an advisor for 4 years. Currently, he is an advisor of Hamari Chemicals. He also served as a board member for many years and a vice president (2009−2011) in the Society of Synthetic Organic Chemistry, Japan, as well as a board member of the Japanese Society for Process Chemistry. His research interest is in the field of organic synthesis utilizing amino acids and nucleosides. He has published over 200 scientific papers and patents.

Hong Liu received her M.S. and Ph.D. in medicinal chemistry from the China Pharmaceutical University, under the supervision of Prof. Weiyi Hua. After a postdoctoral stay with Prof. Ruyun Ji and Prof. Kaixian Chen at the Shanghai Institute of Materia Medica, she joined the Shanghai Institute of Materia Medica and is group leader now. As a visiting scientist, she stayed with Prof. James Halpert at University of Texas Medical Branch at Galveston. Her research interests include medicinal chemistry, organic chemistry, computer modeling, and pharmacological active molecules, especially those targeting antitumor and antidiabetes. Her scientific research has found recognition by a variety of scientific prizes and research awards, international lectureships, and the invitation to join the advisory boards of scientific journals.

DOI: 10.1021/acs.chemrev.5b00392
Chem. Rev. 2016, 116, 422−518

ACKNOWLEDGMENTS

We gratefully acknowledge financial support from IKERBASQUE, Basque Foundation for Science, and the National Natural Science Foundation of China (Grants 91229204 and 81220108025).

REFERENCES

(1) Liang, Y.; Feng, D.; Wu, Y.; Tsai, S.-T.; Li, G.; Ray, C.; Yu, L. Highly Efficient Solar Cell Polymers Developed via Fine-Tuning of Structural and Electronic Properties. *J. Am. Chem. Soc.* **2009**, *131*, 7792−7799.
(2) Son, H. J.; Wang, W.; Xu, T.; Liang, Y.; Wu, Y.; Li, G.; Yu, L. Synthesis of Fluorinated Polythienothiophene-*co*-benzodithiophenes and Effect of Fluorination on the Photovoltaic Properties. *J. Am. Chem. Soc.* **2011**, *133*, 1885−1894.
(3) Stuart, A. C.; Tumbleston, J. R.; Zhou, H.; Li, W.; Liu, S.; Ade, H.; You, W. Fluorine Substituents Reduce Charge Recombination and Drive Structure and Morphology Development in Polymer Solar Cells. *J. Am. Chem. Soc.* **2013**, *135*, 1806−1815.
(4) Cai, L.; Lu, S.; Pike, V. W. Chemistry with [^{18}F]Fluoride Ion. *Eur. J. Org. Chem.* **2008**, *2008*, 2853−2873.
(5) Brooks, A. F.; Topczewski, J. J.; Ichiishi, N.; Sanford, M. S.; Scott, P. J. H. Late-Stage [^{18}F]Fluorination: New Solutions to Old Problems. *Chem. Sci.* **2014**, *5*, 4545−4553.
(6) Chen, H.; Viel, S.; Ziarelli, F.; Peng, L. ^{19}F NMR: A Valuable Tool for Studying Biological Events. *Chem. Soc. Rev.* **2013**, *42*, 7971−7982.
(7) Marsh, E. N. G.; Suzuki, Y. Using ^{19}F NMR to Probe Biological Interactions of Proteins and Peptides. *ACS Chem. Biol.* **2014**, *9*, 1242−1250.
(8) Smits, R.; Cadicamo, C. D.; Burger, K.; Koksch, B. Synthetic Strategies to α-Trifluoromethyl and α-Difluoromethyl Substituted α-Amino Acids. *Chem. Soc. Rev.* **2008**, *37*, 1727−1739.
(9) Qiu, X.-L.; Qing, F.-L. Recent Advances in the Synthesis of Fluorinated Amino Acids. *Eur. J. Org. Chem.* **2011**, *2011*, 3261−3278.
(10) Mikami, K.; Fustero, S.; Sánchez-Roselló, M.; Aceña, J. L.; Soloshonok, V.; Sorochinsky, A. Synthesis of Fluorinated β-Amino Acids. *Synthesis* **2011**, *2011*, 3045−3079.
(11) Aceña, J. L.; Sorochinsky, A. E.; Soloshonok, V. A. Recent Advances in the Asymmetric Synthesis of α-(Trifluoromethyl)-Containing α-Amino Acids. *Synthesis* **2012**, *44*, 1591−1602.
(12) Yoder, N. C.; Kumar, K. Fluorinated Amino Acids in Protein Design and Engineering. *Chem. Soc. Rev.* **2002**, *31*, 335−341.
(13) Jäckel, C.; Koksch, B. Fluorine in Peptide Design and Protein Engineering. *Eur. J. Org. Chem.* **2005**, *2005*, 4483−4503.
(14) Salwiczek, M.; Nyakatura, E. K.; Gerling, U. I. M.; Ye, S.; Koksch, B. Fluorinated Amino Acids: Compatibility with Native Protein Structures and Effects on Protein−Protein Interactions. *Chem. Soc. Rev.* **2012**, *41*, 2135−2171.
(15) Marsh, E. N. G. Fluorinated Proteins: From Design and Synthesis to Structure and Stability. *Acc. Chem. Res.* **2014**, *47*, 2878−2886.
(16) Tirotta, I.; Dichiarante, V.; Pigliacelli, C.; Cavallo, G.; Terraneo, G.; Bombelli, F. B.; Metrangolo, P.; Resnati, G. ^{19}F Magnetic Resonance Imaging (MRI): From Design of Materials to Clinical Applications. *Chem. Rev.* **2015**, *115*, 1106−1129.
(17) Berger, R.; Resnati, G.; Metrangolo, P.; Weber, E.; Hulliger, J. Organic Fluorine Compounds: A Great Opportunity for Enhanced Materials Properties. *Chem. Soc. Rev.* **2011**, *40*, 3496−3508.
(18) Studer, A.; Hadida, S.; Ferritto, R.; Kim, S.-Y.; Jeger, P.; Wipf, P.; Curran, D. P. Fluorous Synthesis: A Fluorous-Phase Strategy for Improving Separation Efficiency in Organic Synthesis. *Science* **1997**, *275*, 823−826.
(19) Zhang, W. Fluorous Linker-Facilitated Chemical Synthesis. *Chem. Rev.* **2009**, *109*, 749−795.
(20) Zhang, W. Green Chemistry Aspects of Fluorous Techniques−Opportunities and Challenges for Small-Scale Organic Synthesis. *Green Chem.* **2009**, *11*, 911−920.
(21) Jeschke, P. The Unique Role of Fluorine in the Design of Active Ingredients for Modern Crop Protection. *ChemBioChem* **2004**, *5*, 570−589.
(22) Jeschke, P. The Unique Role of Halogen Substituents in the Design of Modern Agrochemicals. *Pest Manage. Sci.* **2010**, *66*, 10−27.
(23) Isanbor, C.; O'Hagan, D. Fluorine in Medicinal Chemistry: A Review of Anti-Cancer Agents. *J. Fluorine Chem.* **2006**, *127*, 303−319.
(24) Bégué, J.-P.; Bonnet-Delpon, D. Recent Advances (1995−2005) in Fluorinated Pharmaceuticals Based on Natural Products. *J. Fluorine Chem.* **2006**, *127*, 992−1012.
(25) Müller, K.; Faeh, C.; Diederich, F. Fluorine in Pharmaceuticals: Looking Beyond Intuition. *Science* **2007**, *317*, 1881−1886.
(26) O'Hagan, D. Fluorine in Health Care: Organofluorine Containing Blockbuster Drugs. *J. Fluorine Chem.* **2010**, *131*, 1071−1081.
(27) Böhm, H.-J.; Banner, D.; Bendels, S.; Kansy, M.; Kuhn, B.; Müller, K.; Obst-Sander, U.; Stahl, M. Fluorine in Medicinal Chemistry. *ChemBioChem* **2004**, *5*, 637−643.
(28) Kirk, K. L. Fluorine in Medicinal Chemistry: Recent Therapeutic Applications of Fluorinated Small Molecules. *J. Fluorine Chem.* **2006**, *127*, 1013−1029.
(29) Purser, S.; Moore, P. R.; Swallow, S.; Gouverneur, V. Fluorine in Medicinal Chemistry. *Chem. Soc. Rev.* **2008**, *37*, 320−330.
(30) Hagmann, W. K. The Many Roles for Fluorine in Medicinal Chemistry. *J. Med. Chem.* **2008**, *51*, 4359−4369.
(31) Gillis, E. P.; Eastman, K. J.; Hill, M. D.; Donnelly, D. J.; Meanwell, N. A. Applications of Fluorine in Medicinal Chemistry. *J. Med. Chem.* **2015**, *58*, 8315−8359.
(32) Huchet, Q. A.; Kuhn, B.; Wagner, B.; Kratochwil, N. A.; Fischer, H.; Kansy, M.; Zimmerli, D.; Carreira, E. M.; Müller, K. Fluorination Patterning: A Study of Structural Motifs that Impact Physicochemical Properties of Relevance to Drug Discovery. *J. Med. Chem.* **2015**, *58*, 9041−9060.
(33) Wang, J.; Sánchez-Roselló, M.; Aceña, J. L.; del Pozo, C.; Sorochinsky, A. E.; Fustero, S.; Soloshonok, V. A.; Liu, H. Fluorine in Pharmaceutical Industry: Fluorine-Containing Drugs Introduced to the Market in the Last Decade (2001−2011). *Chem. Rev.* **2014**, *114*, 2432−2506.
(34) Zhu, W.; Wang, J.; Wang, S.; Gu, Z.; Aceña, J. L.; Izawa, K.; Liu, H.; Soloshonok, V. A. Recent Advances in the Trifluoromethylation Methodology and New CF_3-Containing Drugs. *J. Fluorine Chem.* **2014**, *167*, 37−54.
(35) Izawa, K.; Aceña, J. L.; Wang, J.; Soloshonok, V. A.; Liu, H. Small-Molecule Therapeutics for Ebola Virus (EBOV) Disease Treatment. *Eur. J. Org. Chem.* **2016**, 8−16.
(36) Fried, J.; Sabo, E. F. 9α-Fluoro Derivatives of Cortisone and Hydrocortisone. *J. Am. Chem. Soc.* **1954**, *76*, 1455−1456.
(37) Ilardi, E. A.; Vitaku, E.; Njardarson, J. T. Data-Mining for Sulfur and Fluorine: An Evaluation of Pharmaceuticals To Reveal Opportunities for Drug Design and Discovery. *J. Med. Chem.* **2014**, *57*, 2832−2842.
(38) McGrath, N. A.; Brichacek, M.; Njardarson, J. T. A Graphical Journey of Innovative Organic Architectures that Have Improved our Lives. *J. Chem. Educ.* **2010**, *87*, 1348−1349.
(39) Top 100 US Prescription and Brand Name Drugs Products. http://cbc.arizona.edu/njardarson/group/sites/default/files/Top%20US%20Pharmaceutical%20Products%20of%202013.pdf (accessed July 2, 2015).
(40) Ridker, P. M.; Danielson, E.; Fonseca, F. A. H.; Genest, J.; Gotto, A. M., Jr.; Kastelein, J. J. P.; Koenig, W.; Libby, P.; Lorenzatti, A. J.; MacFadyen, J. G.; et al. Rosuvastatin to Prevent Vascular Events in Men and Women with Elevated C-Reactive Protein. *N. Engl. J. Med.* **2008**, *359*, 2195−2207.
(41) LaRosa, J. C.; Grundy, S. M.; Waters, D. D.; Shear, C.; Barter, P.; Fruchart, J.-C.; Gotto, A. M.; Greten, H.; Kastelein, J. J. P.; Shepherd, J.; et al. Intensive Lipid Lowering with Atorvastatin in Patients with Stable Coronary Disease. *N. Engl. J. Med.* **2005**, *352*, 1425−1435.

DOI: 10.1021/acs.chemrev.5b00392
Chem. Rev. 2016, 116, 422−518

(42) Calverley, P. M. A.; Anderson, J. A.; Celli, B.; Ferguson, G. T.; Jenkins, C.; Jones, P. W.; Yates, J. C.; Vestbo, J. Salmeterol and Fluticasone Propionate and Survival in Chronic Obstructive Pulmonary Disease. *N. Engl. J. Med.* **2007**, *356*, 775−789.
(43) Gallant, J. E.; Dejesus, E.; Arribas, J. R.; Pozniak, A. L.; Gazzard, B.; Campo, R. E.; Lu, B.; McColl, D.; Chuck, S.; Enejosa, J.; et al. Tenofovir DF, Emtricitabine, and Efavirenz vs. Zidovudine, Lamivudine, and Efavirenz for HIV. *N. Engl. J. Med.* **2006**, *354*, 251−260.
(44) Kim, D.; Wang, L.; Beconi, M.; Eiermann, G. J.; Fisher, M. H.; He, H.; Hickey, G. J.; Kowalchick, J. E.; Leiting, B.; Lyons, K.; et al. (2*R*)-4-Oxo-4-[3-(trifluoromethyl)-5,6-dihydro[1,2,4]triazolo[4,3-*a*]-pyrazin-7(8*H*)-yl]-1-(2,4,5-trifluorophenyl)butan-2-amine: A Potent, Orally Active Dipeptidyl Peptidase IV Inhibitor for the Treatment of Type 2 Diabetes. *J. Med. Chem.* **2005**, *48*, 141−151.
(45) Penning, T. D.; Talley, J. J.; Bertenshaw, S. R.; Carter, J. S.; Collins, P. W.; Docter, S.; Graneto, M. J.; Lee, L. F.; Malecha, J. W.; Miyashiro, J. M.; et al. Synthesis and Biological Evaluation of the 1,5-Diarylpyrazole Class of Cyclooxygenase-2 Inhibitors: Identification of 4-[5-(4-Methylphenyl)-3-(trifluoromethyl)-1H-pyrazol-1-yl]-benzenesulfonamide (SC-58635, Celecoxib). *J. Med. Chem.* **1997**, *40*, 1347−1365.
(46) Besset, T.; Poisson, T.; Pannecoucke, X. Recent Progress in Direct Introduction of Fluorinated Groups on Alkenes and Alkynes by means of C−H Bond Functionalization. *Chem. - Eur. J.* **2014**, *20*, 16830−16845.
(47) Wu, J. Review of Recent Advances in Nucleophilic C-F Bond-Forming Reactions at sp^3 Centers. *Tetrahedron Lett.* **2014**, *55*, 4289−4294.
(48) Li, Y.; Wu, Y.; Li, G.-S.; Wang, X.-S. Palladium-Catalyzed C-F Bond Formation via Directed C-H Activation. *Adv. Synth. Catal.* **2014**, *356*, 1412−1418.
(49) Yang, X.; Wu, T.; Phipps, R. J.; Toste, F. D. Advances in Catalytic Enantioselective Fluorination, Mono-, Di-, and Trifluoromethylation, and Trifluoromethylthiolation Reactions. *Chem. Rev.* **2015**, *115*, 826−870.
(50) Ahrens, T.; Kohlmann, J.; Ahrens, M.; Braun, T. Functionalization of Fluorinated Molecules by Transition-Metal-Mediated C-F Bond Activation To Access Fluorinated Building Blocks. *Chem. Rev.* **2015**, *115*, 931−972.
(51) Alonso, C.; Martínez de Marigorta, E.; Rubiales, G.; Palacios, F. Carbon Trifluoromethylation Reactions of Hydrocarbon Derivatives and Heteroarenes. *Chem. Rev.* **2015**, *115*, 1847−1935.
(52) Kirk, K. L. Fluorination in Medicinal Chemistry: Methods, Strategies, and Recent Developments. *Org. Process Res. Dev.* **2008**, *12*, 305−321.
(53) Campbell, M. G.; Ritter, T. Late-Stage Fluorination: From Fundamentals to Application. *Org. Process Res. Dev.* **2014**, *18*, 474−480.
(54) Cresswell, A. J.; Davies, S. G.; Roberts, P. M.; Thomson, J. E. Beyond the Balz−Schiemann Reaction: The Utility of Tetrafluoroborates and Boron Trifluoride as Nucleophilic Fluoride Sources. *Chem. Rev.* **2015**, *115*, 566−611.
(55) Sun, H.; DiMagno, S. G. Anhydrous Tetrabutylammonium Fluoride. *J. Am. Chem. Soc.* **2005**, *127*, 2050−2051.
(56) Furuya, T.; Kamlet, A. S.; Ritter, T. Catalysis for Fluorination and Trifluoromethylation. *Nature* **2011**, *473*, 470−477.
(57) Campbell, M. G.; Ritter, T. Modern Carbon−Fluorine Bond Forming Reactions for Aryl Fluoride Synthesis. *Chem. Rev.* **2015**, *115*, 612−633.
(58) Champagne, P. A.; Desroches, J.; Hamel, J.-D.; Vandamme, M.; Paquin, J.-F. Monofluorination of Organic Compounds: 10 Years of Innovation. *Chem. Rev.* **2015**, *115*, 9073−9174.
(59) Hull, K. L.; Anani, W. Q.; Sanford, M. S. Palladium-Catalyzed Fluorination of Carbon-Hydrogen Bonds. *J. Am. Chem. Soc.* **2006**, *128*, 7134−7135.
(60) Watson, D. A.; Su, M.; Teverovskiy, G.; Zhang, Y.; García-Fortanet, J.; Kinzel, T.; Buchwald, S. L. Formation of ArF from LPdAr(F): Catalytic Conversion of Aryl Triflates to Aryl Fluorides. *Science* **2009**, *325*, 1661−1664.
(61) Prakash, G. K. S.; Yudin, A. K. Perfluoroalkylation with Organosilicon Reagents. *Chem. Rev.* **1997**, *97*, 757−786.
(62) Liu, X.; Xu, C.; Wang, M.; Liu, Q. Trifluoromethyltrimethylsilane: Nucleophilic Trifluoromethylation and Beyond. *Chem. Rev.* **2015**, *115*, 683−730.
(63) Cho, E. J.; Senecal, T. D.; Kinzel, T.; Zhang, Y.; Watson, D. A.; Buchwald, S. L. The Palladium-Catalyzed Trifluoromethylation of Aryl Chlorides. *Science* **2010**, *328*, 1679−1681.
(64) Umemoto, T. Electrophilic Perfluoroalkylating Agents. *Chem. Rev.* **1996**, *96*, 1757−1777.
(65) Kieltsch, I.; Eisenberger, P.; Togni, A. Mild Electrophilic Trifluoromethylation of Carbon- and Sulfur-Centered Nucleophiles by a Hypervalent Iodine(III)-CF_3 reagent. *Angew. Chem., Int. Ed.* **2007**, *46*, 754−757.
(66) Charpentier, J.; Früh, N.; Togni, A. Electrophilic Trifluoromethylation by Use of Hypervalent Iodine Reagents. *Chem. Rev.* **2015**, *115*, 650−682.
(67) Nagib, D. A.; MacMillan, D. W. C. Trifluoromethylation of Arenes and Heteroarenes by Means of Photoredox Catalysis. *Nature* **2011**, *480*, 224−228.
(68) Ji, Y.; Brueckl, T.; Baxter, R. D.; Fujiwara, Y.; Seiple, I. B.; Su, S.; Blackmond, D. G.; Baran, P. S. Innate C-H Trifluoromethylation of Heterocycles. *Proc. Natl. Acad. Sci. U. S. A.* **2011**, *108*, 14411−144150.
(69) Scherer, K. V., Jr.; Ono, T.; Yamanouchi, K.; Fernandez, R.; Henderson, P.; Goldwhite, H. *F*-2,4-Dimethyl-3-ethyl-3-pentyl and *F*-2,4-Dimethyl-3-isopropyl-3-pentyl: Stable *tert*-Perfluoroalkyl Radicals Prepared by Addition of Fluorine or Trifluoromethyl to a Perfluoroalkene. *J. Am. Chem. Soc.* **1985**, *107*, 718−719.
(70) Yogesh, P.; Ono, T.; Bruno, A. Innovative Trifluoromethyl Radical from Persistent Radical as Efficient Initiator for the Radical Copolymerization of Vinylidene Fluoride with *tert*-Butyl α-Trifluoromethacrylate. *ACS Macro Lett.* **2012**, *1*, 315−320.
(71) Boschet, F.; Ono, T.; Ameduri, B. Novel Source of Trifluoromethyl Radical As Efficient Initiator for the Polymerization of Vinylidene Fluoride. *Macromol. Rapid Commun.* **2012**, *33*, 302−308.
(72) Patil, Y.; Alaaeddine, A.; Ono, T.; Ameduri, B. Novel Method to Assess the Molecular Weights of Fluoropolymers by Radical Copolymerization of Vinylidene Fluoride with Various Fluorinated Comonomers Initiated by a Persistent Radical. *Macromolecules* **2013**, *46*, 3092−3106.
(73) Sato, A.; Han, J.; Ono, T.; Wzorek, A.; Aceña, J. L.; Soloshonok, V. A. Introducing a New Radical Trifluoromethylation Reagent. *Chem. Commun.* **2015**, *51*, 5967−5970.
(74) Middleton, W. J. New Fluorinating Reagents. Dialkylaminosulfur Fluorides. *J. Org. Chem.* **1975**, *40*, 574−578.
(75) Lal, G. S.; Pez, G. P.; Syvret, R. G. Electrophilic NF Fluorinating Agents. *Chem. Rev.* **1996**, *96*, 1737−1755.
(76) Ma, J.-A.; Cahard, D. Update 1 of: Asymmetric Fluorination, Trifluoromethylation, and Perfluoroalkylation Reactions. *Chem. Rev.* **2008**, *108*, PR1−PR43.
(77) Marigo, M.; Fielenbach, D.; Braunton, A.; Kjaersgaard, A.; Jørgensen, K. A. Enantioselective Formation of Stereogenic Carbon−Fluorine Centers by a Simple Catalytic Method. *Angew. Chem., Int. Ed.* **2005**, *44*, 3703−3706.
(78) Steiner, D. D.; Mase, N.; Barbas, C. F., III Direct Asymmetric α-Fluorination of Aldehydes. *Angew. Chem., Int. Ed.* **2005**, *44*, 3706−3710.
(79) Beeson, T. D.; MacMillan, D. W. C. Enantioselective Organocatalytic α-Fluorination of Aldehydes. *J. Am. Chem. Soc.* **2005**, *127*, 8826−8828.
(80) Nagib, D. A.; Scott, M. E.; MacMillan, D. W. C. Enantioselective α-Trifluoromethylation of Aldehydes via Photoredox Organocatalysis. *J. Am. Chem. Soc.* **2009**, *131*, 10875−10877.
(81) Bégué, J.-P.; Bonnet-Delpon, D.; Crousse, B.; Legros, J. The Chemistry of Trifluoromethyl Imines and Related Acetals Derived from Fluoral. *Chem. Soc. Rev.* **2005**, *34*, 562−572.

DOI: 10.1021/acs.chemrev.5b00392
Chem. Rev. 2016, 116, 422−518

(82) Truong, V. L.; Ménard, M. S.; Dion, I. Asymmetric Syntheses of 1-Aryl-2,2,2-trifluoroethylamines via Diastereoselective 1,2-Addition of Arylmetals to 2-Methyl-*N*-(2,2,2-trifluoroethylidene)propane-2-sulfinamide. *Org. Lett.* **2007**, *9*, 683−685.
(83) Truong, V. L.; Pfeiffer, J. Y. Rhodium-Catalyzed Diastereoselective 1,2-Addition of Arylboronic Acids to Chiral Trifluoroethyl Imine. *Tetrahedron Lett.* **2009**, *50*, 1633−1635.
(84) Liu, J.; Hu, J. Synthesis of Fluorinated Chiral Amines Using *N*-*tert*-Butylsulfinyl Imines. *Future Med. Chem.* **2009**, *1*, 875−888.
(85) Soloshonok, V. A.; Avilov, D. V.; Kukhar, V. P. Asymmetric Aldol Reactions of Trifluoromethyl Ketones with a Chiral Ni(II) Complex of Glycine: Stereocontrolling Effect of the Trifluoromethyl Group. *Tetrahedron* **1996**, *52*, 12433−12442.
(86) Soloshonok, V. A.; Hayashi, T.; Ishikawa, K.; Nagashima, N. Highly Diastereoselective Aldol Reaction of Fluoroalkyl Aryl Ketones with Methyl Isocyanoacetate Catalyzed by Silver(I)/Triethylamine. *Tetrahedron Lett.* **1994**, *35*, 1055−1058.
(87) Bravo, P.; Guidetti, M.; Viani, F.; Zanda, M.; Markovsky, A. L.; Sorochinsky, A. E.; Soloshonok, I. V.; Soloshonok, V. A. Chiral Sulfoxide Controlled Asymmetric Additions to C-N Double Bond. An Efficient Approach to Stereochemically Defined α-Fluoroalkyl Amino Compounds. *Tetrahedron* **1998**, *54*, 12789−12806.
(88) Robak, M. T.; Herbage, M. A.; Ellman, J. A. Synthesis and Applications of *tert*-Butanesulfinamide. *Chem. Rev.* **2010**, *110*, 3600−3740.
(89) Ellman, J. A.; Owens, T. D.; Tang, T. P. *N*-*tert*-Butanesulfinyl Imines: Versatile Intermediates for the Asymmetric Synthesis of Amines. *Acc. Chem. Res.* **2002**, *35*, 984−985.
(90) Liu, G.; Cogan, D. A.; Owens, T. D.; Tang, T. P.; Ellman, J. A. Synthesis of Enantiomerically Pure *N*-*tert*-Butanesulfinyl Imines (*tert*-Butanesulfinimines) by the Direct Condensation of *tert*-Butanesulfinamide with Aldehydes and Ketones. *J. Org. Chem.* **1999**, *64*, 1278−1284.
(91) Mimura, H.; Kawada, K.; Yamashita, T.; Sakamoto, T.; Kikugawa, Y. Trifluoroacetaldehyde: A Useful Industrial Bulk Material for the Synthesis of Trifluoromethylated Amino Compounds. *J. Fluorine Chem.* **2010**, *131*, 477−486.
(92) Qian, P.; Dai, Y.; Mei, H.; Soloshonok, V. A.; Han, J.; Pan, Y. Ni-Catalyzed Asymmetric Decarboxylative Mannich Reaction for the Synthesis of β-Trifluoromethyl-β-Amino Ketones. *RSC Adv.* **2015**, *5*, 26811−26814.
(93) Mei, H.; Xiong, Y.; Han, J.; Pan, Y. A Facile Process for the Asymmetric Synthesis of β-Trifluoromethylated β-Amino Ketones via Addition of Ketone Enolates to Sulfinylimine. *Org. Biomol. Chem.* **2011**, *9*, 1402−1406.
(94) Xie, C.; Mei, H.; Wu, L.; Soloshonok, V. A.; Han, J.; Pan, Y. LDA-Promoted Asymmetric Synthesis of β-trifluoromethyl-β-amino Indanone Derivatives with Virtually Complete Stereochemical Outcome. *RSC Adv.* **2014**, *4*, 4763−4768.
(95) Wu, L.; Xie, C.; Mei, H.; Soloshonok, V. A.; Han, J.; Pan, Y. Highly Efficient and Generalized Asymmetric Synthesis of Quaternary Stereogenic Carbon-Containing β-amino Indanones/Indanoles *via* Mannich-Type Additions between 1-Indanones and *N*-*tert*-Butanesulfinylketimines. *Org. Biomol. Chem.* **2014**, *12*, 4620−4627.
(96) Qian, P.; Xie, C.; Wu, L.; Mei, H.; Soloshonok, V. A.; Han, J.; Pan, Y. Asymmetric Synthesis of (3*S*,1′*S*)-3-(1-Amino-2,2,2-trifluoroethyl)-1-(alkyl)-indolin-2-one Derivatives by Additions of (*S*)-*N*-*t*-Butylsulfinyl-3,3,3-trifluoroacetaldimine to 1-(Alkyl)-indolin-2-ones. *Org. Biomol. Chem.* **2014**, *12*, 7909−7913.
(97) Wu, L.; Xie, C.; Mei, H.; Dai, Y.; Han, J.; Soloshonok, V. A.; Pan, Y. Synthesis of Trifluoromethyl-Containing Vicinal Diamines by Asymmetric Decarboxylative Mannich Addition Reactions. *J. Org. Chem.* **2015**, *80*, 3187−3194.
(98) Mei, H.; Xie, C.; Wu, L.; Soloshonok, V. A.; Han, J.; Pan, Y. Asymmetric Mannich Reactions of Imidazo[2,1-*b*]-thiazole-Derived Nucleophiles with (S_S)-*N*-*tert*-Butanesulfinyl-(3,3,3)-trifluoroacetaldimine. *Org. Biomol. Chem.* **2013**, *11*, 8018−8021.
(99) Mei, H.; Xiong, Y.; Xie, C.; Soloshonok, V. A.; Han, J.; Pan, Y. Concise and Scalable Asymmetric Synthesis of 5-(1-Amino-2,2,2-trifluoroethyl)thiazolo[3,2-*b*][1,2,4]triazoles. *Org. Biomol. Chem.* **2014**, *12*, 2108−2113.
(100) Mei, H.; Dai, Y.; Wu, L.; Soloshonok, V. A.; Han, J.; Pan, Y. Mannich-Type Addition Reactions between Lithium Derivatives of Benzo[*d*]thiazoles and *N*-*tert*-Butylsulfinyl-3,3,3-trifluoroacetaldimine: Convenient Generalized Synthesis of Bis(benzothiazole)s. *Eur. J. Org. Chem.* **2014**, *2014*, 2429−2433.
(101) Dai, Y.; Xie, C.; Wu, L.; Mei, H.; Soloshonok, V. A.; Han, J.; Pan, Y. Asymmetric Synthesis of Amino-benzothiazol Derivatives by Additions of 2-Lithiated Benzothiazoles to (*S*)-*N*-*t*-Butylsulfinylketimines. *RSC Adv.* **2015**, *5*, 3491−3497.
(102) Wu, L.; Xie, C.; Zhou, J.; Mei, H.; Soloshonok, V. A.; Han, J.; Pan, Y. General Asymmetric Synthesis of 2,2,2-Trifluoro-1-(1*H*-indol-3- and −2-yl)ethanamines. *J. Fluorine Chem.* **2015**, *170*, 57−65.
(103) Xie, C.; Mei, H.; Wu, L.; Soloshonok, V. A.; Han, J.; Pan, Y. Concise Asymmetric Synthesis of β-Trifluoromethylated α,β-Diamino Esters through Addition Reactions of Glycine Esters to CF_3-Sulfinylimine. *Eur. J. Org. Chem.* **2014**, *2014*, 1445−1451.
(104) Kawamura, A.; Moriwaki, H.; Röschenthaler, G.-V.; Kawada, K.; Aceña, J. L.; Soloshonok, V. A. Synthesis of (2*S*,3*S*)-β-(Trifluoromethyl)-α,β-diamino Acid by Mannich Addition of Glycine Schiff Base Ni(II) Complexes to *N*-*tert*-Butylsulfinyl-3,3,3-trifluoroacetaldimine. *J. Fluorine Chem.* **2015**, *171*, 67−72.
(105) Shevchuk, M. V.; Kukhar, V. P.; Röschenthaler, G.-V.; Bassil, B. S.; Kawada, K.; Soloshonok, V. A.; Sorochinsky, A. E. New Asymmetric Approach to β-Trifluoromethyl Isoserines. *RSC Adv.* **2013**, *3*, 6479−6484.
(106) Shibata, N.; Nishimine, T.; Shibata, N.; Tokunaga, E.; Kawada, K.; Kagawa, T.; Aceña, J. L.; Sorochinsky, A. E.; Soloshonok, V. A. Asymmetric Mannich Reaction between (*S*)-*N*-(*tert*-Butanesulfinyl)-3,3,3-trifluoroacetaldimine and Malonic Acid Derivatives. Stereodivergent Synthesis of (*R*)- and (*S*)-3-Amino-4,4,4-trifluorobutanoic acids. *Org. Biomol. Chem.* **2014**, *12*, 1454−1462.
(107) Shibata, N.; Nishimine, T.; Shibata, N.; Tokunaga, E.; Kawada, K.; Kagawa, T.; Sorochinsky, A. E.; Soloshonok, V. A. Organic Base-Catalyzed Stereodivergent Synthesis of (*R*)- and (*S*)-3-Amino-4,4,4-trifluorobutanoic Acids. *Chem. Commun.* **2012**, *48*, 4124−4126.
(108) Wu, L.; Xie, C.; Mei, H.; Soloshonok, V. A.; Han, J.; Pan, Y. Asymmetric Friedel-Crafts Reactions of *N*-*tert*-Butylsulfinyl-3,3,3-trifluoroacetaldimines: General Access to Enantiomerically Pure Indoles Containing a 1-Amino-2,2,2-trifluoroethyl Group. *J. Org. Chem.* **2014**, *79*, 7677−7681.
(109) Milcent, T.; Hao, J.; Kawada, K.; Soloshonok, V. A.; Ongeri, S.; Crousse, B. Highly Stereoselective aza-Baylis−Hillman Reactions of CF_3-Sulfinylimines: Straightforward Access to α-Methylene β-CF_3 β-Amino Acids. *Eur. J. Org. Chem.* **2014**, *2014*, 3072−3075.
(110) Röschenthaler, G.-V.; Kukhar, V. P.; Kulik, I. B.; Belik, M. Y.; Sorochinsky, A. E.; Rusanov, E. B.; Soloshonok, V. A. Asymmetric Synthesis of Phosphonotrifluoroalanine and its Derivatives using *N*-*tert*-Butanesulfinyl Imine Derived from Fluoral. *Tetrahedron Lett.* **2012**, *53*, 539−542.
(111) Turcheniuk, K. V.; Poliashko, K. O.; Kukhar, V. P.; Rozhenko, A. B.; Soloshonok, V. A.; Sorochinsky, A. E. Efficient Asymmetric Synthesis of Trifluoromethylated β-Aminophosphonates and their Incorporation into Dipeptides. *Chem. Commun.* **2012**, *48*, 11519−11521.
(112) Röschenthaler, G.-V.; Kukhar, V. P.; Kulik, I. B.; Sorochinsky, A. E.; Soloshonok, V. A. Convenient Synthesis of Fluoroalkyl α- and β-Aminophosphonates. *J. Fluorine Chem.* **2011**, *132*, 834−837.
(113) Liu, Y.; Liu, J.; Huang, Y.; Qing, F.-L. Lewis Acid-Catalyzed Regioselective Synthesis of Chiral α-Fluoroalkyl Amines via Asymmetric Addition of Silyl Dienolates to Fluorinated Sulfinylimines. *Chem. Commun.* **2013**, *49*, 7492−7494.
(114) Jiang, W.; Chen, C.; Marinkovic, D.; Tran, J. A.; Chen, C. W.; Arellano, L. M.; White, N. S.; Tucci, F. C. Practical Asymmetric Synthesis of α-Branched 2-Piperazinylbenzylamines by 1,2-Additions of Organometallic Reagents to *N*-*tert*-Butanesulfinyl Imines. *J. Org. Chem.* **2005**, *70*, 8924−8931.

DOI: 10.1021/acs.chemrev.5b00392
Chem. Rev. 2016, 116, 422−518

(115) Zhang, H.; Li, Y.; Xu, W.; Zheng, W.; Zhou, P.; Sun, Z. Practical and Stereoselective Synthesis of β-Amino Sulfones from Alkyl Phenyl Sulfones and N-(tert-Butylsulfinyl) Aldimines. *Org. Biomol. Chem.* **2011**, *9*, 6502−6505.
(116) Liu, Y.; Yang, Y.; Huang, Y.; Xu, X.-H.; Qing, F.-L. Regio- and Diastereoselective Vinylogous Mannich Addition of 3-Alkenyl-2-oxindoles to α-Fluoroalkyl Aldimines. *Synlett* **2015**, *26*, 67−72.
(117) Xie, C.; Mei, H.; Wu, L.; Han, J.; Soloshonok, V. A.; Pan, Y. Large-Scale Mannich-Type Reactions of (S_S)-*N*-*tert*-Butanesulfinyl-(3,3,3)-trifluoroacetaldimine with *C*-Nucleophiles. *J. Fluorine Chem.* **2014**, *165*, 67−75.
(118) Yamana, M.; Ishihara, T.; Ando, T. A Convenient Synthesis of 2,2-Difluoro Enol Silyl Ethers from Chlorodifluoromethyl Ketones. *Tetrahedron Lett.* **1983**, *24*, 507−510.
(119) Brigaud, T.; Doussot, P.; Portella, C. Synthesis of Difluoroenoxysilanes from Acylsilanes and Trifluoromethyltrimethylsilane (TFMTMS). Dramatic Effect of the Catalytic Fluoride Source. *J. Chem. Soc., Chem. Commun.* **1994**, 2117−2118.
(120) Amii, H.; Kobayashi, T.; Hatamoto, Y.; Uneyama, K. Mg^0-Promoted Selective C−F Bond Cleavage of Trifluoromethyl Ketones: A Convenient Method for the Synthesis of 2,2-Difluoro Enol Silanes. *Chem. Commun.* **1999**, 1323−1324.
(121) Mei, H.; Xie, C.; Aceña, J. L.; Soloshonok, V. A.; Röschenthaler, G.-V.; Han, J. Recent Progress in the in situ Detrifluoroacetilative Generation of Fluoro Enolates and Their Reactions with Electrophiles. *Eur. J. Org. Chem.* **2015**, *2015*, 6401−6412.
(122) McBee, E. T.; Burton, T. M. The Bromination of 1,1,1-Trifluoropropanone. *J. Am. Chem. Soc.* **1952**, *74*, 3902−3904.
(123) Haszeldine, R. N. 361. Perfluoroalkyl Grignard Reagents. Part II. Reaction of Heptafluoropropylmagnesium Iodide with Carbonyl Compounds, and the Mechanism of Reduction During Grignard Reactions. *J. Chem. Soc.* **1953**, 1748−1757.
(124) Hauptschein, M.; Braun, R. A. The Reaction of Ethyl Perfluorobutyrate with Sodium. An Improved Synthesis of Perfluoroheptan-4-one. *J. Am. Chem. Soc.* **1955**, *77*, 4930−4931.
(125) Simmons, H. E.; Wiley, D. W. Fluoroketones. I. *J. Am. Chem. Soc.* **1960**, *82*, 2288−2296.
(126) Prager, J. H.; Ogden, P. H. Metal Derivatives of Fluorinated *gem*-Diols. *J. Org. Chem.* **1968**, *33*, 2100−2102.
(127) Soloshonok, V. A.; Gerus, I. I.; Yagupolskii, Y. L.; Kukhar, V. P. Azomethine-Azomethine Isomerization in Fluorinated N-Benzylimines. *Zh. Org. Khim.* **1988**, *24*, 993−997. *Chem. Abstr.* **1989**, *110*, 134824.
(128) Soloshonok, V. A.; Yagupolskii, Y. L.; Kukhar, V. P. Fluorine-Containing Amino Acids. V. Imines of Trifluoropyruvic Acid in the Synthesis of *N*-Substituted Trifluoroalanines. *Zh. Org. Khim.* **1988**, *24*, 1638−1644. *Chem. Abstr.* **1989**, *110*, 154827.
(129) Ohkura, H.; Berbasov, D. O.; Soloshonok, V. A. Chemo- and Regioselectivity in the Reactions between Highly Electrophilic Fluorine Containing Dicarbonyl Compounds and Amines. Improved Synthesis of the Corresponding Imines/Enamines. *Tetrahedron* **2003**, *59*, 1647−1656.
(130) Berbasov, D. O.; Ojemaye, I. D.; Soloshonok, V. A. Synthesis of Highly 1,3-Proton Shift Transferable *N*-Benzyl Imines of Trifluoroacetophenone under the "Low-Basicity" Reaction Conditions. *J. Fluorine Chem.* **2004**, *125*, 603−607.
(131) Xie, C.; Wu, L.; Mei, H.; Soloshonok, V. A.; Han, J.; Pan, Y. Generalized Access to Fluorinated β-Keto Amino Compounds through Asymmetric Additions of α,α-Difluoroenolates to CF_3-Sulfinylimine. *Org. Biomol. Chem.* **2014**, *12*, 7836−7843.
(132) Xie, C.; Wu, L.; Mei, H.; Soloshonok, V. A.; Han, J.; Pan, Y. Operationally Convenient Method for Preparation of Sulfonamides Containing α,α-Difluoro-β-amino Carbonyl Moiety. *Tetrahedron Lett.* **2014**, *55*, 5908−5910.
(133) Xie, C.; Wu, L.; Zhou, J.; Mei, H.; Soloshonok, V. A.; Han, J.; Pan, Y. Synthesis of α,α-Difluoro-β-amino Carbonyl-Containing Sulfonamides and Related Compounds. *J. Fluorine Chem.* **2015**, *172*, 13−21.
(134) Xie, C.; Dai, Y.; Mei, H.; Han, J.; Soloshonok, V. A.; Pan, Y. Asymmetric Synthesis of Quaternary α-Fluoro-β-keto-amines *via* Detrifluoroacetylative Mannich Reactions. *Chem. Commun.* **2015**, *51*, 9149−9152.
(135) Han, C.; Kim, E. H.; Colby, D. A. Cleavage of Carbon−Carbon Bonds through the Mild Release of Trifluoroacetate: Generation of α,α-Difluoroenolates for Aldol Reactions. *J. Am. Chem. Soc.* **2011**, *133*, 5802−5805.
(136) Zhang, P.; Wolf, C. Synthesis of Pentafluorinated β-Hydroxy Ketones. *J. Org. Chem.* **2012**, *77*, 8840−8844.
(137) Zhang, P.; Wolf, C. Catalytic Enantioselective Difluoroalkylation of Aldehydes. *Angew. Chem., Int. Ed.* **2013**, *52*, 7869−7873.
(138) Xie, C.; Wu, L.; Han, J.; Soloshonok, V. A.; Pan, Y. Assembly of Fluorinated Quaternary Stereogenic Centers through Catalytic Enantioselective Detrifluoroacetylative Aldol Reactions. *Angew. Chem., Int. Ed.* **2015**, *54*, 6019−6023.
(139) John, J. P.; Colby, D. A. Synthesis of α-Halo-α,α-difluoromethyl Ketones by a Trifluoroacetate Release/Halogenation Protocol. *J. Org. Chem.* **2011**, *76*, 9163−9168.
(140) Singer, T.; Platz, S.; Colbatzky, F. PCT Int. Appl. WO2003094921A2, 2003; *Chem. Abstr.* **2003**, *139*, 391384.
(141) Miller, V. A.; Hirsh, V.; Cadranel, J.; Chen, Y.-M.; Park, K.; Kim, S.-W.; Zhou, C.; Su, W.-C.; Wang, M.; Sun, Y.; et al. Afatinib versus Placebo for Patients with Advanced, Metastatic Non-Small-Cell Lung Cancer after Failure of Erlotinib, Gefitinib, or Both, and One or Two Lines of Chemotherapy (LUX-Lung 1): A Phase 2b/3 Randomised Trial. *Lancet Oncol.* **2012**, *13*, 528−538.
(142) Ramalingam, S. S.; Blackhall, F.; Krzakowski, M.; Barrios, C. H.; Park, K.; Bover, I.; Heo, D. S.; Rosell, R.; Talbot, D. C.; Frank, R.; et al. Randomized Phase II Study of Dacomitinib (PF-00299804), an Irreversible Pan−Human Epidermal Growth Factor Receptor Inhibitor, Versus Erlotinib in Patients With Advanced Non−Small-Cell Lung Cancer. *J. Clin. Oncol.* **2012**, *30*, 3337−3344.
(143) Trinks, U.; Buchdunger, E.; Furet, P.; Kump, W.; Mett, H.; Meyer, T.; Müller, M.; Regenass, U.; Rihs, G.; Lydon, N.; et al. Dianilinophthalimides: Potent and Selective, ATP-Competitive Inhibitors of the EGF-Receptor Protein Tyrosine Kinase. *J. Med. Chem.* **1994**, *37*, 1015−1027.
(144) Smaill, J. B.; Palmer, B. D.; Rewcastle, G. W.; Denny, W. A.; McNamara, D. J.; Dobrusin, E. M.; Bridges, A. J.; Zhou, H.; Showalter, H. D. H.; Winters, R. T.; et al. Tyrosine Kinase Inhibitors. 15. 4-(Phenylamino)quinazoline and 4-(Phenylamino)pyrido[*d*]pyrimidine Acrylamides as Irreversible Inhibitors of the ATP Binding Site of the Epidermal Growth Factor Receptor. *J. Med. Chem.* **1999**, *42*, 1803−1815.
(145) Fry, D. W.; Bridges, A. J.; Denny, W. A.; Doherty, A.; Greis, K. D.; Hicks, J. L.; Hook, K. E.; Keller, P. R.; Leopold, W. R.; Loo, J. A.; et al. Specific, Irreversible Inactivation of the Epidermal Growth Factor Receptor and Erbb2, by a New Class of Tyrosine Kinase Inhibitor. *Proc. Natl. Acad. Sci. U. S. A.* **1998**, *95*, 12022−12027.
(146) Thompson, A. M.; Murray, D. K.; Elliott, W. L.; Fry, D. W.; Nelson, J. A.; Showalter, H. D. H.; Roberts, B. J.; Vincent, P. W.; Denny, W. A. Tyrosine Kinase Inhibitors. 13. Structure-Activity Relationships for Soluble 7-Substituted 4-[(3-Bromophenyl)amino]-pyrido[4,3-*d*]pyrimidines Designed as Inhibitors of the Tyrosine Kinase Activity of the Epidermal Growth Factor Receptor. *J. Med. Chem.* **1997**, *40*, 3915−3925.
(147) Smaill, J. B.; Showalter, H. D. H.; Zhou, H.; Bridges, A. J.; McNamara, D. J.; Fry, D. W.; Nelson, J. M.; Sherwood, V.; Vincent, P. W.; Roberts, B. J.; et al. Tyrosine Kinase Inhibitors. 18. 6-Substituted 4-Anilinoquinazolines and 4-Anilinopyrido[3,4-*d*]pyrimidines as Soluble, Irreversible Inhibitors of the Epidermal Growth Factor Receptor. *J. Med. Chem.* **2001**, *44*, 429−440.
(148) Smaill, J. B.; Rewcastle, G. W.; Loo, J. A.; Greis, K. D.; Chan, O. H.; Reyner, E. L.; Lipka, E.; Showalter, H. D. H.; Vincent, P. W.; Elliott, W. L.; et al. Tyrosine Kinase Inhibitors. 17. Irreversible Inhibitors of the Epidermal Growth Factor Receptor: 4-(Phenylamino)quinazoline- and 4-(Phenylamino)pyrido[3,2-*d*]-

DOI: 10.1021/acs.chemrev.5b00392
Chem. Rev. 2016, 116, 422−518

pyrimidine-6-acrylamides Bearing Additional Solubilizing Functions. *J. Med. Chem.* **2000**, *43*, 1380−1397.
(149) Tsou, H.-R.; Mamuya, N.; Johnson, B. D.; Reich, M. F.; Gruber, B. C.; Ye, F.; Nilakantan, R.; Shen, R.; Discafani, C.; DeBlanc, R.; et al. 6-Substituted-4-(3-bromophenylamino)quinazolines as Putative Irreversible Inhibitors of the Epidermal Growth Factor Receptor (EGFR) and Human Epidermal Growth Factor Receptor (HER-2) Tyrosine Kinases with Enhanced Antitumor Activity. *J. Med. Chem.* **2001**, *44*, 2719−2734.
(150) Solca, F.; Dahl, G.; Zoephel, A.; Bader, G.; Sanderson, M.; Klein, C.; Kraemer, O.; Himmelsbach, F.; Haaksma, E.; Adolf, G. R. Target Binding Properties and Cellular Activity of Afatinib (BIBW 2992), an Irreversible ErbB Family Blocker. *J. Pharmacol. Exp. Ther.* **2012**, *343*, 342−350.
(151) Xie, W. Chin. Patent CN1515542A, 2004; *Chem. Abstr.* **2005**, *143*, 7489.
(152) Schroeder, J.; Dziewas, G.; Fachinger, T.; Jaeger, B.; Reichel, C.; Renner, S. PCT Int. Appl. WO2007085638A1, 2007; *Chem. Abstr.* **2007**, *147*, 235190.
(153) Fakhoury, S. A.; Lee, H. T.; Reed, J. E.; Schlosser, K. M.; Sexton, K. E.; Tecle, H.; Winters, R. T. U.S. Patent US20050250761A1, 2005; *Chem. Abstr.* **2005**, *143*, 460178.
(154) Miller, C. R.; Oliver, K. E.; Farley, J. H. MEK1/2 Inhibitors in the Treatment of Gynecologic Malignancies. *Gynecol. Oncol.* **2014**, *133*, 128−137.
(155) Martin-Liberal, J.; Lagares-Tena, L.; Larkin, J. Prospects for MEK Inhibitors for Treating Cancer. *Expert Opin. Drug Saf.* **2014**, *13*, 483−495.
(156) Salama, A. K. S.; Kim, K. B. MEK Inhibition in the Treatment of Advanced Melanoma. *Curr. Oncol. Rep.* **2013**, *15*, 473−482.
(157) Salama, A. K. S.; Kim, K. B. Trametinib (GSK1120212) in the treatment of Melanoma. *Expert Opin. Pharmacother.* **2013**, *14*, 619−627.
(158) Yamaguchi, T.; Yoshida, T.; Kurachi, R.; Kakegawa, J.; Hori, Y.; Nanayama, T.; Hayakawa, K.; Abe, H.; Takagi, K.; Matsuzaki, Y.; et al. Identification of JTP-70902, a $p15^{INK4b}$-Inductive Compound, as a Novel MEK1/2 Inhibitor. *Cancer Sci.* **2007**, *98*, 1809−1816.
(159) Abe, H.; Kikuchi, S.; Hayakawa, K.; Iida, T.; Nagahashi, N.; Maeda, K.; Sakamoto, J.; Matsumoto, N.; Miura, T.; Matsumura, K.; et al. Discovery of a Highly Potent and Selective MEK Inhibitor: GSK1120212 (JTP-74057 DMSO Solvate). *ACS Med. Chem. Lett.* **2011**, *2*, 320−324.
(160) Fong, P. C.; Boss, D. S.; Yap, T. A.; Tutt, A.; Wu, P.; Mergui-Roelvink, M.; Mortimer, P.; Swaisland, H.; Lau, A.; O'Connor, M. J.; et al. Inhibition of Poly(ADP-Ribose) Polymerase in Tumors from *BRCA* Mutation Carriers. *N. Engl. J. Med.* **2009**, *361*, 123−134.
(161) Gunderson, C. C.; Moore, K. N. Olaparib: An Oral PARP-1 and PARP-2 Inhibitor with Promising Activity in Ovarian Cancer. *Future Oncol.* **2015**, *11*, 747−757.
(162) Deeks, E. D. Olaparib: First Global Approval. *Drugs* **2015**, *75*, 231−240.
(163) Loh, V. M., Jr.; Cockcroft, X.-L.; Dillon, K. J.; Dixon, L.; Drzewiecki, J.; Eversley, P. J.; Gomez, S.; Hoare, J.; Kerrigan, F.; Matthews, I. T. W.; et al. Phthalazinones. Part 1: The Design and Synthesis of a Novel Series of Potent Inhibitors of Poly(ADP-ribose)polymerase. *Bioorg. Med. Chem. Lett.* **2005**, *15*, 2235−2238.
(164) Cockcroft, X.-L.; Dillon, K. J.; Dixon, L.; Drzewiecki, J.; Kerrigan, F.; Loh, V. M., Jr.; Martin, N. M. B.; Menear, K. A.; Smith, G. C. M. Phthalazinones 2: Optimisation and Synthesis of Novel Potent Inhibitors of Poly(ADP-ribose)polymerase. *Bioorg. Med. Chem. Lett.* **2006**, *16*, 1040−1044.
(165) Menear, K. A.; Adcock, C.; Boulter, R.; Cockcroft, X.-L.; Copsey, L.; Cranston, A.; Dillon, K. J.; Drzewiecki, J.; Garman, S.; Gomez, S.; et al. 4-[3-(4-Cyclopropanecarbonylpiperazine-1-carbonyl)-4-fluorobenzyl]-2*H*-phthalazin-1-one: A Novel Bioavailable Inhibitor of Poly(ADP-ribose) Polymerase-1. *J. Med. Chem.* **2008**, *51*, 6581−6591.
(166) Gao, D. PCT Int. Appl. WO2012071684A1, 2012; *Chem. Abstr.* **2012**, *157*, 45188.
(167) Moore, J. L.; Taylor, S. M.; Soloshonok, V. A. An Efficient and Operationally Convenient General Synthesis of Tertiary Amines by Direct Alkylation of Secondary Amines with Alkyl Halides in the Presence of Huenig's Base. *ARKIVOC* **2005**, 287−292.
(168) Lescot, C.; Nielsen, D. U.; Makarov, I. S.; Lindhardt, A. T.; Daasbjerg, K.; Skrydstrup, T. Efficient Fluoride-Catalyzed Conversion of CO_2 to CO at Room Temperature. *J. Am. Chem. Soc.* **2014**, *136*, 6142−6147.
(169) Bowles, D. W.; Kessler, E. R.; Jimeno, A. Multi-targeted Tyrosine Kinase Inhibitors in Clinical Development: Focus on XL-184 (cabozantinib). *Drugs Today* **2011**, *47*, 857−868.
(170) Kurzrock, R.; Sherman, S. I.; Ball, D. W.; Forastiere, A. A.; Cohen, R. B.; Mehra, R.; Pfister, D. G.; Cohen, E. E. W.; Janisch, L.; Nauling, F.; et al. Activity of XL184 (Cabozantinib), an Oral Tyrosine Kinase Inhibitor, in Patients With Medullary Thyroid Cancer. *J. Clin. Oncol.* **2011**, *29*, 2660−2666.
(171) Yakes, F. M.; Chen, J.; Tan, J.; Yamaguchi, K.; Shi, Y. C.; Yu, P. W.; Qian, F.; Chu, F. L.; Bentzien, F.; Cancilla, B.; et al. Cabozantinib (XL184), a Novel MET and VEGFR2 Inhibitor, Simultaneously Suppresses Metastasis, Angiogenesis, and Tumor Growth. *Mol. Cancer Ther.* **2011**, *10*, 2298−2308.
(172) Bannen, L. C.; Chan, D. S.-M.; Chen, J.; Dalrymple, L. E.; Forsyth, T. P.; Huynh, T. P.; Jammalamadaka, V.; Khoury, R. G.; Leahy, J. W.; Mac, M. B.; et al. PCT Int. Appl. WO2005030140A2, 2005; *Chem. Abstr.* **2005**, *142*, 373856.
(173) Wilson, J. A. PCT Int. Appl. WO2012109510A1, 2012; *Chem. Abstr.* **2012**, *157*, 382704.
(174) Wedge, S. R.; Kendrew, J.; Hennequin, L. F.; Valentine, P. J.; Barry, S. T.; Brave, S. R.; Smith, N. R.; James, N. H.; Dukes, M.; Curwen, J. O.; et al. AZD2171: A Highly Potent, Orally Bioavailable, Vascular Endothelial Growth Factor Receptor-2 Tyrosine Kinase Inhibitor for the Treatment of Cancer. *Cancer Res.* **2005**, *65*, 4389−4400.
(175) Batchelor, T. T.; Sorensen, A. G.; di Tomaso, E.; Zhang, W.-T.; Duda, D. G.; Cohen, K. S.; Kozak, K. R.; Cahill, D. P.; Chen, P.-J.; Zhu, M.; et al. AZD2171, a Pan-VEGF Receptor Tyrosine Kinase Inhibitor, Normalizes Tumor Vasculature and Alleviates Edema in Glioblastoma Patients. *Cancer Cell* **2007**, *11*, 83−95.
(176) Matulonis, U. A.; Berlin, S.; Ivy, P.; Tyburski, K.; Krasner, C.; Zarwan, C.; Berkenblit, A.; Campos, S.; Horowitz, N.; Cannistra, S. A.; et al. Cediranib, an Oral Inhibitor of Vascular Endothelial Growth Factor Receptor Kinases, Is an Active Drug in Recurrent Epithelial Ovarian, Fallopian Tube, and Peritoneal Cancer. *J. Clin. Oncol.* **2009**, *27*, 5601−5606.
(177) Cai, Z.-W.; Zhang, Y.; Borzilleri, R. M.; Qian, L.; Barbosa, S.; Wei, D.; Zheng, X.; Wu, L.; Fan, J.; Shi, Z.; et al. Discovery of Brivanib Alaninate ((*S*)-((*R*)-1-(4-(4-Fluoro-2-methyl-1*H*-indol-5-yloxy)-5-methylpyrrolo[2,1-*f*][1,2,4]triazin-6-yloxy)propan-2-yl)2-aminopropanoate), A Novel Prodrug of Dual Vascular Endothelial Growth Factor Receptor-2 and Fibroblast Growth Factor Receptor-1 Kinase Inhibitor (BMS-540215). *J. Med. Chem.* **2008**, *51*, 1976−1980.
(178) Hennequin, L. F. A.; Ple, P.; Stokes, E. S. E.; Mckerrecher, D. PCT Int. Appl. WO2000047212A1, 2000; *Chem. Abstr.* **2000**, *133*, 177183.
(179) Hennequin, L. F. A. PCT Int. Appl. WO2005014582A1, 2005; *Chem. Abstr.* **2005**, *142*, 240453.
(180) Hunt, J. T.; Mitt, T.; Borzilleri, R.; Gullo-Brown, J.; Fargnoli, J.; Fink, B.; Han, W.-C.; Mortillo, S.; Vite, G.; Wautlet, B.; et al. Discovery of the Pyrrolo[2,1-*f*][1,2,4]triazine Nucleus as a New Kinase Inhibitor Template. *J. Med. Chem.* **2004**, *47*, 4054−4059.
(181) Borzilleri, R. M.; Cai, Z.-W.; Ellis, C.; Fargnoli, J.; Fura, A.; Gerhardt, T.; Goyal, B.; Hunt, J. T.; Mortillo, S.; Qian, L.; et al. Synthesis and SAR of 4-(3-Hydroxyphenylamino)pyrrolo-[2,1-*f*]-[1,2,4]triazine Based VEGFR-2 Kinase Inhibitors. *Bioorg. Med. Chem. Lett.* **2005**, *15*, 1429−1433.
(182) Bhide, R. S.; Cai, Z.-W.; Zhang, Y.-Z.; Qian, L.; Wei, D.; Barbosa, S.; Lombardo, L. J.; Borzilleri, R. M.; Zheng, X.; Wu, L. I.; et al. Discovery and Preclinical Studies of (*R*)-1-(4-(4-Fluoro-2-methyl-1*H*-indol-5-yloxy)-5-methylpyrrolo[2,1-*f*][1,2,4]triazin-6-

DOI: 10.1021/acs.chemrev.5b00392
Chem. Rev. 2016, 116, 422−518

yloxy)propan-2-ol (BMS-540215), an In Vivo Active Potent VEGFR-2 Inhibitor. *J. Med. Chem.* **2006**, *49*, 2143−2146.
(183) Wang, B.; Wang, J. Chin. Patent CN1357530A, 2002; *Chem. Abstr.* **2003**, *139*, 100923.
(184) Traynor, K. Idelalisib Approved for Three Blood Cancers. *Am. J. Health-Syst. Pharm.* **2014**, *71*, 1430.
(185) Furman, R. R.; Sharman, J. P.; Coutre, S. E.; Cheson, B. D.; Pagel, J. M.; Hillmen, P.; Barrientos, J. C.; Zelenetz, A. D.; Kipps, T. J.; Flinn, I.; et al. Idelalisib and Rituximab in Relapsed Chronic Lymphocytic Leukemia. *N. Engl. J. Med.* **2014**, *370*, 997−1007.
(186) Markham, A. Idelalisib: First Global Approval. *Drugs* **2014**, *74*, 1701−1070.
(187) Khan, M.; Saif, A.; Sandler, S.; Mirrakhimov, A. E. Idelalisib for the Treatment of Chronic Lymphocytic Leukemia. *ISRN Oncol.* **2014**, *2014*, 931858.
(188) Somoza, J. R.; Koditek, D.; Villaseñor, A. G.; Novikov, N.; Wong, M. H.; Liclican, A.; Xing, W.; Lagpacan, L.; Wang, R.; Schultz, B. E.; et al. Structural, Biochemical, and Biophysical Characterization of Idelalisib Binding to Phosphoinositide 3-Kinase δ. *J. Biol. Chem.* **2015**, *290*, 8439−8446.
(189) Burger, J. A.; Okkenhaug, K. Haematological Cancer: Idelalisib-Targeting PI3Kδ in Patients with B-Cell Malignancies. *Nat. Rev. Clin. Oncol.* **2014**, *11*, 184−186.
(190) Evarts, J. B.; Lannutti, B.; Webb, H. PCT Int. Appl. WO 2013082540A1, 2013; *Chem. Abstr.* **2013**, *159*, 75917.
(191) Beight, D. W.; Craft, T. J.; Denny, C. P.; Franciskovich, J. B.; Goodson, T., Jr.; Hall, S. E.; Herron, D. K.; Joseph, S. P.; Klimkowski, V. J.; Masters, J. J.; et al. PCT Int. Appl. WO2000039118A1, 2000; *Chem. Abstr.* **2000**, *133*, 89437.
(192) Fowler, K. W.; Huang, D.; Kesicki, E. A.; Ooi, H. C.; Oliver, A. R.; Ruan, F.; Treiberg, J. PCT Int. Appl. WO2005113554, 2005; *Chem. Abstr.* **2005**, *144*, 22759.
(193) Ball, S.; Dellva, M. A.; D'Souza, D. N.; Marangell, L. B.; Russell, J. M.; Goldberger, C. A Double-Blind, Placebo-Controlled Study of Edivoxetine as an Adjunctive Treatment for Patients with Major Depressive Disorder who are Partial Responders to Selective Serotonin Reuptake Inhibitor Treatment. *J. Affective Disord.* **2014**, *167*, 215−223.
(194) Pangallo, B.; Dellva, M. A.; D'Souza, D. N.; Essink, B.; Russell, J.; Goldberger, C. A Randomized, Double-Blind Study Comparing LY2216684 and Placebo in the Treatment of Major Depressive Disorder. *J. Psychiatr. Res.* **2011**, *45*, 748−755.
(195) Chancellor, D. The Depression Market. *Nat. Rev. Drug Discovery* **2011**, *10*, 809−810.
(196) Kielbasa, W.; Quinlan, T.; Jin, L.; Xu, W.; Lachno, D. R.; Dean, R. A.; Allen, A. J. Pharmacokinetics and Pharmacodynamics of Edivoxetine (LY2216684), a Norepinephrine Reuptake Inhibitor, in Pediatric Patients with Attention-Deficit/ Hyperactivity Disorder. *J. Child Adolesc. Psychopharmacol.* **2012**, *22*, 269−276.
(197) Markowitz, J. S.; Brinda, B. J. A Pharmacokinetic Evaluation of Oral Edivoxetine Hydrochloride for the Treatment of Attention Deficit-Hyperactivity Disorder. *Expert Opin. Drug Metab. Toxicol.* **2014**, *10*, 1289−1299.
(198) Kielbasa, W.; Tesfaye, E.; Luffer-Atlas, D.; Mitchell, M. I.; Turik, M. A. The Effect of Hepatic or Renal Impairment on the Pharmacokinetics of Edivoxetine, a Selective Norepinephrine Transporter Reuptake Inhibitor. *Eur. J. Clin. Pharmacol.* **2013**, *69*, 2011−2019.
(199) Campbell, G. I.; Cases-Thomas, M. J.; Man, T.; Masters, J. J.; Rudyk, H. C. E.; Walter, M. W. PCT Int. Appl. WO2005047272A1, 2005; *Chem. Abstr.* **2005**, *142*, 482071.
(200) Deeks, E. D.; Keating, G. M. Blonanserin: A Review of its Use in the Management of Schizophrenia. *CNS Drugs* **2010**, *24*, 65−84.
(201) Kishi, T.; Matsuda, Y.; Nakamura, H.; Iwata, N. Blonanserin for Schizophrenia: Systematic Review and Meta-Analysis of Double-Blind, Randomized, Controlled Trials. *J. Psychiatr. Res.* **2013**, *47*, 149−154.
(202) Ohno, Y.; Okano, M.; Imaki, J.; Tatara, A.; Okumura, T.; Shimizu, S. Atypical antipsychotic properties of blonanserin, a novel dopamine D_2 and 5-HT_{2A} antagonist. *Pharmacol., Biochem. Behav.* **2010**, *96*, 175−180.
(203) Yang, J.; Bahk, W.-M.; Cho, H.-S.; Jeon, Y.-W.; Jon, D.-I.; Jung, H.-Y.; Kim, C.-H.; Kim, H.-C.; Kim, Y.-K.; Kim, Y.-H.; et al. Efficacy and Tolerability of Blonanserin in the Patients With Schizophrenia: A Randomized, Double-Blind, Risperidone-Compared Trial. *Clin. Neuropharmacol.* **2010**, *33*, 169−175.
(204) Kato, K.; Yamada, K.; Maehara, M.; Akama, F.; Kimoto, K.; Saito, M.; Yano, H.; Ichimura, A.; Matsumoto, H. Blonanserin in the Treatment of Delirium. *Psychiatry Clin. Neurosci.* **2011**, *65*, 389−391.
(205) Oka, M.; Noda, Y.; Ochi, Y.; Furukawa, K.; Une, T.; Kurumiya, S.; Hino, K.; Karasawa, T. Pharmacological Profile of AD-5423, a Novel Antipsychotic with Both Potent Dopamine-D_2 and Serotonin-S_2 Antagonist Properties. *J. Pharmacol. Exp. Ther.* **1993**, *264*, 158−165.
(206) Murasaki, M. Clinical Evaluation of Blonanserin for Schizophrenia: A Double-Blind Trial Comparing Blonanserin with Haloperidol. *Jpn. J. Clin. Psychopharmacol.* **2007**, *10*, 2059−2079.
(207) Ochi, T.; Sakamoto, M.; Minamida, A.; Suzuki, K.; Ueda, T.; Une, T.; Toda, H.; Matsumoto, K.; Terauchi, Y. Syntheses and Properties of the Major Hydroxy Metabolites in Humans of Blonanserin AD-5423, a Novel Antipsychotic Agent. *Bioorg. Med. Chem. Lett.* **2005**, *15*, 1055−1059.
(208) Hino, K.; Kai, N.; Sakamoto, M.; Kon, T.; Oka, M.; Furakawa, K.; Ochi, Y. Eur. Pat. Appl. EP385237A2; *Chem. Abstr.* **1991**, *114*, 143438.
(209) Morrow, D. A.; Scirica, B. M.; Fox, K. A. A.; Berman, G.; Strony, J.; Veltri, E.; Bonaca, M. P.; Fish, P.; McCabe, C. H.; Braunwald, E. Evaluation of a Novel Antiplatelet Agent for Secondary Prevention in Patients with a History of Atherosclerotic Disease: Design and Rationale for the Thrombin-Receptor Antagonist in Secondary Prevention of Atherothrombotic Ischemic Events (TRA 2°P)-TIMI 50 Trial. *Am. Heart J.* **2009**, *158*, 335−341.
(210) Frampton, J. E. Vorapaxar: A Review of Its Use in the Long-Term Secondary Prevention of Atherothrombotic Events. *Drugs* **2015**, *75*, 797−808.
(211) Becker, R. C.; Moliterno, D. J.; Jennings, L. K.; Pieper, K. S.; Pei, J.; Niederman, A.; Ziada, K. M.; Berman, G.; Strony, J.; Joseph, D.; et al. Safety and Tolerability of SCH 530348 in Patients Undergoing Non-Urgent Percutaneous Coronary Intervention: A Randomised, Double-Blind, Placebo-Controlled Phase II Study. *Lancet* **2009**, *373*, 919−928.
(212) Coccheri, S. Antiplatelet Therapy: Controversial Aspects. *Thromb. Res.* **2012**, *129*, 225−229.
(213) Doller, D.; Chackalamannil, S.; Czarniecki, M.; McQuade, R.; Ruperto, V. Design, Synthesis, and Structure-Activity Relationship Studies of Himbacine Derived Muscarinic Receptor Antagonists. *Bioorg. Med. Chem. Lett.* **1999**, *9*, 901−906.
(214) Chackalamannil, S.; Xia, Y.; Greenlee, W. J.; Clasby, M.; Doller, D.; Tsai, H.; Asberom, T.; Czarniecki, M.; Ahn, H.-S.; Boykow, G.; et al. Discovery of Potent Orally Active Thrombin Receptor (Protease Activated Receptor 1) Antagonists as Novel Antithrombotic Agents. *J. Med. Chem.* **2005**, *48*, 5884−5887.
(215) Clasby, M. C.; Chackalamannil, S.; Czarniecki, M.; Doller, D.; Eagen, K.; Greenlee, W.; Kao, G.; Lin, Y.; Tsai, H.; Xia, Y.; et al. Metabolism-Based Identification of a Potent Thrombin Receptor Antagonist. *J. Med. Chem.* **2007**, *50*, 129−138.
(216) Chelliah, M. V.; Chackalamannil, S.; Xia, Y.; Eagen, K.; Clasby, M. C.; Gao, X.; Greenlee, W.; Ahn, H.-S.; Agans-Fantuzzi, J.; Boykow, G.; et al. Heterotricyclic Himbacine Analogs as Potent, Orally Active Thrombin Receptor (Protease Activated Receptor-1) Antagonists. *J. Med. Chem.* **2007**, *50*, 5147−5160.
(217) Chackalamannil, S.; Wang, Y.; Greenlee, W. J.; Hu, Z.; Xia, Y.; Ahn, H.-S.; Boykow, G.; Hsieh, Y.; Palamanda, J.; Agans-Fantuzzi, J.; et al. Discovery of a Novel, Orally Active Himbacine-Based Thrombin Receptor Antagonist (SCH 530348) with Potent Antiplatelet Activity. *J. Med. Chem.* **2008**, *51*, 3061−3064.
(218) Zhang, C.; Srinivasan, Y.; Arlow, D. H.; Fung, J. J.; Palmer, D.; Zheng, Y.; Green, H. F.; Pandey, A.; Dror, R. O.; Shaw, D. E.; et al.

DOI: 10.1021/acs.chemrev.5b00392
Chem. Rev. 2016, 116, 422−518

High-Resolution Crystal Structure of Human Protease-Activated Receptor 1. *Nature* **2012**, *492*, 387−392.
(219) Kanafani, Z. A.; Corey, G. R. Tedizolid (TR-701): A New Oxazolidinone with Enhanced Potency. *Expert Opin. Invest. Drugs* **2012**, *21*, 515−522.
(220) Ford, C. W.; Zurenko, G. E.; Barbachyn, M. R. The Discovery of Linezolid, the First Oxazolidinone Antibacterial Agent. *Curr. Drug Targets: Infect. Disord.* **2001**, *1*, 181−199.
(221) Brickner, S. J.; Barbachyn, M. R.; Hutchinson, D. K.; Manninen, P. R. Linezolid (ZYVOX), the First Member of a Completely New Class of Antibacterial Agents for Treatment of Serious Gram-Positive Infections. *J. Med. Chem.* **2008**, *51*, 1981−1990.
(222) Jo, Y. W.; Im, W. B.; Rhee, J. K.; Shim, M. J.; Kim, W. B.; Choi, E. C. Synthesis and Antibacterial Activity of Oxazolidinones Containing Pyridine Substituted with Heteroaromatic Ring. *Bioorg. Med. Chem.* **2004**, *12*, 5909−5915.
(223) Im, W. B.; Choi, S. H.; Park, J.-Y.; Choi, S. H.; Finn, J.; Yoon, S.-H. Discovery of Torezolid as a Novel 5-Hydroxymethyl-Oxazolidinone Antibacterial Agent. *Eur. J. Med. Chem.* **2011**, *46*, 1027−1039.
(224) Rhee, J. K.; Im, W. B.; Cho, C. H.; Choi, S. H.; Lee, T. H. PCT Int. Appl. WO2005058886A1, 2005; *Chem. Abstr.* **2005**, *143*, 97343.
(225) Costello, C. A.; Simson, J. A.; Duguid, R. J.; Phillipson, D. PCT Int. Appl. WO2010042887A1, 2010; *Chem. Abstr.* **2010**, *152*, 454112.
(226) Zhang, T.; Li, X. Chin. Patent CN101367738A, 2009; *Chem. Abstr.* **2009**, *150*, 329397.
(227) Bartoli, S.; Cipollone, A.; Squarcia, A.; Madami, A.; Fattori, D. Electrophilic Bromination of *meta*-Substituted Anilines with *N*-Bromosuccinimide: Regioselectivity and Solvent Effect. *Synthesis* **2009**, *2009*, 1305−1308.
(228) Park, H. S.; Jung, S. J.; Kwak, J.-H.; Choi, D.-R.; Choi, E.-C. DNA Gyrase and Topoisomerase IV Are Dual Targets of Zabofloxacin in *Streptococcus Pneumoniae*. *Int. J. Antimicrob. Agents* **2010**, *36*, 97−98.
(229) Gootz, T. D.; Brighty, K. E. Fluoroquinolone Antibacterials: SAR, Mechanism of Action, Resistance, and Clinical Aspects. *Med. Res. Rev.* **1996**, *16*, 433−486.
(230) Chu, D. T. W.; Fernandes, P. B. Structure-Activity Relationships of the Fluoroquinolones. *Antimicrob. Agents Chemother.* **1989**, *33*, 131−135.
(231) Yoon, S.-J.; Chung, Y.-H.; Lee, C.-W.; Oh, Y.-S.; Kim, N.-D.; Lim, J.-K.; Jin, Y.-H. PCT Int. Appl. WO199900393A1, 1999; *Chem. Abstr.* **1999**, *130*, 110281.
(232) Kim, E.-J.; Shin, W.-H.; Kim, K.-S.; Han, S.-S. Safety Pharmacology of DW-224a, a Novel Fluoroquinolone Antibiotic Agent. *Drug Chem. Toxicol.* **2004**, *27*, 295−307.
(233) Jones, R.; Biedenbach, D.; Sader, H.; Fritsche, T.; Ambrose, P.; Wikler, M. Comparative in Vitro Activity of Zabofloxacin (DW-224a) Tested Against Multidrug-Resistant *Neisseria gonorrhoeae*. *Int. J. Infect. Dis.* **2008**, *12*, e181.
(234) Lee, J. H.; Choi, B. S.; Chang, J. H.; Kim, S. S.; Shin, H. *Org. Process Res. Dev.* **2007**, *11*, 1062−1064.
(235) Shin, H.-I.; Chang, J.-H.; Lee, K.-W. PCT Int. Appl. WO2005040164A1, 2005; *Chem. Abstr.* **2005**, *142*, 430256.
(236) Morrissey, I.; Fernandes, P.; Keedy, K.; Lemos, B.; Hawser, S. P. Activity of Solithromycin and Comparators against Antimicrobial-Resistant *Streptococcus pneumoniae* Isolated from Respiratory Samples Collected 2012−2013. *54th Interscience Conference on Antimicrobial Agents and Chemotherapy (ICAAC), Washington, DC, September 5−9, 2014*; C1472.
(237) Llano-Sotelo, B.; Dunkle, J.; Klepacki, D.; Zhang, W.; Fernandes, P.; Cate, J. H. D.; Mankin, A. S. Binding and Action of CEM-101, a New Fluoroketolide Antibiotic that Inhibits Protein Synthesis. *Antimicrob. Agents Chemother.* **2010**, *54*, 4961−4970.
(238) Bryskier, A. Ketolides-Telithromycin, an Example of a New Class of Antibacterial Agents. *Clin. Microbiol. Infect.* **2000**, *6*, 661−669.
(239) Hwang, C.; Duffield, J.; Chiu, Y.; Liang, C.; Yao, S.; Babakhani, F.; Sears, P.; Ichikawa, Y.; Fernandes, P.; Pereira, D.; et al. SAR of 11,12-Carbamate Macrolides/Ketolides Linked with 1,4-Substituted-[1,2,3]-triazoles. *48th Interscience Conference on Antimicrobial Agents and Chemotherapy (ICAAC), Washington, DC, October 25−28, 2008*; F1-3973.
(240) Liang, C.-H.; Duffield, J.; Romero, A.; Chiu, Y.-H.; Rabuka, D.; Yao, S.; Sucheck, S.; Marby, K.; Shue, Y.-K.; Ichikawa, Y.; et al. PCT Int. Appl. WO2004080391A2, 2004; *Chem. Abstr.* **2004**, *141*, 296244.
(241) Soloshonok, V. A.; Gerus, I. I.; Yagupolskii, Y. L. *N*-(Methoxycarbonyl)imine of Trifluoropyruvic Acid. *Zh. Org. Khim.* **1986**, *22*, 1335−1337. *Chem. Abstr.* **1987**, *106*, 195861.
(242) Soloshonok, V. A.; Gerus, I. I.; Yagupolskii, Y. L.; Kukhar, V. P. Fluorine-Containing Amino Acids. III. α-Trifluoromethyl-α-Amino Acids. *Zh. Org. Khim.* **1987**, *23*, 2308−2313. *Chem. Abstr.* **1988**, *109*, 55185.
(243) Fernandes, P.; Pereira, D.; Jamieson, B.; Keedy, K. Solitrhomycin. *Drugs Future* **2011**, *36*, 751.
(244) Pereira, D. E.; Patel, M. K.; Deo, K. PCT Int. Appl. WO2009055557A1, 2009; *Chem. Abstr.* **2009**, *150*, 448270.
(245) World Health Organization. Hepatitis C, Fact Sheet No. 164, updated April 2014. http://www.who.int/mediacentre/factsheets/fs164/en (accessed July 2, 2015).
(246) U.S. Department of Health & Human Services, Office of Population Affairs. Hepatitis C, The Facts. http://www.hhs.gov/opa/pdfs/hepatitis-c-fact-sheet.pdf (accessed July 2, 2015).
(247) Kawashima, A.; Xie, C.; Mei, H.; Takeda, R.; Kawamura, A.; Sato, T.; Moriwaki, H.; Izawa, K.; Han, J.; Aceña, J. L.; et al. Asymmetric Synthesis of (1*R*,2*S*)-1-Amino-2-vinylcyclopropanecarboxylic Acid by Sequential S_N2-S_N2' Dialkylation of (*R*)-*N*-(Benzyl)-proline-derived Glycine Schiff Base Ni(II) Complex. *RSC Adv.* **2015**, *5*, 1051−1058 and references therein..
(248) Zeuzem, S.; Berg, T.; Moeller, B.; Hinrichsen, H.; Mauss, S.; Wedemeyer, H.; Sarrazin, C.; Hueppe, D.; Zehnter, E.; Manns, M. P. Expert Opinion on the Treatment of Patients with Chronic Hepatitis C. *J. Viral Hepatitis* **2009**, *16*, 75−90.
(249) De Clercq, E. Current Race in the Development of DAAs (Direct-Acting Antivirals) against HCV. *Biochem. Pharmacol.* **2014**, *89*, 441−452.
(250) Clark, J. L.; Hollecker, L.; Mason, J. C.; Stuyver, L. J.; Tharnish, P. M.; Lostia, S.; McBrayer, T. R.; Schinazi, R. F.; Watanabe, K. A.; Otto, M. J.; et al. Design, Synthesis, and Antiviral Activity of 2′-Deoxy-2′-fluoro-2′-*C*-methylcytidine, a Potent Inhibitor of Hepatitis C Virus Replication. *J. Med. Chem.* **2005**, *48*, 5504−5508.
(251) Stuyver, L. J.; McBrayer, T. R.; Tharnish, P. M.; Clark, J.; Hollecker, L.; Lostia, S.; Nachman, T.; Grier, J.; Bennett, M. A.; Xie, M.-Y.; et al. Inhibition of Hepatitis C Replicon RNA Synthesis by β-D-2′-Deoxy-2′-fluoro-2′-*C*-Methylcytidine: A Specific Inhibitor of Hepatitis C Virus Replication. *Antiviral Chem. Chemother.* **2006**, *17*, 79−87.
(252) Pierra, C.; Amador, A.; Benzaria, S.; Cretton-Scott, E.; D'Amours, M.; Mao, J.; Mathieu, S.; Moussa, A.; Bridges, E. G.; Standring, D. N.; et al. Synthesis and Pharmacokinetics of Valopicitabine (NM283), an Efficient Prodrug of the Potent Anti-HCV Agent 2′-*C*-Methylcytidine. *J. Med. Chem.* **2006**, *49*, 6614−6620.
(253) Sofia, M. J.; Bao, D.; Chang, W.; Du, J.; Nagarathnam, D.; Rachakonda, S.; Reddy, P. G.; Ross, B. S.; Wang, P.; Zhang, H.-R.; et al. Discovery of a β-D-2′-Deoxy-2′-α-fluoro-2′-β-C-methyluridine Nucleotide Prodrug (PSI-7977) for the Treatment of Hepatitis C Virus. *J. Med. Chem.* **2010**, *53*, 7202−7218.
(254) Murakami, E.; Niu, C.; Bao, H.; Micolochick Steuer, H. M.; Whitaker, T.; Nachman, T.; Sofia, M. A.; Wang, P.; Otto, M. J.; Furman, P. A. The Mechanism of Action of β-D-2′-Deoxy-2′-fluoro-2′-*C*-methylcytidine Involves a Second Metabolic Pathway Leading to β-D-2′-Deoxy-2′-fluoro-2′-*C*-Methyluridine 5′-Triphosphate, a Potent Inhibitor of the Hepatitis C Virus RNA-Dependent RNA Polymerase. *Antimicrob. Agents Chemother.* **2008**, *52*, 458−464.
(255) McGuigan, C.; Cahard, D.; Sheeka, H. M.; De Clercq, E.; Balzarini, J. Aryl Phosphoramidate Derivatives of d4T Have Improved Anti-HIV Efficacy in Tissue Culture and May Act by the Generation of a Novel Intracellular Metabolite. *J. Med. Chem.* **1996**, *39*, 1748−1753.
(256) Keating, G. M.; Vaidya, A. Sofosbuvir: First Global Approval. *Drugs* **2014**, *74*, 273−282.

DOI: 10.1021/acs.chemrev.5b00392
Chem. Rev. 2016, 116, 422−518

(257) Ritzmann, G.; Klein, R. S.; Hollenberg, D. H.; Fox, J. J. Nucleosides LXXXIX. Synthesis of 1-(2-Chloro-2-deoxy-α- and -β-D-Arabinofuranosyl)cytosines. *Carbohydr. Res.* **1975**, *39*, 227−236.
(258) Clark, J. L.; Mason, J. C.; Hobbs, A. J.; Hollecker, L.; Schinazi, R. F. Synthesis of 2-Deoxy-2-fluoro-2-C-methyl-D-ribofuranoses. *J. Carbohydr. Chem.* **2006**, *25*, 461−470.
(259) Mayes, B. A.; Moussa, A. PCT Int. Appl. WO2007075876A2, 2007; *Chem. Abstr.* **2007**, *147*, 143619.
(260) Gao, Y.; Sharpless, K. B. Vicinal Diol Cyclic Sulfates: Like Epoxides Only More Reactive. *J. Am. Chem. Soc.* **1988**, *110*, 7538−7539.
(261) Wang, P.; Chun, B.-K.; Rachakonda, S.; Du, J.; Khan, N.; Shi, J.; Stec, W.; Cleary, D.; Ross, B. S.; Sofia, M. J. An Efficient and Diastereoselective Synthesis of PSI-6130: A Clinically Efficacious Inhibitor of HCV NS5B Polymerase. *J. Org. Chem.* **2009**, *74*, 6819−6824.
(262) Ross, B. S.; Ganapati Reddy, P. G.; Zhang, H.-R.; Rachakonda, S.; Sofia, M. J. Synthesis of Diastereomerically Pure Nucleotide Phosphoramidates. *J. Org. Chem.* **2011**, *76*, 8311−8319.
(263) Chu, C. K.; Ma, T.; Shanmuganathan, K.; Wang, Y.; Xiang, Y.; Pai, S. B.; Yao, G. Q.; Sommadossi, J.-P.; Cheng, Y.-C. Use of 2′-Fluoro-5-methyl-β-L-arabinofuranosyluracil as a Novel Antiviral Agent for Hepatitis B Virus and Epstein-Barr Virus. *Antimicrob. Agents Chemother.* **1995**, *39*, 979−981.
(264) Kim, B. K.; Oh, J.; Kwon, S. Y.; Choe, W. H.; Ko, S. Y.; Rhee, K. H.; Seo, T. H.; Lim, S. D.; Lee, C. H. Clevudine Myopathy in Patients with Chronic Hepatitis B. *J. Hepatol.* **2009**, *51*, 829−834.
(265) Seok, J. J.; Lee, D. K.; Lee, C. H.; Park, M. S.; Kim, S. Y.; Kim, H.-S.; Jo, H.-Y.; Lee, C. H.; Kim, D.-S. Long-Term Therapy with Clevudine for Chronic Hepatitis B Can Be Associated with Myopathy Characterized by Depletion of Mitochondrial DNA. *Hepatology* **2009**, *49*, 2080−2086.
(266) Tak, W. Y.; Yang, J. M.; Kim, B. I.; Baik, S. K.; Cheon, G. J.; Byun, K. S.; Kim, D. Y.; Yoo, B. C. A Randomized, Open-Label Study Comparing Low-Dose Clevudine plus Adefovir Combination Therapy with Clevudine Monotherapy in Naïve Chronic Hepatitis B Patients. *Hepatol. Int.* **2014**, *8*, 375−381.
(267) Pai, S. B.; Liu, S.-H.; Zhu, Y.-L.; Chu, C. K.; Cheng, Y.-C. Inhibition of Hepatitis B Virus by a Novel L-Nucleoside, 2′-Fluoro-5-methyl-β-L-arabinofuranosyl Uracil. *Antimicrob. Agents Chemother.* **1996**, *40*, 380−386.
(268) Chong, Y.; Chu, C. K. Understanding the Unique Mechanism of L-FMAU (Clevudine) against Hepatitis B Virus: Molecular Dynamics Studies. *Bioorg. Med. Chem. Lett.* **2002**, *12*, 3459−3462.
(269) Yao, G.-Q.; Liu, S.-H.; Chou, E.; Kukhanova, M.; Chu, C. K.; Cheng, Y.-C. Inhibition of Epstein-Barr Virus Replication by a Novel L-Nucleoside, 2′-Fluoro-5-methyl-β-L-arabinofuranosyluracil. *Biochem. Pharmacol.* **1996**, *51*, 941−947.
(270) Jones, S. A.; Murakami, E.; Delaney, W.; Furman, P.; Hu, J. Noncompetitive Inhibition of Hepatitis B Virus Reverse Transcriptase Protein Priming and DNA Synthesis by the Nucleoside Analog Clevudine. *Antimicrob. Agents Chemother.* **2013**, *57*, 4181−4189.
(271) Niu, C.; Bao, H.; Tolstykh, T.; Micolochick Steuer, H. M.; Murakami, E.; Korba, B.; Furman, P. A. Evaluation of the In Vitro Anti-HBV Activity of Clevudine in Combination with Other Nucleoside/Nucleotide Inhibitors. *Antiviral Ther.* **2010**, *15*, 401−412.
(272) De Clercq, E.; Férir, G.; Kaptein, S.; Neyts, J. Antiviral Treatment of Chronic Hepatitis B Virus (HBV) Infections. *Viruses* **2010**, *2*, 1279−1305.
(273) Jones, S. A.; Murakami, E.; Delaney, W.; Furman, P.; Hu, J. Noncompetitive Inhibition of Hepatitis B Virus Reverse Transcriptase Protein Priming and DNA Synthesis by the Nucleoside Analog Clevudine. *Antimicrob. Agents Chemother.* **2013**, *57*, 4181−4189.
(274) Mathé, C.; Gosselin, G. L-Nucleoside enantiomers as antivirals drugs: A mini-review. *Antiviral Res.* **2006**, *71*, 276−281.
(275) Du, J.; Choi, Y.; Lee, L.; Chun, B. K.; Hong, J. H.; Chu, C. K. A Practical Synthesis of L-FMAU from L-Arabinose. *Nucleosides Nucleotides* **1999**, *18*, 187−195.
(276) Korba, B. E.; Furman, P. A.; Otto, M. J. Clevudine: A Potent Inhibitor of Hepatitis B Virus *In Vitro* And *In Vivo*. *Expert Rev. Anti-Infect. Ther.* **2006**, *4*, 549−561.
(277) Lim, S. G.; Leung, N.; Hann, H. W. L.; Lau, G. K. K.; Trepo, C.; Mommeja-Marin, H.; Moxham, C.; Sorbel, J.; Snow, A.; Blum, M. R.; et al. Clinical Trial: A Phase II, Randomized Study Evaluating the Safety, Pharmacokinetics and Anti-Viral Activity of Clevudine for 12 Weeks in Patients with Chronic Hepatitis B. *Aliment. Pharmacol. Ther.* **2008**, *27*, 1282−1292.
(278) Tann, C. H.; Brodfuehrer, P. R.; Brundidge, S. P.; Sapino, C., Jr; Howell, H. G. Fluorocarbohydrates in Synthesis. An Efficient Synthesis of 1-(2-Deoxy-2-fluoro-β-D-arabinofuranosyl)-5-iodouracil (β-FIAU) and l-(2-Deoxy-2-fluoro-β-D-arabinofuranosyl)thymine (β-FMAU). *J. Org. Chem.* **1985**, *50*, 3644−3647.
(279) Ma, T.; Pai, S. B.; Zhu, Y. L.; Lin, J. S.; Shanmuganathan, K.; Du, J.; Wang, C.; Kim, H.; Newton, M. G.; Cheng, Y. C.; et al. Structure-Activity Relationships of 1-(2-Deoxy-2-fluoro-β-L-arabinofuranosyl)pyrimidine Nucleosides as Anti-Hepatitis B Virus Agents. *J. Med. Chem.* **1996**, *39*, 2835−2843.
(280) Balog, A.; Yu, M. S.; Curran, D. P.; Yu, G.; Carcanague, D. R.; Shue, Y.-K. A Practical Asymmetric Synthesis of a Pseudomonic Acid Precursor from D-Arabinose or D-Xylose. *Synth. Commun.* **1996**, *26*, 935−944.
(281) Sznaidman, M. L.; Almond, M. R.; Pesyan, A. New Synthesis of L-Fmau from L-Arabinose. *Nucleosides, Nucleotides Nucleic Acids* **2002**, *21*, 155−163.
(282) Craigie, R. HIV Integrase, a Brief Overview from Chemistry to Therapeutics. *J. Biol. Chem.* **2001**, *276*, 23213−23216.
(283) Pommier, Y.; Johnson, A. A.; Marchand, C. Integrase Inhibitors to Treat HIV/Aids. *Nat. Rev. Drug Discovery* **2005**, *4*, 236−248.
(284) Deeks, S. G.; Kar, S.; Gubernick, S. I.; Kirkpatrick, P. Raltegravir. *Nat. Rev. Drug Discovery* **2008**, *7*, 117−118.
(285) Gu, W.-G. Newly Approved Integrase Inhibitors for Clinical Treatment of AIDS. *Biomed. Pharmacother.* **2014**, *68*, 917−921.
(286) Serrao, E.; Odde, S.; Ramkumar, K.; Neamati, N. Raltegravir, Elvitegravir, and Metoogravir: The Birth of "Me-Too" HIV-1 Integrase Inhibitors. *Retrovirology* **2009**, *6*, 25.
(287) Wang, Y.; Serradell, N.; Bolos, J.; Rosa, E. MK-0518. HIV Integrase Inhibitor. *Drugs Future* **2007**, *32*, 118−122.
(288) Summa, V.; Petrocchi, A.; Bonelli, F.; Crescenzi, B.; Donghi, M.; Ferrara, M.; Fiore, F.; Gardelli, C.; Gonzalez Paz, O.; Hazuda, D. J.; et al. Discovery of Raltegravir, a Potent, Selective Orally Bioavailable HIV-Integrase Inhibitor for the Treatment of HIV-AIDS Infection. *J. Med. Chem.* **2008**, *51*, 5843−5855.
(289) Sato, M.; Motomura, T.; Aramaki, H.; Matsuda, T.; Yamashita, M.; Ito, Y.; Kawakami, H.; Matsuzaki, Y.; Watanabe, W.; Yamataka, K.; et al. Novel HIV-1 Integrase Inhibitors Derived from Quinolone Antibiotics. *J. Med. Chem.* **2006**, *49*, 1506−1508.
(290) Dayam, R.; Al-Mawsawi, L. Q.; Zawahir, Z.; Witvrouw, M.; Debyser, Z.; Neamati, N. Quinolone 3-Carboxylic Acid Pharmacophore: Design of Second Generation HIV-1 Integrase Inhibitors. *J. Med. Chem.* **2008**, *51*, 1136−1144.
(291) Sato, M.; Kawakami, H.; Motomura, T.; Aramaki, H.; Matsuda, T.; Yamashita, M.; Ito, Y.; Matsuzaki, Y.; Yamataka, K.; Ikeda, S.; et al. Quinolone Carboxylic Acids as a Novel Monoketo Acid Class of Human Immunodeficiency Virus Type 1 Integrase Inhibitors. *J. Med. Chem.* **2009**, *52*, 4869−4882.
(292) Zhang, J.-A. Synthesis of 2,4-Difluorobenzoic Acid. *Zhongguo Yiyao Gongye Zazhi* **2000**, *31*, 468−469. *Chem. Abstr.* **2001**, *134*, 326233.
(293) Zhou, S.; Li, J.; Wang, X.; Huang, J. Improved Synthesis of 2,4-Difluorobenzoic Acid. *Zhongguo Yiyao Gongye Zazhi* **2001**, *32*, 420. *Chem. Abstr.* **2001**, *137*, 93577.
(294) Wild, J.; Goetz, N. Ger. Offen. DE3820979A1, 1989; *Chem. Abstr.* **1990**, *113*, 40150.
(295) Aebi, J.; Amrein, K.; Chen, W.; Hornsperger, B.; Kuhn, B.; Liu, Y.; Maerki, H. P.; Mayweg, A. V.; Mohr, P.; Tan, X.; et al. PCT Int. Appl. WO2013079452A1, 2013; *Chem. Abstr.* **2013**, *159*, 75813.

DOI: 10.1021/acs.chemrev.5b00392
Chem. Rev. 2016, 116, 422−518

(296) Dowdy, E.; Pfeiffer, S. PCT Int. Appl. WO2009036161A1, 2009; *Chem. Abstr.* **2009**, *150*, 329633.
(297) Traynor, K. Riociguat Approved for Pulmonary Hypertension. *Am. J. Health-Syst. Pharm.* **2013**, *70*, 1960.
(298) Ko, F.-N.; Wu, C.-C.; Kuo, S.-C.; Lee, F.-Y.; Teng, C.-M. YC-1, a Novel Activator of Platelet Guanylate Cyclase. *Blood* **1994**, *84*, 4226−4233.
(299) Stasch, J.-P.; Becker, E. M.; Alonso-Alija, C.; Apeler, H.; Dembowsky, K.; Feurer, A.; Gerzer, R.; Minuth, T.; Perzborn, E.; Pleiβ, U.; et al. NO-Independent Regulatory Site on Soluble Guanylate Cyclase. *Nature* **2001**, *410*, 212−215.
(300) Stasch, J.-P.; Alonso-Alija, C.; Apeler, H.; Dembowsky, K.; Feurer, A.; Minuth, T.; Perzborn, E.; Schramm, M.; Straub, A. Pharmacological Actions of a Novel NO-Independent Guanylyl Cyclase Stimulator, BAY 41−8543: *In Vitro* Studies. *Br. J. Pharmacol.* **2002**, *135*, 333−343.
(301) Straub, A.; Benet-Buchholz, J.; Frode, R.; Kern, A.; Kohlsdorfer, C.; Schmitt, P.; Schwarz, T.; Siefert, H.-M.; Stasch, J.-P. Metabolites of Orally Active NO-Independent Pyrazolopyridine Stimulators of Soluble Guanylate Cyclase. *Bioorg. Med. Chem.* **2002**, *10*, 1711−1717.
(302) Mittendorf, J.; Weigand, S.; Alonso-Alija, C.; Bischoff, E.; Feurer, A.; Gerisch, M.; Kern, A.; Knorr, A.; Lang, D.; Muenter, K.; et al. Discovery of Riociguat (BAY 63−2521): A Potent, Oral Stimulator of Soluble Guanylate Cyclase for the Treatment of Pulmonary Hypertension. *ChemMedChem* **2009**, *4*, 853−865.
(303) Nagata, K.; Hirai, H. The Second PGD2 Receptor CRTH2: Structure, Properties, and Functions in Leukocytes. *Prostaglandins, Leukotrienes Essent. Fatty Acids* **2003**, *69*, 169−177.
(304) Fretz, H.; Valdenaire, A.; Pothier, J.; Hilpert, K.; Gnerre, C.; Peter, O.; Leroy, X.; Riederer, M. A. Identification of 2-(2-(1-Naphthoyl)-8-fluoro-3,4-dihydro-1*H*-pyrido[4,3-*b*]indol-5(2H)-yl)-acetic Acid (Setipiprant/ACT-129968), a Potent, Selective, and Orally Bioavailable Chemoattractant Receptor-Homologous Molecule Expressed on Th2 Cells (CRTH2) Antagonist. *J. Med. Chem.* **2013**, *56*, 4899−4911.
(305) Diamant, Z.; Sidharta, P. N.; Singh, D.; O'Connor, B. J.; Zuiker, R.; Leaker, B. R.; Silkey, M.; Dingemanse, J. Setipiprant, a Selective CRTH2 Antagonist, Reduces Allergen-Induced Airway Responses in Allergic Asthmatics. *Clin. Exp. Allergy* **2014**, *44*, 1044−1052.
(306) Norman, P. Update on the Status of DP2 Receptor Antagonists; from Proof of Concept through Clinical Failures to Promising New Drugs. *Expert Opin. Invest. Drugs* **2014**, *23*, 55−56.
(307) Valdenaire, A.; Pothier, J.; Renneberg, D.; Riederer, M. A.; Peter, O.; Leroy, X.; Gnerre, C.; Fretz, H. Evolution of Novel Tricyclic CRTh2 Receptor Antagonists from a (*E*)-2-Cyano-3-(1*H*-indol-3-yl)acrylamide Scaffold. *Bioorg. Med. Chem. Lett.* **2013**, *23*, 944−948.
(308) Brunavs, M.; Cowley, P.; Ward, S. E.; Weber, P. Recent Disclosures of Clinical Candidates. *Drugs Future* **2013**, *38*, 127−133.
(309) Pettipher, R.; Whittaker, M. Update on the Development of Antagonists of Chemoattractant Receptor-Homologous Molecule Expressed on Th2 Cells (CRTH2). From Lead Optimization to Clinical Proof-of-Concept in Asthma and Allergic Rhinitis. *J. Med. Chem.* **2012**, *55*, 2915−2931.
(310) Hoch, M.; Wank, J.; Kluge, I.; Wagner-Redeker, W.; Dingemanse, J. Disposition and Metabolism of Setipiprant, a Selective Oral CRTH2 Antagonist, in Humans. *Drugs R&D* **2013**, *13*, 253−269.
(311) Bridoux, A.; Goossens, L.; Houssin, R.; Héanichart, J.-P. Synthesis of 8-Substituted Tetrahydro-γ-carbolines. *J. Heterocycl. Chem.* **2006**, *43*, 571−578.
(312) Robinson, M. Proton Pump Inhibitors: Update on their Role in Acid-Related Gastrointestinal Diseases. *Int. J. Clin. Pract.* **2005**, *59*, 709−715.
(313) Fass, R.; Shapiro, M.; Dekel, R.; Sewell, J. Systematic Review: Proton-Pump Inhibitor Failure in Gastro-Oesophageal Reflux Disease − Where Next? *Aliment. Pharmacol. Ther.* **2005**, *22*, 79−94.
(314) Arikawa, Y.; Nishida, H.; Kurasawa, O.; Hasuoka, A.; Hirase, K.; Inatomi, N.; Hori, Y.; Matsukawa, J.; Imanishi, A.; Kondo, M.; et al. Discovery of a Novel Pyrrole Derivative 1-[5-(2-Fluorophenyl)-1-(pyridin-3-ylsulfonyl)-1*H*-pyrrol-3-yl]-*N*-methylmethanamine Fumarate (TAK-438) as a Potassium-Competitive Acid Blocker (P-CAB). *J. Med. Chem.* **2012**, *55*, 4446−4456.
(315) Hori, Y.; Imanishi, A.; Matsukawa, J.; Tsukimi, Y.; Nishida, H.; Arikawa, Y.; Hirase, K.; Kajino, M.; Inatomi, N. 1-[5-(2-Fluorophenyl)-1-(pyridin-3-ylsulfonyl)-1*H*-pyrrol-3-yl]-*N*-methylmethanamine Monofumarate (TAK-438), a Novel and Potent Potassium-Competitive Acid Blocker for the Treatment of Acid-Related Diseases. *J. Pharmacol. Exp. Ther.* **2010**, *335*, 231−238.
(316) Hori, Y.; Matsukawa, J.; Takeuchi, T.; Nishida, H.; Kajino, M.; Inatomi, N. A Study Comparing the Antisecretory Effect of TAK-438, a Novel Potassium-Competitive Acid Blocker, with Lansoprazole in Animals. *J. Pharmacol. Exp. Ther.* **2011**, *337*, 797−804.
(317) Shin, J. M.; Inatomi, N.; Munson, K.; Strugatsky, D.; Tokhtaeva, E.; Vagin, O.; Sachs, G. Characterization of a Novel Potassium-Competitive Acid Blocker of the Gastric H,K-ATPase, 1-[5-(2-Fluorophenyl)-1-(pyridin-3-ylsulfonyl)-1*H*-pyrrol-3-yl]-*N*-methylmethanamine Monofumarate (TAK-438). *J. Pharmacol. Exp. Ther.* **2011**, *339*, 412−420.
(318) Garnock-Jones, K. P. Vonoprazan: First Global Approval. *Drugs* **2015**, *75*, 439−443.
(319) Kondo, M.; Kawamoto, M.; Hasuoka, A.; Kajino, M.; Inatomi, N.; Tarui, N. High-Throughput Screening of Potassium-Competitive Acid Blockers. *J. Biomol. Screening* **2012**, *17*, 177−182.
(320) Nishida, H.; Hasuoka, A.; Arikawa, Y.; Kurasawa, O.; Hirase, K.; Inatomi, N.; Hori, Y.; Sato, F.; Tarui, N.; Imanishi, A.; et al. Discovery, Synthesis, and Biological Evaluation of Novel Pyrrole Derivatives as Highly Selective Potassium-Competitive Acid Blockers. *Bioorg. Med. Chem.* **2012**, *20*, 3925−3938.
(321) Kajino, M.; Hasuoka, A.; Nishida, H. PCT Int. Appl. WO2007026916A1, 2007; *Chem. Abstr.* **2007**, *146*, 316771.
(322) Milner, D. J. Fluoroaromatics from Arylamines. A Convenient One-Pot Conversion Using Nitrosonium Tetrafluoroborate. *Synth. Commun.* **1992**, *22*, 73−82.
(323) Döbele, M.; Vanderheiden, S.; Jung, N.; Bräse, S. Synthesis of Aryl Fluorides on a Solid Support and in Solution by Utilizing a Fluorinated Solvent. *Angew. Chem., Int. Ed.* **2010**, *49*, 5986−5988.
(324) Hoveyda, H. R.; Marsault, E.; Gagnon, R.; Mathieu, A. P.; Vézina, M.; Landry, A.; Wang, Z.; Benakli, K.; Beaubien, S.; Saint-Louis, C.; et al. Optimization of the Potency and Pharmacokinetic Properties of a Macrocyclic Ghrelin Receptor Agonist (Part I): Development of Ulimorelin (TZP-101) from Hit to Clinic. *J. Med. Chem.* **2011**, *54*, 8305−8320.
(325) Hellström, P. Ulimorelin. Ghrelin (GHS) Receptor Agonist Treatment of Postoperative Ileus Treatment of Gastroparesis. *Drugs Future* **2011**, *36*, 899−907.
(326) Fraser, G. L.; Hoveyda, H. R.; Tannenbaum, G. S. Pharmacological Demarcation of the Growth Hormone, Gut Motility and Feeding Effects of Ghrelin Using a Novel Ghrelin Receptor Agonist. *Endocrinology* **2008**, *149*, 6280−6288.
(327) Colca, J. R. Discontinued Drugs in 2012: Endocrine and Metabolic. *Expert Opin. Invest. Drugs* **2013**, *22*, 1305−1313.
(328) Camilleri, M.; Acosta, A. A Ghrelin Agonist Fails to Show Benefit in Patients with Diabetic Gastroparesis: Let's Not Throw the Baby Out with the Bath Water. *Neurogastroenterol. Motil.* **2013**, *25*, 859−863.
(329) Hoveyda, H. R.; Peterson, M. L.; Fraser, G. L.; Ramaseshan, M. U.S. Patent US20060025566A1, 2006; *Chem. Abstr.* **2006**, *144*, 171265.
(330) Yoshida, Y.; Kimura, Y. A Convenient Synthesis of Fluorobenzaldehydes by KF/Ph4PBr/18-crown-6 Reagent System. *Chem. Lett.* **1988**, 1355−1358.
(331) Yoshida, Y.; Kimura, Y. U.S. Patent US4845304A, 1989; *Chem. Abstr.* **1989**, *110*, 114444.

DOI: 10.1021/acs.chemrev.5b00392
Chem. Rev. 2016, 116, 422−518

(332) Yoshida, Y.; Kimura, Y. An Improved and Practical Synthesis of 4-Fluorobenzaldehyde by Halogen-Exchange Fluorination Reaction. *J. Fluorine Chem.* **1989**, *44*, 291−298.
(333) Kliukiene, R.; Maroziene, A.; Pociene, D.; Stumbreviciute, Z.; Laukaitis, V.; Karpavicius, K. Fluorinated Phenylalanines and their Derivatives. 1. Synthesis and Antitumor Activity of Some Cytoactive Derivatives of p-Fluoro-DL-phenylalamine. *Chemija* **1993**, 47−51. *Chem. Abstr.* **1994**, *120*, 218445.
(334) Zhang, Z. Enantioselective Scavenging Using Homogenate of Rhodotorula Graminis: A Facile Preparation of D-Amino Acid Derivatives in Enantiopure Form. *Tetrahedron Lett.* **2008**, *49*, 6468−6470.
(335) Yasukawa, K.; Asano, Y. Enzymatic Synthesis of Chiral Phenylalanine Derivatives by a Dynamic Kinetic Resolution of Corresponding Amide and Nitrile Substrates with a Multi-Enzyme System. *Adv. Synth. Catal.* **2012**, *354*, 3327−3332.
(336) Rozzell, D. J.; Novick, S. J. U.S. Patent US20080182972A1, 2008; *Chem. Abstr.* **2006**, *145*, 450835.
(337) Latacz, G.; Pękala, E.; Ciopińska, A.; Kieć-Kononowicz, K. Unnatural D-Amino Acids as Building Blocks of New Peptidomimetics. *Acta Pol. Pharm.* **2006**, *62*, 430−433.
(338) Maguire, N. E.; McLaren, A. B.; Sweeney, J. B. Asymmetric Synthesis of Arylalanines via Asymmetric aza-Darzens (ADZ) Reaction. *Synlett* **2003**, 1898−1900.
(339) Krause, H.-W.; Kreuzfeld, H.-J.; Döbler, C. Unusual Amino Acids: II. Asymmetric Synthesis of Fluorine Containing Phenylalanines. *Tetrahedron: Asymmetry* **1992**, *3*, 555−566.
(340) Soloshonok, V. A.; Cai, C.; Hruby, V. J.; Van Meervelt, L.; Mischenko, N. Stereochemically Defined *C*-Substituted Glutamic Acids and their Derivatives. 1. An Efficient Asymmetric Synthesis of (2*S*,3*S*)-3-Methyl- and −3-Trifluoromethylpyroglutamic Acids. *Tetrahedron* **1999**, *55*, 12031−12044.
(341) Jörres, M.; Aceña, J. L.; Soloshonok, V. A.; Bolm, C. Asymmetric Carbon−Carbon Bond Formation under Solventless Conditions in Ball Mills. *ChemCatChem* **2015**, *7*, 1265−1269.
(342) Jörres, M.; Chen, X.; Aceña, J. L.; Merkens, C.; Bolm, C.; Liu, H.; Soloshonok, V. A. Asymmetric Synthesis of α-Amino Acids under Operationally Convenient Conditions. *Adv. Synth. Catal.* **2014**, *356*, 2203−2208.
(343) Takeda, R.; Kawamura, A.; Kawashima, A.; Moriwaki, H.; Sato, T.; Aceña, J. L.; Soloshonok, V. A. Design and Synthesis of (*S*)- and (*R*)-α-(Phenyl)-ethylamine-Derived NH-Type Ligands and their Application for the Chemical Resolution of α-Amino Acids. *Org. Biomol. Chem.* **2014**, *12*, 6239−6249.
(344) Wang, J.; Liu, H.; Aceña, J. L.; Houck, D.; Takeda, R.; Moriwaki, H.; Soloshonok, V. A.; Sato, T. Synthesis of Bis-α,α-amino Acids through Diastereoselective Bis-alkylations of Chiral Ni(II)-Complexes of Glycine. *Org. Biomol. Chem.* **2013**, *11*, 4508−4515.
(345) Ellis, T. K.; Ueki, H.; Yamada, T.; Ohfune, Y.; Soloshonok, V. A. The Design, Synthesis and Evaluation of a New Generation of Modular Nucleophilic Glycine Equivalents for the Efficient Synthesis of Sterically Constrained α-Amino Acids. *J. Org. Chem.* **2006**, *71*, 8572−8578.
(346) Ellis, T. K.; Ueki, H.; Soloshonok, V. A. New Generation of Nucleophilic Glycine Equivalents. *Tetrahedron Lett.* **2005**, *46*, 941−944.
(347) Soloshonok, V. A.; Ueki, H.; Ellis, T. K.; Yamada, T.; Ohfune, Y. Application of Modular Nucleophilic Glycine Equivalents for Truly Practical Asymmetric Synthesis of β-Substituted Pyroglutamic Acids. *Tetrahedron Lett.* **2005**, *46*, 1107−1110.
(348) Sorochinsky, A. E.; Aceña, J. L.; Moriwaki, H.; Sato, T.; Soloshonok, V. A. Asymmetric Synthesis of α-Amino Acids via Homologation of Ni(II) Complexes of Glycine Schiff Bases; Part 1: Alkyl Halide Alkylations. *Amino Acids* **2013**, *45*, 691−718.
(349) Sorochinsky, A. E.; Aceña, J. L.; Moriwaki, H.; Sato, T.; Soloshonok, V. Asymmetric Synthesis of α-Amino Acids via Homologation of Ni(II) Complexes of Glycine Schiff Bases. Part 2: Aldol, Mannich Addition Reactions, Deracemization and (*S*) To (*R*) Interconversion of α-Amino Acids. *Amino Acids* **2013**, *45*, 1017−1033.
(350) Aceña, J. L.; Sorochinsky, A. E.; Soloshonok, V. Asymmetric Synthesis of α-Amino Acids via Homologation of Ni(II) Complexes of Glycine Schiff Bases. Part 3: Michael Addition Reactions and Miscellaneous Transformations. *Amino Acids* **2014**, *46*, 2047−2073.
(351) Soloshonok, V. A.; Sorochinsky, A. E. Practical Methods for the Synthesis of Symmetrically α,α-Disubstituted-α-Amino Acids. *Synthesis* **2010**, *2010*, 2319−2344.
(352) Zhou, S.; Wang, J.; Chen, X.; Aceña, J. L.; Soloshonok, V. A.; Liu, H. Chemical Kinetic Resolution of Unprotected β-Substituted β-Amino Acids Using Recyclable Chiral Ligands. *Angew. Chem., Int. Ed.* **2014**, *53*, 7883−7886.
(353) Takeda, R.; Kawamura, A.; Kawashima, A.; Sato, T.; Moriwaki, H.; Izawa, K.; Akaji, K.; Wang, S.; Liu, H.; Aceña, J. L.; et al. Chemical Dynamic Kinetic Resolution and *S*/*R* Interconversion of Unprotected α-Amino Acids. *Angew. Chem., Int. Ed.* **2014**, *53*, 12214−12217.
(354) Soloshonok, V. A.; Ellis, T. K.; Ueki, H.; Ono, T. Resolution/Deracemization of Chiral α-Amino Acids Using Resolving Reagents with Flexible Stereogenic Centers. *J. Am. Chem. Soc.* **2009**, *131*, 7208−7209.
(355) Sorochinsky, A. E.; Ueki, H.; Aceña, J. L.; Ellis, T. K.; Moriwaki, H.; Sato, T.; Soloshonok, V. A. Chemical Deracemization and (*S*) to (*R*) Interconversion of Some Fluorine-Containing α-Amino Acids. *J. Fluorine Chem.* **2013**, *152*, 114−118.
(356) Sorochinsky, A. E.; Ueki, H.; Aceña, J. L.; Ellis, T. K.; Moriwaki, H.; Sato, T.; Soloshonok, V. A. Chemical Approach for Interconversion of (*S*)- and (*R*)-α-Amino Acids. *Org. Biomol. Chem.* **2013**, *11*, 4503−4507.
(357) Yamamoto, K.; Maruyama, K.; Himori, N.; Omodaka, K.; Yokoyama, Y.; Shiga, Y.; Morin, R.; Nakazawa, T. The Novel Rho Kinase (ROCK) Inhibitor K-115: A New Candidate Drug for Neuroprotective Treatment in Glaucoma. *Invest. Ophthalmol. Visual Sci.* **2014**, *55*, 7126−7136.
(358) Tanihara, H.; Inoue, T.; Yamamoto, T.; Kuwayama, Y.; Abe, H.; Araie, M. Phase 2 Randomized Clinical Study of a Rho Kinase Inhibitor, K-115, in Primary Open-Angle Glaucoma and Ocular Hypertension. *Am. J. Ophthalmol.* **2013**, *156*, 731−736.
(359) Graul, A. I.; Cruces, E.; Stringer, M. The Year's New Drugs & Biologics, 2014: Part I. *Drugs Today* **2015**, *51*, 37−87.
(360) Garnock-Jones, K. P. Ripasudil: First Global Approval. *Drugs* **2014**, *74*, 2211−2215.
(361) Gomi, N.; Ohgiya, T.; Shibuya, K.; Katsuyama, J.; Masumoto, M.; Sakai, H. A Practical Synthesis of Novel Rho-Kinase Inhibitor, (*S*)-4-Fluoro-5-(2-methyl-1,4-diazepan-1-ylsulfonyl)isoquinoline. *Heterocycles* **2011**, *83*, 1771−1781.
(362) Tamura, M.; Nakao, H.; Yoshizaki, H.; Shiratsuchi, M.; Shigyo, H.; Yamada, H.; Ozawa, T.; Totsuka, J.; Hidaka, H. Development of Specific Rho-Kinase Inhibitors and their Clinical Application. *Biochim. Biophys. Acta, Proteins Proteomics* **2005**, *1754*, 245−252.
(363) Sasaki, Y.; Suzuki, M.; Hidaka, H. The Novel and Specific Rho-Kinase Inhibitor (S)-(+)-2-Methyl-1-[(4-methyl-5-isoquinoline)-sulfonyl]-momopiperazine as a Probing Molecule for Rho-Kinase-Involved Pathway. *Pharmacol. Ther.* **2002**, *93*, 225−232.
(364) Breitenlechner, C.; Gaβel, M.; Hidaka, H.; Kinzel, V.; Huber, R.; Engh, R. A.; Bossemeyer, D. Protein Kinase A in Complex with Rho-Kinase Inhibitors Y-27632, Fasudil, and H-1152P: Structural Basis of Selectivity. *Structure* **2003**, *11*, 1595−1607.
(365) Jacobs, M.; Hayakawa, K.; Swenson, L.; Bellon, S.; Fleming, M.; Taslimi, P.; Doran, J. The Structure of Dimeric ROCK I Reveals the Mechanism for Ligand Selectivity. *J. Biol. Chem.* **2006**, *281*, 260−268.
(366) Ohba, S.; Gomi, N.; Ohgiya, T.; Shibuya, K. Three Derivatives of 4-Fluoro-5-sulfonylisoquinoline. *Acta Crystallogr., Sect. C: Cryst. Struct. Commun.* **2012**, *68*, o427−o430.
(367) Hidaka, H.; Matsuura, A. PCT Int. Appl. WO9920620A1, 1999; *Chem. Abstr.* **1999**, *130*, 306596.
(368) Gomi, N.; Ohgiya, T.; Shibuya, K. U.S. Patent US20130144054A1, 2013; *Chem. Abstr.* **2012**, *156*, 311083.
(369) Gomi, N.; Kouketsu, A.; Ohgiya, T.; Shibuya, K. A Practical Synthesis of (*S*)-*tert*-Butyl 3-Methyl-1,4-diazepane-1-carboxylate, the

DOI: 10.1021/acs.chemrev.5b00392
Chem. Rev. 2016, 116, 422−518

Key Intermediate of Rho−Kinase Inhibitor K-115. *Synthesis* **2012**, *44*, 3171−3178.
(370) Polidori, D.; Sha, S.; Mudaliar, S.; Ciaraldi, T. P.; Ghosh, A.; Vaccaro, N.; Farrell, K.; Rothenberg, P.; Henry, R. R. Canagliflozin Lowers Postprandial Glucose and Insulin by Delaying Intestinal Glucose Absorption in Addition to Increasing Urinary Glucose Excretion: Results of a randomized, placebo-controlled study. *Diabetes Care* **2013**, *36*, 2154−2161.
(371) Clar, C.; Gill, J. A.; Court, R.; Waugh, N. Systematic Review of SGLT2 Receptor Inhibitors in Dual or Triple Therapy in Type 2 Diabetes. *BMJ. Open* **2012**, *2*, e001007.
(372) Kanwal, A.; Banerjee, S. K. SGLT Inhibitors: A Novel Target for Diabetes. *Pharm. Pat. Anal.* **2013**, *2*, 77−91.
(373) Rosenstock, J.; Aggarwal, N.; Polidori, D.; Zhao, Y.; Arbit, D.; Usiskin, K.; Capuano, G.; Canovatchel, W. Dose-Ranging Effects of Canagliflozin, a Sodium-Glucose Cotransporter 2 Inhibitor, as Add-On to Metformin in Subjects With Type 2 Diabetes. *Diabetes Care* **2012**, *35*, 1232−1238.
(374) Polidori, D.; Mari, A.; Ferrannini, E. Canagliflozin, a Sodium Glucose Co-Transporter 2 Inhibitor, Improves Model-Based Indices of Beta Cell Function in Patients With Type 2 Diabetes. *Diabetologia* **2014**, *57*, 891−901.
(375) Imamura, M.; Nakanishi, K.; Suzuki, T.; Ikegai, K.; Shiraki, R.; Ogiyama, T.; Murakami, T.; Kurosaki, E.; Noda, A.; Kobayashi, Y.; et al. Discovery of Ipragliflozin (ASP1941): A Novel *C*-Glucoside with Benzothiophene Structure as a Potent and Selective Sodium Glucose Co-Transporter 2 (SGLT2) Inhibitor for the Treatment of Type 2 Diabetes Mellitus. *Bioorg. Med. Chem.* **2012**, *20*, 3263−3279.
(376) Poole, R. M.; Dungo, R. T. Ipragliflozin: First Global Approval. *Drugs* **2014**, *74*, 611−617.
(377) Wielert-Badt, S.; Lin, J.-T.; Lorenz, M.; Fritz, S.; Kinne, R. K.-H. Probing the Conformation of the Sugar Transport Inhibitor Phlorizin by 2D-NMR, Molecular Dynamics Studies, and Pharmacophore Analysis. *J. Med. Chem.* **2000**, *43*, 1692−1698.
(378) Oku, A.; Ueta, K.; Arakawa, K.; Ishihara, T.; Nawano, M.; Kuronuma, Y.; Matsumoto, M.; Saito, A.; Tsujihara, K.; Anai, M.; et al. T-1095, an Inhibitor of Renal Na+-Glucose Cotransporters, May Provide a Novel Approach to Treating Diabetes. *Diabetes* **1999**, *48*, 1794−1800.
(379) Meng, W.; Ellsworth, B. A.; Nirschl, A. A.; McCann, P. J.; Patel, M.; Girotra, R. N.; Wu, G.; Sher, P. M.; Morrison, E. P.; Biller, S. A.; et al. Discovery of Dapagliflozin: A Potent, Selective Renal Sodium-Dependent Glucose Cotransporter 2 (SGLT2) Inhibitor for the Treatment of Type 2 Diabetes. *J. Med. Chem.* **2008**, *51*, 1145−1149.
(380) Nomura, S.; Sakamaki, S.; Hongu, M.; Kawanishi, E.; Koga, Y.; Sakamoto, T.; Yamamoto, Y.; Ueta, K.; Kimata, H.; Nakayama, K.; et al. Discovery of Canagliflozin, a Novel *C*-Glucoside with Thiophene Ring, as Sodium-Dependent Glucose Cotransporter 2 Inhibitor for the Treatment of Type 2 Diabetes Mellitus. *J. Med. Chem.* **2010**, *53*, 6355−6360.
(381) Yale, J.-F.; Bakris, G.; Cariou, B.; Yue, D.; David-Neto, E.; Xi, L.; Figueroa, K.; Wajs, E.; Usiskin, K.; Meininger, G. Efficacy and Safety of Canagliflozin in Subjects with Type 2 Diabetes and Chronic Kidney Disease. *Diabetes, Obes. Metab.* **2013**, *15*, 463−473.
(382) Inagaki, N.; Kondo, K.; Yoshinari, T.; Ishii, M.; Sakai, M.; Kuki, H.; Furihata, K. Pharmacokinetic and Pharmacodynamic Profiles of Canagliflozin in Japanese Patients with Type 2 Diabetes Mellitus and Moderate Renal Impairment. *Clin. Drug Invest.* **2014**, *34*, 731−742.
(383) Forst, T.; Guthrie, R.; Goldenberg, R.; Yee, J.; Vijapurkar, U.; Meininger, G.; Stein, P. Efficacy and Safety of Canagliflozin over 52 Weeks in Patients with Type 2 Diabetes on Background Metformin and Pioglitazone. *Diabetes, Obes. Metab.* **2014**, *16*, 467−477.
(384) Schwartz, S. L.; Akinlade, B.; Klasen, S.; Kowalski, D.; Zhang, W.; Wilpshaar, W. Safety, Pharmacokinetic, and Pharmacodynamic Profiles of Ipragliflozin (ASP1941), a Novel and Selective Inhibitor of Sodium-Dependent Glucose Co-Transporter 2, in Patients with Type 2 Diabetes Mellitus. *Diabetes Technol. Ther.* **2011**, *13*, 1219−1227.
(385) Veltkamp, S. A.; Kadokura, T.; Krauwinkel, W. J. J.; Smulders, R. A. Effect of Ipragliflozin (ASP1941), a Novel Selective Sodium-Dependent Glucose Co-Transporter 2 Inhibitor, on Urinary Glucose Excretion in Healthy Subjects. *Clin. Drug Invest.* **2011**, *31*, 839−851.
(386) Tahara, A.; Kurosaki, E.; Yokono, M.; Yamajuku, D.; Kihara, R.; Hayashizaki, Y.; Takasu, T.; Imamura, M.; Qun, L.; Tomiyama, H.; et al. Pharmacological Profile of Ipragliflozin (ASP1941), a Novel Selective SGLT2 Inhibitor, In Vitro and In Vivo. *Naunyn-Schmiedeberg's Arch. Pharmacol.* **2012**, *385*, 423−436.
(387) Lemaire, S.; Houpis, I. N.; Xiao, T.; Li, J.; Digard, E.; Gozlan, C.; Liu, R.; Gavryushin, A.; Diène, C.; Wang, Y.; et al. Stereoselective C-Glycosylation Reactions with Arylzinc Reagents. *Org. Lett.* **2012**, *14*, 1480−1483.
(388) Henschke, J. P.; Wu, P.-Y.; Lin, C.-W.; Chen, S.-F.; Chiang, P.-C.; Hsiao, C.-N. *β*-Selective *C*-Arylation of Silyl Protected 1,6-Anhydroglucose with Arylalanes: The Synthesis of SGLT2 Inhibitors. *J. Org. Chem.* **2015**, *80*, 2295−2309.
(389) Henschke, J. P.; Lin, C.-W.; Wu, P.-Y.; Tsao, W.-S.; Liao, J.-H.; Chiang, P.-C. *β*-Selective *C*-Arylation of Diisobutylaluminum Hydride Modified 1,6-Anhydroglucose: Synthesis of Canagliflozin without Recourse to Conventional Protecting Groups. *J. Org. Chem.* **2015**, *80*, 5189−5195.
(390) Juillerat-Jeanneret, L. Dipeptidyl Peptidase IV and Its Inhibitors: Therapeutics for Type 2 Diabetes and What Else? *J. Med. Chem.* **2014**, *57*, 2197−2212.
(391) Kushwaha, R. N.; Haq, W.; Katti, S. B. Discovery of 17 Gliptins in 17-Years of Research for the Treatment of Type 2 Diabetes: A Synthetic Overview. *Chem. Biol. Interface* **2014**, *4*, 137−162.
(392) Schwehm, C.; Li, J.; Song, H.; Hu, X.; Kellam, B.; Stocks, M. J. Synthesis of New DPP-4 Inhibitors Based on a Novel Tricyclic Scaffold. *ACS Med. Chem. Lett.* **2015**, *6*, 324−328.
(393) Zhang, Z.; Wallace, M. B.; Feng, J.; Stafford, J. A.; Skene, R. J.; Shi, L.; Lee, B.; Aertgeerts, K.; Jennings, A.; Xu, R.; et al. Design and Synthesis of Pyrimidinone and Pyrimidinedione Inhibitors of Dipeptidyl Peptidase IV. *J. Med. Chem.* **2011**, *54*, 510−524.
(394) Inagaki, N.; Onouchi, H.; Sano, H.; Funao, N.; Kuroda, S.; Kaku, K. SYR-472, a Novel Once-Weekly Dipeptidyl Peptidase-4 (DPP-4) Inhibitor, in Type 2 Diabetes Mellitus: A Phase 2, Randomised, Double-Blind, Placebo-Controlled Trial. *Lancet Diabetes Endocrinol.* **2014**, *2*, 125−132.
(395) Inagaki, N.; Onouchi, H.; Maezawa, H.; Kuroda, S.; Kaku, K. Once-Weekly Trelagliptin versus Daily Alogliptin in Japanese Patients with Type 2 Diabetes: A Randomised, Double-Blind, Phase 3, Non-Inferiority Study. *Lancet Diabetes Endocrinol.* **2015**, *3*, 191−197.
(396) Kelly, R. C.; Koztecki, L. H. PCT Int. Appl. WO2008067465A1, 2008; *Chem. Abstr.* **2008**, *149*, 10042.
(397) Biftu, T.; Sinha-Roy, R.; Chen, P.; Qian, X.; Feng, D.; Kuethe, J. T.; Scapin, G.; Gao, Y. D.; Yan, Y.; Krueger, D.; et al. Omarigliptin (MK-3102): A Novel Long-Acting DPP-4 Inhibitor for Once-Weekly Treatment of Type 2 Diabetes. *J. Med. Chem.* **2014**, *57*, 3205−3212.
(398) Burness, C. B. Omarigliptin: First Global Approval. *Drugs* **2015**, *75*, 1947−1957.
(399) Zhou, S.; Wang, J.; Chen, X.; Aceña, J. L.; Soloshonok, V. A.; Liu, H. Chemical Kinetic Resolution of Unprotected *β*-Substituted *β*-Amino Acids Using Recyclable Chiral Ligands. *Angew. Chem., Int. Ed.* **2014**, *53*, 7883−7886.
(400) Gao, Y.-D.; Feng, D.; Sheridan, R. P.; Scapin, G.; Patel, S. B.; Wu, J. K.; Zhang, X.; Sinha-Roy, R.; Thornberry, N. A.; Weber, A. E.; et al. Modeling Assisted Rational Design of Novel, Potent, and Selective Pyrrolopyrimidine DPP-4 Inhibitors. *Bioorg. Med. Chem. Lett.* **2007**, *17*, 3877−3879.
(401) Biftu, T.; Scapin, G.; Singh, S.; Feng, D.; Becker, J. W.; Eiermann, G.; He, H.; Lyons, K.; Patel, S.; Petrov, A.; et al. Rational Design of a Novel, Potent, and Orally Bioavailable Cyclohexylamine DPP-4 Inhibitor by Application of Molecular Modeling and X-Ray Crystallography of Sitagliptin. *Bioorg. Med. Chem. Lett.* **2007**, *17*, 3384−3387.
(402) Jamieson, C.; Moir, E. M.; Rankovic, Z.; Wishart, G. Medicinal Chemistry of hERG Optimizations: Highlights and Hang-Ups. *J. Med. Chem.* **2006**, *49*, 5029−5046.

DOI: 10.1021/acs.chemrev.5b00392
Chem. Rev. 2016, 116, 422−518

(403) Biftu, T.; Qian, X.; Chen, P.; Feng, D.; Scapin, G.; Gao, Y.-D.; Cox, J.; Sinha Roy, R.; Eiermann, G.; He, H.; et al. Novel Tetrahydropyran Analogs as Dipeptidyl Peptidase IV Inhibitors: Profile of Clinical Candidate (2*R*,3*S*,5*R*)-2-(2,5-Difluorophenyl)-5-[2-(methylsulfonyl)-2,6-dihydropyrrolo[3,4-*c*]pyrazol-5(4*H*)-yl]-tetrahydro-2*H*-pyran-3-amine (23). *Bioorg. Med. Chem. Lett.* **2013**, *23*, 5361−5366.
(404) Chen, S. C.-A.; Playford, E. G.; Sorrell, T. C. Antifungal Therapy in Invasive Fungal Infections. *Curr. Opin. Pharmacol.* **2010**, *10*, 522−530.
(405) Guinea, J.; Peláez, T.; Recio, S.; Torres-Narbona, M.; Bouza, E. In Vitro Antifungal Activities of Isavuconazole (BAL4815), Voriconazole, and Fluconazole against 1,007 Isolates of Zygomycete, *Candida*, *Aspergillus*, *Fusarium*, and *Scedosporium* Species. *Antimicrob. Agents Chemother.* **2008**, *52*, 1396−1400.
(406) Lepak, A. J.; Marchillo, K.; VanHecker, J.; Andes, D. R. Isavuconazole (BAL4815) Pharmacodynamic Target Determination in an *In Vivo* Murine Model of Invasive Pulmonary Aspergillosis against Wild-Type and *cyp51* Mutant Isolates of *Aspergillus fumigatus*. *Antimicrob. Agents Chemother.* **2013**, *57*, 6284−6289.
(407) Guinea, J.; Bouza, E. Isavuconazole: A New and Promising Antifungal Triazole for the Treatment of Invasive Fungal Infections. *Future Microbiol.* **2008**, *3*, 603−615.
(408) McCormack, P. L. Isavuconazonium: First Global Approval. *Drugs* **2015**, *75*, 817−822.
(409) Seyedmousavi, S.; Verweij, P. E.; Mouton, J. W. Isavuconazole, a Broad-Spectrum Triazole for the Treatment of Systemic Fungal Diseases. *Expert Rev. Anti-Infect. Ther.* **2015**, *13*, 9−27.
(410) Falci, D. R.; Pasqualotto, A. C. Profile of Isavuconazole and its Potential in the Treatment of Severe Invasive Fungal Infections. *Infect. Drug Resist.* **2013**, *6*, 163−174.
(411) Thompson, G. R., III; Wiederhold, N. P. Isavuconazole: A Comprehensive Review of Spectrum of Activity of a New Triazole. *Mycopathologia* **2010**, *170*, 291−313.
(412) Schmitt-Hoffmann, A.; Roos, B.; Heep, M.; Schleimer, M.; Weidekamm, E.; Brown, T.; Roehrle, M.; Beglinger, C. Single-Ascending-Dose Pharmacokinetics and Safety of the Novel Broad-Spectrum Antifungal Triazole BAL4815 after Intravenous Infusions (50, 100, and 200 mg) and Oral Administrations (100, 200, and 400 mg) of its Prodrug, BAL8557, in Healthy Volunteers. *Antimicrob. Agents Chemother.* **2006**, *50*, 279−285.
(413) Livermore, J.; Hope, W. Evaluation of the Pharmacokinetics and Clinical Utility of Isavuconazole for Treatment of Invasive Fungal Infections. *Expert Opin. Drug Metab. Toxicol.* **2012**, *8*, 759−765.
(414) Hayase, T.; Ichihara, S.; Isshiki, Y.; Liu, P.; Ohwada, J.; Sakai, T.; Shimma, N.; Tsukazaki, M.; Umeda, I.; Yamazaki, T. PCT Int. Appl. WO9945008A1, 1999; *Chem. Abstr.* **1999**, *131*, 199700.
(415) Soukup, M. PCT Int. Appl. WO2011042827A1, 2011; *Chem. Abstr.* **2011**, *154*, 459788.
(416) Pendri, A.; Meanwell, N. A.; Peese, K. M.; Walker, M. A. New First and Second Generation Inhibitors of Human Immunodeficiency Virus-1 Integrase. *Expert Opin. Ther. Pat.* **2011**, *21*, 1173−1189.
(417) Lennox, J. L.; DeJesus, E.; Lazzarin, A.; Pollard, R. B.; Valdez Ramalho Madruga, J.; Berger, D. S.; Zhao, J.; Xu, X.; Williams-Diaz, A.; Rodgers, A. J.; et al. Safety and Efficacy of Raltegravir-Based versus Efavirenz-Based Combination Therapy in Treatment-Naive Patients with HIV-1 Infection: A Multicentre, Double-Blind Randomised Controlled Trial. *Lancet* **2009**, *374*, 796−806.
(418) Ceccherini-Silberstein, F.; Malet, I.; D'Arrigo, R.; Antinori, A.; Marcelin, A.-G.; Perno, C.-F. Characterization and Structural Analysis of HIV-1 Integrase Conservation. *AIDS Rev.* **2009**, *11*, 17−29.
(419) Johnson, V. A.; Brun-Vézinet, F.; Clotet, B.; Günthard, H. F.; Kuritzkes, D. R.; Pillay, D.; Schapiro, J. M.; Richman, D. D. Update of the Drug Resistance Mutations in HIV-1: December 2010. *Top. HIV Med.* **2010**, *18*, 156−163.
(420) Quashie, P. K.; Sloan, R. D.; Wainberg, M. A. Novel Therapeutic Strategies Targeting HIV Integrase. *BMC Med.* **2012**, *10*, 34.
(421) Ramanathan, S.; Mathias, A. A.; German, P.; Kearney, B. P. Clinical Pharmacokinetic and Pharmacodynamic Profile of the HIV Integrase Inhibitor Elvitegravir. *Clin. Pharmacokinet.* **2011**, *50*, 229−244.
(422) Blanco, J.-L.; Varghese, C.; Rhee, S.-Y.; Gatell, J. M.; Shafer, R. W. HIV-1 Integrase Inhibitor Resistance and Its Clinical Implications. *J. Infect. Dis.* **2011**, *203*, 1204−1214.
(423) Kawasuji, T.; Johns, B. A.; Yoshida, H.; Taishi, T.; Taoda, Y.; Murai, H.; Kiyama, R.; Fuji, M.; Yoshinaga, T.; Seki, T.; et al. Carbamoyl Pyridone HIV-1 Integrase Inhibitors. 1. Molecular Design and Establishment of an Advanced Two-Metal Binding Pharmacophore. *J. Med. Chem.* **2012**, *55*, 8735−8744.
(424) Kawasuji, T.; Johns, B. A.; Yoshida, H.; Weatherhead, J. G.; Akiyama, T.; Taishi, T.; Taoda, Y.; Mikamiyama-Iwata, M.; Murai, H.; Kiyama, R.; et al. Carbamoyl Pyridone HIV-1 Integrase Inhibitors. 2. Bi- and Tricyclic Derivatives Result in Superior Antiviral and Pharmacokinetic Profiles. *J. Med. Chem.* **2013**, *56*, 1124−1135.
(425) Johns, B. A.; Kawasuji, T.; Weatherhead, J. G.; Taishi, T.; Temelkoff, D. P.; Yoshida, H.; Akiyama, T.; Taoda, Y.; Murai, H.; Kiyama, R.; et al. Carbamoyl Pyridone HIV-1 Integrase Inhibitors 3. A Diastereomeric Approach to Chiral Nonracemic Tricyclic Ring Systems and the Discovery of Dolutegravir (S/GSK1349572) and (S/GSK1265744). *J. Med. Chem.* **2013**, *56*, 5901−5916.
(426) Yoshida, H.; Taoda, Y.; Johns, B. A. PCT Int. Appl. WO2010068253A1, 2010; *Chem. Abstr.* **2010**, *153*, 62289.
(427) Johns, B. A.; Weatherhead, J. G. PCT Int. Appl. WO2010011812A1, 2010; *Chem. Abstr.* **2010**, *152*, 192163.
(428) Sumino, Y.; Okamoto, K.; Masui, M.; Yamada, D.; Ikarashi, F. PCT Int. Appl. WO2012018065A1, 2012; *Chem. Abstr.* **2012**, *156*, 257808.
(429) Werkmeister, S.; Bornschein, C.; Junge, K.; Beller, M. Selective Ruthenium-Catalyzed Transfer Hydrogenations of Nitriles to Amines with 2-Butanol. *Chem. - Eur. J.* **2013**, *19*, 4437−4440.
(430) Shevlin, M. Sulfate Additives Generate Robust and Highly Active Palladium Catalysts for the Cyanation of Aryl Chlorides. *Tetrahedron Lett.* **2010**, *51*, 4833−4836.
(431) Zhu, X.-D.; Zhu, X.-F. Synthesis of m-Difluorobenzene from m-Dichlorobenzene. *Qufu Shifan Daxue Xuebao, Ziran Kexueban* **2001**, *27*, 61−64. *Chem. Abstr.* **2001**, *136*, 355007.
(432) Gu, L.; Lu, T.; Zhang, M.; Tou, L.; Zhang, Y. Efficient Oxidative Chlorination of Aromatics on Saturated Sodium Chloride Solution. *Adv. Synth. Catal.* **2013**, *355*, 1077−1082.
(433) Link, J. O.; Taylor, J. G.; Xu, L.; Mitchell, M.; Guo, H.; Liu, H.; Kato, D.; Kirschberg, T.; Sun, J.; Squires, N.; et al. Discovery of Ledipasvir (GS-5885): A Potent, Once-Daily Oral NS5A Inhibitor for the Treatment of Hepatitis C Virus Infection. *J. Med. Chem.* **2014**, *57*, 2033−2046.
(434) Ghany, M. G.; Nelson, D. R.; Strader, D. B.; Thomas, D. L.; Seeff, L. B. An Update on Treatment of Genotype 1 Chronic Hepatitis C Virus Infection: 2011 Practice Guideline by the American Association for the Study of Liver Diseases. *Hepatology* **2011**, *54*, 1433−1444.
(435) Harrison, S. A. Management of Anemia in Patients Receiving Protease Inhibitors. *Gastroenterol. Hepatol.* **2012**, *8*, 254−256.
(436) Cordek, D. G.; Bechtel, J. T.; Maynard, A. T.; Kazmierski, W. M.; Cameron, C. E. Targeting the NS5A Protein of HCV: An Emerging Option. *Drugs Future* **2011**, *36*, 691−711.
(437) Romine, J. L.; Martin, S. W.; Snyder, L. B.; Serrano-Wu, M.; Deshpande, M.; Whitehouse, D.; Lemm, J.; O'Boyle, D.; Gao, M.; Colonno, R. PCT Int. Appl. WO2004014852A2, 2004; *Chem. Abstr.* **2004**, *140*, 199315.
(438) Serrano-Wu, M.; Belema, M.; Snyder, L. B.; Meanwell, N.; St. Laurent, D.; Kakaria, R.; Nguyen, V. N.; Qui, Y.; Yang, X.; Leet, J. E.; et al. PCT Int. Appl. WO2006133326A1, 2006; *Chem. Abstr.* **2006**, *146*, 45728.
(439) Gao, M.; Nettles, R. E.; Belema, M.; Snyder, L. B.; Nguyen, V. N.; Fridell, R. A.; Serrano-Wu, M. H.; Langley, D. R.; Sun, J.-H.; O'Boyle, D. R., II; et al. Chemical Genetics Strategy Identifies an HCV

DOI: 10.1021/acs.chemrev.5b00392
Chem. Rev. 2016, 116, 422−518

NS5A Inhibitor with a Potent Clinical Effect. *Nature* **2010**, *465*, 96−100.
(440) Belema, M.; Meanwell, N. A. Discovery of Daclatasvir, a Pan-Genotypic Hepatitis C Virus NS5A Replication Complex Inhibitor with Potent Clinical Effect. *J. Med. Chem.* **2014**, *57*, 5057−5071.
(441) Guo, H.; Kato, D.; Kirschberg, T. A.; Liu, H.; Link, J. O.; Mitchell, M. L.; Parrish, J. P.; Squires, N.; Sun, J.; Taylor, J.; et al. PCT Int. Appl. WO2010132601A1, 2010; *Chem. Abstr.* **2010**, *153*, 643864.
(442) Delaney, W. E., IV; Lee, W. A.; Oldach, D. W.; Rousseau F. PCT Int. Appl. WO2011156757A1, 2011; *Chem. Abstr.* **2011**, *156*, 74254.
(443) Tymtsunik, A. V.; Bilenko, V. A.; Ivon, Y. M.; Grygorenko, O. O.; Komarov, I. V. Synthesis of a Novel Boc-Protected Cyclopropane-Modified Proline Analogue. *Tetrahedron Lett.* **2012**, *53*, 3847−3849.
(444) Aebi, J.; Bur, D.; Chucholowski, A.; Dehmlow, H.; Kitas, E. A.; Obst, U.; Wessel, H. P. PCT Int. Appl. WO2002008185A1, 2002; *Chem. Abstr.* **2002**, *136*, 151068.
(445) Stella, L.; Abraham, H.; Feneau-Dupont, J.; Tinant, B.; Declercq, J. P. Asymmetric Aza-Diels-Alder Reaction Using the Chiral 1-Phenyl Ethyl Imine of Methyl Glyoxylate. *Tetrahedron Lett.* **1990**, *31*, 2603−2606.
(446) L'Heureux, A.; Beaulieu, F.; Bennett, C.; Bill, D. R.; Clayton, S.; LaFlamme, F.; Mirmehrabi, M.; Tadayon, S.; Tovell, D.; Couturier, M. Aminodifluorosulfinium Salts: Selective Fluorination Reagents with Enhanced Thermal Stability and Ease of Handling. *J. Org. Chem.* **2010**, *75*, 3401−3411.
(447) Kotoris, C. C.; Chen, M.-J.; Taylor, S. D. Novel Phosphate Mimetics for the Design of Non-Peptidyl Inhibitors of Protein Tyrosine Phosphatases. *Bioorg. Med. Chem. Lett.* **1998**, *8*, 3275−3280.
(448) Ikemoto, N.; Liu, J.; Brands, K. M. J.; McNamara, J. M.; Reider, P. J. Practical Routes to the Triarylsulfonyl Chloride Intermediate of a β3 Adrenergic Receptor Agonist. *Tetrahedron* **2003**, *59*, 1317−1325.
(449) Differding, D.; Poss, A. J.; Cahard, D.; Shibata, N. *N*-Fluoro-*N*-(phenylsulfonyl)benzenesulfonamide - Second Update. *e-EROS, Encyclopedia of Reagents for Organic Synthesis*; John Wiley & Sons: 2013. (accessed July 2, 2015). DOI: 10.1002/047084289X.rf011.pub3.
(450) Rheault, T. R.; Stellwagen, J. C.; Adjabeng, G. M.; Hornberger, K. R.; Petrov, K. G.; Waterson, A. G.; Dickerson, S. H.; Mook, R. A., Jr.; Laquerre, S. G.; King, A. J.; et al. Discovery of Dabrafenib: A Selective Inhibitor of Raf Kinases with Antitumor Activity against B-Raf-Driven Tumors. *ACS Med. Chem. Lett.* **2013**, *4*, 358−362.
(451) Stellwagen, J. C.; Adjabeng, G. M.; Arnone, M. R.; Dickerson, S. H.; Han, C.; Hornberger, K. R.; King, A. J.; Mook, R. A., Jr.; Petrov, K. G.; Rheault, T. R.; et al. Development of Potent B-Raf^{V600E} Inhibitors Containing an Arylsulfonamide Headgroup. *Bioorg. Med. Chem. Lett.* **2011**, *21*, 4436−4440.
(452) Wong, H.; Vernillet, L.; Peterson, A.; Ware, J. A.; Lee, L.; Martini, J.-F.; Yu, P.; Li, C.; Del Rosario, G.; Choo, E. F.; et al. Bridging the Gap between Preclinical and Clinical Studies Using Pharmacokinetic−Pharmacodynamic Modeling: An Analysis of GDC-0973, a MEK Inhibitor. *Clin. Cancer Res.* **2012**, *18*, 3090−3099.
(453) Hoeflich, K. P.; Merchant, M.; Orr, C.; Chan, J.; Den Otter, D.; Berry, L.; Kasman, I.; Koeppen, H.; Rice, K.; Yang, N.-Y.; et al. Intermittent Administration of MEK Inhibitor GDC-0973 plus PI3K Inhibitor GDC-0941 Triggers Robust Apoptosis and Tumor Growth Inhibition. *Cancer Res.* **2012**, *72*, 210−219.
(454) Hatzivassiliou, G.; Haling, J. R.; Chen, H.; Song, K.; Price, S.; Heald, R.; Hewitt, J. F. M.; Zak, M.; Peck, A.; Orr, C.; et al. Mechanism of MEK Inhibition Determines Efficacy in Mutant KRAS- versus BRAF-Driven Cancers. *Nature* **2013**, *501*, 232−236.
(455) Barrett, S. D.; Bridges, A. J.; Dudley, D. T.; Saltiel, A. R.; Fergus, J. H.; Flamme, C. M.; Delaney, A. M.; Kaufman, M.; LePage, S.; Leopold, W. R.; et al. The Discovery of the Benzhydroxamate MEK Inhibitors CI-1040 and PD 0325901. *Bioorg. Med. Chem. Lett.* **2008**, *18*, 6501−6504.
(456) Rice, K. D.; Aay, N.; Anand, N. K.; Blazey, C. M.; Bowles, O. J.; Bussenius, J.; Costanzo, S.; Curtis, J. K.; Defina, S. C.; Dubenko, L.; et al. Novel Carboxamide-Based Allosteric MEK Inhibitors: Discovery and Optimization Efforts toward XL518 (GDC-0973). *ACS Med. Chem. Lett.* **2012**, *3*, 416−421.
(457) Beak, P.; Lee, W. K. α-Lithioamine Synthetic Equivalents: Syntheses of Diastereoisomers from the Boc Piperidines. *J. Org. Chem.* **1990**, *55*, 2578−2580.
(458) Manley, P. W.; Stiefl, N.; Cowan-Jacob, S. W.; Kaufman, S.; Mestan, J.; Wartmann, M.; Wiesmann, M.; Woodman, R.; Gallagher, N. Structural Resemblances and Comparisons of the Relative Pharmacological Properties of Imatinib and Nilotinib. *Bioorg. Med. Chem.* **2010**, *18*, 6977−6986.
(459) Kim, S.-H.; Menon, H.; Jootar, S.; Saikia, T.; Kwak, J.-Y.; Sohn, S.-K.; Park, J. S.; Jeong, S. H.; Kim, H. J.; Kim, Y.-K.; et al. Efficacy and Safety of Radotinib in Chronic Phase Chronic Myeloid Leukemia Patients with Resistance or Intolerance to BCR-ABL1 Tyrosine Kinase Inhibitors. *Haematologica* **2014**, *99*, 1191−1196.
(460) Duveau, D. Y.; Hu, X.; Walsh, M. J.; Shukla, S.; Skoumbourdis, A. P.; Boxer, M. B.; Ambudkar, S. V.; Shen, M.; Thomas, C. J. Synthesis and Biological Evaluation of Analogues of the Kinase Inhibitor Nilotinib as Abl and Kit Inhibitors. *Bioorg. Med. Chem. Lett.* **2013**, *23*, 682−686.
(461) O'Hare, T.; Pollock, R.; Stoffregen, E. P.; Keats, J. A.; Abdullah, O. M.; Moseson, E. M.; Rivera, V. M.; Tang, H.; Metcalf, C. A., III; Bohacek, R. S.; et al. Inhibition of Wild-Type and Mutant Bcr-Abl by AP23464, a Potent ATP-Based Oncogenic Protein Kinase Inhibitor: Implications for CML. *Blood* **2004**, *104*, 2532−2539.
(462) Weisberg, E.; Manley, P. W.; Breitenstein, W.; Brüggen, J.; Cowan-Jacob, S. W.; Ray, A.; Huntly, B.; Fabbro, D.; Fendrich, G.; Hall-Meyers, E.; et al. Characterization of AMN107, a Selective Inhibitor of Native and Mutant Bcr-Abl. *Cancer Cell* **2005**, *7*, 129−141.
(463) Huang, W.-S.; Zhu, X.; Wang, Y.; Azam, M.; Wen, D.; Sundaramoorthi, R.; Thomas, R. M.; Liu, S.; Banda, G.; Lentini, S. P.; et al. C. 9-(Arenethenyl)purines as Dual Src/Abl Kinase Inhibitors Targeting the Inactive Conformation: Design, Synthesis, and Biological Evaluation. *J. Med. Chem.* **2009**, *52*, 4743−4756.
(464) Huang, W.-S.; Metcalf, C. A.; Sundaramoorthi, R.; Wang, Y.; Zou, D.; Thomas, R. M.; Zhu, X.; Cai, L.; Wen, D.; Liu, S.; et al. Discovery of 3-[2-(Imidazo[1,2-b]pyridazin-3-yl)ethynyl]-4-methyl-N-{4-[(4-methylpiperazin-1-yl)-methyl]-3-(trifluoromethyl)phenyl}-benzamide (AP24534), a Potent, Orally Active Pan-Inhibitor of Breakpoint Cluster Region-Abelson (BCR-ABL) Kinase Including the T315I Gatekeeper Mutant. *J. Med. Chem.* **2010**, *53*, 4701−4719.
(465) Kim, D.-Y.; Cho, D.-J.; Lee, G.-Y.; Kim, H.-Y.; Woo, S.-H.; Kim, Y.-S.; Lee, S.-A.; Han, B.-C. PCT Int. Appl. WO2007018325A1, 2007; *Chem. Abstr.* **2007**, *146*, 251858.
(466) Kim, D.-Y.; Cho, D.-J.; Lee, G.-Y.; Kim, H.-Y.; Woo, S.-H. PCT Int. Appl. WO2010018895A1, 2010; *Chem. Abstr.* **2010**, *152*, 238984.
(467) Oguro, Y.; Miyamoto, N.; Takagi, T.; Okada, K.; Awazu, Y.; Miki, H.; Hori, A.; Kamiyama, K.; Imamura, S. *N*-Phenyl-*N*′-[4-(5*H*-pyrrolo[3,2-*d*]pyrimidin-4-yloxy)phenyl]ureas as Novel Inhibitors of VEGFR and FGFR Kinases. *Bioorg. Med. Chem.* **2010**, *18*, 7150−7163.
(468) Shieh, W.-C.; McKenna, J.; Sclafani, J. A.; Xue, S.; Girgis, M.; Vivelo, J.; Radetich, B.; Prasad, K. Syntheses of a Triad of Flt3 Kinase Inhibitors: From Bench to Pilot Plant. *Org. Process Res. Dev.* **2008**, *12*, 1146−1155.
(469) Isaacs, J. T. The Long and Winding Road for the Development of Tasquinimod as an Oral Second-Generation Quinoline-3-Carboxamide Antiangiogenic Drug for the Treatment of Prostate Cancer. *Expert Opin. Invest. Drugs* **2010**, *19*, 1235−1243.
(470) Jennbacken, K.; Welén, K.; Olsson, A.; Axelsson, B.; Törngren, M.; Damber, J.-E.; Leanderson, T. Inhibition of Metastasis in a Castration Resistant Prostate Cancer Model by the Quinoline-3-Carboxamide Tasquinimod (ABR-215050). *Prostate* **2012**, *72*, 913−924.
(471) Raymond, E.; Dalgleish, A.; Damber, J.-E.; Smith, M.; Pili, R. Mechanisms of Action of Tasquinimod on the Tumour Microenvironment. *Cancer Chemother. Pharmacol.* **2014**, *73*, 1−8.
(472) Williamson, S. C.; Hartley, A. E.; Heer, R. A Review of Tasquinimod in the Treatment of Advanced Prostate Cancer. *Drug Des., Dev. Ther.* **2013**, *7*, 167−174.

DOI: 10.1021/acs.chemrev.5b00392
Chem. Rev. 2016, 116, 422−518

(473) Dalrymple, S. L.; Becker, R. E.; Isaacs, J. T. The Quinoline-3-carboxamide Anti-Angiogenic Agent, Tasquinimod, Enhances the Anti-Prostate Cancer Efficacy of Androgen Ablation and Taxotere without Effecting Serum PSA Directly in Human Xenografts. *Prostate* **2007**, *67*, 790−797.
(474) Yamada, T.; Okada, T.; Sakaguchi, K.; Ohfune, Y.; Ueki, H.; Soloshonok, V. A. Efficient Asymmetric Synthesis of Novel 4-Substituted and Configurationally Stable Analogs of Thalidomide. *Org. Lett.* **2006**, *8*, 5625−5628.
(475) Soloshonok, V. A.; Kirilenko, A. G.; Fokina, N. A.; Kukhar, V. P.; Galushko, S. V.; Švedas, V. K.; Resnati, G. Chemo-Enzymatic Approach to the Synthesis of Each of the Four Isomers of α-Alkyl-β-Fluoroalkyl-Substituted β-Amino Acids. *Tetrahedron: Asymmetry* **1994**, *5*, 1225−1228.
(476) Bravo, P.; Farina, A.; Kukhar, V. P.; Markovsky, A. L.; Meille, S. V.; Soloshonok, V. A.; Sorochinsky, A. E.; Viani, F.; Zanda, M.; Zappalà, C. Stereoselective Additions of α-Lithiated Alkyl-*p*-tolylsulfoxides to *N*-PMP(fluoroalkyl)aldimines. An Efficient Approach to Enantiomerically Pure Fluoro Amino Compounds. *J. Org. Chem.* **1997**, *62*, 3424−3425.
(477) Isaacs, J. T.; Pili, R.; Qian, D. Z.; Dalrymple, S. L.; Garrison, J. B.; Kyprianou, N.; Björk, A.; Olsson, A.; Leanderson, T. Identification of ABR-215050 as Lead Second Generation Quinoline-3-carboxamide Anti-Angiogenic Agent for the Treatment of Prostate Cancer. *Prostate* **2006**, *66*, 1768−1778.
(478) Jönsson, S.; Andersson, G.; Fex, T.; Fristedt, T.; Hedlund, G.; Jansson, K.; Abramo, L.; Fritzson, I.; Pekarski, O.; Runström, A.; et al. Synthesis and Biological Evaluation of New 1,2-Dihydro-4-hydroxy-2-oxo-3-quinolinecarboxamides for Treatment of Autoimmune Disorders: Structure-Activity Relationship. *J. Med. Chem.* **2004**, *47*, 2075−2088.
(479) Kulke, M. H.; O'Dorisio, T.; Phan, A.; Bergsland, E.; Law, L.; Banks, P.; Freiman, J.; Frazier, K.; Jackson, J.; Yao, J. C.; et al. Telotristat Etiprate, a Novel Serotonin Synthesis Inhibitor, in Patients with Carcinoid Syndrome and Diarrhea Not Adequately Controlled by Octreotide. *Endocr.-Relat. Cancer* **2014**, *21*, 705−714.
(480) Li, Q.; Hu, W.; Yang, X.; Zhao, J.; Zhao, M. M. PCT Int. Appl. WO2012061576A1, 2012; *Chem. Abstr.* **2012**, *156*, 638087.
(481) Jin, H.; Cianchetta, G.; Devasagayaraj, A.; Gu, K.; Marinelli, B.; Samala, L.; Scott, S.; Stouch, T.; Tunoori, A.; Wang, Y.; et al. Substituted 3-(4-(1,3,5-Triazin-2-yl)-phenyl)-2-aminopropanoic Acids as Novel Tryptophan Hydroxylase Inhibitors. *Bioorg. Med. Chem. Lett.* **2009**, *19*, 5229−5232.
(482) Shi, Z.-C.; Devasagayaraj, A.; Gu, K.; Jin, H.; Marinelli, B.; Samala, L.; Scott, S.; Stouch, T.; Tunoori, A.; Wang, Y.; et al. Modulation of Peripheral Serotonin Levels by Novel Tryptophan Hydroxylase Inhibitors for the Potential Treatment of Functional Gastrointestinal Disorders. *J. Med. Chem.* **2008**, *51*, 3684−3687.
(483) Bednarz, M. S.; Burgoon, H. A., Jr.; Iimura, S.; Kanamarlapudi, R. C.; Song, Q.; Wu, W.; Yan, J.; Zhang, H. PCT Int. Appl. WO2009029499A1, 2009; *Chem. Abstr.* **2009**, *150*, 283077.
(484) Cantley, L. C. The Phosphoinositide 3-Kinase Pathway. *Science* **2002**, *296*, 1655−1657.
(485) Azab, F.; Muz, B.; de la Puente, P.; Salama, N.; Azab, A. K. Buparlisib (NVP-BKM-120). *Drugs Future* **2013**, *38*, 73−80.
(486) Maira, S.-M.; Pecchi, S.; Huang, A.; Burger, M.; Knapp, M.; Sterker, D.; Schnell, C.; Guthy, D.; Nagel, T.; Wiesmann, M.; et al. Identification and Characterization of NVP-BKM120, an Orally Available Pan-Class I PI3-Kinase Inhibitor. *Mol. Cancer Ther.* **2012**, *11*, 317−328.
(487) Pecchi, S.; Renhowe, P. A.; Taylor, C.; Kaufman, S.; Merritt, H.; Wiesmann, M.; Shoemaker, K. R.; Knapp, M. S.; Ornelas, E.; Hendrickson, T. F.; et al. Identification and Atructure−Activity Relationship of 2-Morpholino 6-(3-Hydroxyphenyl) Pyrimidines, a Class of Potent and Selective PI3 Kinase Inhibitors. *Bioorg. Med. Chem. Lett.* **2010**, *20*, 6895−6898.
(488) Burger, M. T.; Knapp, M.; Wagman, A.; Ni, Z.-J.; Hendrickson, T.; Atallah, G.; Zhang, Y.; Frazier, K.; Verhagen, J.; Pfister, K.; et al. Synthesis and in Vitro and in Vivo Evaluation of Phosphoinositide-3-kinase Inhibitors. *ACS Med. Chem. Lett.* **2011**, *2*, 34−38.
(489) Burger, M. T.; Pecchi, S.; Wagman, A.; Ni, Z.-J.; Knapp, M.; Hendrickson, T.; Atallah, G.; Pfister, K.; Zhang, Y.; Bartulis, S.; et al. Identification of NVP-BKM120 as a Potent, Selective, Orally Bioavailable Class I PI3 Kinase Inhibitor for Treating Cancer. *ACS Med. Chem. Lett.* **2011**, *2*, 774−779.
(490) Narayanan, R.; Mohler, M. L.; Bohl, C. E.; Miller, D. D.; Dalton, J. T. Selective Androgen Receptor Modulators in Preclinical and Clinical Development. *Nucl. Recept. Signal.* **2008**, *6*, e010.
(491) Gao, W.; Kim, J.; Dalton, J. T. Pharmacokinetics and Pharmacodynamics of Nonsteroidal Androgen Receptor Ligands. *Pharm. Res.* **2006**, *23*, 1641−1658.
(492) He, Y.; Yin, D.; Perera, M.; Kirkovsky, L.; Stourman, N.; Li, W.; Dalton, J. T.; Miller, D. D. Novel Nonsteroidal Ligands with High Binding Affinity and Potent Functional Activity for the Androgen Receptor. *Eur. J. Med. Chem.* **2002**, *37*, 619−634.
(493) Yin, D.; Xu, H.; He, Y.; Kirkovsky, L. I.; Miller, D. D.; Dalton, J. T. Pharmacology, Pharmacokinetics, and Metabolism of Acetothiolutamide, a Novel Nonsteroidal Agonist for the Androgen Receptor. *J. Pharmacol. Exp. Ther.* **2003**, *304*, 1323−1333.
(494) Yin, D.; Gao, W.; Kearbey, J. D.; Xu, H.; Chung, K.; He, Y.; Marhefka, C. A.; Veverka, K. A.; Miller, D. D.; Dalton, J. T. Pharmacodynamics of Selective Androgen Receptor Modulators. *J. Pharmacol. Exp. Ther.* **2003**, *304*, 1334−1340.
(495) Gao, W.; Reiser, P. J.; Coss, C. C.; Phelps, M. A.; Kearbey, J. D.; Miller, D. D.; Dalton, J. T. Selective Androgen Receptor Modulator Treatment Improves Muscle Strength and Body Composition and Prevents Bone Loss in Orchidectomized Rats. *Endocrinology* **2005**, *146*, 4887−4897.
(496) Kearbey, J. D.; Wu, D.; Gao, W.; Miller, D. D.; Dalton, J. T. Pharmacokinetics of *S*-3-(4-Acetylamino-phenoxy)-2-hydroxy-2-methyl-*N*-(4-nitro-3-trifluoromethyl-phenyl)-propionamide in Rats, a Non-Steroidal Selective Androgen Receptor Modulator. *Xenobiotica* **2004**, *34*, 273−280.
(497) Kim, J.; Wu, D.; Hwang, D. J.; Miller, D. D.; Dalton, J. T. The *Para* Substituent of *S*-3-(Phenoxy)-2-hydroxy-2-methyl-*N*-(4-nitro-3-trifluoromethyl-phenyl)-propionamides Is a Major Structural Determinant of in Vivo Disposition and Activity of Selective Androgen Receptor Modulators. *J. Pharmacol. Exp. Ther.* **2005**, *315*, 230−239.
(498) Ahn, T.; Dalton, J. T.; Dickason, D.; Hong, D.; Bird, T. G. PCT Int. Appl. WO2009036206A1, 2009; *Chem. Abstr.* **2009**, *150*, 329423.
(499) Pan, S.; Gray, N. S.; Gao, W.; Mi, Y.; Fan, Y.; Wang, X.; Tuntland, T.; Che, J.; Lefebvre, S.; Chen, Y.; et al. Discovery of BAF312 (Siponimod), a Potent and Selective S1P Receptor Modulator. *ACS Med. Chem. Lett.* **2013**, *4*, 333−337.
(500) Gergely, P.; Nuesslein-Hildesheim, B.; Guerini, D.; Brinkmann, V.; Traebert, M.; Bruns, C.; Pan, S.; Gray, N. S.; Hinterding, K.; Cooke, N. G.; et al. The Selective Sphingosine 1-Phosphate Receptor Modulator BAF312 Redirects Lymphocyte Distribution and Has Species-Specific Effects on Heart Rate. *Br. J. Pharmacol.* **2012**, *167*, 1035−1047.
(501) Selmaj, K.; Li, D. K. B.; Hartung, H.-P.; Hemmer, B.; Kappos, L.; Freedman, M. S.; Stüve, O.; Rieckmann, P.; Montalban, X.; Ziemssen, T.; et al. Siponimod for Patients with Relapsing-Remitting Multiple Sclerosis (BOLD): An Adaptive, Dose-Ranging, Randomised, Phase 2 Study. *Lancet Neurol.* **2013**, *12*, 756−767.
(502) Brinkmann, V.; Billich, A.; Baumruker, T.; Heining, P.; Schmouder, R.; Francis, G.; Aradhye, S.; Burtin, P. Fingolimod (FTY720): Discovery and Development of an Oral Drug to Treat Multiple Sclerosis. *Nat. Rev. Drug Discovery* **2010**, *9*, 883−897.
(503) Pan, S.; Gao, W.; Gray, N. S.; Mi, Y.; Fan, Y. PCT Int. Appl. WO2004103306A2, 2004; *Chem. Abstr.* **2004**, *142*, 23084.
(504) Leppert, D.; Wallstroem, E.; Nuesslein-Hildesheim, B. PCT Int. Appl. WO2010020610A1, 2010; *Chem. Abstr.* **2010**, *152*, 304133.
(505) Liu, Y.; Papoutsakis, D.; Roddy, E. PCT Int. Appl. WO2010071794A1, 2010; *Chem. Abstr.* **2010**, *153*, 97605.

DOI: 10.1021/acs.chemrev.5b00392
Chem. Rev. 2016, 116, 422−518

(506) Ciszewski, L.; de la Cruz, M.; Karpinski, P. H.; Mutz, M.; Riegert, C.; Vogel, C.; Schneeberger, R. PCT Int. Appl. WO2010080409A1, 2010; *Chem. Abstr.* **2010**, *153*, 184545.
(507) Gallou, F.; Sedelmeier, J. M.; Vogel, C. PCT Int. Appl. WO2013113915A1, 2013; *Chem. Abstr.* **2013**, *159*, 347862.
(508) Jones, C. W.; Sanderson, W. R.; Sankey, J. P. Eur. Pat. Appl. EP700885A1; *Chem. Abstr.* **1996**, *124*, 342829.
(509) Cowell, A. B.; Tamborski, C. Fluoroalkylation of Aromatic Compounds. *J. Fluorine Chem.* **1981**, *17*, 345−356.
(510) Naumann, D.; Kischkewitz, J. Trifluoromethylation Reactions of Bis(Trifluoromethyl) Telluride with Halobenzenes and with Methylbenzenes. *J. Fluorine Chem.* **1990**, *47*, 283−299.
(511) Wang, C.-L. J. Fluorination by Sulfur Tetrafluoride. *Organic Reactions*; John Wiley & Sons: 2004 (accessed July 2, 2015). DOI: 10.1002/0471264180.or034.02.
(512) Hafner, A.; Bräse, S. Trifluoromethylation of 1-Aryl-3,3-diisopropyltriazenes. *Adv. Synth. Catal.* **2013**, *355*, 996−1000.
(513) Warnke, C.; Meyer zu Hörste, G.; Hartung, H.-P.; Stüve, O.; Kieseier, B. C. Review of Teriflunomide and its Potential in the Treatment of Multiple Sclerosis. *Neuropsychiatr. Dis. Treat.* **2009**, *5*, 333−340.
(514) Wird, S. G. W.; Heubach, G. Ger. Patent DE2524959A1, 1976; *Chem. Abstr.* **1977**, *86*, 72626.
(515) Kaemmerer, F. J.; Schleyerbach, R. U.S. Patent US 4,351,841, 1982; *Chem. Abstr.* **1980**, *93*, 239392.
(516) Williamson, R. A.; Yea, C. M.; Robson, P. A.; Curnock, A. P.; Gadher, S.; Hambleton, A. B.; Woodward, K.; Bruneau, J.-M.; Hambleton, P.; Moss, D.; et al. Dihydroorotate Dehydrogenase Is a High Affinity Binding Protein for A77 1726 and Mediator of a Range of Biological Effects of the Immunomodulatory Compound. *J. Biol. Chem.* **1995**, *270*, 22467−22472.
(517) Liu, S.; Neidhardt, E. A.; Grossman, T. H.; Ocain, T.; Clardy, J. Structures of Human Dihydroorotate Dehydrogenase in Complex with Antiproliferative Agents. *Structure* **2000**, *8*, 25−33.
(518) Bartlett, R. R.; Kämmerer, F.-J. PCT Int. Appl. WO9117748A1, 1991; *Chem. Abstr.* **1992**, *116*, 128908.
(519) Métro, T.-X.; Bonnamour, J.; Reidon, T.; Sarpoulet, J.; Martinez, J.; Lamaty, F. Mechanosynthesis of Amides in the Total Absence of Organic Solvent from Reaction to Product Recovery. *Chem. Commun.* **2012**, *48*, 11781−11783.
(520) Hirth, K. P.; Schwartz, D. P.; Mann, E.; Shawver, L. K.; Keri, G.; Szekely, I.; Bajor, T.; Haimichael, J.; Orfi, L.; Levitzki, A.; et al. U.S. Patent US5990141A, 1999; *Chem. Abstr.* **1999**, *131*, 346563.
(521) Uckun, F. M.; Zheng, Y.; Ghosh, S. PCT Int. Appl. WO9954286A2, 1999; *Chem. Abstr.* **1999**, *131*, 299368.
(522) Hachtel, J.; Neises, B.; Schwab, W.; Utz, R.; Zahn, M. U.S. Patent US20040186173A1, 2004; *Chem. Abstr.* **2004**, *141*, 295750.
(523) Deo, K.; Patel, S.; Dhol, S.; Sanghani, S.; Ray, V. PCT Int. Appl. WO2009147624A2, 2009; *Chem. Abstr.* **2009**, *152*, 37215.
(524) Deo, K.; Patel, S.; Dhol, S.; Sanghani, S.; Ray, V. PCT Int. Appl. WO2010013159A1, 2010; *Chem. Abstr.* **2010**, *152*, 214931.
(525) Chen, G.; Sun, L. Chin. Patent CN102786437A, 2012; *Chem. Abstr.* **2012**, *158*, 11317.
(526) Guidot, G.; Rochin, C.; Saint-Jalmes, L. PCT Int. Appl. WO2001002337A1, 2001; *Chem. Abstr.* **2001**, *134*, 100636.
(527) Du, X.; Xu, Z. Chin. Patent CN101016255A, 2007; *Chem. Abstr.* **2007**, *147*, 322709.
(528) Su, W.; Li, Y.; Cai, H. Chin. Patent CN1475480A, 2004; *Chem. Abstr.* **2004**, *142*, 392187.
(529) DeVita, R. J.; Pinto, S. Current Status of the Research and Development of Diacylglycerol *O*-Acyltransferase 1 (DGAT1) Inhibitors. *J. Med. Chem.* **2013**, *56*, 9820−9825.
(530) Birch, A. M.; Buckett, L. K.; Turnbull, A. V. DGAT1 Inhibitors as Anti-Obesity and Anti-Diabetic Agents. *Curr. Opin. Drug Discovery Dev.* **2010**, *13*, 489−496.
(531) Zhang, X.-D.; Yan, J.-W.; Yan, G.-R.; Sun, X.-Y.; Ji, J.; Li, Y.-M.; Hu, Y.-H.; Wang, H.-Y. Pharmacological Inhibition of Diacylglycerol Acyltransferase 1 Reduces Body Weight Gain, Hyperlipidemia, and Hepatic Steatosis in *Db/Db* Mice. *Acta Pharmacol. Sin.* **2010**, *31*, 1470−1477.
(532) Jian, Z.; Ray, T.; Wu, A.; Jones, L.; Forseth, R. Proton Exchange Reactions in Isotope Chemistry (II) Synthesis of Stable Isotope-Labeled LCQ908. *J. Labelled Compd. Radiopharm.* **2014**, *57*, 670−673.
(533) Fox, B. M.; Sugimoto, K.; Iio, K.; Yoshida, A.; Zhang, J. K.; Li, K.; Hao, X.; Labelle, M.; Smith, M.-L.; Rubenstein, S. M.; et al. Discovery of 6-Phenylpyrimido[4,5-b][1,4]oxazines as Potent and Selective Acyl CoA:Diacylglycerol Acyltransferase 1 (DGAT1) Inhibitors with in Vivo Efficacy in Rodents. *J. Med. Chem.* **2014**, *57*, 3464−3483.
(534) Serrano-Wu, M. H.; Coppola, G. M.; Gong, Y.; Neubert, A. D.; Chatelain, R.; Clairmont, K. B.; Commerford, R.; Cosker, T.; Daniels, T.; Hou, Y.; et al. Intestinally Targeted Diacylglycerol Acyltransferase 1 (DGAT1) Inhibitors Robustly Suppress Postprandial Triglycerides. *ACS Med. Chem. Lett.* **2012**, *3*, 411−415.
(535) Serrano-Wu, M. H.; Kwak, Y.-S.; Liu, W. PCT Int. Appl. WO2007126957A2, 2007; *Chem. Abstr.* **2007**, *147*, 522280.
(536) Saliu, O. Y.; Crismale, C.; Schwander, S. K.; Wallis, R. S. Bactericidal Activity of OPC-67683 against Drug-Tolerant Mycobacterium Tuberculosis. *J. Antimicrob. Chemother.* **2007**, *60*, 994−998.
(537) Xavier, A. S.; Lakshmanan, M. Delamanid: A New Armor in Combating Drug-Resistant Tuberculosis. *J. Pharmacol. Pharmacother.* **2014**, *5*, 222−224.
(538) Gler, M. T.; Skripconoka, V.; Sanchez-Garavito, E.; Xiao, H.; Cabrera-Rivero, J. L.; Vargas-Vasquez, D. E.; Gao, M.; Awad, M.; Park, S.-K.; Shim, T. S.; et al. Delamanid for Multidrug-Resistant Pulmonary Tuberculosis. *N. Engl. J. Med.* **2012**, *366*, 2151−2160.
(539) Blair, H. A.; Scott, L. J. Delamanid: A Review of Its Use in Patients with Multidrug-Resistant Tuberculosis. *Drugs* **2015**, *75*, 91−100.
(540) Ashtekar, D. R.; Costa-Perira, R.; Nagrajan, K.; Vishvanathan, N.; Bhatt, A. D.; Rittel, W. In Vitro and In Vivo Activities of the Nitroimidazole CGI 17341 against *Mycobacterium tuberculosis*. *Antimicrob. Agents Chemother.* **1993**, *37*, 183−186.
(541) Stover, C. K.; Warrener, P.; VanDevanter, D. R.; Sherman, D. R.; Arain, T. M.; Langhorne, M. H.; Anderson, S. W.; Towell, J. A.; Yuan, Y.; McMurray, D. N.; et al. A Small-Molecule Nitroimidazopyran Drug Candidate for the Treatment of Tuberculosis. *Nature* **2000**, *405*, 962−966.
(542) Kmentova, I.; Sutherland, H. S.; Palmer, B. D.; Blaser, A.; Franzblau, S. G.; Wan, B.; Wang, Y.; Ma, Z.; Denny, W. A.; Thompson, A. M. Synthesis and Structure-Activity Relationships of Aza- and Diazabiphenyl Analogues of the Antitubercular Drug (6*S*)-2-Nitro-6-{[4-(trifluoromethoxy)benzyl]oxy}-6,7-dihydro-5H-imidazo-[2,1-b][1,3]oxazine (PA-824). *J. Med. Chem.* **2010**, *53*, 8421−8439.
(543) Sasaki, H.; Haraguchi, Y.; Itotani, M.; Kuroda, H.; Hashizume, H.; Tomishige, T.; Kawasaki, M.; Matsumoto, M.; Komatsu, M.; Tsubouchi, H. Synthesis and Antituberculosis Activity of a Novel Series of Optically Active 6-Nitro-2,3-dihydroimidazo[2,1-*b*]oxazoles. *J. Med. Chem.* **2006**, *49*, 7854−7860.
(544) Matsumoto, M.; Hashizume, H.; Tomishige, T.; Kawasaki, M.; Tsubouchi, H.; Sasaki, H.; Shimokawa, Y.; Komatsu, M. OPC-67683, a Nitro-Dihydro-Imidazooxazole Derivative with Promising Action against Tuberculosis In Vitro and In Mice. *PLoS Med.* **2006**, *3*, e466.
(545) Diacon, A. H.; Dawson, R.; Hanekom, M.; Narunsky, K.; Venter, A.; Hittel, N.; Geiter, L. J.; Wells, C. D.; Paccaly, A. J.; Donald, P. R. Early Bactericidal Activity of Delamanid (OPC-67683) in Smear-Positive Pulmonary Tuberculosis Patients. *Int. J. Tuberc. Lung Dis.* **2011**, *15*, 949−954.
(546) Quartara, L.; Maggi, C. A. The Tachykinin NK_1 Receptor. Part I: Ligands and Mechanisms of Cellular Activation. *Neuropeptides* **1997**, *31*, 537−563.
(547) Almeida, T. A.; Rojo, J.; Nieto, P. M.; Pinto, F. M.; Hernandez, M.; Martín, J. D.; Candenas, M. L. Tachykinins and Tachykinin Receptors: Structure and Activity Relationships. *Curr. Med. Chem.* **2004**, *11*, 2045−2081.

DOI: 10.1021/acs.chemrev.5b00392
Chem. Rev. 2016, 116, 422−518

(548) Gan, T. J. Mechanisms Underlying Postoperative Nausea and Vomiting and Neurotransmitter Receptor Antagonist-Based Pharmacotherapy. *CNS Drugs* **2007**, *21*, 813−833.
(549) Reddy, G. K.; Gralla, R. J.; Hesketh, P. J. Novel Neurokinin-1 Antagonists as Antiemetics for the Treatment of Chemotherapy-Induced Emesis. *Supportive Cancer Ther.* **2006**, *3*, 140−142.
(550) Duffy, R. A. Potential Therapeutic Targets for Neurokinin-1 Receptor Antagonists. *Expert Opin. Emerging Drugs* **2004**, *9*, 9−21.
(551) Quartara, L.; Altamura, M.; Evangelista, S.; Maggi, C. A. Tachykinin Receptor Antagonists in Clinical Trials. *Expert Opin. Invest. Drugs* **2009**, *18*, 1843−1864.
(552) Albert, J. S. Neurokinin Antagonists and their Potential Role in Treating Depression and other Stress Disorders. *Expert Opin. Ther. Pat.* **2004**, *14*, 1421−1433.
(553) Dando, T. M.; Perry, C. M. Aprepitant. A Review of its Use in the Prevention of Chemotherapy-Induced Nausea and Vomiting. *Drugs* **2004**, *64*, 777−794.
(554) Navari, R. M. Profile of Netupitant/Palonosetron (NEPA) Fixed Dose Combination and its Potential in the Treatment of Chemotherapy-Induced Nausea and Vomiting (CINV). *Drug Des., Dev. Ther.* **2015**, *9*, 155−161.
(555) Gan, T. J.; Gu, J.; Singla, N.; Chung, F.; Pearman, M. H.; Bergese, S. D.; Habib, A. S.; Candiotti, K. A.; Mo, Y.; Huyck, S.; et al. Rolapitant for the Prevention of Postoperative Nausea and Vomiting: A Prospective, Double-Blinded, Placebo-Controlled Randomized Trial. *Anesth. Analg.* **2011**, *112*, 804−812.
(556) Duffy, R. A.; Morgan, C.; Naylor, R.; Higgins, G. A.; Varty, G. B.; Lachowicz, J. E.; Parker, E. M. Rolapitant (SCH 619734): A Potent, Selective and Orally Active Neurokinin NK1 Receptor Antagonist with Centrally-Mediated Antiemetic Effects in Ferrets. *Pharmacol., Biochem. Behav.* **2012**, *102*, 95−100.
(557) Syed, Y. Y. Rolapitant: First Global Approval. *Drugs* **2015**, *75*, 1941−1945.
(558) Hoffmann, T.; Bös, M.; Stadler, H.; Schnider, P.; Hunkeler, W.; Godel, T.; Galley, G.; Ballard, T. M.; Higgins, G. A.; Poli, S. M.; et al. Design and Synthesis of a Novel, Achiral Class of Highly Potent and Selective, Orally Active Neurokinin-1 Receptor Antagonists. *Bioorg. Med. Chem. Lett.* **2006**, *16*, 1362−1365.
(559) Harrison, T.; Williams, B. J.; Swain, C. J. *Gem*-Disubstituted Amino-Ether Based Substance P Antagonists. *Bioorg. Med. Chem. Lett.* **1994**, *4*, 2733−2734.
(560) Xiao, D.; Lavey, B. J.; Palani, A.; Wang, C.; Aslanian, R. G.; Kozlowski, J. A.; Shih, N.-Y.; McPhail, A. T.; Randolph, G. P.; Lachowicz, J. E.; et al. Selective Benzylic Lithiation of *N*-Boc-2-Phenylpiperidine and Pyrrolidine: Expedient Synthesis of a 2,2-Disubstituted Piperidine NK1 Antagonist. *Tetrahedron Lett.* **2005**, *46*, 7653−7656.
(561) Xiao, D.; Wang, C.; Tsui, H.-C.; Palani, A.; Aslanian, R.; Buevich, A. V. Conformation of *gem*-Disubstituted Alkylarylpiperidines and their Implication in Design and Synthesis of a Conformationally-Rigidified NK_1 Antagonist. *Tetrahedron Lett.* **2013**, *54*, 6199−6203.
(562) Paliwal, S.; Reichard, G. A.; Wang, C.; Xiao, D.; Tsui, H.-C.; Shih, N.-Y.; Arredondo, J. D.; Wrobleski, M. L.; Palani, A. PCT Int. Appl. WO2003051840A1, 2003; *Chem. Abstr.* **2003**, *139*, 69145.
(563) Duffy, R. A.; Varty, G. B.; Morgan, C. A.; Lachowicz, J. E. Correlation of Neurokinin (NK) 1 Receptor Occupancy in Gerbil Striatum with Behavioral Effects of NK1 Antagonists. *J. Pharmacol. Exp. Ther.* **2002**, *301*, 536−542.
(564) Hoffmann-Emery, F.; Hilpert, H.; Scalone, M.; Waldmeier, P. Efficient Synthesis of Novel NK1 Receptor Antagonists: Selective 1,4-Addition of Grignard Reagents to 6-Chloronicotinic Acid Derivatives. *J. Org. Chem.* **2006**, *71*, 2000−2008.
(565) Harrington, P. J.; Johnston, D.; Moorlag, H.; Wong, J.-W.; Hodges, L. M.; Harris, L.; McEwen, G. K.; Smallwood, B. Research and Development of an Efficient Process for the Construction of the 2,4,5-Substituted Pyridines of NK-1 Receptor Antagonists. *Org. Process Res. Dev.* **2006**, *10*, 1157−1166.
(566) Mergelsberg, I.; Scherer, D. H.; Huttenloch, M. E.; Tsui, H.-C.; Paliwal, S.; Shih, N.-Y. PCT Int. Appl. WO2008118328A2, 2008; *Chem. Abstr.* **2008**, *149*, 425823.
(567) Wu, G. G.; Werne, G.; Fu, X.; Orr, R. K.; Chen, F. X.; Cui, J.; Sprague, V. M.; Zhang, F.; Xie, J.; Zeng, L.; et al. PCT Int. Appl. WO2010028232A1, 2010; *Chem. Abstr.* **2010**, *152*, 335075.
(568) Li, C.; Zhang, W.; Zhou, F.; Chen, C.; Zhou, L.; Li, Y.; Liu, L.; Pei, F.; Luo, H.; Hu, Z.; et al. Cholesteryl Ester Transfer Protein Inhibitors in the Treatment of Dyslipidemia: A Systematic Review and Meta-Analysis. *PLoS One* **2013**, *8*, e77049.
(569) Katz, P. M.; Leiter, L. A. Drugs Targeting High-Density Lipoprotein Cholesterol for Coronary Artery Disease Management. *Can. J. Cardiol.* **2012**, *28*, 667−677.
(570) Cao, G.; Beyer, T. P.; Zhang, Y.; Schmidt, R. J.; Chen, Y. Q.; Cockerham, S. L.; Zimmerman, K. M.; Karathanasis, S. K.; Cannady, E. A.; Fields, T.; et al. Evacetrapib is a Novel, Potent, and Selective Inhibitor of Cholesteryl Ester Transfer Protein that Elevates HDL Cholesterol without Inducing Aldosterone or Increasing Blood Pressure. *J. Lipid Res.* **2011**, *52*, 2169−2176.
(571) Nicholls, S. J.; Brewer, H. B.; Kastelein, J. J. P.; Krueger, K. A.; Wang, M.-D.; Shao, M.; Hu, B.; McErlean, E.; Nissen, S. E. Effects of the CETP Inhibitor Evacetrapib Administered as Monotherapy or in Combination With Statins on HDL and LDL Cholesterol. *JAMA, J. Am. Med. Assoc.* **2011**, *306*, 2099−2109.
(572) Mantlo, N. B.; Escribano, A. Update on the Discovery and Development of Cholesteryl Ester Transfer Protein Inhibitors for Reducing Residual Cardiovascular Risk. *J. Med. Chem.* **2014**, *57*, 1−17.
(573) Soloshonok, V. A.; Yasumoto, M. Simple and Convenient Synthesis of 3,5-bis-(Trifluoromethyl)benzylamine via 1,3-Proton Shift Reaction. *J. Fluorine Chem.* **2006**, *127*, 889−893.
(574) Chen, X.; Frank, S. A.; Remick, D. M.; Pedersen, S. W. U.S. Patent US2010331309A1, 2010; *Chem. Abstr.* **2010**, *154*, 118675.
(575) Frederick, M. O.; Frank, S. A.; Vicenzi, J. T.; LeTourneau, M. E.; Berglund, K. D.; Edward, A. W.; Alt, C. A. Development of a Hydrogenative Reductive Amination for the Synthesis of Evacetrapib: Unexpected Benefits of Water. *Org. Process Res. Dev.* **2014**, *18*, 546−551.
(576) Dumas, L.; Payne, H.; Chowdhury, S. The Evolution of Antiandrogens: MDV3100 Comes of Age. *Expert Rev. Anticancer Ther.* **2012**, *12*, 131−133.
(577) Tran, C.; Ouk, S.; Clegg, N. J.; Chen, Y.; Watson, P. A.; Arora, V.; Wongvipat, J.; Smith-Jones, P. M.; Yoo, D.; Kwon, A.; et al. Development of a Second-Generation Antiandrogen for Treatment of Advanced Prostate Cancer. *Science* **2009**, *324*, 787−790.
(578) Nadal, R.; Taplin, M.-E.; Bellmunt, J. Enzalutamide for the Treatment of Prostate Cancer: Results and Implications of the AFFIRM Trial. *Future Oncol.* **2014**, *10*, 351−362.
(579) Jung, M. E.; Ouk, S.; Yoo, D.; Sawyers, C. L.; Chen, C.; Tran, C.; Wongvipat, J. Structure-Activity Relationship for Thiohydantoin Androgen Receptor Antagonists for Castration-Resistant Prostate Cancer (CRPC). *J. Med. Chem.* **2010**, *53*, 2779−2796.
(580) Acar, Ö.; Esen, T.; Lack, N. A. New Therapeutics to Treat Castrate-Resistant Prostate Cancer. *Sci. World J.* **2013**, *2013*, 379641.
(581) Hoffman-Censits, J.; Kelly, W. K. Enzalutamide: A Novel Antiandrogen for Patients with Castrate-Resistant Prostate Cancer. *Clin. Cancer Res.* **2013**, *19*, 1335−1339.
(582) Jain, R. P.; Angelaud, R.; Thompson, A.; Lamberson, C.; Greenfield, S. PCT Int. Appl. WO2011106570A1, 2011; *Chem. Abstr.* **2011**, *155*, 380335.
(583) Miura, K.; Satoh, M.; Kinouchi, M.; Yamamoto, K.; Hasegawa, Y.; Philchenkov, A.; Kakugawa, Y.; Fujiya, T. The Preclinical Development of Regorafenib for the Treatment of Colorectal Cancer. *Expert Opin. Drug Discovery* **2014**, *9*, 1087−1101.
(584) Wilhelm, S. M.; Dumas, J.; Adnane, L.; Lynch, M.; Carter, C. A.; Schütz, G.; Thierauch, K.-H.; Zopf, D. Regorafenib (BAY 73−4506): A New Oral Multikinase Inhibitor of Angiogenic, Stromal and Oncogenic Receptor Tyrosine Kinases with Potent Preclinical Antitumor Activity. *Int. J. Cancer* **2011**, *129*, 245−255.

DOI: 10.1021/acs.chemrev.5b00392
Chem. Rev. 2016, 116, 422−518

(585) Smith, R. A.; Barbosa, J.; Blum, C. L.; Bobko, M. A.; Caringal, Y. V.; Dally, R.; Johnson, J. S.; Katz, M. E.; Kennure, N.; Kingery-Wood, J.; et al. Discovery of Heterocyclic Ureas as a New Class of Raf Kinase Inhibitors: Identification of a Second Generation Lead by a Combinatorial Chemistry Approach. *Bioorg. Med. Chem. Lett.* **2001**, *11*, 2775−2778.
(586) Khire, U. R.; Bankston, D.; Barbosa, J.; Brittelli, D. R.; Caringal, Y.; Carlson, R.; Dumas, J.; Gane, T.; Heald, S. L.; Hibner, B.; et al. Omega-carboxypyridyl substituted ureas as Raf kinase inhibitors: SAR of the amide substituent. *Bioorg. Med. Chem. Lett.* **2004**, *14*, 783−786.
(587) Lowinger, T. B.; Riedl, B.; Dumas, J.; Smith, R. A. Design and Discovery of Small Molecules Targeting Raf-1 Kinase. *Curr. Pharm. Des.* **2002**, *8*, 2269−2278.
(588) Wilhelm, S.; Carter, C.; Lynch, M.; Lowinger, T.; Dumas, J.; Smith, R. A.; Schwartz, B.; Simantov, R.; Kelley, S. Discovery and Development of Sorafenib: A Multikinase Inhibitor for Treating Cancer. *Nat. Rev. Drug Discovery* **2006**, *5*, 835−844.
(589) Stiehl, J.; Heilmann, W.; Lögers, M.; Rehse, J.; Gottfried, M.; Wichmann, S. PCT Int. Appl. WO2011128261A1, 2011; *Chem. Abstr.* **2011**, *155*, 536001.
(590) Pinard, E.; Alanine, A.; Alberati, D.; Bender, M.; Borroni, E.; Bourdeaux, P.; Brom, V.; Burner, S.; Fischer, H.; Hainzl, D.; et al. Selective GlyT1 Inhibitors: Discovery of [4-(3-Fluoro-5-trifluoromethylpyridin-2-yl)piperazin-1-yl]-[5-methanesulfonyl-2-((*S*)-2,2,2-trifluoro-1-methylethoxy)phenyl]methanone (RG1678), a Promising Novel Medicine To Treat Schizophrenia. *J. Med. Chem.* **2010**, *53*, 4603−4614.
(591) Lindsley, C. W.; Wolkenberg, S. E.; Kinney, G. G. Progress in the Preparation and Testing of Glycine Transporter Type-1 (GlyT1) Inhibitors. *Curr. Top. Med. Chem.* **2006**, *6*, 1883−1896.
(592) Javitt, D. C. Glutamate and Schizophrenia: Phencyclidine, N-Methyl-D-Aspartate Receptors, and Dopamine−Glutamate Interactions. *Int. Rev. Neurobiol.* **2007**, *78*, 69−108.
(593) Pinard, E.; Alberati, D.; Borroni, E.; Fischer, H.; Hainzl, D.; Jolidon, S.; Moreau, J.-L.; Narquizian, R.; Nettekoven, M.; Norcross, R. D.; et al. Discovery of Benzoylpiperazines as a Novel Class of Potent and Selective GlyT1 Inhibitors. *Bioorg. Med. Chem. Lett.* **2008**, *18*, 5134−5139.
(594) Purohit, V.; Basu, A. K. Mutagenicity of Nitroaromatic Compounds. *Chem. Res. Toxicol.* **2000**, *13*, 673−692.
(595) Sanguinetti, M. C.; Tristani-Firouzi, M. hERG Potassium Channels and Cardiac Arrhythmia. *Nature* **2006**, *440*, 463−469.
(596) Jamieson, C.; Moir, E. M.; Rankovic, Z.; Wishart, G. Medicinal Chemistry of hERG Optimizations: Highlights and Hang-Ups. *J. Med. Chem.* **2006**, *49*, 5029−5046.
(597) Chen, C.; Wu, D.; Guo, Z.; Xie, Q.; Reinhart, G. J.; Madan, A.; Wen, J.; Chen, T.; Huang, C. Q.; Chen, M.; et al. Discovery of Sodium *R*-(+)-4-{2-[5-(2-Fluoro-3-methoxyphenyl)-3-(2-fluoro-6-[trifluoromethyl]-benzyl)-4-methyl-2,6-dioxo-3,6-dihydro-2*H*-pyrimidin-1-yl]-1-phenylethylamino}butyrate (Elagolix), a Potent and Orally Available Nonpeptide Antagonist of the Human Gonadotropin-Releasing Hormone Receptor. *J. Med. Chem.* **2008**, *51*, 7478−7485.
(598) Betz, S. F.; Zhu, Y.-F.; Chen, C.; Struthers, R. S. Non-Peptide Gonadotropin-Releasing Hormone Receptor Antagonists. *J. Med. Chem.* **2008**, *51*, 3331−3348.
(599) Zhu, Y.-F.; Struthers, R. S.; Connors, P. J., Jr.; Gao, Y.; Gross, T. D.; Saunders, J.; Wilcoxen, K.; Reinhart, G. J.; Ling, N.; Chen, C. Initial Structure−Activity Relationship Studies of a Novel Series of Pyrrolo[1,2-a]pyrimid-7-ones as GnRH Receptor Antagonists. *Bioorg. Med. Chem. Lett.* **2002**, *12*, 399−402.
(600) Zhu, Y.-F.; Wilcoxen, K.; Saunders, J.; Guo, Z.; Gao, Y.; Connors, P. J., Jr.; Gross, T. D.; Tucci, F. C.; Struthers, R. S.; Reinhart, G. J.; et al. A Novel Synthesis of 2-Arylpyrrolo[1,2-a]pyrimid-7-ones and Their Structure−Activity Relationships as Potent GnRH Receptor Antagonists. *Bioorg. Med. Chem. Lett.* **2002**, *12*, 403−406.
(601) Zhu, Y.-F.; Guo, Z.; Gross, T. D.; Gao, Y.; Connors, P. J., Jr.; Struthers, R. S.; Xie, Q.; Tucci, F. C.; Reinhart, G. J.; Wu, D.; et al. Design and Structure-Activity Relationships of 2-Alkyl-3-aminomethyl-6-(3-methoxyphenyl)-7-methyl-8-(2-fluorobenzyl)imidazolo[1,2-*a*]-pyrimid-5-ones as Potent GnRH Receptor Antagonists. *J. Med. Chem.* **2003**, *46*, 1769−1772.
(602) Zhu, Y.-F.; Gross, T. D.; Guo, Z.; Connors, P. J., Jr.; Gao, Y.; Tucci, F. C.; Struthers, R. S.; Reinhart, G. J.; Saunders, J.; Chen, T. K.; et al. Identification of 1-Arylmethyl-3-(2-aminoethyl)-5-aryluracil as Novel Gonadotropin-Releasing Hormone Receptor Antagonists. *J. Med. Chem.* **2003**, *46*, 2023−2026.
(603) Guo, Z.; Zhu, Y.-F.; Tucci, F. C.; Gao, Y.; Struthers, R. S.; Saunders, J.; Gross, T. D.; Xie, Q.; Reinhart, G. J.; Chen, C. Synthesis and Structure−Activity Relationships of 1-Arylmethyl-3-(2-aminopropyl)-5-aryl-6-methyluracils as Potent GnRH Receptor Antagonists. *Bioorg. Med. Chem. Lett.* **2003**, *13*, 3311−3315.
(604) Tucci, F. C.; Zhu, Y.-F.; Guo, Z.; Gross, T. D.; Connors, P. J., Jr.; Struthers, R. S.; Reinhart, G. J.; Saunders, J.; Chen, C. Synthesis and Structure−Activity Relationships of 1-Arylmethyl-3-(1-methyl-2-amino)ethyl-5-aryl-6-methyluracils as Antagonists of the Human GnRH Receptor. *Bioorg. Med. Chem. Lett.* **2003**, *13*, 3317−3322.
(605) Guo, Z.; Zhu, Y.-F.; Gross, T. D.; Tucci, F. C.; Gao, Y.; Moorjani, M.; Connors, P. J., Jr.; Rowbottom, M. W.; Chen, Y.; Struthers, R. S.; et al. Synthesis and Structure-Activity Relationships of 1-Arylmethyl-5-aryl-6-methyluracils as Potent Gonadotropin-Releasing Hormone Receptor Antagonists. *J. Med. Chem.* **2004**, *47*, 1259−1271.
(606) Tucci, F. C.; Zhu, Y.-F.; Struthers, R. S.; Guo, Z.; Gross, T. D.; Rowbottom, M. W.; Acevedo, O.; Gao, Y.; Saunders, J.; Xie, Q.; et al. 3-[(2*R*)-Amino-2-phenylethyl]-1-(2,6-difluorobenzyl)-5-(2-fluoro-3-methoxyphenyl)-6-methylpyrimidin-2,4-dione (NBI 42902) as a Potent and Orally Active Antagonist of the Human Gonadotropin-Releasing Hormone Receptor. Design, Synthesis, and in Vitro and in Vivo Characterization. *J. Med. Chem.* **2005**, *48*, 1169−1178.
(607) Ekins, S.; Stresser, D. M.; Williams, J. A. *In vitro* and Pharmacophore Insights into CYP3A Enzymes. *Trends Pharmacol. Sci.* **2003**, *24*, 161−166.
(608) Papachristou, D. J.; Basdra, E. K.; Papavassiliou, A. G. Bone Metastases: Molecular Mechanisms and Novel Therapeutic Interventions. *Med. Res. Rev.* **2012**, *32*, 611−636.
(609) Palmer, J. T.; Bryant, C.; Wang, D.-X.; Davis, D. E.; Setti, E. L.; Rydzewski, R. M.; Venkatraman, S.; Tian, Z.-Q.; Burrill, L. C.; Mendonca, R. V.; et al. Design and Synthesis of Tri-Ring P_3 Benzamide-Containing Aminonitriles as Potent, Selective, Orally Effective Inhibitors of Cathepsin K. *J. Med. Chem.* **2005**, *48*, 7520−7534.
(610) Sani, M.; Volonterio, A.; Zanda, M. The Trifluoroethylamine Function as Peptide Bond Replacement. *ChemMedChem* **2007**, *2*, 1693−1700.
(611) Isabel, E.; Mellon, C.; Boyd, M. J.; Chauret, N.; Deschênes, D.; Desmarais, S.; Falgueyret, J.-P.; Gauthier, J. Y.; Khougaz, K.; Lau, C. K.; et al. Difluoroethylamines as an Amide Isostere in Inhibitors of Cathepsin K. *Bioorg. Med. Chem. Lett.* **2011**, *21*, 920−923.
(612) Li, C. S.; Deschenes, D.; Desmarais, S.; Falgueyret, J.-P.; Gauthier, J. Y.; Kimmel, D. B.; Léger, S.; Massé, F.; McGrath, M. E.; McKay, D. J.; et al. Identification of a Potent and Selective Non-Basic Cathepsin K Inhibitor. *Bioorg. Med. Chem. Lett.* **2006**, *16*, 1985−1989.
(613) Gauthier, J. Y.; Chauret, N.; Cromlish, W.; Desmarais, S.; Duong, L. T.; Falgueyret, J.-P.; Kimmel, D. B.; Lamontagne, S.; Léger, S.; LeRiche, T.; et al. The Discovery of Odanacatib (MK-0822), a Selective Inhibitor of Cathepsin K. *Bioorg. Med. Chem. Lett.* **2008**, *18*, 923−928.
(614) Gosselin, F.; O'Shea, P. D.; Roy, S.; Reamer, R. A.; Chen, C.-Y.; Volante, R. P. Unprecedented Catalytic Asymmetric Reduction of N-H Imines. *Org. Lett.* **2005**, *7*, 355−358.
(615) Hughes, G.; Devine, P. N.; Naber, J. R.; O'Shea, P. D.; Foster, B. S.; McKay, D. J.; Volante, R. P. Diastereoselective Reductive Amination of Aryl Trifluoromethyl Ketones and α-Amino Esters. *Angew. Chem., Int. Ed.* **2007**, *46*, 1839−1842.
(616) Soloshonok, V. A.; Ohkura, H.; Yasumoto, M. Operationally Convenient Asymmetric Synthesis of (*S*)- and (*R*)-3-Amino-4,4,4-trifluorobutanoic Acid Part II. Enantioselective Biomimetic Trans-

DOI: 10.1021/acs.chemrev.5b00392
Chem. Rev. 2016, 116, 422−518

amination of 4,4,4-Trifluoro-3-oxo-*N*-[(*R*)-1-phenylethyl)butanamide. *J. Fluorine Chem.* **2006**, *127*, 930−935.
(617) Soloshonok, V. A.; Yasumoto, M. Catalytic Asymmetric Synthesis of α-(Trifluoromethyl)benzylamine *via* Cinchonidine Derived Base-Catalyzed Biomimetic 1,3-Proton Shift Reaction. *J. Fluorine Chem.* **2007**, *128*, 170−173.
(618) Soloshonok, V. A.; Ohkura, H.; Yasumoto, M. Operationally Convenient Asymmetric Synthesis of (*S*)- and (*R*)-3-Amino-4,4,4-trifluorobutanoic Acid Part I: Enantioselective Biomimetic Transamination of Isopropyl 4,4,4-Trifluoro-3-oxobutanoate. *J. Fluorine Chem.* **2006**, *127*, 924−929.
(619) Yasumoto, M.; Ueki, H.; Soloshonok, V. A. Thermal 1,3-Proton Shift Reaction and its Application for Operationally Convenient and Improved Synthesis of α-(Trifluoromethyl)-benzylamine. *J. Fluorine Chem.* **2007**, *128*, 736−739.
(620) O'Shea, P. D.; Chen, C.-Y.; Gauvreau, D.; Gosselin, F.; Hughes, G.; Nadeau, C.; Volante, R. P. A Practical Enantioselective Synthesis of Odanacatib, a Potent Cathepsin K Inhibitor, via Triflate Displacement of an α-Trifluoromethylbenzyl Triflate. *J. Org. Chem.* **2009**, *74*, 1605−1610.
(621) Tall, A. R. Functions of Cholesterol Ester Transfer Protein and Relationship to Coronary Artery Disease Risk. *J. Clin. Lipidol.* **2010**, *4*, 389−393.
(622) Krishna, R.; Anderson, M. S.; Bergman, A. J.; Jin, B.; Fallon, M.; Cote, J.; Rosko, K.; Chavez-Eng, C.; Lutz, R.; Bloomfield, D. M.; et al. Effect of the Cholesteryl Ester Transfer Protein Inhibitor, Anacetrapib, on Lipoproteins in Patients with Dyslipidaemia and on 24-h Ambulatory Blood Pressure in Healthy Individuals: Two Double-Blind, Randomised Placebo-Controlled Phase I Studies. *Lancet* **2007**, *370*, 1907−1914.
(623) Lu, Z.; Napolitano, J. B.; Theberge, A.; Ali, A.; Hammond, M. L.; Tan, E.; Tong, X.; Xu, S. S.; Latham, M. J.; Peterson, L. B.; et al. Design of a Novel Class of Biphenyl CETP Inhibitors. *Bioorg. Med. Chem. Lett.* **2010**, *20*, 7469−7472.
(624) Thompson, C. F.; Ali, A.; Quraishi, N.; Lu, Z.; Hammond, M. L.; Sinclair, P. J.; Anderson, M. S.; Eveland, S. S.; Guo, Q.; Hyland, S. A.; et al. Discovery of Substituted Biphenyl Oxazolidinone Inhibitors of Cholesteryl Ester Transfer Protein. *ACS Med. Chem. Lett.* **2011**, *2*, 424−427.
(625) Smith, C. J.; Ali, A.; Hammond, M. L.; Li, H.; Lu, Z.; Napolitano, J.; Taylor, G. E.; Thompson, C. F.; Anderson, M. S.; Chen, Y.; et al. Biphenyl-Substituted Oxazolidinones as Cholesteryl Ester Transfer Protein Inhibitors: Modifications of the Oxazolidinone Ring Leading to the Discovery of Anacetrapib. *J. Med. Chem.* **2011**, *54*, 4880−4895.
(626) Lu, Z.; Chen, Y.-H.; Napolitano, J. B.; Taylor, G.; Ali, A.; Hammond, M. L.; Deng, Q.; Tan, E.; Tong, X.; Xu, S. S.; et al. SAR Studies on the Central Phenyl Ring of Substituted Biphenyl Oxazolidinone-Potent CETP Inhibitors. *Bioorg. Med. Chem. Lett.* **2012**, *22*, 199−203.
(627) Tan, E. Y.; Hartmann, G.; Chen, Q.; Pereira, A.; Bradley, S.; Doss, G.; Zhang, A. S.; Ho, J. Z.; Braun, M. P.; Dean, D. C.; et al. Pharmacokinetics, Metabolism, and Excretion of Anacetrapib, a Novel Inhibitor of the Cholesteryl Ester Transfer Protein, in Rats and Rhesus Monkeys. *Drug Metab. Dispos.* **2010**, *38*, 459−473.
(628) Kumar, S.; Tan, E. Y.; Hartmann, G.; Biddle, Z.; Bergman, A. J.; Dru, J.; Ho, J. Z.; Jones, A. N.; Staskiewicz, S. J.; Braun, M. P.; et al. Metabolism and Excretion of Anacetrapib, a Novel Inhibitor of the Cholesteryl Ester Transfer Protein, in Humans. *Drug Metab. Dispos.* **2010**, *38*, 474−843.
(629) Meanwell, N. A. Improving Drug Candidates by Design: A Focus on Physicochemical Properties as a Means of Improving Compound Disposition and Safety. *Chem. Res. Toxicol.* **2011**, *24*, 1420−1456.
(630) Ouellet, S. G.; Roy, A.; Molinaro, C.; Angelaud, R.; Marcoux, J.-F.; O'Shea, P. D.; Davies, I. W. Preparative Scale Synthesis of the Biaryl Core of Anacetrapib via a Ruthenium-Catalyzed Direct Arylation Reaction: Unexpected Effect of Solvent Impurity on the Arylation Reaction. *J. Org. Chem.* **2011**, *76*, 1436−1439.
(631) Ogawa, T.; Kumagai, N.; Shibasaki, M. Self-Assembling Neodymium/Sodium Heterobimetallic Asymmetric Catalyst Confined in a Carbon Nanotube Network. *Angew. Chem., Int. Ed.* **2013**, *52*, 6196−6201.
(632) Cai, A.; Zheng, D.; Qiu, R.; Mai, W.; Zhou, Y. Lipoprotein-Associated Phospholipase A2 (Lp-PLA_2): A Novel and Promising Biomarker for Cardiovascular Risks Assessment. *Dis. Markers* **2013**, *34*, 323−331.
(633) Dennis, E. A.; Cao, J.; Hsu, Y.-H.; Magrioti, V.; Kokotos, G. Phospholipase A_2 Enzymes: Physical Structure, Biological Function, Disease Implication, Chemical Inhibition, and Therapeutic Intervention. *Chem. Rev.* **2011**, *111*, 6130−6185.
(634) Bui, Q. T.; Wilensky, R. L. Darapladib. *Expert Opin. Invest. Drugs* **2010**, *19*, 161−168.
(635) Boyd, H. F.; Fell, S. C. M.; Flynn, S. T.; Hickey, D. M. B.; Ife, R. J.; Leach, C. A.; Macphee, C. H.; Milliner, K. J.; Moores, K. E.; Pinto, I. L.; et al. N-1 Substituted Pyrimidin-4-ones: Novel, Orally Active Inhibitors of Lipoprotein-Associated Phospholipase A_2. *Bioorg. Med. Chem. Lett.* **2000**, *10*, 2557−2564.
(636) Boyd, H. F.; Fell, S. C. M.; Hickey, D. M. B.; Ife, R. J.; Leach, C. A.; Macphee, C. H.; Milliner, K. J.; Pinto, I. L.; Rawlings, D. A.; Smith, S. A.; et al. Potent, Orally Active Inhibitors of Lipoprotein-Associated Phospholipase A_2: 1-(Biphenylmethylamidoalkyl)-pyrimidones. *Bioorg. Med. Chem. Lett.* **2002**, *12*, 51−55.
(637) Blackie, J. A.; Bloomer, J. C.; Brown, M. J. B.; Cheng, H.-Y.; Elliott, R. L.; Hammond, B.; Hickey, D. M. B.; Ife, R. J.; Leach, C. A.; Lewis, V. A.; et al. The Discovery of SB-435495: A Potent, Orally Active Inhibitor of Lipoprotein-Associated Phospholipase A_2 for Evaluation in Man. *Bioorg. Med. Chem. Lett.* **2002**, *12*, 2603−2606.
(638) Blackie, J. A.; Bloomer, J. C.; Brown, M. J. B.; Cheng, H.-Y.; Hammond, B.; Hickey, D. M. B.; Ife, R. J.; Leach, C. A.; Lewis, V. A.; Macphee, C. H.; et al. The Identification of Clinical Candidate SB-480848: A Potent Inhibitor of Lipoprotein-Associated Phospholipase A_2. *Bioorg. Med. Chem. Lett.* **2003**, *13*, 1067−1070.
(639) Hickey, D. M. B.; Ife, R. J.; Leach, C. A.; Pinto, I. L.; Smith, S. A.; Stanway, S. J. PCT Int. Appl. WO2001060805A1, 2001; *Chem. Abstr.* **2001**, *135*, 195570.
(640) Cardwell, K. S.; Crawford, C. F.; Davies, S. H.; Wade, C. E. PCT Int. Appl. WO2011146494A1, 2011; *Chem. Abstr.* **2011**, *155*, 683770.
(641) Leermann, T.; Leroux, F. R.; Colobert, F. Highly Efficient One-Pot Access to Functionalized Arylboronic Acids via Noncryogenic Bromine/Magnesium Exchanges. *Org. Lett.* **2011**, *13*, 4479−4481.
(642) Soloshonok, V. A.; Berbasov, D. O. Self-Disproportionation of Enantiomers on Achiral Phase Chromatography. One More Example of Fluorine's Magic Powers. *Chim. Oggi/Chem. Today* **2006**, *24*, 44−47.
(643) Soloshonok, V. A. Remarkable Amplification of the Self-Disproportionation of Enantiomers on Achiral-Phase Chromatography Columns. *Angew. Chem., Int. Ed.* **2006**, *45*, 766−769.
(644) Soloshonok, V. A.; Roussel, C.; Kitagawa, O.; Sorochinsky, A. E. Self-Disproportionation of Enantiomers via Achiral Chromatography: A Warning and Extra Dimension in Optical Purifications. *Chem. Soc. Rev.* **2012**, *41*, 4180−4188.
(645) Sorochinsky, A. E.; Katagiri, T.; Ono, T.; Wzorek, A.; Aceña, J. L.; Soloshonok, V. A. Optical Purifications via Self-Disproportionation of Enantiomers by Achiral Chromatography: Case Study of a Series of α-CF_3-Containing Secondary Alcohols. *Chirality* **2013**, *25*, 365−368.
(646) Wzorek, A.; Klika, K. D.; Drabowicz, J.; Sato, A.; Aceña, J. L.; Soloshonok, V. A. The Self-Disproportionation of the Enantiomers (SDE) of Methyl *n*-Pentyl Sulfoxide *via* Achiral, Gravity-Driven Column Chromatography: A Case Study. *Org. Biomol. Chem.* **2014**, *12*, 4738−4746.
(647) Suzuki, Y.; Han, J.; Kitagawa, O.; Aceña, J. L.; Klika, K. D.; Soloshonok, V. A. A Comprehensive Examination of the Self-Disproportionation of Enantiomers (SDE) of Chiral Amides *via* Achiral, Laboratory-Routine, Gravity-Driven Column Chromatography. *RSC Adv.* **2015**, *5*, 2988−2993.

DOI: 10.1021/acs.chemrev.5b00392
Chem. Rev. 2016, 116, 422−518

(648) Katagiri, T.; Yoda, C.; Furuhashi, K.; Ueki, K.; Kubota, T. Separation of an Enantiomorph and its Racemate by Distillation: Strong Chiral Recognizing Ability of Trifluorolactates. *Chem. Lett.* **1996**, 115−116.
(649) Yasumoto, M.; Ueki, H.; Ono, T.; Katagiri, T.; Soloshonok, V. A. Self-Disproportionation of Enantiomers of Isopropyl 3,3,3-(Trifluoro)lactate *via* Sublimation: Sublimation Rates vs. Enantiomeric Composition. *J. Fluorine Chem.* **2010**, *131*, 535−539.
(650) Ueki, H.; Yasumoto, M.; Soloshonok, V. A. Rational Application of Self-Disproportionation of Enantiomers via Sublimation—A Novel Methodological Dimension for Enantiomeric Purifications. *Tetrahedron: Asymmetry* **2010**, *21*, 1396−1400.
(651) Yasumoto, M.; Ueki, H.; Soloshonok, V. A. Self-Disproportionation of Enantiomers of 3,3,3-Trifluorolactic Acid Amides via Sublimation. *J. Fluorine Chem.* **2010**, *131*, 266−269.
(652) Yasumoto, M.; Ueki, H.; Soloshonok, V. A. Self-Disproportionation of Enantiomers of α-Trifluoromethyl Lactic Acid Amides via Sublimation. *J. Fluorine Chem.* **2010**, *131*, 540−544.
(653) Basiuk, V. A.; Gromovoy, T. Y.; Chuiko, A. A.; Soloshonok, V. A.; Kukhar, V. P. A Novel Approach to the Synthesis of Symmetric Optically Active 2,5-Dioxopiperazines. *Synthesis* **1992**, *1992*, 449−451.
(654) Han, J.; Nelson, D. J.; Sorochinsky, A. E.; Soloshonok, V. A. Self-Disproportionation of Enantiomers *via* Sublimation; New and Truly Green Dimension in Optical Purification. *Curr. Org. Synth.* **2011**, *8*, 310−317.
(655) Sorochinsky, A. E.; Aceña, J. L.; Soloshonok, V. A. Self-Disproportionation of Enantiomers of Chiral, Non-Racemic Fluoroorganic Compounds: Role of Fluorine as Enabling Element. *Synthesis* **2013**, *45*, 141−152.
(656) Aceña, J. L.; Sorochinsky, A. E.; Katagiri, T.; Soloshonok, V. A. Unconventional Preparation of Racemic Crystals of Isopropyl 3,3,3-Trifluoro-2-hydroxypropanoate and their Unusual Crystallographic Structure: The Ultimate Preference for Homochiral Intermolecular Interactions. *Chem. Commun.* **2013**, *49*, 373−375.
(657) Soloshonok, V. A.; Berbasov, D. O. Self-Disproportionation of Enantiomers of (*R*)-Ethyl 3-(3,5-Dinitrobenzamido)-4,4,4-trifluorobutanoate on Achiral Silica Gel Stationary Phase. *J. Fluorine Chem.* **2006**, *127*, 597−603.
(658) Maeno, M.; Tokunaga, E.; Yamamoto, T.; Suzuki, T.; Ogino, Y.; Ito, E.; Shiro, M.; Asahi, T.; Shibata, N. Self-Disproportionation of Enantiomers of Thalidomide and its Fluorinated Analogue via Gravity-Driven Achiral Chromatography: Mechanistic Rationale and Implications. *Chem. Sci.* **2015**, *6*, 1043−1048.
(659) Ogawa, S.; Nishimine, T.; Tokunaga, E.; Nakamura, S.; Shibata, N. Self-Disproportionation of Enantiomers of Heterocyclic Compounds Having a Tertiary Trifluoromethyl Alcohol Center on Chromatography with a Non-Chiral System. *J. Fluorine Chem.* **2010**, *131*, 521−524.

DOI: 10.1021/acs.chemrev.5b00392
Chem. Rev. 2016, 116, 422−518